UNIVERSITE LILLE NORD DE FRANCE

ÉCOLE DOCTORALE BIOLOGIE-SANTE DE LILLE
FACULTY OF PHARMACEUTICAL AND BIOLOGICAL SCIENCES

THÈSE
Pour l'obtention de grade de
DOCTEUR en Biologie-Santé de l'Université de Lille
Discipline : Biologie cellulaire et Parasitologie
Présentée par

Asma Sarah KHELIFA

Study of the transcriptional and post-transcriptional regulation of the *Toxoplasma gondii* tachyzoite cell cycle.

Soutenue le 2 Novembre 2021
Composition du jury :

Madame la Docteur, Martine Duterque, Présidente du Jury
Madame la Professeure, Dominique Soldati, Rapporteur
Monsieur le Professeur, Marc-Jan Gubbels, Rapporteur
Monsieur le Docteur, Moritz Treeck, Examinateur
Madame la Docteur, Clare Harding, Examinateur
Monsieur le Docteur, Mathieu Gissot, Directeur de Thèse.

Résumé

Au cours de son cycle de vie complexe, *Toxoplasma gondii* se différencie en stades de développement distincts. Ces transitions sont associées à des modifications du transcriptome du parasite. Les facteurs de transcription (FT) spécifiques de la famille ApiAP2 jouent un rôle dans la régulation de l'expression des gènes au cours de ces transitions développementales. Les FT de la famille des ApiAP2 se caractérisent par la présence d'un domaine de liaison à l'ADN de l'intégrase Apetala2/ERF similaires à ceux des plantes. Alors qu'il a été démontré que certains FT ApiAP2 jouent un rôle dans le contrôle de la transition développementale du tachyzoïte au bradyzoïte, un grand nombre de ces protéines n'ont pas encore été étudiées. Ainsi, pour la première partie de cette thèse, le rôle biologique de deux FT ApiAP2, TgAP2X-10 et TgAP2III-1 a été étudié. L'effet de TgAP2X-10 et TgAP2III-1 sur la différenciation des bradyzoïtes a été déterminé en utilisant différents modèles de différenciation *in vitro*. Nous avons également étudié l'effet de la perte de TgAP2X-10 et TgAP2III-1 *in vivo* chez la souris. Les données accumulées tendent à montrer que ces deux FT pourraient être des régulateurs potentiels de la différenciation des bradyzoïtes. Afin de poursuivre la caractérisation des FT ApiAP2, un troisième FT, TgAP2IX-5 a été étudié. L'étude de cette protéine fait partie de la deuxième partie de ce projet de thèse. Nous avons démontré que TgAP2IX-5 avait un rôle dans la division asexuée du tachyzoïte de *T. gondii.* Plus précisément, cette protéine contrôle la production des cellules filles lors du cycle cellulaire. La création d'un mutant d'expression conditionnel pour la protéine TgAP2IX-5 nous a permis de montrer que l'absence de cette protéine bloque la division du plaste précisément après son allongement et avant sa ségrégation. En étudiant le transcriptome de ces mutants par RNA-seq, nous avons déterminé que la protéine TgAP2IX-5 régule des centaines de gènes, dont la majorité est adressée au complexe de la membrane interne (IMC) et au complexe apical. TgAP2IX-5 est présent sur de nombreux promoteurs de gènes qui sont nécessaires à la progression du cycle cellulaire et la production des cellules filles. De plus, TgAP2IX-5 contrôle aussi le destin cellulaire en activant des répresseurs bradyzoïtes connus, promouvant ainsi la division cellulaire du tachyzoïte. De manière surprenante, nous démontrons que la réexpression de TgAP2IX-5 réinitie la division du cycle cellulaire, mais le parasite change son mode de division de l'endodyogénie à l'endopolygénie. Des études complémentaires montrent aussi que d'autres domaines protéiques jouent un rôle essentiel dans l'activité biologique de TgAP2IX-5. Dans une troisième et dernière partie de cette thèse, nous démontrons le rôle essentiel de la protéine TgPP1 dans la production de l'IMC ainsi que dans le cycle suggère que TgPP1 est important pour contrôler les événements de phosphorylation dans le cycle cellulaire asexué du tachyzoïte.

Abstract

During its complex life cycle, the *T. gondii* parasite differentiates into distinct developmental stages. The transition between these life stages is associated with changes in the parasite's transcriptome. In *Toxoplasma*, it has been demonstrated that specific transcription factors of the ApiAP2 family play a role in regulating gene expression during these developmental transitions. ApiAP2 transcription factors are characterized by the presence of an AP2 domain. These AP2 TFs possess an Apetala2/ERF integrase DNA binding domain similar to those of plants. While certain ApiAP2 TFs have been demonstrated to play a role in controlling the tachyzoite to bradyzoite developmental transition, several remain unstudied. Thus, for the first part of this thesis, the role of two constitutively expressed ApiAP2 TFs, TgAP2X-10 and TgAP2III-1was studied. The effect of TgAP2X-10 and TgAP2III-1 on bradyzoite differentiation was determined using two *in vitro* models. We also study the effect of TgAP2X-10 and TgAP2III-1 loss *in vivo* in mice and demonstrate that these proteins might be potential regulators of bradyzoite differentiation. In an attempt to continue with the characterization of ApiAP2 TFs, a third ApiAP2 TF, TgAP2IX-5 was studied. The study of TgAP2IX-5 represents the second part of this PhD project. TgAP2IX-5 was demonstrated to have a role in asexual cell cycle division of the *T. gondii* tachyzoite. The conditional depletion of TgAP2IX-5 blocks the progression of the cell cycle at a precise time-point when the plastid is elongated before its segregation. By using RNA-seq, we determined that TgAP2IX-5 differentially regulates hundreds of genes, a majority of which are targeted to the Inner Membrane Complex (IMC) and apical complex. ChIP-seq allowed to identify the promoters of hundreds of genes targeted by TgAP2IX-5 which are necessary for the progression of the budding cycle. In addition, TgAP2IX-5 was demonstrated to activate known bradyzoite repressors. Strikingly, we demonstrate that the re-expression of TgAP2IX-5 re-initiates cell cycle division, yet the parasite switches its mode of division from endodyogeny to endopolygeny. Further studies regarding the elucidation of the different regions of the TgAP2IX-5 protein were carried out and a novel domain was identified and shown to be essential for the function of TgAP2IX-5. In the third and final part of this PhD study, we demonstrated the crucial role of the TgPP1 phosphatase in the cell cycle. The production of the daughter cell IMC and the nuclear cycle is affected in absence of this protein. Phospho-proteomics analysis revealed that the depletion of TgPP1 results in the differential phosphorylation of several IMC proteins. Overall, this study suggests that TgPP1 is important for controlling phosphorylation events within the tachyzoite's cell cycle.

Acknowledgments

As a beginning statement of this PhD thesis, I would like to express my most heartfelt thanks to the people who have helped me throughout this three-year PhD journey. It is with my sincerest gratitude that I thank the people who have assisted me in completing this work.

First and foremost, I would like to thank my thesis supervisor, Dr Mathieu Gissot for giving me this amazing opportunity and for allowing me to pursue this PhD under his supervision. I would like to thank him for his advice, patience, and guidance throughout this PhD. I am grateful for the numerous scientific discussions; I have learned a lot from him and cannot thank him enough. It has been a privilege to be his PhD student.

Next, I would like to thank all the lab members, Dr Jamal Khalife, Dr Christine Pierrot, Dr El Moukhtar Aliouat, and Dr Sabrina Marion for their feedback during the laboratory meetings and for the scientific discussions. I would also like to thank Emmanuel, Caroline, Veronique, and Tom.

My gratitude towards my lab colleagues, Thomas, Claudianne, Claire, Hala, Amir, Lola, Cecilia, Anais, Sylia, Benedicte, and Aline for their friendship and support. We shared memorable moments together in the lab which I will always look back upon and remember.

My sincere gratitude to the jury members, Prof. Soldati-Favre, Prof. Gubbels, Dr Treeck, Dr Harding, and Dr Duterque, who have agreed to evaluate and review this work.

My appreciation to Ms. Elisabeth Werkmeister and Ms. Sophie Desnoulez for help with the microscopy platform.

I would like to thank the administrative team at the EDBSL, Mr Francois Delcroix, Ms Marjorie Vanderhove, and Ms Tanya Florida for their help with administrative aspects of this PhD.

Most importantly, I would like to extend my thanks to my parents, for their unconditional love and support. They have selflessly encouraged me throughout this PhD journey. I am forever indebted to them for all that they have offered me throughout my years of academic education. Their support has allowed me to persevere when times became challenging and rough. I would not have been able to reach this milestone without them. "I will forever be indebted to you for an education of which I am sincerely proud of.". Special thanks to my grandparents for their endless encouragement. I could have not made it to this day without their support. I am forever grateful for their endless prayers. My gratitude to all three of my brothers, whom I cherish dearly and whose encouragements are greatly appreciated.

Finally, I would like to thank my extended family; my aunt, uncles, and cousins, for always checking on me since I was so far away from home. My most heartfelt gratitude to all my friends across the Atlantic who have supported me throughout the course of this PhD.

Summary

Cette thèse de doctorat comprend trois projets différents. Dans la première partie du doctorat, la caractérisation de deux facteurs de transcription ApiAP2 a été réalisée. Des parasites mutants ont été générés dans les souches de Type I, RHΔKu80, et de Type II, Pru ΔKu80, pour lesquelles les gènes AP2X-10 et AP2III-1 ont été supprimés. Les analyses de croissance n'ont démontré aucun défaut de croissance. L'étude de la différenciation des souches de Type II en bradyzoïte, dans un modèle de stress alcalin, a montré qu'il n'y avait pas de différence significative dans le nombre de kystes identifiés. Cependant, dans un nouveau modèle de différenciation spontanée utilisant des cellules primaires de cerveaux de rat, les parasites mutants pour le gène AP2X-10 ont montré une augmentation significative du pourcentage de kystes tissulaires suggérant qu'AP2X-10 aurait un rôle dans la différenciation. En outre, afin d'examiner si les deux souches mutantes ont un rôle dans la différenciation des bradyzoïtes *in vivo*, nous avons réalisé deux expériences d'infection de souris par les souches mutantes et sauvages. Dans les deux expériences, le nombre de kystes étaient significativement plus faibles pour les souches mutantes par rapport au sauvage. Ces résultats *in vivo* suggèrent que TgAP2X-10 et TgAP2III-1 ont un rôle dans la différenciation des bradyzoïtes *in vivo*. Une analyse du transcriptome des souches mutantes en condition normales et de stress alcalin, n'ont pas révélé d'expression différentielle, reflétant les données de caractérisation des mutants obtenues pour ces conditions.

Dans une deuxième partie, un troisième facteur de transcription ApiAP2, TgAP2IX-5, a été caractérisé. Un mutant inductible de cette protéine a été généré à l'aide du système de dégradation inductible par l'auxine (AID). En présence d'auxine, la déplétion de TgAP2IX-5 est effective après une heure. Les expériences testant la croissance et la prolifération du mutant ont montré que cette protéine est essentielle pour le parasite. En outre, le mutant a un défaut extrêmement marqué de production des cellules filles, induisant la production de parasites comportant un grand nombre de noyaux. Le suivi de la ségrégation des organelles lors du cycle cellulaire dans le mutant a montré le rôle essentiel de ce facteur de transcription précisément après l'allongement du plastide et avant sa ségrégation. Des expériences d'immuno-précipitation de la chromatine (ChIP-seq) ont permis d'identifier les promoteurs sur lesquels TgAP2IX-5 se lie. L'intégration de ces données avec celles de transcriptomique des parasites iKD TgAP2IX-5 traités avec de l'auxine pendant 6 heures a permis d'identifier les gènes directement sous le contrôle de ce facteur de transcription. Ces gènes sont exprimés pendant la phase S/M et sont en majorité adressés au complexe membranaire interne (IMC) et au complexe apical. Des expériences de réexpression de TgAP2IX-5 après déplétion de cette protéine a permis de démontrer que cette protéine jouait un rôle central dans le contrôle de la production des cellules filles. Nous pu montrer que le moment de production des cellules filles est l'évènement crucial du cycle cellulaire permettant le passage d'un mode de division par endodyogenie à l'endopolygénie, qui est normalement réalisée par les mérozoïtes chez l'hôte félidé définitif. Ce travail a été suivi d'un ensemble d'expériences complémentaires. Notamment, des expériences explorant le transcriptome des parasites traités avec de l'auxine pendant une ou deux heures ont permis l'identification d'un panel plus large de

gènes ciblés directement par TgAP2IX-5. De plus, différents domaines de la protéine TgAP2IX-5 ont été caractérisés. Les régions étudiées, grâce à des expériences de complémentation du mutant iKD AP2IX-5, sont le domaine AP2 et un nouveau domaine non caractérisé nommé « domaine 1 ». Ces expériences ont démontré que le domain 1 est essentiel pour la fonction biologique de TgAP2IX-5 alors que le domaine AP2 ne l'est pas.

Dans une troisième et dernière partie, la phosphatase TgPP1 a été caractérisée. Les analyses de croissance pour ce mutant ont montré un défaut de croissance après le traitement avec de l'auxine. Une étude de l'impact de la déplétion de la protéine TgPP1 sur la division des organites a démontré un role de cette protéine sur la division du plastide et l'intégrité structurelle du centrosome. Nous avons aussi observé un impact majeur sur la formation de l'IMC. Les expériences de microscopie électronique ont confirmé les conséquences de la déplétion de TgPP1sur l'IMC tandis que la membrane plasmique demeure intacte. Des expériences de phosphoprotéomique ont montré un impact majeur de TgPP1 sur l'état de phosphorylation de plusieurs protéines IMC, telles que IMC4, IMC5, IMC18, IMC20 et IMC24. En résumé, TgPP1 joue un rôle essentiel dans la formation et le maintien de la structure de l'IMC. Cependant, d'autres études sont nécessaires afin de mieux comprendre le role de la phosphorylation dans la structuration de l'IMC.

Article :

- TgAP2IX-5 is a key transcriptional regulator of the asexual cell cycle division in *Toxoplasma gondii*

Asma S. Khelifa[1], Cecilia Guillen Sanchez[1], Kevin M. Lesage[1], Ludovic Huot[1], Thomas Mouveaux[1], Pierre Pericard[2], Nicolas Barois[1], Helene Touzet[2,3], Guillemette Marot[2,4], Emmanuel Roger[1], and Mathieu Gissot[1*]

1 Univ. Lille, CNRS, Inserm, CHU Lille, Institut Pasteur de Lille, U1019-UMR 9017-CIIL-Center for Infection and Immunity of Lille, F-59000, Lille, France
2 Univ. Lille, CNRS, Inserm, CHU Lille, Institut Pasteur de Lille, US 41-UMS 2014-PLBS, bilille, F-59000, Lille, France
3 Univ. Lille, CNRS, Centrale Lille, UMR 9189-CRIStAL-Centre de Recherche en Informatique Signal et Automatique de Lille, F-59000, Lille, France
4 Univ. Lille, Inria, CHU Lille, ULR 2694-METRICS : Evaluation des technologies de santé et des pratiques médicales, F-59000, Lille, France

*Corresponding author

Table of Contents

List of Figures

List of Tables

List of Abbreviations

ABA Abscissic Acid

AAP Apical Annuli Protein

AC Apical Cap

AID Auxin Inducible Degradation

AIP ARO-Interacting Protein

AMA1 Apical Membrane Antigen 1

AP2 Apetala-2

APH Acylated Pleckstrin Homology domain-containing protein

APR Apical Polar Ring

ARO Armadillo Repeats Only protein

ATFs Activating Transcription Factors

BFD1 Bradyzoite Formation Deficient 1

BIC Basal Inner Collar

BIR Basal Inner Ring

BLAST Basic Local Alignment Search Tool

CAM Calmodulin-like

CDPK Calcium Dependent Protein Kinase

CORVET Class C Core Vacuole/Endosome Transport

CPE Core Promoter Elements

CRISPR/Cas9 Clustered Regularly Interspersed Short Palindromic Repeats/CRISPR associated protein 9

CRC Corepressor Complex

CrK Cyclin related Kinase

CT Congenital Transmission

CTD Carboxyl-Terminal Domain

DAG Diacylglycerol

DAPI Di Aminido Phenyl Indol

DBA Dolichos biflorus Agglutinin

DCX Doublecortin protein

DGK1 Daicylglycerol Kinase 1

DHFR Dihydrofolate Reductase-thymidine synthase

DLC Dynein Light Chain

DLC8a Dynein Light Chain 8a

DMEM Dulbecco's Modified Eagle's Medium

DPE Downstream Promoter Elements

DrpA Dynamin-related Protein A

DT Dye Test

ELISA Enzyme-Linked ImmunoSorbent Assay

ENO1 Enolase-1

ENO2 Enolase-2

ER Endoplasmic Reticulum

ERAD Endoplasmic Reticulum Associated Degradation

ERK7 Extracellular Signal-Regulated Kinase 7

ERF Ethylene Response Factor

FBS Fetal Bovine Serum

FCP FIIF-associating carboxyl-terminal domain protein

FLU Fluoridone

GAC Glideosome Associated Connector

GAP Glideosome Activating Protein

GAPM glideosome associated protein with transmembrane domain

GC Guanylate Cyclase

GCN5 lysine acetyltransferase

cGMP Cyclic Guanosine Monophosphate

GPI Glycosyl-phosphatidyl-inositol

GRA Dense GRAnules Proteins

GTFs General Transcription Factors

GTP Guanosine Triphosphate

GVBD Germinal Vesicle Breakdown

HAD Haloacid Dehalogenase

HAT Histone Acetylase enzyme

HDAC Histone Deacetylase enzyme

HFF Human Foreskin Fibroblasts

HOPS Homotypic Vacuole Fusion and Protein Sorting

H.O.S.T Host Organelle Sequestering Tubulostructures

HXGPRT Hypohanthine Xanthine Guanine PhosphRibosylTransferase

hyperLOPIT hyperplexed Localization of Organelle Proteins by Isotope Tagging

IAA Indole-3-Acetic Acid

IECs Intestinal Epithelial Cells

IFA Immunofluorescence Assay

IFAT Indirect Fluorescent Antibody Test

IF-like Intermediate filament-like

IFN-γ Interferon γ

Ig Immunoglobulin

IHA Indirect Hemaglutination Assay

IMC Inner Membrane Complex

IMP Inner Membranous Particle

IP Immunoprecipitation

IP$_3$ Inositol-1,4,5-triphosphate

IPP Isopentenyl diphosphate

IRG Immune-related GTPases

ISAGA Immunosorbent Agglutination Assay

ISC IMC suture component

ISP IMC Sub-compartment Proteins

IST Inhibitor of STAT1 Transcriptional activity

ITS-1 Internal Transcribed Spacer

IVN Intravacuolar Network

KAT Lysine Acetyltransferase

KD Knock-down

KDAC Lysine Deacetyltransferase enzyme

KI Knock-in

KMT Lysine methyltransferase

KO Knock-out

M Mitosis

MAF1b Mitochondrial Association Factor 1b

M2AP MIC2-associated protein

MAF1 Mitochondrial Associating Factor1

MAPK Mitogen Activated Protein Kinase

MAP Microtubule associated Protein

MIC Microneme proteins

MJ Moving Junction

MLC Myosin Light Chain

MORC Microchidia

MORN1 Membrane Occupation and Recognition Nexus1 protein

mRNA Messenger Ribonucleic Acid

MSC1a Mature Soluble Cytoskeletal 1a protein

MT Microtubules

MTOC Microtubule Organizing Center

Myo Myosin

NFAT4 Nuclear Factor of Activated T cell 4

OA Okadaic Acid

PA Phosphatidic Acid

PAGE Polyacrylamide Gel Electrophoresis

PBS Phosphate Buffer Saline

PCRs Pre-conoidal Rings

PCR Polymerase Chain Reaction

PFA Paraformaldehyde

pI Isoelectric point

PIC Pre-initiation Complex

PI-PLC Phosphinositide Phospholipase C

PIPs Phosphatase Type 1-Interacting proteins

PKG Protein Kinase G/cGMP-dependent Protein Kinase

PPKL Protein Phosphatase with characteristic Kelch-like domain

PLP1 Perforin-like Protein 1

PM Plasma membrane

PMSF Phenylmethyl Sulfonyl Fluoride

PP2C Protein Phosphatase 2C

PPM Periplastid membrane

PPMs Protein Phosphatases that are Mg^{2+}/Mn^{2+}- dependent

PPPs Phospho-Protein Phosphatases

PRMT Protein Arginine Methyltransferase

PRP1 Parafusin Related Protein 1

PSPs Protein Serine/Threonine Phosphatases

PV Parasitophorous Vacuole

PVM Parasitophorous Vacuole Membrane

PYR Pyremethamine

RNG1 Ring-1

RNG-2 Ring-2

RON Rhoptry Neck Protein

ROP Rhoptry Bulb Protein

rRNA Ribosomal Ribonumcleic Acid

SAG Surface Antigen Glycoprotein

SAGE Serial Analysis of Gene Expression

SAS6L SAS6 centriole associated-like protein

SFA Striated-Fiber Assemblin

SLP Shewanella-Like Phosphatase

SPM1 Subpellicular Microtubule Protein 1

SPMTs Sub-Pellicular Microtubules

SPN Subpellicular Network

SRS SAG1 related sequence

SR-SIM Super-resolution Structured Illumination Microscopy

STAT Signal Transducer and Activator of Transcription

TAFs TBP Associated Factors

TAU Tautomycin

TBP TATA Binding Proteins

TFA Trifluoracetic acid

TMP Trimethoprime

TRANSFAC Transcription Factor Database

tRNA Transfer Ribonucleic Acid

TSC Transverse suture component

TSSs Transcription Start Sites

TVN Tubulo-Vesicular Network

U-ExM Ultrastructure Expansion Microscopy

WB Western Blot

Introduction

Chapter I - Introduction

1 *Toxoplasma gondii*, member of the Apicomplexa phylum

1.1 History of the *Toxoplasma gondii* parasite

Toxoplasma gondii is a protozoan parasite that was first discovered more than 100 years ago by scientists in North Africa and Brazil. It was Charles Nicolle and Louis Manceaux who first identified the parasite in Tunisia in a hamster-like rodent, *Ctenodactylus gundi*, in 1908 (Nicolle & Manceaux, 1908). When first discovered Nicolle thought the parasite to be a piroplasm and then *Leishmania,* but it was soon realized that a new organism was discovered and was named *T. gondii* based on its morphology. *Toxoplasma* is derived from the Greek word 'taxon'. "Toxo" refers to "bow" or "arc" whereas "plasma" refers to "form". Splendore also discovered the same parasite in a rabbit in Brazil in 1908 and he thought it to be *Leishmania* without naming the parasite (Splendore, 1908).

During the next 30 years, *T. gondii* was discovered in several other hosts specifically in birds (J. P. Dubey, 2002). In 1937, viable *T. gondii* was first isolated and proven identical to the human isolate (Sabin and Olitsky, 1937). The taxonomic classification of *T. gondii* according to NCBI (Taxonomy ID: 5811) is included in the following table:

Domain	*Eukaryota*
Kingdom	*Alveolata*
Phylum	*Apicomplexa*
Class	*Conoidasida*
Sub-class	*Coccidia*
Order	*Eucoccidiorida*
Sub-Order	*Eimeriorina*
Family	*Sarcocystidae*
Genus	*Toxoplasma*
Species	*Toxoplasma gondii*

Table 1- Taxonomic Classification of *Toxoplasma gondii* according to NCBI

Several *T. gondii* genotypes are present worldwide (Su et al., 2012). However, previous studies demonstrated that *T. gondii* had a clonal population structure comprised of three main genotypic lineages: Type I, Type II, and Type III (Howe

& Sibley, 1995). These lineages were mainly characterized based on their distinguished virulence in mice and their cyst-forming capability (Howe & Sibley, 1995). The three clonal lineages were found in diverse hosts in different regions mainly located in North America and Europe. The expansion of the three main clonal lineages is most likely due to their spread through the food chain (Howe & Sibley, 1995). However, more recent studies have identified that *T. gondii* isolates consist of six major clades classified into several haplogroups (Su et al., 2012).

Type I strains are extremely virulent *in vivo* where the inoculation with a single parasite is deadly (Boothroyd & Grigg, 2002). Type II and Type III strains are characterized by low virulence when relatively compared to the Type I strain and exhibit lethality *in vivo* by the inoculation of 1000 parasites (Saeij et al., 2005). Type II strains are characterized by the production of a large number of tissue cysts *in vivo* (Hunter et al., 1992), and may become reactivated in the case of immunocompromised individuals such as those who are diagnosed with AIDS or are undergoing chemotherapy or organ transplantation. The Type II strain is predominantly associated with disease and is responsible for around two-thirds of the globe's human cases of toxoplasmosis (Howe & Sibley, 1995). In a study carried out in France, Type II strains were found to be associated with disease in the French population and constitute over 90% of human and animal isolates (Robert-Gangneux & Darde, 2012). The correlation of Type II strains with disease has made strains of type II the focus of study for investigating the implications of toxoplasmosis as well as potential discovery of treatments.

Atypical strains account for large genetic diversity within South America. A recent study grouped the atypical strains into 11 distinct haplogroups. Most of the strains classified under haplogroups 1-3 occur in North America and Europe coinciding with the previously defined lineages I, II, and III. However, haplogroup strains 4,5, and 8-10 occur mainly in South America whereas haplogroup 6 strains are spread widely and appear in Europe, South America, and Africa. Strains that were previously designated as 'exotic' were discovered to be common in South America and are 'uncommon' solely in the case when compared to the defined lineages in North America and Europe (Khan et al., 2007). Furthermore, the recent study carried out by Su et al. (2012) identified 15 haplogroups defining the six major clades of *T. gondii* isolates.

1.2 The Apicomplexa phylum

The Apicomplexa phylum consists of a large and diverse group of unicellular protists that have a wide geographic distribution. It is the only taxonomic group that is uniquely formed of obligate intracellular parasites. Many of its members are pathogens of humans and domesticated animals. The phylum belongs to the taxonomic kingdom *Alveolata* which consists of Dinoflagellates and Ciliates in addition to Apicomplexans (Gould et al., 2008; Moore et al., 2008; Yoon et al., 2008). The Apicomplexa taxonomic group consists of four sub-groups: the Coccidia, the Gregarines, the Cryptosporidia, and the Hematozoa (Figure 1). The current classification of Apicomplexan members is characterized by its conservation far from the extents of modern molecular data (Kaya, 2001). Many morphological features are shared among Apicomplexan parasites that are regarded as a hallmark of the phylum. These shared traits include the elongated shape, and several specialized organelles that constitute the apical complex which include:

rhoptries, micronemes, and the apical polar ring. The apical complex is essential for the parasite's survival and invasion of the host cell. Furthermore, Apicomplexans have other specialized structures such as the apicoplast, which is an essential chloroplast-like organelle (N. S. Morrissette & Sibley, 2002).
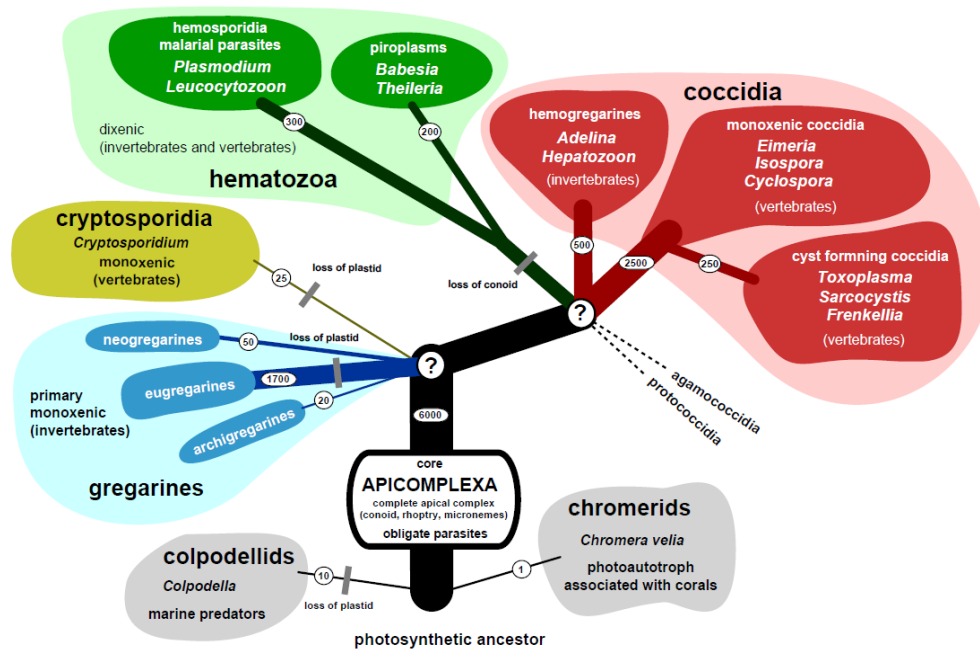
Figure 1 – Schematic representation of the various Apicomplexa taxonomic sub-classes (Portman & Šlapeta, 2014). Apicomplexa phylum members and their closest related relatives are represented in the phylogenetic tree. There are four main sub-groups present in the Apicomplexa phylum and include: Cryptosporidia, Gregarines, Hematozoa, and Coccidia.

This phylum contains pathogens such as *Plasmodium, Cryptosporidium, Babesia,* and *Eimeria.*

2 *Toxoplasma gondii* life cycle and transmission

T. gondii can infect any type of nucleated cell whether it be mammalian or avian. The life cycle of *T. gondii* is divided between an intermediate host and a definitive host correlating to asexual and sexual replication, respectively. Transmission of *T. gondii* can occur when a warm-blooded intermediate host ingests either tissue cysts or oocysts from the external environment. Tissue cysts release bradyzoites which then differentiate into tachyzoites. Sporulated oocysts release sporozoites which then also differentiate into tachyzoites. Tachyzoites replicate throughout the intermediate host until they differentiate into the latent bradyzoite form in different types of tissue such as the brain, skeletal muscle tissue, the eyes, and even cardiac tissue.

The sexual cycle occurs exclusively in the intestinal lumen of the definitive host which includes many members of the Felidae. After the felid ingests tissue cysts or oocysts, the parasites invade and replicate within the definitive host's intestinal epithelial cells (IECs). The parasite undergoes several rounds of asexual division known as endopolygeny and is characterized by the development of merozoites within schizonts (J. P. Dubey & Frenkel, 1972). This is then followed by the formation of microgametocytes and macrogametocytes. These gametocytes fuse to form a zygote, which then develops into an oocyst. The sporozoite-containing oocysts are released into the environment and ingested by a secondary host (intermediate host), where the sporozoites differentiate into the rapidly replicating tachyzoites causing the 'acute' form of toxoplasmosis. The parasite can be a cause of 'chronic' disease, when the rapidly replicating tachyzoites differentiate into the slowly replicating bradyzoites (Figure 2). These bradyzoites can re-emerge occasionally but usually are not a factor of serious illness in healthy individuals (Ajioka et al., 2001). However, cerebral toxoplasmosis is developed in the case of bradyzoite re-activation and differentiation into tachyzoites in immune-compromised individuals (Lee & Lee, 2017; Luft et al., 2010). In these cases, the uncontrolled proliferation of tachyzoites is the cause of life-threatening illness, especially when the reactivating cysts are located in the brain of the infected host (cerebral toxoplasmosis).
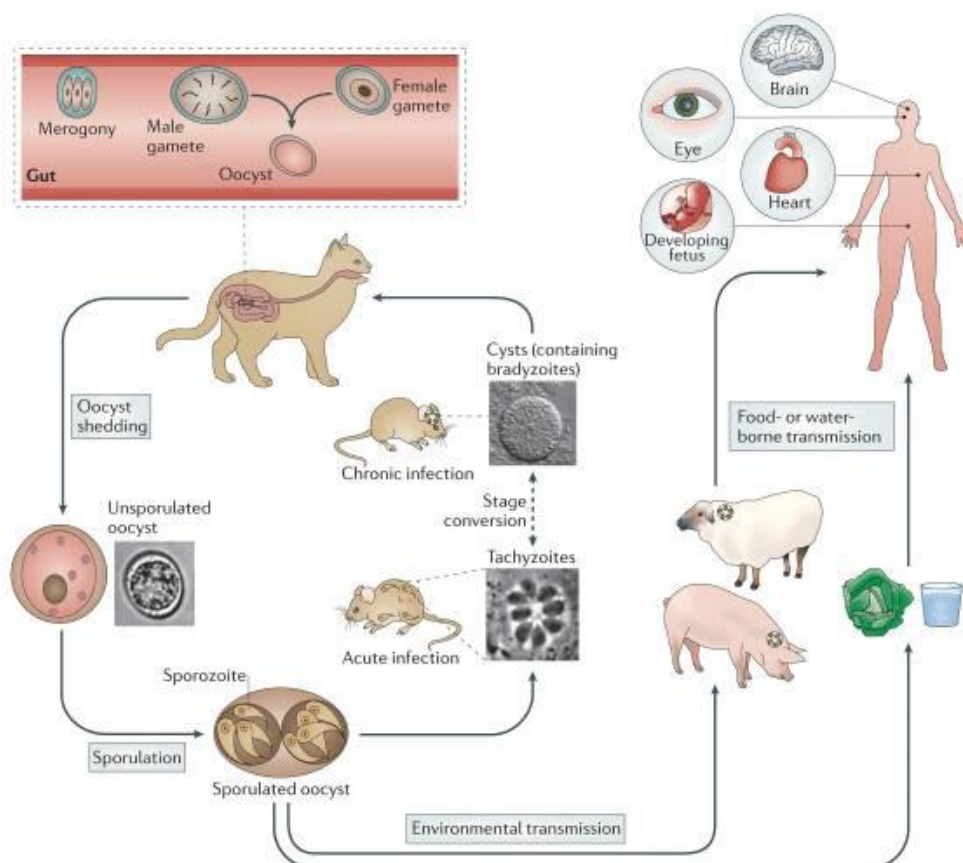
Figure 2 − Schematic representation of the complex life cycle of *T. gondii* divided between the intermediate and the definitive host (Hunter & Sibley, 2012). Sexual reproduction of the *T. gondii* life cycle occurs in the felid definitive host whereas asexual reproduction occurs in the warm-blooded intermediate host and the

definitive host. Merogony which involves the division of merozoites within the feline enterocytes is followed by the formation of female and male gametes. The two gametes fuse to form an oocyst which is excreted with the feline's feces. Oocysts released by the definitive host into the environment withstand extreme conditions and ensure transmission of the parasite when ingested by the intermediate host. Within the intermediate host, asexual division occurs. The oocysts release sporozoites which differentiate into tachyzoites and disseminate throughout the body. The tachyzoites may then differentiate into the latent bradyzoite form forming tissue cysts that remain dormant in muscle, heart, brain, and eye tissues. Intermediate hosts including humans can become infected by ingesting tissue cysts where bradyzoites that reach the intestinal lumen convert into tachyzoites and disseminate throughout the body. Vertical transmission can have detrimental effects on a pregnant women's fetus.

2.1 Sexual stage of *Toxoplasma gondii* life cycle

The sexual life cycle of *T. gondii* occurring in the definitive host (Felidae) is characterized by oocyst shedding in the feces 3 to 10 days after initial ingestion of bradyzoites, around 18 days after ingesting sporulated oocysts, and around 13 days after the ingestion of tachyzoites (J. P. Dubey, 1998). After the felid (domestic and wild cats) ingest tissue cysts of an intermediate host, the cyst wall is disrupted by specific gastric enzymes and bradyzoites are released from the tissue cysts before they invade enterocytes carrying out multiple rounds of asexual replication resulting in merozoite-containing schizonts. This is then followed by the sexual development phase also known as gametogony, where the formation of male and female gametes, microgametes and macrogametes, respectively is carried out (Ferguson, 2002). Microgametes are bi-flagellated and fertilize macrogametes by using their flagella to swim and displace towards the macrogametes (Speer & Dubey, 2005). After fertilization, a zygote is formed which develops into an oocyst. Oocysts are liberated from the enterocytes by disruption of the epithelial cells. This is then followed by excretion of the oocysts in an un-sporulated form in cat feces. Once the oocysts are released within the external environment, sporogony is carried out after a few days. The oocyst undergoes morphological changes and a meiotic reduction. This produces a sporulated oocyst containing two sporocysts, within each sporocyst are four haploid sporozoites (Figure 3).

The excretion of oocysts can start as early as 3 days after tissue cyst ingestion and can continue throughout the following 20 days. The number of shed oocysts in a cat's feces can reach up to 100 million oocysts. The released oocysts can infect any warm-blooded intermediate host, usually through food contamination. However, oocysts remain less infectious for cats based on a study which examined the infectivity of oocysts in cats (definitive host) and mice (intermediate host). In the case when 29 cats were fed 1-10 million oocysts, only one single cat shed oocysts and all cats were asymptomatic. However, when administering 1-10 million oocysts to mice, all of the mice died of toxoplasmosis. This study therefore confirmed that oocyst infectivity to cats is less than that to mice. In addition, non-pathogenicity of oocysts in cats was determined (Dubey, 2006; Robert-Gangneux & Darde, 2012).

2.2 Asexual stage of *Toxoplasma gondii* life cycle

The asexual stage of *T. gondii* occurs in the warm-blooded intermediate host. After the intermediate host ingests oocysts which release sporozoites, the sporozoites invade and replicate within the intestinal epithelium of the intermediate host and differentiate into tachyzoites. Similarly, cysts containing bradyzoites that are developed within muscle and brain tissues can be ingested by another intermediate host by consuming raw or uncooked meat. In that case, the cyst wall is ruptured by digestive tract enzymes allowing for the release of bradyzoites which infect the epithelial cells of the intermediate host and differentiate into tachyzoites (Figure 3).

These tachyzoites replicate within cells by undergoing a process termed 'endodyogeny' and disseminate via the bloodstream throughout the body. The tachyzoites then differentiate into a slower replicating form of the parasite known as 'bradyzoites' which give rise to tissue cysts within 7 to 10 days after infection *in vivo* in mice (Black & Boothroyd, 2000; Robert-Gangneux & Darde, 2012).

Tissue cysts remain throughout the entire lifespan of the intermediate host, and reside most prominently in muscle tissues and the brain (Black & Boothroyd, 2000; J. P. Dubey, 1997b; Robert-Gangneux & Darde, 2012). Life-long persistence of tissue cysts has been proven in mice (J. P. Dubey, 1997a).

The development of tissue cysts defines the chronic phase of toxoplasmosis. Tissue cysts can then be consumed by either an intermediate or definitive host. In the case when consumed by the definitive felid host, asexual replication occurs primarily followed by initiation of the sexual phase (Figure 3, following page).

.

2.3 Modes of Transmission

The modes of transmission of *T. gondii* were elucidated when the discovery of its life cycle came into light and can be classified into horizontal and vertical modes of transmission.

Congenital transmission (vertical)

Congenital transmission (CT) represents the vertical method of *T. gondii* transmission in which transplacental transmission occurs when the mother of the fetus becomes infected with the *T. gondii* parasite during pregnancy for the first time. The risk of transmission is elevated as the primary infection of the mother occurs later in pregnancy. The transmission rate in the third trimester is 65% compared to 25% in the first trimester and 54% in the second trimester (McAuley, 2014).
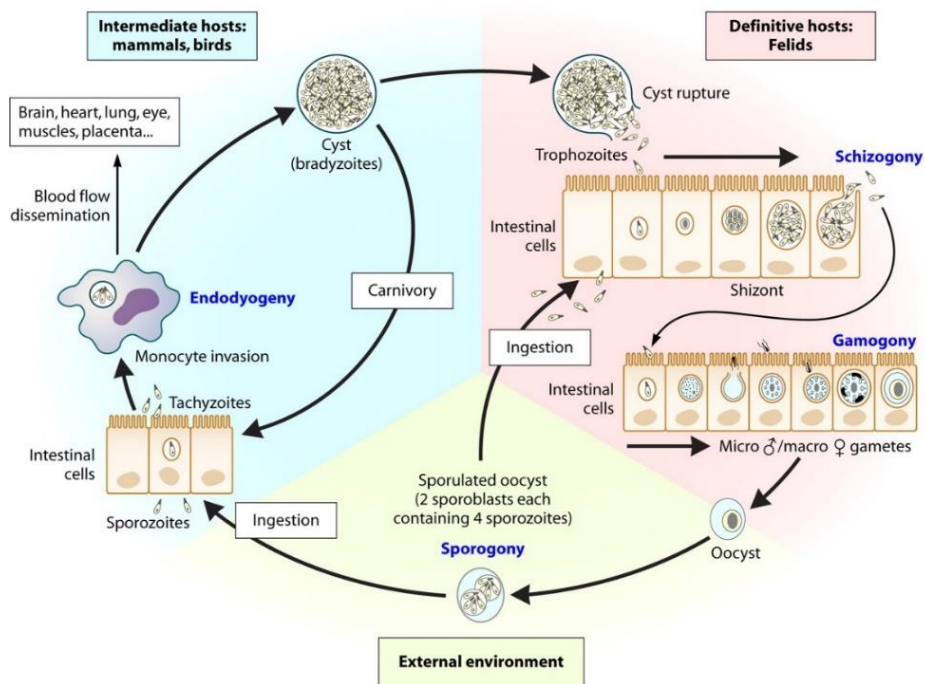
Figure 3 – Schematic representation of *T. gondii* life cycle's three main infective stages (Robert-Gangneux & Darde, 2012). *T. gondii* has three main infective stages of development. Within the felid definitive host, the **sexual phase** takes place where the ingestion of tissue cysts is followed by the disruption of the tissue cyst wall with gastric enzymes leading to the release of bradyzoites which infects cells of the intestinal epithelium. The parasite undergoes several rounds of asexual replication and schizonts consisting of merozoites are developed through schizogony. This is then followed by gamogony which entails the differentiation of merozoites into microgametes and macrogametes. After the fusion of these two types of gametes, oocysts are formed and released into the external environment via the felid's feces. These oocysts remain within the external environment where they undergo an **environmental phase**. Several environmental factors affect the Oocysts such as temperature, pH, pressure, etc. and result in their sporulation. The **asexual phase** takes place in the intermediate host and consists of the ingestion of the sporulated Oocysts or tissue cysts. Sporozoites released from oocysts or bradyzoites released from tissue cysts differentiate into tachyzoites and spread throughout the organism by asexual replication termed endodyogeny. The tachyzoites can convert into bradyzoites and form tissue cysts in different types of tissue such as the brain, heart, lungs, the eyes, etc.

There are three mechanisms by which congenital toxoplasmosis can occur: One method is through transmission to the fetus in the case where the mother is seronegative and immunocompetent and acquires infection during the first trimester of pregnancy or three months before conceiving. The second method that CT can occur by is through reactivation of toxoplasmosis in an immune woman that suddenly becomes immunocompromised when pregnant. The third method by which CT can occur is in the case where an immune mother gets infected with a new *T. gondii* strain that is more virulent than the one she was initially infected

with (Maldonado et al., 2017). CT is known to be a cause of miscarriage and in some cases can cause severe ocular disease and mental retardation in newborns.

Carnivorism (horizontal)
This method of transmission occurs when infected raw or undercooked meat is ingested by a naïve intermediate host. The transmission of the parasite through ingestion of infected meat was proven by experiments carried out on children in a Paris sanitorium by comparing acquisition rates of infection in the children before and after admission to the sanitorium. The annual acquisition rate of *T. gondii* infection increased from 10% to 50% after addition of undercooked meat (beef or horse) to the diet whereas the acquisition rate increased to 100% when adding undercooked lamb meat to the diet. This coincides with *T. gondii* prevalence rates which are higher in sheep compared to other animal types (horse and cattle) (J. P. Dubey, 2008).

Fecal-oral (horizontal)
The widespread prevalence of *T. gondii* in vegetarians and herbivores can be explained by ingestion of oocysts that are excreted in cat feces. Shedding of oocysts within the environment has been a cause of numerous outbreaks of Toxoplasmosis in humans. Epidemiological studies have demonstrated a complete absence of *Toxoplasma* in habitats without cats particularly in isolated islands. Therefore, affirming the importance of the fecal-oral route for natural *T. gondii* transmission (J. P. Dubey, 2008).

In addition to carnivorism and fecal-oral transmission, horizontal transmission of *T. gondii* may rarely occur through blood transfusion and during organ transplants consisting of tissue cysts (Katzer et al., 2014).

3 Toxoplasmosis, a devastating infectious disease
Toxoplasmosis, the disease associated and caused by the intracellular parasite, *T. gondii*, is a world-wide public health problem of significant importance. In the United States, an estimation of 8-22% of the population is infected. In other parts of the world such as Africa, Europe and Central America, infection rates range from 30-90% (Aguirre et al., 2019). These high rates of infection across the world have a negative impact on mortality, human health, and overall quality of life.

In the United States alone, more than one million individuals are infected by *T. gondii* every year with an estimate that the parasite is a cause for more than 8% of hospitalizations and 24% of deaths in the United States due to foodborne diseases (Scallan et al., 2011).

3.1 Clinical history of toxoplasmosis
T. gondii was first identified as a cause of disease in humans in 1939 in an infant girl who was delivered by Caesarean section in New York. After 3 days, the infant experienced seizures and chorioretinitis and died at 1 month of age. The *T. gondii* strain responsible for the death of the child was isolated and demonstrated to be no different to other *T. gondii* strains that were isolated from animals in terms of biology and immunology (Wolf et al., 1939). Following the initial case of *T. gondii* infection, several other cases were reported in infants, and it was concluded that

encephalitis and chorioretinitis were recognizable syndromes due to *T. gondii* infection.

In 1951, the first ocular toxoplasmosis clinical description was carried out in detail and in the 1960s, studies regarding seroconversion in pregnant women were initiated (Couvreur,1974). In the 1960s, *T. gondii* was initially recorded to cause encephalitis in immune-compromised patients under immunosuppressive drugs for Hodgkin's disease (Flament-Durand et al., 1967).

3.2 Toxoplasmosis pathogenesis

About one third of the world is infected with the latent form of toxoplasmosis. The prevalence of this infectious disease is different from one region to another based on eating habits, hygiene conditions, and ethnic factors (Tenter et al., 2000). However, underdeveloped countries are known to have a higher incidence rate of infections than developed countries. A high seroprevalence of 80% is present in Africa and Southern America relative to North America and Southeast Asia where the seroprevalence rate is around 30%. 80% of infections in immunocompetent individuals are asymptomatic. However, the remaining ~ 10-20% of cases of *T. gondii* infections in immune-competent hosts are symptomatic (Montoya & Liesenfeld, 2004). Asymptomatic cervical lymphadenopathy usually manifests. *T. gondii* causes around 3-7 % of lymphadenopathy which is clinically significant (McCabe et al., 1987). There are particular groups of people who are at high risk of severe *T. gondii* infection, and these include fetuses who are infected via CT, infants, and immune-compromised individuals. For example, those who receive corticosteroids and cytotoxic treatments, individuals suffering from hematological malignancies, those who have received organ transplants and those diagnosed with HIV/AIDS (Weiss & Dubey, 2009).

Three types of toxoplasmosis can be developed:

Cerebral toxoplasmosis

This type of clinical manifestation is the most common among immune-deficient individuals. Cerebral toxoplasmosis is caused by the re-activation of the latent tissue cyst forms. This occurs when the chronic infection is re-activated through the conversion of the tissue cysts containing bradyzoites into tachyzoites in the brain (Lee & Lee, 2017; Luft et al., 2010). In this case, the parasite replicates through its tachyzoite form causing severe brain tissue lesions.

It has many common symptoms such as headaches, deficiency in coordinating motor and sensory functions, as well as psychiatric complications. It was a leading cause of death in patients diagnosed with AIDS until the development of antiretroviral treatments.

Ocular toxoplasmosis

This type of toxoplasmosis affects the eye's retina and usually occurs when a local tissue cyst reactivates within the retinal region. The latent tissue cysts re-activate into tachyzoites in eye tissues. Common symptoms include blurred vision and the appearance of floating bodies at the posterior region of the eye. Ocular toxoplasmosis was initially thought to be a consequence of congenital toxoplasmosis. However, recent advances in the field have demonstrated that this

specific form of parasitic infection can be acquired post birth as well (Montoya & Liesenfeld, 2004).

affects immunocompromised individuals in rare cases and can lead to severe pneumonia which can be deadly in merely a few days (Rabaud et al., 1996). This is a result of the re-activation of latent tissue cysts containing the bradyzoite form into tachyzoites. In addition, a fulminant pneumonia can also develop as a result of acute toxoplasmosis and is considered as a severe disseminated systemic disease termed 'Amazonian toxoplasmosis' (Demar et al., 2012).

3.3 Toxoplasmosis Diagnosis
The development of the serological test allowed for great advancements in studying the world-wide prevalence of the toxoplasmosis disease and is characterized by sensitivity and specificity.

Since the clinical symptoms of infection with the *T. gondii* parasite are non-specific, medical doctors have relied on other methods to diagnose this parasitic disease. Traditional diagnosis of toxoplasmosis includes bioassays and serological tests. The gold standard procedure for *T. gondii* infection detection is by isolation of *T. gondii* by using laboratory animals. The specimens used for parasite isolation include secretions, excretions, lymph nodes, muscle, and brain tissues (Aubert et al., 2010; J. P. Dubey et al., 2013). INF-γ knock-out mice ensure higher success rates of *T. gondii* isolation since these mice are extremely sensitive to infection with the parasite. However, the bioassay remains an overall costly and time-consuming detection method and can take up to six weeks (Q. Liu et al., 2015).

Alternatively, a variety of serological tests exist such as the dye test (DT) first developed by Sabin and Feldman and is considered the gold standard for *T. gondii* infection detection in human individuals. The modified agglutination test (MAT) is known to be utilized in epidemiological studies. The enzyme-linked immunosorbent assays (ELISA), has the advantage of testing a large sample number using a single ELISA plate. The immunosorbent agglutination assay (ISAGA) necessitates great numbers of tachyzoites. There are also two other assays, indirect fluorescent antibody test (IFAT) and indirect hemagglutination assays (IHA), in addition to several others. These serological tests have the ability to detect various antigens. IgM antibodies can be detected in an infected individual around 1 week after infection, these antibodies are able to remain for several months or years. Detection of IgA antibodies allow for the determination of acute infection whereas IgE antibodies can determine current infection but are only present for a short period. Infection by *T. gondii* is confirmed by the presence of IgG antibodies, however, it does not convey any information regarding the timing of its occurrence (Q. Liu et al., 2015).

Traditional diagnostic methods are limiting in the case of prenatal toxoplasmosis diagnosis and immunocompromised patients. Therefore, molecular approaches in detecting *T. gondii* infection are relied upon in addition to the traditional serological test. The most prominent molecular detection method being PCR which allows for amplification of DNA from a minimal quantity of initial material. Increased sensitivity of PCR is achieved by using many multicopy targeting genes for *T. gondii* detection. These targeting genes include genes such as the B1 gene

and ITS-1 (internal transcribed spacer or 18S rDNA sequences). Single copy genes have also been used to detect *T. gondii* and include SAG1, SAG2, and GRA1 (Q. Liu et al., 2015).

3.4 Treatments and vaccine

Despite the several gaps that have been filled in toxoplasmosis diagnosis, epidemiology, and *T. gondii* parasite-cell interaction, only a few advances have been established in the field of toxoplasmosis treatment. Globally, CT still remains a burden with 1.2 million disability-adjusted life-years (DALY) corresponding to 190,000 cases annually (Torgerson & Mastroiacovo, 2013). Furthermore, HIV-associated toxoplasmosis remains a burden in countries with low-income where antiretroviral therapy is not available with an estimate of 87% of the 13 million HIV-infected people that are Toxoplasma seropositive, and at an elevated risk of developing cerebral toxoplasmosis, residing in the sub-Saharan African region (Z.-D. Wang et al., 2017).

Treatment options for toxoplasmosis remain limited and are usually administered in the case of CT or HIV-infected individuals. The main pathway that is targeted by anti-*Toxoplasma* drugs is the folate pathway. There are two main enzymes that are specifically targeted in this pathway: dihydrofolate reductase (DHFR) enzyme and dihydropteroate synthetase (DHPS) enzyme. The two major drugs that are used against the DHFR enzyme are pyrimethamine (PYR) and trimethoprime (TMP). However, the most prominent drawback of these drugs is that they are not able to differentiate between the DHFR enzyme of the parasite and that of the human host cell and need to be taken by patients in association with sulphonamides that block DHPS and only have an effect against toxoplasmosis during the acute phase of infection. One of the major side effects of the current treatments used against toxoplasmosis is myelotoxicity which consists of a lack of leukocytes, erythrocytes, and blood platelets. This creates a major concern in the case of immunocompromised patients and is extremely life-threatening. Furthermore, there are no drugs available that target the latent form of the disease; the *T. gondii* tissue cysts. The search for potent novel drug candidates that is effective and safe in a wide range of patients and can act against both forms of Toxoplasma (tachyzoite and bradyzoite) is an ideal future perspective and remains an important concern in the field of Toxoplasmosis (Konstantinovic et al., 2019). Aspects of protection against toxoplasmosis are also being studied and several vaccination trials against toxoplasmosis have been carried out yet resulting in only partial protection against the infection (Rezaei et al., 2019). Furthermore, there is a single approved vaccine 'TOXOVAX' that is only valid for veterinary use and consists of live attenuated parasite of the S48 *T. gondii* strain (Buxton, 1993).

4 Ultrastructure of *Toxoplasma gondii*

The tachyzoite remains to be the most substantially studied stage in the life cycle of *T. gondii*. This is due to the ease of obtaining large numbers of tachyzoites *in vitro* and *in vivo*. The tachyzoite is characterized by a crescent shape and has dimensions of approximately 2 x 7 µm. The anterior apical end of

the parasite which defines the direction of motility is slightly pointed compared to the posterior basal end.

4.1 Toxoplasma gondii tachyzoite ultrastructure

The tachyzoite is made up of a unique cytoskeleton (composed of subpellicular microtubules and the conoid), secretory organelles (including the rhoptries, micronemes and dense granules), organelles of endosymbiotic origin such as the mitochondrion and the apicoplast. In addition to conventional eukaryotic organelles (for example the nucleus, endoplasmic reticulum, Golgi, and ribosomes). All the previously mentioned components of the *T. gondii* tachyzoite are enclosed within a complex structure known as the cortical cytoskeleton (Black & Boothroyd, 2000) (Figure 4).

A

B
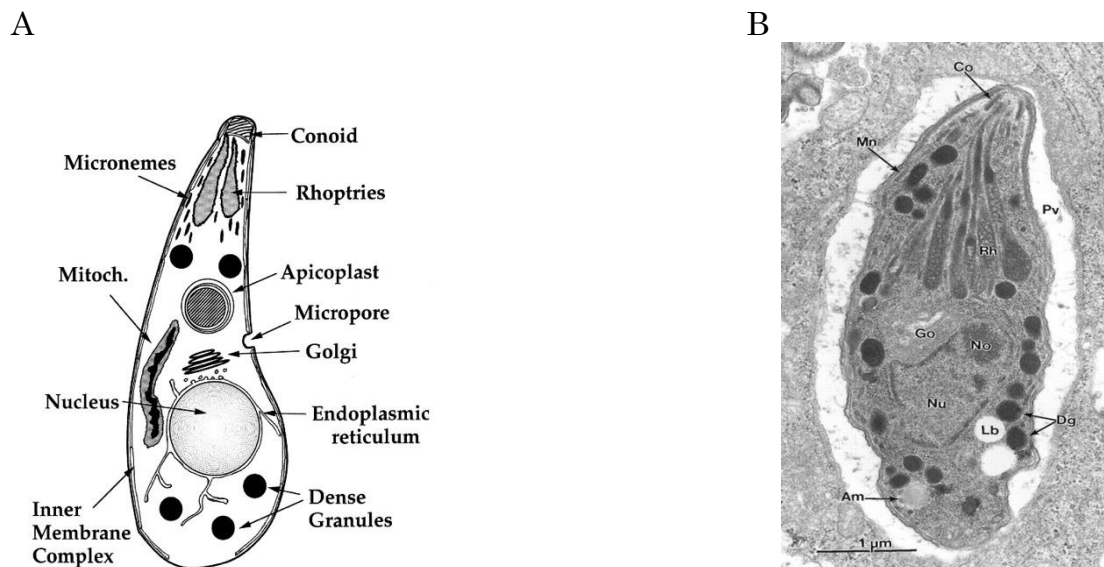
Figure 4 - Ultrastructure of *T. gondii* tachyzoite (Black & Boothroyd, 2000; J. P. Dubey et al., 1998). **(A)** Schematic representation of *T. gondii* tachyzoite including the subcellular components within this parasitic form. **(B)** Transmission electron micrograph scan of a tachyzoite of VEG *T. gondii* strain. Amylopectin granules are abbreviated as **Am**. The conoid is represented by **Co**. The Golgi complex is represented by **Go**. Dense granules are represented by **Dg**. Micronemes are represented by **Mn**. The nucleolus is represented by **No** and the nucleus by **Nu**. **PV** stands for parasitophorous vacuole and **Rh** stands for rhoptries.

4.1.1. *Toxoplasma gondii* cytoskeleton

The cortical *Toxoplasma* cytoskeleton is composed of the microtubular network enclosed within a complex and layered structure comprised of the plasma membrane and the inner membrane complex (IMC) known as the pellicle.

Plasma membrane

The plasma membrane comprises of a lipid bilayer that is enriched with glycosyl-phosphatidylinositol (GPI) clusters (Nagel & Boothroyd, 1989;Tomavo et al.,

1989). GPI proteins allow for the anchorage of *T. gondii* characteristic surface proteins and play a role in host cell adhesion and evasion of the host's immune response (Lekutis et al., 2001; Mineo & Kasper, 1994; He et al., 2002). Surface antigen (SAG) proteins are known to coat the surface of the parasite (G. Couvreur et al., 1988). *Tg*SAG1 (P30) is the most abundant antigen found on the surface of the tachyzoite within the plasma membrane and belongs to the SRS (SAG1 related sequence) family (Lekutis et al., 2001; Manger et al., 1998). Recent studies utilizing single-cell RNA sequencing (scRNA-seq) of asynchronous populations demonstrated that SRS gene expression is dependent on the cell cycle as well as the stage of the parasite's life cycle (Waldman et al., 2020; Xue et al., 2020). Furthermore, around 50% of the SRS genes of the *T. gondii* genome (111 SRS genes in genome) have a significantly increased expression during the entero-epithelial stage of the definitive host (cat) in merozoites whereas only about 10% of SRS genes are expressed in the tachyzoite form (Behnke et al., 2014; Hehl et al., 2015).

Inner Membrane Complex (IMC)

The Inner Membrane complex (IMC) consists of a double membrane system situated 15nm beneath the plasma membrane. The IMC spans longitudinally along the length of the parasite and has openings at each end of the parasite, one at the apical end (conoid level), the other at the posterior end (basal end). An opening is also present at the micropore level which is situated in the apical half of the parasite and consists of an invagination of the membrane and most likely has a role in endocytosis (Nichols et al., 1994). The membranous structures of the IMC are made up of flattened vesicles termed alveoli which are Golgi-associated and give rise to membranous sheets enveloping the parasite (Morrissette et al., 1997). The alveoli are a unique feature of the Alveolata, which is a superphylum made of ciliates, dinoflagellates, and apicomplexans (Keeling et al., 2005). The subpellicular network (SPN) consists of an underlying protein mesh which comprises of 8-10 nm wide filaments. These filaments contain intermediate filament-like (IF-like) proteins which align along the cytoplasmic edge of the alveoli and coat the subpellicular microtubules and are termed alveolins (Gould et al., 2008; Mann, 2001; Porchet & Torpier, 1977).

The IMC consisting of the alveoli and associated cytoskeletal proteins provide structure to cells, are responsible for daughter parasite scaffold formation as well as have a role in glideosome-associated motility (Mann, 2001; Gaskins et al., 2004). The double membranes of the alveoli contain intramembranous particles (IMPs) which interact with the microtubules in order to provide further stabilization to the cytoskeleton (Morrissette & Sibley, 2002; Morrissette et al., 1997).

The IMC initiates exactly below the apex of the parasite which is limited by the plasma membrane only. Below the apical tip, the flattened IMC sacs spiral around the parasite body in a similar manner to the underlying microtubules and are organized as three rows of joined rectangular membrane plates which are sutured together by suture proteins. The suture proteins are responsible for bridging transverse segments or connecting individual plates by association with both their longitudinal and lateral boundaries (A. L. Chen et al., 2015, 2017; Lentini et al., 2015; Tilley et al., 2014). The flattened IMC sacs are capped with an alveolar plate

at the apical tip of the parasite (Porchet & Torpier, 1977) which is composed of a single IMC compartment characterized by a ring shape and consists of an IMC sub-compartment protein, TgISP1 in addition to nine apical complex proteins (Beck et al., 2010; A. L. Chen et al., 2015, 2017; Fung et al., 2012). The central IMC compartment includes TgISP2 and TgISP4 (Beck et al., 2010; Fung et al., 2012). In addition to this, the central compartment also includes TgISP3. However, TgISP3 is shared with the basal IMC compartment as well (Beck et al., 2010). Targeting of TgISP1, TgISP2, and TgISP3 to their associated IMC compartments requires coordinated myristoylation and palmitoylation (Beck et al., 2010). Alternatively, targeting of TgISP4 exclusively necessitates palmitoylation rather than myristoylation (Fung et al., 2012). Parasite mutants lacking in TgISP2 exhibited severe defects in daughter cell formation (Beck et al., 2010). However, loss of TgISP4 did not lead to any major replicative or growth impairments (Fung et al., 2012).

The apical IMC plate is connected to the central and basal plates by a number of proteins termed 'IMC suture components' (ISCs) localized at the lateral and longitudinal boundaries of the plates (Chen et al., 2015, 2017). To date, TgISC1, TgISC2, TgISC3, TgISC4, TgISC5, and TgISC6 have been identified. Among these proteins, TgISC1, TgISC4, and TgISC5 are detergent insoluble and embedded within the IMC filamentous network (Chen et al., 2015, 2017). By carrying out BLAST analyses, it was demonstrated that TgISC1, TgISC2, and TgISC4 are devoid of any known functional domains. However, TgISC3 is similar to choline transporter-like proteins therefore suggesting a possible role in the formation of IMC membranes (Chen et al., 2015; Michel et al., 2016). In addition, there is a specific set of proteins which are exclusively localized at the transverse IMC sutures and not the longitudinal sutures and are designated 'Transverse Suture Components' (TSCs) (Chen et al., 2017). There exists a total of six TSCs designated TgTSC1-6. Mutant parasites where TgTSC1 (also termed as TgCBAP and TgSIP) is disrupted are shorter compared to the wild-type parasites and demonstrate defects in gliding motility, invasion impairment, and decreased infectivity *in vivo* (Chen et al., 2017; Gaelle Lentini et al., 2015; Tilley et al., 2014). Three TSC proteins are insoluble when detergent-extracted : TgTSC2, TgTSC3, and TgTSC4 (Chen et al., 2017).

The IMC sutures are also known to be residence to a total of seven apical annuli proteins (AAPs) of which 5 consist of coiled-coil regions suggesting functions associated with structure (Engelberg et al., 2020). These TgAAPs are embedded within the junctions between the lateral IMC plates located at the apical end of the parasite and the apical IMC compartment. In addition, super-resolution microscopy (SR-SIM) demonstrated that the AAP proteins are organized into concentric rings 200-400 nm in diameter (Engelberg et al., 2020). TgCentrin2 localizes at the intermediate annuli ring and apical annuli methyltransferase AAMT is present on the annuli exclusively in intracellular parasites (Engelberg et al., 2020; Hu et al., 2006; Suvorova et al., 2015). Mutant knock-out parasites of TgAAP4 had a significantly slower proliferation rate compared to that of the parental strain. Normal proliferation was restored when the knock-out strain was

complemented with *AAP4* gene. Furthermore, *in vivo* experiments demonstrated that mice infected with TgAAP4 knock-out strain were able to survive acute infection for one more additional day compared to the mice infected with wild type strain (Engelberg et al., 2020). Phylogenetic analysis of AAPs demonstrated that AAPs are conserved across Coccidia dividing by means of internal budding suggesting a potential role of AAPs in the internal budding process Furthermore, AAPs possess a pore-like structure suggesting roles in signaling and material exchange across the IMC membranes (Engelberg et al., 2020).

To date, there have been 30 proteins dubbed IMC proteins based on their localization to the IMC compartment. There are several subtypes of IMC proteins which can either be integral or peripheral membrane proteins, members of the alveolin cytoskeleton, or proteins localized to the IMC that are not designated as IMC proteins but have distinguished names such as TgPhIL1, TgILP1, and TgMSC1b (Morrissette & Gubbels, 2020). Currently, there is no standard categorization organizing the different IMC proteins. However, it would be of use to assign specific names reflecting the particular subcategories which include the alveolins, cytoskeletal proteins embedded within the IMC network, and proteins anchored to the IMC sacs that are detergent soluble (Morrissette & Gubbels, 2020).

The first 15 IMC proteins are intermediate filament-like alveolin proteins with the exception of TgIMC2 which consists of an N-terminal transmembrane domain (Mann, 2001). Recent studies have identified novel IMC proteins which are non-alveolin and are designated as IMC proteins 16-29 (Butler et al., 2014; Chen et al., 2015, 2017). These proteins are targeted to the central and basal sub-compartments of the IMC save for TgIMC28 which is targeted to all 3 sub-compartments (apical sub-compartment included) (Chen et al., 2017). Among the non-alveolin IMC proteins, there are those that are suggested to being membrane cytoskeletal constituents due to their characteristic detergent-insoluble nature. This subset of IMC proteins comprises of TgIMC16, TgIMC17, TgIMC21, and TgIMC25. Some IMC proteins are localized to both mature and nascent developing buds such as TgIMC19, TgIMC21, and TgIMC25. Some are exclusively specific to mature parasites such as TgIMC17, TgIMC18, and TgIMC20 while others are specific to the developing daughter buds and consist of TgIMC16 and TgIMC29 (Chen et al., 2015, 2017).

The 14 alveolin IMC proteins provide the parasite with pellicle tensile strength and are characterized by the presence of conserved repeats "EKIVEVP", "EVVR", or "VPV" sub-repeats within domains rich in valine and proline residues (Gould et al., 2008; Mann, 2001). These alveolin proteins are localized to the mother and daughter cytoskeletons. TgIMC1 and TgIMC4 are characterized by equal distribution between the mother and nascent daughter IMCs whereas TgIMC3, TgIMC6, and TgIMC10 are heavily localized to the forming daughters. TgIMC3, TgIMC6, and TgIMC10 disappear once the daughter parasites mature (Anderson-White et al., 2011). TgIMC7, TgIMC12, and TgIMC14 are solely localized to the mature parasite's cortical cytoskeleton specifically during the G1 phase of the cell cycle, these proteins are not found on the developing daughter cells (Anderson-White et al., 2011). These three IMC proteins have an important role in controlling

mature and daughter parasite structural stability. TgIMC11 localizes to the apical and basal poles of the parasite (Anderson-White et al., 2011). In the middle of the process entailing daughter parasite formation, TgIMC5, TgIMC8, TgIMC9, and TgIMC13 are targeted from the developing daughter buds towards the basal complex of the daughter parasites. TgIMC15 is involved in the initiation of daughter parasite budding and is associated with centrosome replication (Anderson-White et al., 2011). TgIMC14 and TgIMC15 ensure a single round of nuclear division is carried out since the absence of either of these proteins triggers the production of multiple buds within the mother parasite per round of division and therefore TgIMC14 and TgIMC15 can be considered as proteins influencing the development decision to either divide by endodyogeny or endopolygeny (Dubey et al., 2017). The assembly of IMCs in daughter parasites follows a sequential order. After TgIMC15 is recruited to the daughter parasite cytoskeletons, this is followed by the recruitment of other IMC proteins in the following order: TgIMC1, TgIMC3, TgIMC4, TgIMC5, TgIMC6, TgIMC8, TgIMC9, TgIMC10, and TgIMC13 (Anderson-White et al., 2011). A recent study demonstrated that TgIMC32 is a conserved protein across the Apicomplexa phylum which is essential for the survival of the parasite (Torres et al., 2021). IMC32 localizes at the IMC's body portion and is deposited on the nascent daughter buds early during the internal budding process. Mutant parasites where IMC32 is conditionally depleted exhibit a collapsed IMC (Torres et al., 2021)..

In addition to its main role in the formation of daughter parasites during endodyogeny, the IMC also has essential functions in the motility and invasion of the parasite. These motility characteristics of the IMC are shared across Apicomplexan members. For the parasites to move forward, a myosin motor tethered to the outer membrane of the IMC must pull the actin filaments which are situated between the plasma membrane and the IMC and their associated adhesins rearward. During this process, it is crucial that the IMC-anchored myosins in association with glideosome associated proteins (GAP) remain intact and fixed to the IMC most likely by interactions connecting the glideosome motor to the cytoskeleton laying beneath. Subpellicular microtubules and the alveolin network are key to achieving IMC stability which is important for the resistance of IMC myosin displacement (Johnson et al., 2007).

GAPM (gildeosome associated proteins with transmembrane domain) link the IMC alveoli to the cortical cytoskeleton (Harding et al., 2019). Proteins which belong to the GAPM family are extremely conserved and Apicomplexa-specific. Phylogenetic analysis revealed that members of the GAPM family belong to one of the following orthologous groups: GAPM1, GAPM2, and GAPM3 (Bullen et al., 2009). GAPM proteins are six-pass transmembrane proteins which are localized to the IMC of both mature and nascent parasites and are characterized by their SDS-resistant nature (Harding et al., 2019; Bullen et al., 2009).

GAPM1a, GAPM2a, and GAPM3 are expressed abundantly within the tachyzoite form. However, GAPM1b and GAPM2b are expressed at a relatively lower level (Harding et al., 2019). Based on CRISPR genome-wide screens, loss of GAPM1a, GAPM2a, and GAPM3 decreases *in vitro* fitness of the tachyzoite. GAPM1b and GAPM2b do not have much of an effect on *in vitro* fitness and are most likely dispensable (Sidik et al., 2016). Mutant parasites conditionally depleted of

TgGAPM1a displayed a severe defect in replication. In addition, the conditional loss of TgGAPM1a resulted in impaired organisation of cortical microtubules followed by their disassembly leading to morphological changes to the tachyzoite rendering it rounder and shorter (Harding et al., 2019).

Inner membranous particles (IMPs) are present at the surface of the IMC and are arranged in longitudinal spiraling rows organized with a 32 nm periodicity, reflecting the periodicity of the subpellicular microtubules of the underlying cytoskeleton (Morrissette et al., 1997). It has been suggested that the tethering of the alveolar membrane to the cytoskeleton is most likely not achieved by the direct interaction of GAPM proteins with the cytoskeleton microtubules but rather microtubule associated proteins (MAPS) which decorate the cytoskeleton microtubules, IMPs and linkers that bridge the space between the microtubules and the IMC membrane are suggested to have a role in mediating this connection. (Harding et al., 2019).

Despite the studies that have been carried out so far regarding IMC proteins, several of these proteins remain unstudied and thus the complete IMC proteome remains uncharacterized. Therefore, a novel technique based on the application of the spatial proteomic method hyperplexed localization of organelle proteins by isotope tagging (hyperLOPIT) resulted in identifying the location of thousands of proteins in the parasite including those associated with specific parasite compartments among them the IMC (Barylyuk et al., 2020).

The study utilizing the hyperLOPIT method allowed for the identification of a total of 81 IMC proteins including previously characterized and verified IMC proteins (38 IMC proteins) as well as newly assigned IMC protein predictions (43 IMC proteins) thus expanding the IMC proteome (Barylyuk et al., 2020). In addition, this study provided knowledge regarding the physical association of *T. gondii* proteins and sub-compartments with each other. Insights into the IMC sub-compartment associations indicated that the IMC as a definitive complex component of the pellicle resolves into a total of four hyperLOPIT clusters; a major IMC cluster which resolved separately from that of the PM, two apical IMC clusters; apical 1 and apical 2, and a microtubule-associated proteins (MAPs) cluster (Barylyuk et al., 2020). The study additionally provided information regarding the strength of attachment of the IMC's different entities. Since the known apical cap and apical annuli proteins located at the posterior boundary resolved separately from the remaining IMC proteins, this suggested that the posterior boundary is disassociated and that the association of the apical annuli to the IMC alveoli is weaker than the association of the apical annuli to the apical cap (Barylyuk et al., 2020).

Overall, the IMC has many integral functions in *T. gondii*. It is implicated in maintaining the tachyzoite's structural integrity, several IMC proteins are essential for providing tensile strength for the parasite (R. Dubey et al., 2017). The IMC has additional key roles in replication, motility, and invasion (Beck et al., 2010; R. Dubey et al., 2017). Furthermore, it is a highly dynamic compartment

and is disassembled and re-built during cell division (Harding & Frischknecht, 2020; Ouologuem & Roos, 2014).

Microtubule network

The microtubule network is a component of the *T. gondii* cytoskeleton. Microtubules are important components of various structures that are used throughout the parasite's life cycle. *T. gondii*'s microtubule cytoskeleton morphology is highly conserved throughout the "four" zoite stages (tachyzoites, bradyzoites, merozoites, and sporozoites). Similar to other eukaryotes, spindle microtubules are a crucial element for chromosome segregation during cell division. Membrane-associated microtubules give rise to the elongated appearance of the invasive forms of the parasite. In addition, microtubules have a role in the spiral trajectory pathway that *T. gondii* has due to its unique motility (Morrissette, 2015).

There is a total of 22 microtubules situated within the subpellicular region of the *T. gondii* tachyzoite. A microtubule organizing center (MTOC) anchors the negative ends of the microtubules, this region is also known as the apical polar ring (APR). Growth of the microtubules starts from the apical end of the parasite in the direction of the posterior end. The positive ends of the microtubules remain in a condition of hindered depolymerization (Anderson-White et al., 2012).

T. gondii microtubules are very stable compared to those in other eukaryotes and this is due to microtubule-associated proteins (MAPs) which connect the microtubules to the pellicle such as subpellicular microtubule protein 1 (SPM1) (Tran et al., 2012). MAPs allow the microtubules to coordinate crucial roles in mitosis and meiosis, motility, and cytoplasmic structure. Microtubules are polymers composed of α-β-tubulin heterodimers. There are five type of structures containing tubulin within *T. gondii*: spindle microtubules, centrioles, subpellicular microtubules (SPMTs), the conoid, and intraconoid microtubules (Figure 5B).
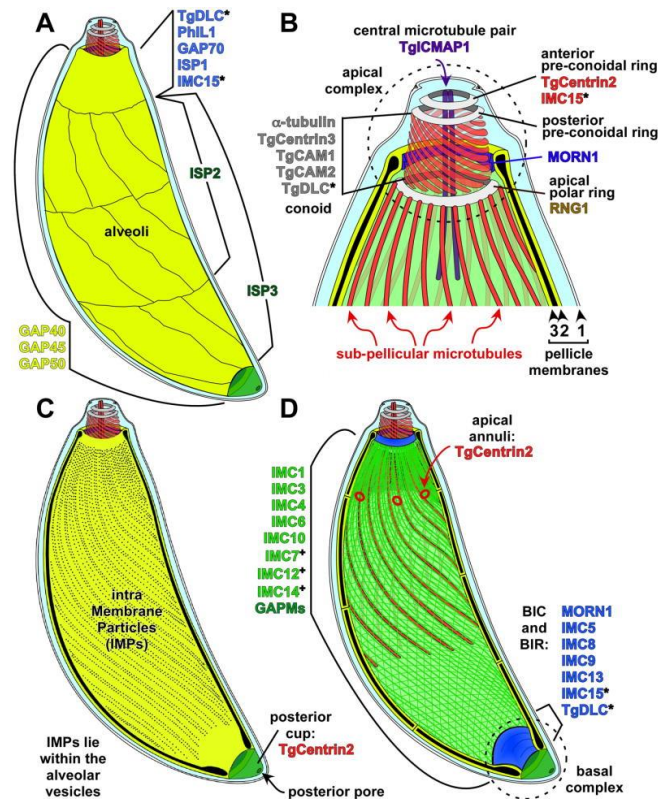
Figure 5- Schematic representation of the *T. gondii* cytoskeleton- (Anderson-White et al., 2012). A. Representation of the alveolar vesicles that are situated directly under the plasma membrane are represented in yellow. The top-most alveolar vesicle termed the apical cap is structured in the form of a cone at the apical tip of the parasite. The three rectangular-shaped vesicles occupy the IMC. **B.** Representation of the apical complex structure and the associated apical complex proteins (MORN1, RNG1, TgCentrin2, IMC15). **C.** Representation of the Intra-Membrane Particles (IMPs) localized within the alveolar vesicles. **D.** Representation of the IMC protein network including associated IMC proteins as well as proteins localised to both sides of the alveoli. Proteins that are indicated with an asterisk (*) represent proteins which are present in various regions. Proteins that are present only in mature daughter parasites are indicated with a (+) symbol.

The apical complex

The Apicomplexa phylum name is based on the apical complex region present within its members. The apical complex region contains specialized organelles that orchestrate parasite-host interactions. These organelles are apical secretory organelles consisting of micronemes and rhoptries which carry out key roles for parasite motility, invasion, and parasitophorous vacuole formation (Frénal, Dubremetz et al., 2017). Members of the Gregarine and Coccidian subgroups of the Apicomplexa phylum possess an additional apical structure named the conoid (Leander & Keeling, 2003).

The apical complex is comprised of three main structural components: 1) the apical cap which is the most apical part of the IMC. In *T. gondii*, the apical cap is characterized by a single conical shaped alveolar plate and is delimited at its base

by several annuli structures dubbed 'apical annuli'. 2) the conoid which is situated within the apical polar ring (APR) and 3) rhoptries and micronemes, the secretory organelles, that secrete their contents to ensure the dissemination of the parasite (reviewed in Dos Santos Pacheco et al., 2020). Furthermore, the apical complex consists of three main tubulin-based components: 1) the pre-conoidal rings located at the most distant tip of the conoid and from which the fibers of the conoid originate. 2) the polar ring from which the 22 subpellicular microtubule (SPMTs) fibers originate and 3) two short intraconoidal microtubule fibers (Hu et al., 2006). In addition to the apical complex's main role in invasion, regulated secretion from the apical complex is responsible for providing factors which are critical for the formation of the parasitophorous vacuole (Carruthers & Sibley, 1997). The apical complex in addition to daughter conoids is the first structure to emerge during daughter cell formation and represents a focal point for the building of the daughter parasites.

The apical cap is characterized by several proteins among them TgISP1 which is clearly restricted to the apical cap region and is associated with the IMC at the periphery. However, ISP1 is not found embedded in the protein meshwork underlying the IMC (Beck et al., 2010). TgISP1 consists of conserved N-terminal cysteine residues which are critical for targeting TgISP1 to its proper location at the extremity of the apical cap. To determine the functional role of TgISP1, the *ISP1* gene was disrupted. Disruption of the *ISP1* gene did not have a major impact on the growth of the parasite *in vitro*. However, an interesting observation was noted where instead of the mutant parasites exhibiting a loss of TgISP1 at the apical cap, two other closely related ISP proteins, TgISP2 and TgISP3 were localized to the apical cap where TgISP1 should normally be localized (Beck et al., 2010). In addition to TgISP1, the apical cap is home to several apical cap proteins (ACs) which are exclusively restricted to the apical cap region. Proximity-labelling experiments using the BIOID technique allowed for the identification of this novel set of apical proteins. Apical cap protein 1 (TgAC1) and Apical cap protein 2 (TgAC2) were identified by using ISP3 as bait for BIOID proximity labelling. The two identified proteins were found to be localized to different IMC sub-compartments. TgAC1 was found to be associated with the membrane sacs whereas TgAC2 was found to be associated with the cytoskeleton network (Chen et al., 2015). In order to identify additional apical cap proteins in *T. gondii*, another BIOID proximity labelling experiment was carried out using TgAC2 as bait which resulted in the identification of 5 additional AC proteins: TgAC3, TgAC4, TgAC5, TgAC6, and TgAC7. All 5 AC proteins colocalized with TgISP1 in mature and nascent parasites (Chen et al., 2015). In a following study carried out by Chen et al. (2017), two additional AC proteins were identified by using proximity labelling. However, this time, ISC4, a protein localized within the sutures at the very base of the apical IMC plate was used as bait. TgAC8 and TgAC9 were identified and verified by immunofluorescence to localize to the apical cap region (Chen et al., 2017). A tenth AC protein designated TgAC10 has also been identified by using the BIOID technique (Tosetti et al., 2020). TgAC9 and TgAC10 are recruited early on during endodyogeny to the apical caps of the forming daughter parasites even prior to the recruitment of TgISP1. Super-resolution microscopy using the stimulated emission depletion (STED) technique demonstrated that TgAC9 and

TgAC10 belong to the alveolin cytoskeleton and are organized in rows following a regular periodicity. TgAC9 was found to colocalize with TgGAP45 and TgISP1, thus confirming that TgAC9 is localized at the IMC and confined to the sub-pellicular microtubules (SPMTs) side. Furthermore, a newly developed type of electron microscopy termed ultrastructure expansion microscopy (U-ExM) showed that TgAC9 and TgAC10 colocalize between the SPMTs below the conoid and the APR (Tosetti et al., 2020). Mutant parasites that are conditionally depleted of TgAC9 and TgAC10 exhibit extreme defects in microneme secretion, invasion, and egress. In addition, these mutant parasites harbor severe morphological defects of the apical complex region and are devoid of the conoid and the APR. This loss occurs at the final stage of the division process and/or during the emergence of the daughter parasites from the mother cell (Tosetti et al., 2020). Furthermore, by using U-ExM microscopy, parasites depleted of TgAC9 and TgAC10 exhibited SPMTs that are significantly disorganized (Tosetti et al., 2020). TgAC9 was demonstrated to form a complex with TgERK7 (extracellular signal-regulated kinase 7), a conserved mitogen activated protein kinase (MAPK) (Back et al., 2020). TgERK7 was found to be essential for proper conoid formation (O'Shaughnessy et al., 2020) and its localization at the apical cap region requires TgAC9. TgERK7 interacts with TgAC9 by means of its C terminus where the C-terminus of TgAC9 is inserted into the active site of TgERK7 leading to its subsequent inhibition (Back et al., 2020).

Furthermore, two other proteins were demonstrated to localize within the apical cap region, TgPhIL and TgIMC11. TgPhIL is a cytoskeletal IMC protein which colocalizes with TgIMC11 (Gilk et al., 2006; Anderson-White et al., 2011). In an attempt to functionally characterize TgPhIL, a mutant strain in which the *TgPhIL* gene was disrupted by homologous recombination, was produced. The morphology of mutant TgPhIL knock-out parasites was altered and resulted in mutant parasites which were shorter and wider compared to the wildtype parasites. In addition, mutant parasites depleted of TgPhIL demonstrated a growth defect *in vitro* and reduced fitness *in vivo* (Barkhuff et al., 2011).

The apical complex in *T. gondii* is constructed around the conoid. This structure is characterized by its motile activity during the invasion process. The conoid is 380 nm wide in diameter and is comprised of 10-14 filaments which are~430 nm long. These filaments are arranged in a left-handed spiral pattern and structured to resemble a funnel shape (Hu et al., 2002; Nichols & Chiappino, 1987; Morrissette et al., 1997). The conoid is characterized by the arrangement of its α-tubulin microtubule filaments into a spiral similar to a compacted spring. The anterior face of the conoid has two pre-conoidal rings. The α-tubulin filaments of the conoid link the apical polar ring (APR) to the pre-conoidal rings (Anderson-White et al., 2012; Hu et al., 2002; Swedlow et al., 2002). Within the conoid, two intraconoidal microtubules are present and have a role in secretion of proteins from the apical region of the parasite during invasion of the host cell (Figure 5).

The extrusion and retraction of the conoid is apparent during invasion of the host cells. This specific conoid movement can be initiated in extracellular tachyzoites by pharmacologically increasing Ca^{2+} ion concentrations intracellularly (Del

Carmen et al., 2009). The conoid is characterized by the presence of apicortin/doublecortin protein referred to as DCX, which contains two domains that bind tubulin,(Nagayasu et al., 2017) P25-α and DCX (Orosz, 2009). TgDCX localizes solely to the conoid and has an important role in the stability of the conoid and the overall fitness of the parasite (Nagayasu et al., 2017). The loss of TgDCX results in morphological defects of the conoid structure hence it becomes shorter and disordered and subsequently leads to a defect in host cell invasion (Nagayasu et al., 2017). TgDCX has the striking ability to stabilize the curvature of the microtubules forming the conoid to support effective host cell invasion (Leung et al., 2020). The conoid consists of several proteins which are implicated in parasite motility such as TgMyoH which interacts with myosin light chain proteins (MLCs) such as TgMLC3, TgMLC5, and TgMLC7 (Graindorge et al., 2016). In addition, TgMyoH most likely interacts with calmodulin-like proteins designated TgCAM1, TgCAM2, and TgCAM3 present within the conoid and likely regulate the activity of MyoH in a calcium-dependent manner (Long et al., 2017).

On top of the conoid are the two pre-conoidal rings (PCRs). The specific function of these two rings remains to be elucidated. Dynein light chain 8a (DLC8a) is localized within the apical complex region when expressed as a second copy localizing at the apical polar ring, the conoid, spindle poles, the centrosome and basal ring (Hu et al., 2006). However, other studies in which TgDLC8a is C-terminally tagged demonstrated that TgDLC8a localizes exclusively to the apical cap (Qureshi et al., 2013). An even more recent study exhibited that TgDLC8a localizes to the parasite's centrosome and the apical cap but is more strongly concentrated at the APR (Lentini et al., 2019). DLC8a has been suggested to be essential for the tachyzoite's lytic cycle based on the genome wide CRISPR screen carried out by Sidik et al (2016). In an attempt to functionally characterize the role of TgDLC8a, a mutant cell-line in which TgDLC8a is depleted was generated. The depletion of TgDLC8a has a major impact on invasion and microneme secretion yet does not as strongly affect the parasite's motility, attachment, and egress from host cells (Lentini et al., 2019). Furthermore, depletion of TgDLC8a affects rhoptry positioning impacting rhoptry discharge which is important for proper invasion of the host cell (Lentini et al., 2019).

TgCentrin2, a calcium-binding protein localizes to the anterior of the preconoidal rings at the extremity of the apex of the *T. gondii* parasite. TgCentrin2 can also be found in the annuli present at the apical region's posterior edge and is also found within the basal complex and the centrioles (Hu et al., 2006; Lentini et al., 2019; Leung et al., 2019). TgCentrin2 is essential for the tachyzoite's lytic cycle (Lentini et al., 2019; Leung et al., 2019). TgCentrin2 depleted parasites demonstrated defects in motility, adhesion, invasion, and egress. The ability of TgCentrin2 depleted parasites to secrete micronemes was drastically affected. However, the overall morphology and positioning of micronemes and rhoptries remained unaffected (Lentini et al., 2019). In addition, TgCentrin2 has an essential role in maintaining the architecture of the peripheral annuli. In mutant parasites conditionally depleted of TgCentrin2, around 70% of mutant parasites demonstrated a faint peripheral annuli protein 2 (TgPAP2) signal, unproper PAP2 localization, or a significantly decreased number of parasites possessing PAP2 at

annuli compared to their wildtype counterparts (Lentini et al., 2019). These results were confirmed by a similar study carried out by Leung et al. (2019) in which TgCentrin2 was depleted and indicated the essentiality of TgCentrin2 in lytic cycle stages and microneme exocytosis. TgCentrin2 present within the centrioles most likely has an important role in regulating parasite replication (Leung et al., 2019).

TgSAS6L is a centriole-associated-like protein which localizes at the PCRs. Mutant parasites devoid of *SAS6L* gene resulted in reduced fitness (Leon et al., 2013). It is most likely that TgSAS6-L plays a role in the tethering of straited fiber assemblins (SFA) to the conoid (Leon et al., 2013).

The apical polar ring (APR) is characterized by the presence of the Ring 1 protein (TgRNG1) which localizes to the APR at the very late stages of daughter parasite formation and is apparent within daughter cells before disassembly of the mother parasite cell (Tran et al., 2010).Unsuccessful attempts to generate a knock-out strain of TgRNG1 suggests its essentiality. Another protein localized at the APR is TgRNG2 which connects the APR to the base of the conoid forming a ring with the amino-terminal associated with the conoid and the carboxy-terminal anchored to the APR (Katris et al., 2014). During the extrusion of the conoid, the orientation of the TgRNG2 proteins terminal ends is flipped as the conoid passes through the APR (Katris et al., 2014). As opposed to TgRNG1, TgRNG2 associates with the apical complex early during endodyogeny. An inducible knock-down mutant of TgRNG2 demonstrated that this protein is crucial for the growth of the parasite. Studying the role of TgRNG2 in maintaining the structure of the tachyzoite demonstrated that TgRNG2 has no obvious role in maintaining pellicle structure. However, TgRNG2 knock-down perturbed parasite motility, invasion, and microneme and rhoptry content secretion (Katris et al., 2014). The membrane occupation and recognition nexus 1 protein (MORN1) is yet another protein localized at the apical end of the alveoli. It also localizes to the spindle pole and the spindles (Gubbels, 2006; Hu, 2008). However, TgMORN1 is more highly concentrated at the basal end of the parasite and has an important role in cytokinesis (Lorestani et al., 2010).

The recent study that utilized the novel hyperLOPIT method identified a total of 63 apical proteins . Among the 63 apical proteins, 41 were already known and 22 were newly identified and predicted to localize to the apical region of the parasite (Barylyuk et al., 2020). The resolved apical proteins included known apical cap proteins, apical annuli proteins, known conoid-associated proteins, APR proteins, and structural apical extremity invasion-associated components (Barylyuk et al., 2020). The apical proteins resolved into two clusters, *apical 1* and *apical 2*. Intriguingly, these two clusters did not demonstrate much of spatial differentiation since both clusters consist of conoid-associated proteins and apical cap proteins (Barylyuk et al., 2020). However, there are biophysical properties which distinguish the two clusters. Apical 1 cluster proteins possess a basic pI (isoelectric point) whereas apical 2 cluster proteins possess an acidic pI (Barylyuk et al., 2020). In a follow-up study of the hyperLOPIT experiments carried out by Barylyuk et al. (2020), another 32 proteins were resolved into the apical clusters

which were not reported in the previous study due to less data support (Koreny et al., 2021). Therefore, the number of putative apical proteins assigned by hyperLOPIT expanded to a total of 95 (Koreny et al., 2021). Among these 95 putative apical proteins, 13 were verified in the previous hyperLOPIT study to be localized at the apex extremity (Barylyuk et al., 2020), 23 were verified to be localized to the same apical extremity, 21 are known to localize to the apical cap or other IMC sub-compartments, leaving 38 novel predicted apical proteins with unverified localization (Koreny et al., 2021). Super-resolution microscopy allowed for the verification of the novel apical proteins localization which were found to be located at the conoid body, the conoid base, and the conoid canopy while others were verified to localize to the APR (Koreny et al., 2021).

To conclude, the conoid represents a signalling hub controlling gliding motility, invasion, and egress. Novel insights into the proteins that make up this structure provide a platform for future studies in order to decipher enigmatic conoid mechanisms. Further identification of apical cap proteins has advanced our understanding of how these proteins contribute to the maintenance and stability of the conoid and APRs. Likewise, APR proteins are linked to the integrity of the conoid.

The proteins of these structures are inter-linked and maintain the integrity of each other (Dos Santos Pacheco et al., 2020).

Furthermore, the apical proteome has become expanded due to the hyperLOPIT technique. However, future studies are still needed to explicitly characterize each newly identified and verified apical protein. Studying each apical protein's potential contribution to the function of the apical region is necessary to decipher still outstanding questions regarding the function of its subcomponents such as conoid protrusion, preconoidal ring function as well as the role of intraconoidal microtubules. These are a few questions of many.

The basal complex

The basal complex is a structure located at the posterior end of the IMC, also termed as the posterior cup (Mann, 2001) and functions as a contractile ring during cytokinesis at the late stages of parasite replication (Blader et al., 2015; Gubbels, White, et al., 2008b; Hu, 2008). The assembly of daughter parasite basal complexes occurs early during endodyogeny prior to the formation of daughter parasite cytoskeleton and IMC and prior to the disruption of the cytoskeleton of the mother parasite (Hu, 2008).

The basal complex is characterized by electron dense structures which are ring-shaped and become apparent during budding at the leading edge of the developing daughter parasites (Anderson-White et al., 2011; Gubbels, 2006;Hammarton, 2019; Hu, 2008). The basal complex was determined to be comprised of two electron-dense structures observed by electron microscopy. The first electron-dense structure is directly tethered to the cytoplasmic edge of the basal pole of the IMC and is termed the basal inner ring (BIR). The second electron dense structure is situated along the length of the basal IMC but is not directly attached to the IMC or the BIR but instead bends towards the plasma membrane, this structure is termed the basal inner collar (BIC). In addition to these two electron dense

structures, the basal complex consists of numerous unit membranes (UM) (Anderson-White et al., 2011).

The basal complex is initially marked by TgMORN1 and forms a ring around the already replicated centrioles (Anderson-White et al., 2012; Hu, 2008). TgMORN1 also co-localizes with TgMyoC and most likely functions in conjunction with this protein to generate the driving force necessary for the constriction of the basal complex (Gubbels, 2006; Hu, 2008). TgMORN1 was also found to localize to the centrocone, a key structure for mitotic spindle organization (Gubbels, 2006; Naumov et al., 2017). The formation of TgMORN1 rings is independent of the cytoskeleton microtubules structural integrity (Gubbels, 2006; Hu, 2008). TgMORN1 is essential for the formation of the basal complex. The loss of the basal complex in TgMORN1 depleted parasites resulted in parasites losing their contractile capacity that should normally occur during the late stages of daughter parasite formation. Hence mutant parasites with ablated TgMORN1 resulted in multiple-headed parasites conjoined at the basal end with a defect in apicoplast segregation (Heaslip et al., 2010; Lorestani et al., 2010).

A following study allowed for the dissection of the MORN1 complex components by using a cellular fractionation method followed by immunoprecipitation and mass spectrometry analysis (Lorestani et al., 2012). Several proteins were identified as components of the TgMORN1 complex among them TgMSC1a which creates a ring around TgIMC5 and TgIMC8. TgMSC1a is unique to the basal complex of mature parasites since it appears in the daughter parasites only at the final steps of endodyogeny as they emerge from the mother parasite. TgMSC1a was found to be soluble when extracted with TX-100 detergent and is therefore associated with the IMC membrane which coincides with the presence of several predicted palmitoylation sites (Lorestani et al., 2012). A second protein termed 14-3-3 was demonstrated to localize to the basal complex of the mature parasites and co-localize with TgMORN1. Localization of Tg14-3-3 is independent of TgMORN1. To date, the specific functions of TgMSC1a and Tg14-3-3 remain to be elucidated (Lorestani et al., 2012).

IMC proteins localize to the basal complex. Such IMC proteins include: TgIMC5, TgIMC8, TgIMC9, TgIMC13, and TgIMC15 (Anderson-White et al., 2011). Additional proteins localize to the basal complex as well such as TgCentrin2, TgHAD2a, TgDLC, TgMyoC, and TgMyoJ (Delbac et al., 2001; Hu, 2008; Lorestani et al., 2010).

TgCentrin2 is incorporated into the basal complex at the final stage of interphase and is localized to a compartment that is more distal compared to the compartment to which TgMORN1 localizes to (Hu, 2008). The recruitment of TgCentrin2 to the basal ends of the daughter parasites before the start of cytokinesis coincides with basal complex constriction. TgCentrin2 contains a calcium-binding EF-hand domain and may contribute to generating basal complex contractile force since artificial Ca^{2+} ion treatment induces daughter parasite TgCentrin2 basal ring constriction (Hu, 2008).

TgMyoJ is present at the basal complex and colocalizes with TgCentrin2 (Frénal, Jacot et al., 2017). Parasites depleted of TgMyoJ exhibited unsuccessful basal complex constriction. In addition, the localization of TgCentrin2 in TgMyoJ depleted parasites is undetectable (Frénal, Jacot et al., 2017). Basal complex constriction is absent in mutant parasites lacking TgMoyJ. Similarly, constriction is unsuccessful in inducible knock down TgCentrin2 parasites. These results suggest that both TgMyoJ and TgCentrin2 are essential for basal complex constriction (Frénal, Jacot et al., 2017). Furthermore, treatment of parasites with cytochalasin D which destabilizes actin hindered localization of TgCentrin2 and constriction of the basal complex (Frénal, Jacot et al., 2017). These findings suggested a role for actin in basal complex assembly and constriction. In order to study the role of actin in *T. gondii*, a conditional knockout strain of TgACT1 was characterized (Periz et al., 2017). *Act1* gene is the only gene that encodes for actin in *T. gondii*. Mutant parasites lacking TgACT1 exhibit aberrant basal complex morphology with a flattened appearence (Periz et al., 2017). By using an actin chromobody, it was confirmed that actin does not form a ring-like structure at the basal end of the developing daughter parasites but rather actin is targeted to the IMC and forms a ring-like structure at the residual body (Periz et al., 2017).

TgHAD2a is an enzyme consisting of a conserved haloacid dehalogenase (HAD) phosphotransferase domain. This enzyme localizes to the developing daughter parasite's cytoskeleton but then transitions towards the basal complex during its contraction. TgHAD2A colocalizes with TgMORN1 at the basal complex. However, TgHAD2A labelling in mutant parasites conditionally depleted of TgMORN1 (Lorestani et al., 2010) demonstrated that HAD2a is localized to the cortex of daughter parasites yet detection of HAD2a at the basal complex is no longer present. Therefore, TgHAD2a localization is not dependent of TgMORN1 yet its targeting to the basal complex necessitates TgMORN1 (Engelberg et al., 2016). TgHAD2a has a role in the assembly of the basal complex since the conditional knockout of TgHAD2a results in conjoined daughter parasites due to impaired basal constriction. Overall, these results suggest that TgHAD2a has an important role in basal complex contractile function (Engelberg et al., 2016).

The basal complex most likely functions in resisting to mechanical stress during invasion (B. Anderson-White et al., 2012) in addition to its key role in constriction during cytokinesis allowing for the splitting of the daughter parasites as they emerge from the mother cell (Hu, 2008).

4.2.2. Specific organelles

The apicoplast (apicomplexan plastid)
The first electron micrographs demonstrated different subcellular organelles in *T. gondii*, some of these organelles appeared conventional and have already been identified in other organisms such as the ER, Golgi, and mitochondria. However, there are certain subcellular structures that have not been identified before and are unique features of Apicomplexans such as the apical complex including its associated structures and the apicoplast.

The apicoplast is a double membrane structure that is most likely to have originated from secondary endosymbiosis of a red alga (Janouskovec et al., 2010; Kohler, 1997; McFadden et al., 1996). Several electron micrographs demonstrate that the *T. gondii* plastid possesses four membranes. A primary endosymbiotic event involving the engulfment of a cyanobacterium by a eukaryote is assumed to have preceded the secondary endosymbiotic event consisting of the engulfment of an alga containing a plastid (Figure 6). The two inner-most membranes are assumed to be the original membranes of the apicoplast. The third membrane is believed to be derived from the algal cell's plasma membrane or from the ER of the ancestor host and is termed the periplastid. The fourth outer-most membrane originates from the endomembrane system of the host. Most apicoplast proteins are encoded by the nucleus and it is therefore necessary that they are imported across the apicoplast's four membranes (Mallo et al., 2018).

The second outermost membrane also termed the periplastid membrane (PPM) houses an endoplasmic reticulum associated degradation (ERAD)-like system in which a major component of this system is the ubiquitin pathway which polyubiquitinates misfolded proteins and is a proteasome degradation signal. The ubiquitin machinery has been re-formulated in order to facilitate the transportation of proteins across the PPM (Sommer et al., 2007).
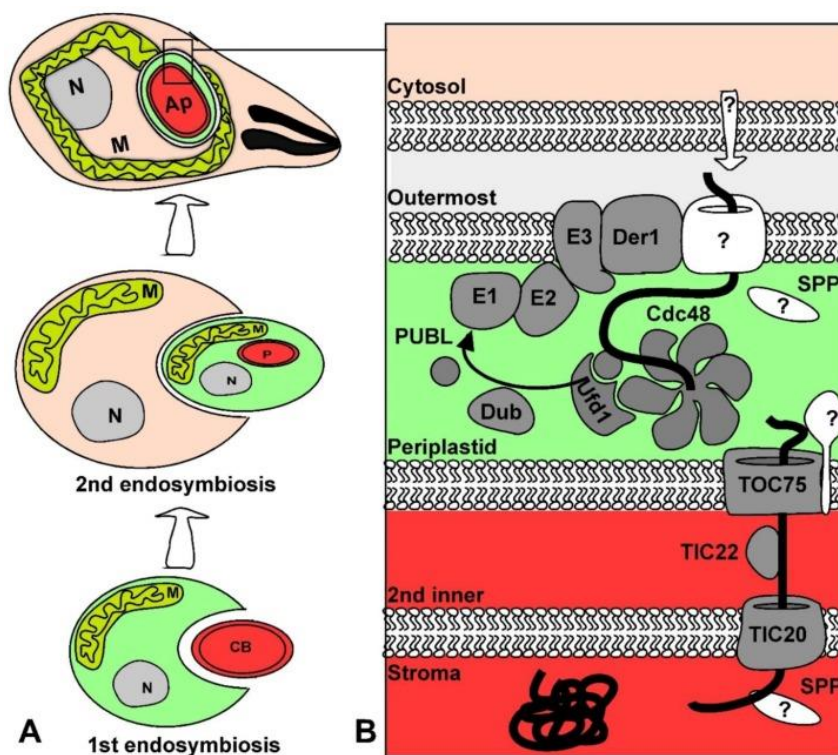
Figure 6- Schematic representation of the history of apicoplast acquisition in *T. gondii* (Mallo et al., 2018). (A) Depiction of the two endosymbiotic events resulting in apicoplast formation. The first endosymbiotic event (bottom), a cyanobacterium represented by CB is engulfed by a eukaryotic cell. During the second endosymbiotic event, the eukaryotic cell engulfs a red alga cell which contains a

primary plastid which then evolves into a secondary apicoplast plastid. **(B)** Schematic representation of the proteins invloved in the import of apicoplast proteins. The direction of protein transportation is indicated by a white arrow starting from the parasite's cytosol passing through the four apicoplast membranes and arriving within the apicoplast stroma. The participants of the endoplasmic reticulum associated degradation (ERAD) and ubiquitination pathways are represented as well.

The genome of the plastid resembles plant and algal chloroplast DNA and comprises of a ~35 kb circular DNA genome. Apicomplexan plastids are non-photosynthetic and their genomes are highly reduced with a great loss of photosynthesis-related genes (Hadariová et al., 2018). Overall, apicomplexan plastid genomes are highly similar in length yet vary in GC content (Cinar et al., 2016). The majority of apicoplast genes code for proteins that are necessary for the expression of the apicoplast genome (Wilson et al., 1996). These genes include genes encoding all tRNAs which are necessary for the synthesis of apicoplast proteins and consist of genes encoding three components of a eubacterial-like RNA polymerase (RPOB, RPOC1, and RPOC2). In addition to 17 ribosomal proteins and Tu, a translation factor of elongation (Wilson et al., 1996).

The apicoplast is an essential organelle for *T. gondii* parasite survival despite losing its photosynthetic properties and houses numerous crucial metabolic pathways such as the production of fatty acids, heme, iron-sulfur clusters, and isoprenoid precursors (Mazumdar et al., 2006; Nair et al., 2011). Isoprenoids are lipid compounds which have many important functions. Isoprenoids allow for cytosolic proteins to interact with membranes of cells (Swiezewska & Danikiewicz, 2005). In addition, isoprenylation is essential for the localization of membranes and the proper function of proteins involved in DNA replication and cell cycle regulation.

Several inhibitors targeting apicoplast biogenesis result in 'delayed death' phenotype. Treatment with inhibitor resulted in parasites which were devoid of apicoplasts or possessed a defective apicoplast. Despite these severe apicoplast defects, the parasite is still able to grow unaffected during the first lytic cycle while treated with the inhibitor. However, during the second lytic cycle, parasite growth is inhibited leading to its death even after removal of the inhibitor. This phenomenon has been observed in several studies. Apicoplast ribosome inhibitors such as clindamycin in addition to inhibitors against DNA gyrase such as ciprofloxacin as well as the actinonin inhibitor targeting the apicoplast membrane metalloprotease, FtsH1 resulted in a delayed death phenotype of the *T. gondii* tachyzoite (Amberg-Johnson et al., 2017; Camps et al., 2002; Fichera et al., 1995;. Fichera & Roos, 1997). Delayed death phenotype was also observed in mutant parasites over-expressing a dominant negative version of TgMyoF-tail (Frénal et al., 2017; Jacot et al., 2013). The deletion of TgMyoJ and TgMyoI in the TgMyoF-tail dominant negative strains resulted in parasite death within the first lytic cycle, thus suggesting that parasite survival during the initial lytic cycle is due to intravacuolar communication (Frénal, Jacot et al., 2017). A recent study

confirmed that the common defect of the delayed death phenotype is the loss of metabolic function of the apicoplast (Amberg-Johnson & Yeh, 2019).

Overall, the essentiality of the plastid for the growth and development of *T. gondii* has made it a very promising drug target (Striepen, 2011).

Micronemes

Micronemes are present in abundance and are clustered mostly at the apical pole of the parasites. These structures are crucial for gliding motility and invasion of the parasite. Micronemes were initially identified by electron microscopy and appear to have a rod-like appearance (Garnham et al., 1962; Scholtyseck et al., 1970). The relative abundance of these organelles is different based on the species and the developmental life stage of the Apicomplexan parasite (V. B. Carruthers & Tomley, 2008; Dubois & Soldati-Favre, 2019).

The secretion of micronemes occurs at the furthermost apical end of the parasite. Microneme secretion has an important role in invasion since the chemical inhibition of microneme secretion greatly hinders the invasion process (Carruthers et al., 1999; Carruthers & Sibley., 1997). Before the secretion of their contents, the micronemes travel through the conoid to reach the plasma membrane where fusion occurs between the micronemes and the plasma membrane and the micronemes' contents are released (Carruthers & Sibley, 1999). This 'fusion' allows micronemes to transfer the components of their membranes to the surface and soluble proteins are released within the extracellular space termed 'adhesins'.

Across the apicomplexan phylum, microneme proteins have been studied by using a variety of approaches including proteomics analyses (Bromley et al., 2003; Soldati et al., 2001; Tomley & Soldati, 2001). In *T. gondii*, adhesins (MICs) are heavily involved in host cell attachment and invasion and form functional complexes (Huynh et al., 2003; Huynh & Carruthers, 2006). Most adhesin proteins consist of adhesive repeat domains which give the parasite the ability to bind to the surface of the host cell. The adhesive domains in MICs include: Thrombospomdin-1-type 1 domains (TSR), Von Willebrand A domain/integrin inserted (I) domain (A/I domain), Apple/PAN domains, EGF-like domains, and lectin domains. These domains are predicted to have a transmembrane configuration across the plasma membrane that involve receptor-ligand interactions (V. B. Carruthers & Tomley, 2008) (Figure 7, following page). For example, MIC2 consists of an A/I domain which is highly conserved across Apicomplexa and is characterized by its ability to bind different ligands such as ICAM- 1 and collagen (Lee et al., 1995; Wan et al., 1997). MIC2 also contains thrombosin-like domains which have a role in adhesion of the *T. gondii* parasite to its host cell (V. B. Carruthers & Tomley, 2008).
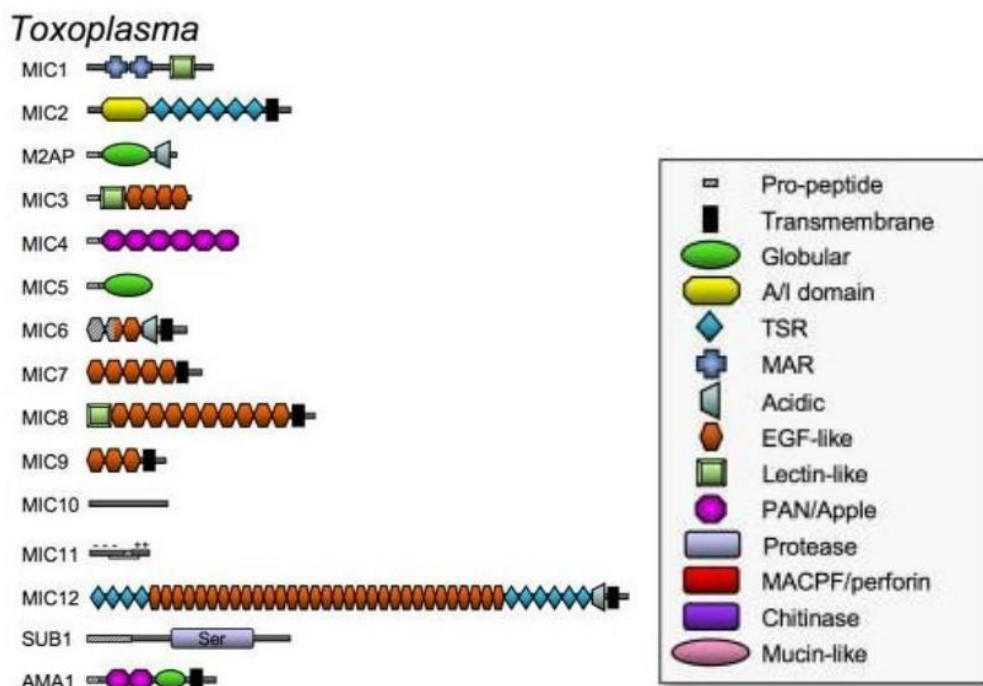
Figure 7 - Schematic representation of the different adhesion domains of MIC proteins in *Toxoplasma gondii* (V. B. Carruthers & Tomley, 2008). Micronemes contain different adhesion repeat domains implicated in various microneme functions.

In *T. gondii*, super resolution microscopy allowed for the identification of two distinct microneme subpopulations which are trafficked differently and have distinct subcellular localizations. One subpopulation involves the transport of microneme proteins MIC3, MIC8, and MIC11 while the other subpopulation includes microneme proteins MIC2, M2AP, PLP1, and AMA1 (Kremer et al., 2013). Further distinctions have been made regarding the distribution of micronemes. Differences between micronemes concentrated at or directly under the conoid and those localized in the peripheral and central area of the parasite body were made based on the exclusive localization of parafusin (PRP1), a protein with a Ca^{2+} dependent exocytosis role, with apical micronemes (Matthiesen et al., 2001, 2003). In addition, lack of certain proteins associated with CORVET/HOPS complexes resulted in absence of peripheral microneme proteins (Morlon-Guyot et al., 2018). Overall, these results suggest that micronemes possess at least two different trafficking pathways of at least two different subpopulations of micronemes that are confined to distinct spatial locations within the parasite.

Microneme proteins exist in two forms, there are soluble microneme proteins and transmembrane ones. Microneme proteins associate with each other in order to form complexes which function in parasite invasion (Sheiner et al., 2010). These complexes are: MIC6/MIC1/MIC4, MIC2/M2AP (MIC-2 associated protein), MIC8/MIC3, and AMA1/RONs (Figure 8, following page). The first complex was

discovered based on the disruption of TgMIC6 which resulted in the mislocalization of two other MIC proteins, TgMIC1 and TgMIC4. (Reiss et al., 2001). By using coimmunoprecipitation, the association of all three MIC proteins was confirmed (Reiss et al., 2001).This complex functions in the attachment and invasion of the parasite (Cérède et al., 2005).

The second complex MIC2/M2AP was discovered to be formed in the ER and then localized at the micronemes. The MIC2/M2AP complex remains on the parasite surface during invasion (Rabenau et al., 2001) and has an important role in attachment, invasion and parasite gliding (Huynh & Carruthers, 2006). TgMIC3 and TgMIC8 are suggested to form a complex based on the association of TgMIC3 to artificially expressed GPI-anchored TgMIC8 (Meissner et al., 2002). TgMIC3 has a synergistic role in association with TgMIC1 in parasite virulence whereas TgMIC8 is implicated in rhoptry secretion (Cérède et al., 2005; Kessler et al., 2008). The AMA1/RONs complex functions in the formation of the moving junction (MJ) (Bargieri et al., 2013; Lamarque et al., 2014; Mital et al., 2005).
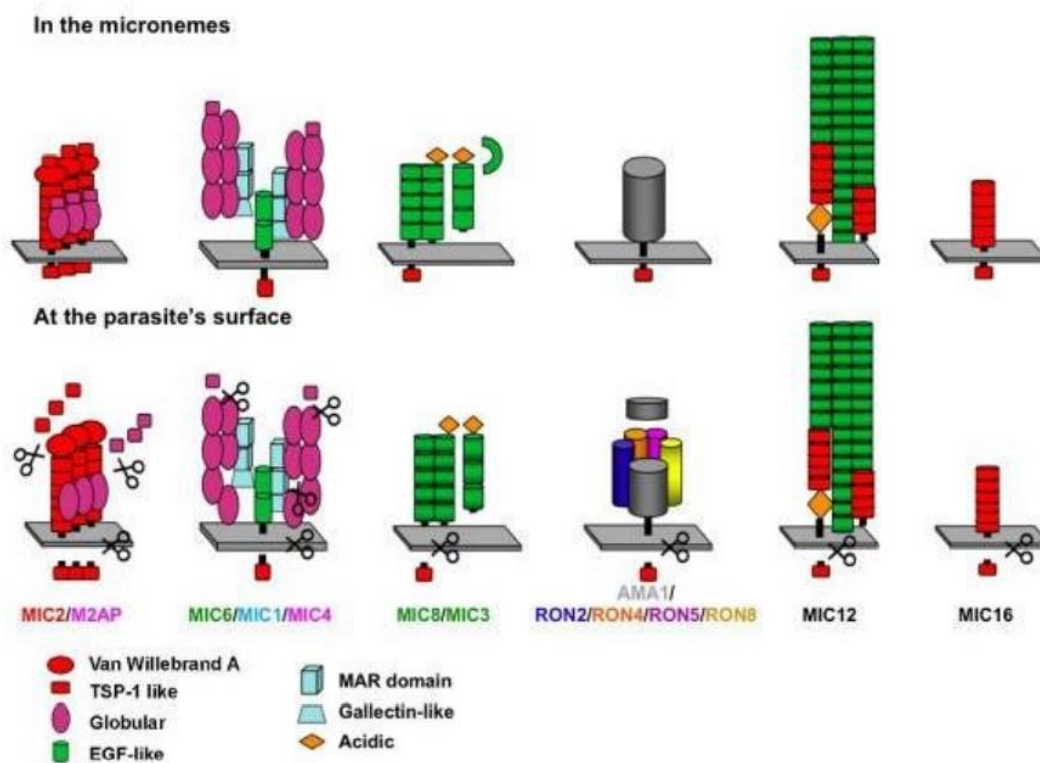
Figure 8 - Microneme complexes in *Toxoplasma gondii* (Sheiner et al., 2010). Schematic representation of different microneme complexes present within the parasite and at its surface.

Rhoptries

Rhoptries are club-shaped organelles present in *T. gondii* in multiples of 8-12 per parasite, and each rhoptry is around 2 -3 µm long (Dubey et al., 1998). Rhoptries have a bulb-like base and an elongated duct and are situated at the apical region of the parasite with the exception of only one to two rhoptries which can access the

interior of the conoid at one given time. There are three sub-compartments within each rhoptry, a sub-compartment for the bulb, one for the neck and a recently identified third sub-compartment separating between the rhoptry bulb and the neck. The latter sub-compartment has been demonstrated to exist by using freeze-fracture and quick-freeze techniques (Lemgruber et al., 2011) showing that this middle region has intermediate electron density and houses particular rhoptry proteins present on the cytoplasmic surface of the rhoptry organelle (Mueller et al., 2016).

Nature Reviews | Microbiology
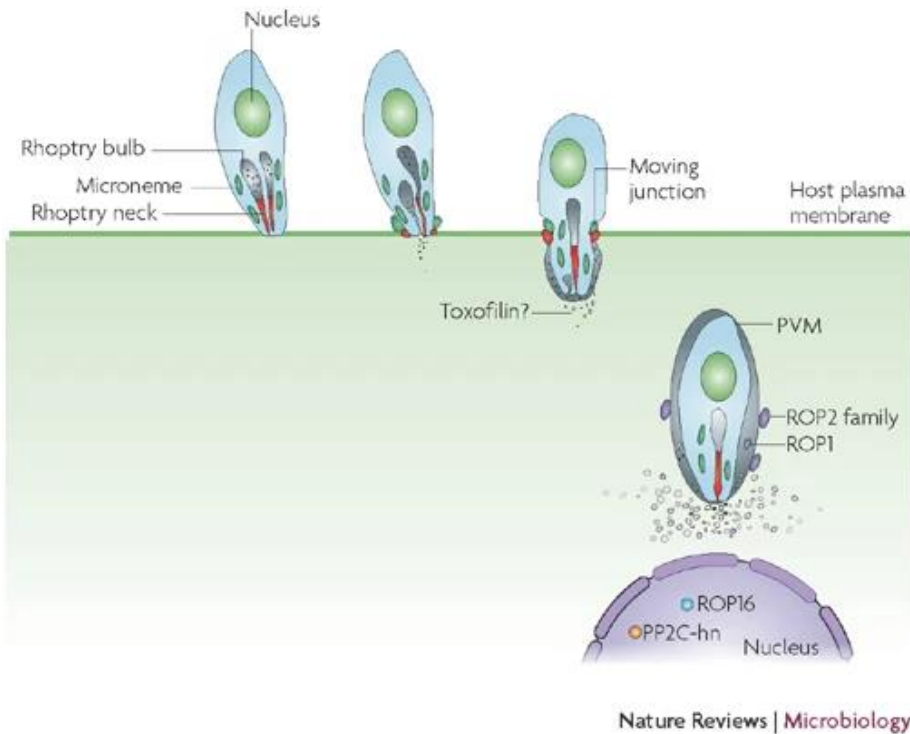
Figure 9- Schematic representation of rhoptry proteins in *T. gondii* (Boothroyd & Dubremetz, 2008). ROP and RON proteins are released from rhoptry bulbs (represented in grey) and rhoptry necks (represented in red) during the *T. gondii* invasion process. The collaboration of RON2, RON4, and RON5 with TgAMA1 results in the formation of the moving junction. The MJ transcends down the parasite's surface and leads to the formation of the parasitophorous vacuole membrane (PVM). ROP16 and PP2C localize within the host nucleus.

Segregation of rhoptry proteins exists between the neck and the bulb region of these organelles (Roger et al., 1988). ROP proteins are the proteins identified to be situated in the bulb region while RON proteins are located within the neck of the rhoptry (Dubey et al., 1998). Rhoptries are a central component of the parasite's secretory system and are produced *de novo* during the formation of daughter cells within the mother parasite through the budding of vesicles which contain newly synthesized rhoptry (ROP, RON) proteins (Nishi et al., 2008). Right before the final cytokinesis phase, pre-rhoptries mature into elongated rhoptries which then localize to the apical end of the parasite (Dubremetz, 2007; Venugopal et al., 2017). The translocation and attachment of rhoptries to the apical end of the parasite is crucially dependent on Armadillo Repeats Only protein (TgARO), Myosin F (TgMyoF) and ARO-Interacting protein (TgAIP) (Mueller et al., 2013). Rhoptries are characterized by their acidic environments; pre-rhoptries are more

acidic than the mature rhoptries. The rhoptries are the only organelles which were found to be acidic within the parasite (Shaw et al., 1998).

The secretion of rhoptries happens early in the invasion process. The exact number of rhoptries that are secreted is not known. However, the secretion process does not follow the conventional exocytosis process which involves the release of cell content extracellularly but rather follows a process where two main steps are coupled (Boothroyd & Dubremetz, 2008). The first step involves the docking and fusion of the rhoptry membrane with the apical plasma membrane of the parasite, representing a process commonly known as 'exocytosis'. The second step involves the transfer of the rhoptry content via the membrane of the host cell, this process is commonly known by 'export'. However, in this specific case, content of the parasite consisting of ROPs/RONs/ and associated lipids are not secreted via synaptic vesicles but are rather directly injected into the host cell (Håkansson et al., 2001).

After the secretion of rhoptry proteins, they associate with various compartments in order to carry out essential functions. These functions include association of TgRONs with the moving junction (MJ) for invasion (Figure 9), disarming of immune defenses by TgROPs, hi-jacking the host during the invasion process by rhoptry proteins that are directly injected into the cytosol of the host, and interference with the signalling pathways of the host particularly the host's transcription factors associated with the production of IFN-γ (Lebrun et al., 2020).

RON proteins such as TgRON2, TgRON4, and TgRON5 are present within the neck region of the rhoptry organelle and are secreted after the MIC proteins. These RON proteins have an implication in the formation of the moving junction (MJ) in association with TgAMA1 during invasion (Alexander et al., 2005; Lebrun et al., 2005). ROP proteins present within the bulb of the rhoptries are secreted after the formation of the MJ and have a crucial role in the formation of the parasitophorous vacuole (PV). ROP proteins are targeted to various compartments which include the parasitophorous vacuole (PV), PV membrane (PVM), in addition to compartments of the host cell (Bradley & Sibley, 2007).

The largest and most extensively studied rhoptry proteins are the ROPK superfamily also referred to as the ROP2 family, known to localize within the bulb region of the rhoptries and consists of more than 50 kinases and pseudokinases termed as "rhoptry kinases" (Peixoto et al., 2010; Talevich & Kannan, 2013). The ROP2 family was initially described as a family of rhoptry proteins consisting of three proteins; each of which were recognized by a single monoclonal antibody (Sadak et al., 1988). The ROPK family proteins have distinct characteristics in common. They share a kinase-fold present at the C-terminus and a basic amino-acid rich region present at the N-terminus of the protein. The N-terminal region of the kinase domain consists of an activation loop and a substrate-binding site and is the most conserved region of the ROPK proteins. Several ROPK proteins are predicted to be active due to the presence of a complete catalytic triad (Peixoto et al., 2010). However, not all members of the ROPK family are enzymatically active since some lack a glycine loop essential for ATP stabilization and a

conserved aspartate in the catalytic loop which is crucial for phosphotransferase function. These inactive ROP proteins are termed "pseudokinases" such as ROP2, ROP4, ROP5, ROP7, ROP8, and ROP54. X-ray crystallography showed that these pseudo-kinases still have a 'kinase-fold'. However, it is different from the conventional one and is characterized by *Toxoplasma*-specific variations. These pseudo-kinases exhibit potential roles in the scaffold and substrate sequestration (Labesse et al., 2009; Qiu et al., 2009; Reese & Boothroyd, 2011). Certain polymorphic ROP proteins are essential factors of virulence for the parasite in type I strains. The complex consisting of ROP5, ROP17, and ROP18 which localizes at the PVM is responsible for triggering the phosphorylation of immunity related GTPases (IRGs) preventing accumulation of IRGs at the PV and subsequently hindering PV lysis within mice (Etheridge et al., 2014; Fleckenstein et al., 2012). In Type II strains, the *ROP5* gene has a polymorphism which renders it inactive (Behnke et al., 2011) and hence results in an alternative outcome leading to disruption of PVM integrity and PV lysis. TgROP18 is also implicated in the modulation of transcription factor ATF6-ß function (Yamamoto et al., 2011). TgROP17 is involved in modulating the host cell transcriptome (Li et al., 2019). TgROP17 additionally has a role in effectively translocating dense granule proteins across the PVM (Panas, Ferrel, et al., 2019).

Another set of ROP proteins are translocated to the nucleus of the host. TgROP16 is a kinase secreted within the cytosol and is quickly targeted towards the nucleus of the host cell by means of a nuclear translocation sequence. TgROP16 has a prominent role in the activation of transcription factors STAT3 and STAT6 (Signal Transducer and Activator of Transcription) resulting in the inhibition of cytokine secretion such as IL-12 (Butcher et al., 2011). Another rhoptry protein TgPP2C which is not a member of the ROPK family is also translocated to the nucleus. Parasites lacking TgPP2C demonstrated a decreased growth phenotype. However, further studies to identify its specific role remain to be carried out (Gilbert et al., 2007).

Furthermore, other rhoptry proteins exhibit an important role in the differentiation of the *T. gondii* parasite. The transcriptome of the parasite was investigated during acute and chronic infection and the gene encoding for the ROP28 protein was found to be 5-fold more abundant during chronic infection compared to acute infection (Pittman et al., 2014). Another study in which 26 ROPK gene loci encoding for 31 unique Type II ROPK proteins were deleted identified several Type II ROPK proteins to have a moderate effect on cyst burden (Fox et al., 2016). However, certain ROPK proteins proved to be essential for the establishment of chronic infection *in vivo* and included: ROP5, ROP17, ROP18, ROP35, and ROP38/29/19 (Fox et al., 2016). Furthermore, in yet another study, the deletion of ROP21, ROP27, ROP28, and ROP30 did not significantly affect bradyzoite differentiation *in vitro*. However, a combined knock-out mutant of ROP21 and ROP17 resulted in a 50% decrease of cyst burden *in vivo* (Jones et al., 2017). Furthermore, a bradyzoite rhoptry protein designated TgBRP1 was characterized. A TgBRP1 knock-out strain was produced and its effect on cyst burden was studied only to demonstrate that TgBRP1 had no major effect on the

formation of tissue cysts but rather is most likely to have an important role in the merozoites of the sexual felid stages (Schwarz et al., 2005).

In addition, subcellular fractionation of the rhoptries allowed for the detection of abundant lipids and particular enrichment in cholesterol (Foussard et al., 1991). However, experimental studies have clearly demonstrated that cholesterol does not deem necessary for invasion (Coppens & Joiner, 2003). The rhoptry proteins and lipids are exported via rhoptry exocytosis and contribute in modifying the PVM (Coppens & Vielemeyer, 2005).

Overall, the rhoptries house several proteins and lipids with critical functions for parasite invasion and production of the parasitophorous vacuole. The contents of these organelles carry out important roles and contribute to the maintenance of the tachyzoite during the acute stage of infection. Moreover, rhoptry proteins contribute to tissue cyst formation during chronic infection.

Dense granules

Dense granules are small electron dense organelles enclosed by a single membrane and are distributed throughout the parasite's cytoplasm. Under an electron microscope, these organelles appear as microspheres ~200 nm in diameter. Dense granules vary in number based on the developmental stage of the parasite. However, they are plentiful within the *T. gondii* tachyzoite stage (Mercier & Cesbron-Delauw, 2015).

The content of dense granules which consists of GRA proteins has been demonstrated to be secreted after the initial invasion steps and most likely before the parasite has been fully incorporated within the confinements of the PVM (Panas & Boothroyd, 2021). GRA proteins are located within different compartments of the PV, they are found within the PV lumen. Other GRAs are located within the PVM while others are located on the PVM. Moreover, certain GRA proteins are located at the host cell nucleus and cytoplasm after their export from the PV (Clough & Frickel, 2017; Mercier & Cesbron-Delauw, 2015; Panas & Boothroyd, 2021). GRA proteins are also secreted by extracellular parasites with the potential to affect cells which are uninfected (Leroux et al., 2015; Wong et al., 2020). The process by which GRA proteins are secreted has proven to be difficult to elucidate. Unlike rhoptries and micronemes, dense granule proteins are not secreted at the apical end of the parasite but rather it has been hypothesized that the fusion of dense granule membranes with the parasite's plasma membrane occurs through gaps located between the IMC plates (Dubremetz et al., 1993). However, the transport of GRA proteins after being newly synthesized from the Golgi to the parasite periphery is carried out by a MyoF motor, which transports cargo along actin filaments (Heaslip et al., 2016). Additionally, TgRab11A has an essential role by contributing to the transport of dense granules (Venugopal et al., 2020).

GRA proteins have an important role in maintaining PV structural integrity by formation of the intra-vacuolar network (Mercier et al., 2002). GRA proteins also function in the import of nutrients from the host cell to the PV (Gold et al., 2015). Additionally, GRA proteins are implicated in modulating the host's immune response (Bougdour et al., 2013; Braun et al., 2013; Gay et al., 2016; Rosowski et

al., 2011). In addition to their role in the formation of the chronic phase tissue cyst (Fox et al., 2011, 2019; Guevara et al., 2019, 2020, 2021).

TgGRA7 interacts with the vacuole Host Organelle Sequestering Tubulostructures (HOST) which are digitations of the PV membrane and functions in internalizing host endo-lysosomes within the parasite's PV (Coppens et al., 2006). Additionally, TgGRA7 has an in implication in IRG clearance, TgGRA7 interacts with the TgROP5/TgROP18 complex which targets and phosphorylates Irga6, an IRG protein contributing to acute virulence in mice (Alaganan et al., 2014; Hermanns et al., 2016). Similarly, TgGRA12 functions in the elimination of IRGs yet the mechanism regarding how this dense granule protein is able to carry this process out remains to be elucidated (Fox et al., 2019; Michelin et al., 2009; J.-L. Wang et al., 2020). In addition, other important roles for TgGRA12 were identified by studying mutant parasites lacking the expression of GRA12. Mutant parasites in which the *GRA12* gene was deleted exhibited a significant decrease in virulence and tissue cyst formation (J.-L. Wang et al., 2020). TgGRA60 is yet another GRA protein that demonstrated an important role in eliminating IRGs (Nyonda et al., 2021). Type I parasites lacking the *TgGRA60* gene resulted in decreased virulence and reduction of cyst burden in addition to the recruitment of IRG proteins, Irgb10 and Irga6. TgGRA60 was also shown to work in concert with the TgROP18 and TgROP5 proteins (Nyonda et al., 2021).

TgMAF1b is yet another GRA protein which mediates the association of the host mitochondria to the PVM (Pernas et al., 2014). The association of the mitochondria to the PV allows the parasite to obtain fatty acids which are needed for the proliferation of the parasite and at the same time might restrict the growth of the parasite by incorporating essential fatty acids as well (Pernas et al., 2018).

GRA proteins take part in modulating host signalling pathways. GRA proteins were demonstrated to interact with host cell transcription factors such as TgGRA6 In Type I strains which activates NFAT4 (Nuclear Factor of Activated T Cells 4), resulting in the recruitment of immune cells only to be cleared by the parasite (Bierly et al., 2008; Coombes et al., 2013; Courret et al., 2006). Another dense granule protein example is TgHCE1/TgTEEGR which binds to E2F3 and E2F4 TFs affecting chromatin remodeler gene *EZH2* (Braun et al., 2019). TgHCE1/TgTEEGR also has an impact on host cell cyclin E and CDK2 impacting cell cycle progression (Panas, Naor, et al., 2019). Furthermore, GRA proteins have an impact on the immune system such as TgIST which regulates STAT-dependent genes blocking IRG clearance (Gay et al., 2016; Olias et al., 2016).

Furthermore, certain GRA proteins have an implication in tissue cyst formation such as TgGRA4, TgGRA6, TgGRA3, TgGRA7, TgGRA8, TgGRA14, TgGRA2, TgGRA9, and TgGRA12 (Fox et al., 2011, 2019; Guevara et al., 2019). The deletion of TgGRA4 and TgGRA6 in Type II parasites resulted in a drastically decreased cyst burden compared to their wildtype counterparts (Fox et al., 2011). The deletion of both TgGRA4 and TgGRA6 in the same strain resulted in an even more drastic defect in tissue cyst burden (Fox et al., 2011). In a following study, PVM-associated GRAs including TgGRA3, TgGRA7, TgGRA8, and TgGRA14 and IVN-

membrane associated GRAs including TgGRA2, TgGRA9, and TgGRA12 were deleted in type II strains. These deletions resulted in severe defects in cyst burden *in vivo* (Fox et al., 2019). During tissue cyst development, GRA proteins are very dynamic, this was shown through studying the localization of IVN-associated GRA proteins (TgGRA1, TgGRA4, TgGRA6, TgGRA9, and TgGRA12) in developing *in vitro* tissue cysts during different time points (Guevara et al., 2019).
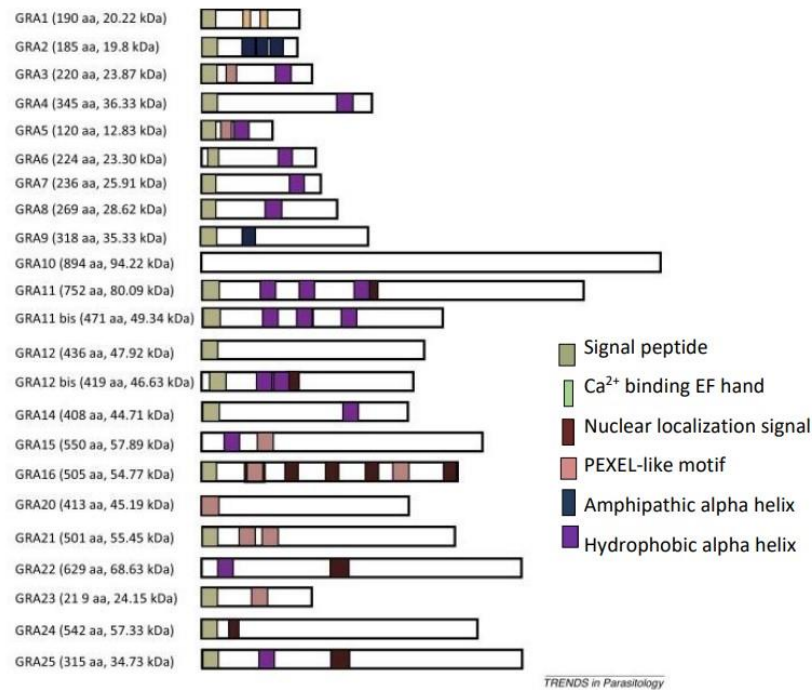
Figure 10- Schematic representation of dense granule GRA proteins in *T. gondii* (Mercier & Cesbron-Delauw, 2015). A compilation of GRA proteins identified in the Type II ME49 strain based on TOXODB database. The associated domains of the GRA proteins are indicated in different colors. Grey represents the signal peptide, light pink represents the PEXEL-like motif, purple represents the hydrophobic alpha-helix, orange represents the Ca^{2+} -binding EF hand, dark red represents the nuclear localization signal.

Proteomics analysis carried out on enriched cyst wall fractions of *in vitro* tissue cysts allowed for the identification of GRA proteins as major components of the tissue cyst wall (Tu et al., 2019). Among these GRA proteins are GRA2, GRA3, GRA4, GRA5, GRA7, GRA8, GRA9, GRA12, GRA14, GRA17, GRA23, GRA25, GRA29, GRA31, GRA33, GRA34, and GRA35 (Tu et al., 2019). In addition, a novel sub-set of dense granule proteins designated as CST proteins was identified. Among them, TgCST2 was demonstrated to have an essential role in establishing an *in vivo* chronic infection (Tu et al., 2019).

In addition, a more recent study characterizing four GRA12-related genes (GRA12A, GRA12B, GRA12C, and GRA12D) indicated that the GRA-12 gene family has an implication in chronic infection (Guevara et al., 2021). Similar to TgGRA12, genes related to TgGRA12 are associated with the IVN in tachyzoites. In immature cysts formed by using the high pH shift, TgGRA12A, TgGRA12B,

and TgGRA12D localize to the cyst wall suggesting that these three proteins have a role in the PV developing into a tissue cyst. Similarly in mature cysts, TgGRA12A, TgGRA12B, and TgGRA12D localize to the cyst wall as well as the cyst matrix (Guevara et al., 2021). Mutant parasites lacking TgGRA12A resulted in a significant decrease in cyst burden *in vivo*. Alternatively, parasites lacking TgGRA12B led to a significant increase in cyst burden *in vivo* (Guevara et al., 2021). Furthermore, parasites lacking TgGRA12A, TgGRA12B, and TgGRA12D demonstrated a decrease in bradyzoite re-activation efficiency yet TgGRA12A deficient-parasites also displayed a delay in re-activation (Guevara et al., 2021). Overall, these findings imply that dense granule proteins have important roles in the formation and maturation of tissue cysts *in vitro* and the establishment of *in vivo* chronic infection.

4.2 *T. gondii* tissue cyst ultrastructure and formation

During the early developmental stage of tissue cysts at around 28 days post-infection, a limited number of dividing tachyzoites remain within the bloodstream and an enlargement of the tissue cysts occurs followed by the appearance of invaginations in the tissue cyst wall, and an underlying amorphous layer. During the early stage of tissue cyst development, the bradyzoites within still retain most of the tachyzoite's ultrastructural features such as the rhoptries despite the expression of bradyzoite markers such as BAG1, ENO1, and LDH2 (Ferguson & Hutchison, 1987b).
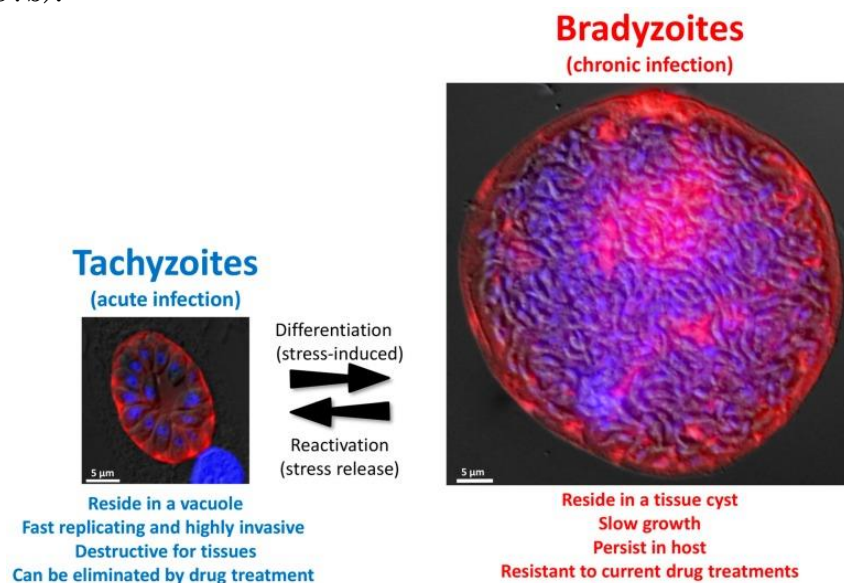
Figure 11 – Tachyzoite – bradyzoite interconversion (Cerutti et al., 2020). Tachyzoites present during acute infection can convert into bradyzoites present during chronic infection and vice versa.

Mature tissue cyst structures were demonstrated to remain unchanged during the entire life span of the mouse. The initial hypothesis was that tissue cysts were extracellular. However, upon ultrastructure observation, the presence of a thin rim of the host cell cytoplasm enclosing the tissue cysts demonstrated otherwise (Ferguson & Hutchison, 1987a). The enclosure of the tissue cyst within the host

cell cytoplasm may be the reason why the tissue cysts avoid the host's immune system. The thickness of cyst walls of different tissue cysts varies; some cysts possess cyst walls with deep invaginations leading to the formation of a network of interconnecting channels fixed within the granular material (Ferguson & Hutchison, 1987b). Bradyzoites enclosed within mature cysts appear to be more elongated compared to tachyzoites and contain a nucleus at the posterior end.

The bradyzoites are characterized by the presence of abundant micronemes and a few dense granules. The rhoptry bulb regions are more enlarged in addition to the appearance of polysaccharide amylopectin granules. Tissue cysts are usually similar in size and shape. However, in some instances, different-sized tissue cysts were observed in mice and it was hypothesized that this may be explained by the formation of daughter tissue cysts following the release of single bradyzoites from initial tissue cysts in order to form new ones (Lainson, 1958). Bradyzoites can be released from the tissue cyst upon reactivation and differentiate into the rapidly replicating tachyzoites (Cerutti et al., 2020).

5 The Lytic Cycle of *Toxoplasma gondii*

The lytic cycle is essential for *T. gondii*'s survival and encompasses five steps which include: attachment (adhesion), invasion of the host cell, parasitophorous vacuole (PV) formation, replication of the parasite within the parasitophorous vacuole, egress, and emergence of new daughter parasites after the destruction of the invaded host cell (Figure 12).
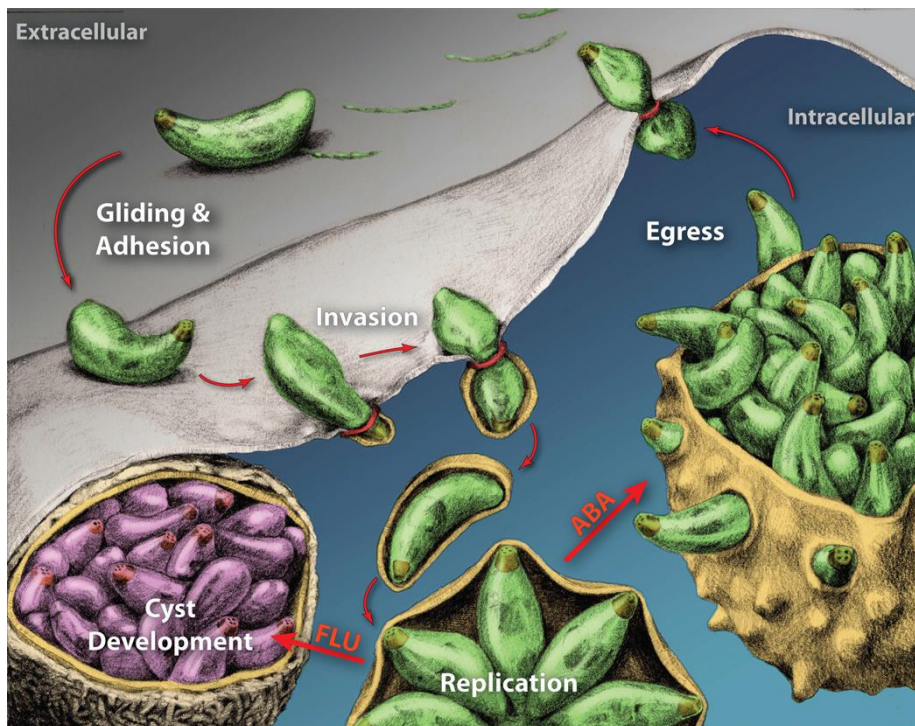
Figure 12 - Schematic representation of the sequential steps involved within the intracellular lytic cycle of *T. gondii* (Billker et al., 2009). Tachyzoites actively invade host cells by means of gliding motility which is based on actin-myosin

motility allowing for active invasion of the host cell. Adhesion to the host cell then results due to microneme protein secretion from the apical complex of the parasite. A tight constriction is formed between the host cell and parasite cell membranes consisting of proteins secreted from the rhoptries and is known as the moving junction (represented by a red ring). Once the parasite has entered the host cell, the parasitophorous vacuole is formed and enlarges as the parasites replicate within it. Abscisic acid (ABA) accumulates and leads to egress. The production of ABA can be blocked by herbicide fluoridone (FLU) and triggers the formation of tissue cysts.

5.1 Motility of the parasite and adhesion

Motility in *T. gondii* is characterized by gliding movement. There are three types of gliding movements when observed on a 2-dimesional coated surface: There is circular gliding, helical rotation gliding, and up-right twirling gliding (Håkansson et al., 1999). However, when observed in a 3-dimensional motility assay, the motility of the parasite can be described as a clockwise corkscrew trajectory and this is due to the nature of the tachyzoite's shape and microtubules present in the tachyzoite's cytoskeleton which are left-handed (Leung et al., 2014).

The machinery involved in the gliding movement is termed the glideosome and is responsible for powering the parasite's motility, migration, invasion, and egress from the host cell. It is situated between the plasma membrane from one side and the IMC from the other and is conserved among members of the Apicomplexa (Opitz & Soldati, 2002). The glideosome consists of Myosin A (TgMyoA), the associated myosin light chain1 (TgMLC1) (Herm-Gotz, 2002), the essential light chain (TgELC1) (Bookwalter et al., 2014; Williams et al., 2015) and three gliding-associated proteins GAP45, GAP50 (Gaskins et al., 2004), and GAP40 (Frénal et al., 2010). TgMLC1 associates with TgGAP45 allowing for the anchoring of TgMyoA to the IMC at its functional location in the pellicle of the parasite's tachyzoite. TgGAP45, a central component of the glideosome is present and produced within the cytosol. Acylation of the GAP45 protein at its N-terminal allows for its targeting towards the plasma membrane while association with the IMC is maintained through the C-terminal of the GAP45 protein (Frénal et al., 2010). TgGAP45 has two other orthologues: TgGAP70 which appears in the glideosome present at the apical region consisting of TgMyoA whereas the TgGAP80 glideosome is present at the basal end and consists of TgMyoC (Figure 13, Frénal et al., 2014).

TgMyoA is the powering motor of gilding motility and has similar mechanical characteristics to that of skeletal muscle myosin with a velocity of ~3μm per second. The chemical energy released from the hydrolysis of ATP is converted by MyoA into mechanical energy and movement is achieved along polymerized actin fibers (Herm-Gotz, 2002). The firm anchorage of TgMyoA to the cytoskeleton of the parasite remains crucial for the generation of traction and this is through TgGAP40 and TgGAP50 on the IMC side whereas on the opposing side, TgMyoA must be anchored to host cell substrates present in the extracellular compartment. Mutant parasites in which the components of the glideosome (TgMyoA, TgMLC1, TgELC1, and TgGAP45) were conditionally depleted had a drastically substantial impact on tachyzoite motility which eventually impacts survival (Frénal, Dubremetz, et al., 2017). *T. gondii* tachyzoites lacking in TgMyoA have been

demonstrated to retain the capacity to replicate within host cells yet the lytic cycle is greatly disrupted (Andenmatten et al., 2013). This is best explained by the presence of another myosin heavy chain TgMyoC which functions with TgGAP45 despite the lack of TgMyoA (Frénal et al., 2014). In more recent studies, a third myosin motor protein has been identified TgMyoH, which is localized at the tachyzoite apex and is anchored at the conoid acts in accordance with conoid protrusion to initiate movement (Graindorge et al., 2016).

It has been hypothesized previously that the link between the parasite and TgMIC2 is due to the aldolase enzyme (TgALD) by means of its ability to bind F-actin (Jewett & Sibley, 2003). Transgenic parasites lacking in TgALD demonstrated an impairment in motility and host cell invasion (Starnes et al., 2009). Strikingly, in recent studies, it has been demonstrated that the *T. gondii* glideosome associated connector (TgGAC) is responsible for binding to F-actin and translocating along the length of the parasite, binding to the TgMIC2 adhesin (Figure 13) while motile and during invasion (Jacot et al., 2016).
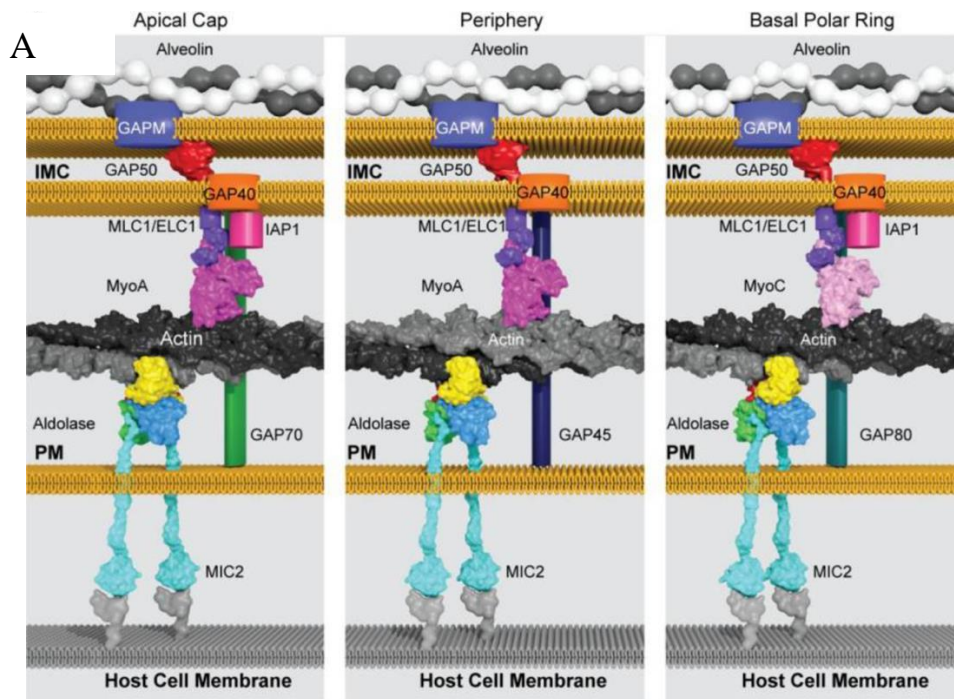
B
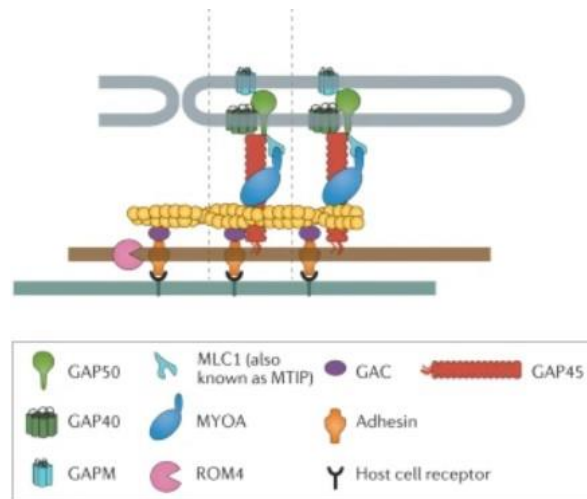
Figure 13- Schematic representation of the glideosome (Boucher & Bosch, 2015; Frénal, Dubremetz et al., 2017). (A) Representation of the different components of the glideosome at the apical cap (left), periphery (middle), and basal polar ring (right). **(B)** Most recent representation of the glideosome which replaces TgALD with TgGAC as the actin connecter linking adhesin TgMIC2.

5.2 Microneme secretion and adhesion of the parasite

The initial attachment of the *T. gondii* parasite to the host cell is through adhesins present at the parasite's surface designated SAGs (Surface Antigen Glycoproteins). These proteins bind to host cell receptors specifically interacting with sulfated proteoglycans (V. Carruthers & Boothroyd, 2007; X. He et al., 2002).

For the parasite to move forward, it is necessary for the glideosome to interact with host cell receptors which is maintained through specific ligands termed 'adhesins' (Paing & Tolia, 2014). Adhesins are secreted into the plasma membrane of the parasite once microneme exocytosis from the parasite's apex has occurred. In *T. gondii*, there are three main adhesion complexes that are exocytosed from the micronemes: TgMIC6-TgMIC1-TgMIC4, TgMIC2-TgM2AP, and TgMIC8-TgMIC3 (V. B. Carruthers & Tomley, 2008). TgMIC2 has an important role in gliding motility since mutations of the TgMIC2 tail region results in a defect in tachyzoite motility (Kappe et al., 1999) whereas the complete absence of TgMIC2 does not totally hinder motility (Andenmatten et al., 2013; Rugarabamu et al., 2015). Therefore, it is highly probable that other microneme proteins have roles in parasite motility.

Microneme protein secretion acts as a response to a decrease in potassium concentration which in turn increases intracellular calcium concentrations. The peak in calcium concentration is involved in signaling through the activation of specific kinases and microneme secretion coordination (Lourido & Moreno, 2015). The presence of several calcium-dependent kinases (CDPKs) which are usually found in plants have been demonstrated to be crucial for microneme secretion (Billker et al., 2009). TgCDPK1 has an important role in microneme exocytosis and is an essential kinase for microneme protein secretion (Lourido et al., 2010). Another *T. gondii* calcium-dependent kinase, TgCDPK3 has an implication in

egress and has an important role in triggering motility following the phosphorylation of myosin protein motor, TgMyoA (Garrison et al., 2012; Lourido et al., 2012; McCoy et al., 2012).

In addition to *T. gondii* CDPKs, there are additional proteins and molecules that play important roles in the signaling pathways associated to *T. gondii*'s motility and glideosome regulation. cGMP-dependent protein kinase (PKG) activates the secretion of micronemes and egress from the host cell in a manner independent of calcium ions (Lourido et al., 2012). Recent studies on TgGC, a purine nucleotide cyclase enzyme which is responsible for converting GTP into cGMP have demonstrated that TgGC is essential for the cell-to-cell transmission in tachyzoites by regulating invasion, migration and egress (Bisio et al., 2019; Brown & Sibley, 2018; L. Yang et al., 2019). TgGC is essential for the production of cGMP which in turn activates TgPKG.

In addition, phosphatidic acid (PA) has been shown to be a lipid which has an important role in regulating microneme secretion (Bullen et al., 2016). Phosphatidylinositol phospholipase C (PI-PLC) in response to an increase in extracellular potassium levels activates a signaling cascade and is responsible for generating second messengers such as diacylglycerol (DAG) and inositol- 1,4,5-triphosphate (IP$_3$). DAG is interconverted into PA by diacylglycerol kinase 1 (DGK1) (Bullen et al., 2016). The downstream product PA is detected by an acylated pleckstrin homology domain-containing protein (APH), an Apicomplexa conserved protein which is situated on the surface of micronemal proteins. In *T. gondii*, TgAPH was demonstrated to have an essential role in microneme secretion since mutant parasites in which TgAPH was conditionally depleted led to a major blockage in the release of microneme proteins and subsequently resulted in a severe impairment in glideosome activity (Bullen et al., 2016).

5.3 Host cell invasion and formation of the Moving Junction (MJ)

The process of invasion is a very rapid process and requires only a few seconds. Following the secretion of microneme and rhoptry proteins, the parasite becomes in intimate contact with the host cell by means of a moving junction (MJ). The MJ appears as a visible constriction encircling the parasite and is apparent as a ring of contact between the parasite and the plasma membrane of the host cell (Figure 14). The formation of such a structure remains necessary for the parasite to successfully invade the host cell (Besteiro et al., 2011).

The MJ is associated with rhoptry neck proteins and microneme apical membrane antigen-1 (TgAMA1) protein (Alexander et al., 2005; M. Lebrun et al., 2005).

TgAMA-1 is a type I transmembrane protein, it possesses a short C-terminal cytoplasmic tail and a large N-terminal extracellular ectodomain consisting of around 16 conserved cysteine residues (Donahue et al., 2000; Hehl et al., 2000). TgAMA1 is secreted on the parasite's surface, followed by cleavage of the N-terminal ectodomain and its shedding. TgRON2, TgRON4, TgRON5 and TgRON8 were identified as members of the TgAMA1-associating MJ complex (Alexander et al., 2005; Besteiro et al., 2009; M. Lebrun et al., 2005). The MJ functions as a flexible, ring-link structure which holds the parasite and the plasma membrane of the host in close proximity by means of a link allowing the membranes of the two organisms to flow around this link.

The interaction between TgRON2 and TgAMA1 bridges the parasite and the host cell (Tonkin et al., 2011). The association of the RON proteins with the host cell cytoplasm function in subverting the host cell protein networks (Guérin et al., 2017). Four host proteins are recruited to the MJ during invasion: ALIX, CD2AP, CIN85, and TSG101 (Guérin et al., 2017). ALIX and TSG101 are components of the endosomal sorting complex which is necessary for transport (Bissig & Gruenberg, 2014) whereas CIN85 and CD2AP are homologs which have an implication in cytoskeletal polarization and cell signaling (Dikic, 2002; Dustin et al., 1998). TgRON4 has an essential role in recruiting ALIX, CD2AP, and CIN85 through specific binding sites whereas TgRON5 contributes to the recruitment of TSG101 (Guérin et al., 2017). Transgenic parasites in which the recruitment of these 4 RON-interacting host proteins is impaired displayed a significantly reduced invasion capacity (Guérin et al., 2017). These results exhibit the parasite's ability to interact with host proteins during the formation of the MJ in order to ensure efficient parasite invasion of the host cell.

Mutant parasites in which TgRON2 was depleted resulted in a significant decrease in invasion which was reduced to 10% compared to that of wildtype parasites (M. H. Lamarque et al., 2014). In addition, these TgRON2 depleted parasites exhibited that TgRON4 and TgRON5 were not expressed and localized correctly and instead of localizing to the rhoptries, they remained dispersed within the PV or perinuclear region of the mutant parasites. These two RON proteins were also absent from the MJ during invasion. However, this was not the case for TgRON8 which localized at the rhoptries and consequently at the MJ in the case of invasion suggesting the presence of additional components that can associate at the MJ (M. H. Lamarque et al., 2014) . In addition, conditional depletion of TgAMA1 demonstrated that *T. gondii* parasites exempt of TgAMA1 expression have a severe impairment in attaching intimately to host cells as well as an impairment in rhoptry protein secretion. These results demonstrate that TgAMA1 is a highly crucial protein for the parasite to robustly adhere to the host cell (M. H. Lamarque et al., 2014; Mital et al., 2005). The direct KO of TgAMA1 confirmed that TgAMA1 is not essential for intimate attachment of the parasite to the host cell. The role of TgAMA1 despite its absence can be compensated for by the expression of homologous proteins of TgAMA1 and TgRON2. Newly identified complexes consisting of TgAMA2-TgRON2, TgAMA3-TgRON2$_{L2}$, and TgAMA4-TgRON2$_{L1}$ indicate the presence of alternative pathways to the TgAMA1 and TgRON2 invasion pathway (M. H. Lamarque et al., 2014).
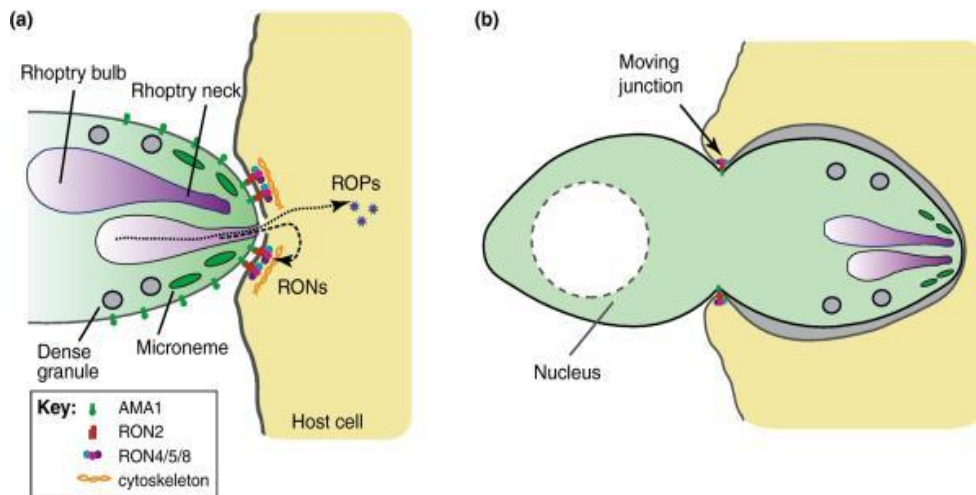
Figure 14- Schematic representation of the invasion process of the *T. gondii* parasite via formation of the moving junction (Tyler, Treeck et al., 2011). **(a)** Schematic representation of the apical portion of the *T. gondii* parasite during the initial steps of invasion demonstrating the presence of secretory organelles such as the micronemes, rhoptries, and dense granules along with key protein members that participate in the formation of the MJ. TgAMA1 is depicted in green, TgRON2 is depicted in red, TgRON4/5/8 are represented as a complex in blue, pink, and purple, respectively. Cytoskeleton microtubules are depicted in dark yellow. **(b)** Schematic representation of the intermediate steps of *T. gondii* invasion and the formation of the constriction ring associated with the MJ. To date, it is not clear whether the constriction is due to cytoskeleton forces or forces generated by the actin/myosin motors.

5.4 Parasitophorous vacuole formation

The parasitophorous vacuole (PV) is an intracellular structure that is formed within the host cell to avoid the host's immune system. Upon entry of the parasite into the host cell and formation of the moving junction (MJ), the parasite creates a force that causes the invagination of the host cell membrane. A study carried out by Suss-Toby *et al* (Suss-Toby et al., 1996) identified that the parasitophorous vacuole lipid bilayer is mainly derived from the plasma membrane of the host cell. The exocytosis of rhoptries has an important role in exporting proteins and lipids that are necessary for the modification of the developing parasitophorous vacuole membrane (PVM). A selective exclusion process of host cell plasma membrane proteins at the MJ is carried out. This sorting or selective exclusion is based on the anchoring of these proteins to the cytoskeleton. Proteins which are excluded include Type I single-spanning TM proteins associated with the cytoskeleton whereas host-lipid anchored proteins remain associated with the PVM (Mordue et al., 1999). The exclusion of proteins is not affected by host cell lipid components hence some raft-associated proteins are excluded while others are included into the composition of the PVM. The parasite's ability to exclude most of the host proteins suggests the prevention of elimination of the parasite by lysosomal fusion (Charron & Sibley, 2004).

Evacuoles which are rhoptry-derived vesicles are secreted into the cytosol of the host cell (Håkansson et al., 2001). These specialized vesicles contain within them the ROP proteins necessary for the making of the PV. The specialized vesicles (evacuoles) appear to have a multilamellar morphological structure of lipids and are similar to the PVM in avoiding fusion with the endosomal components of the host cell.
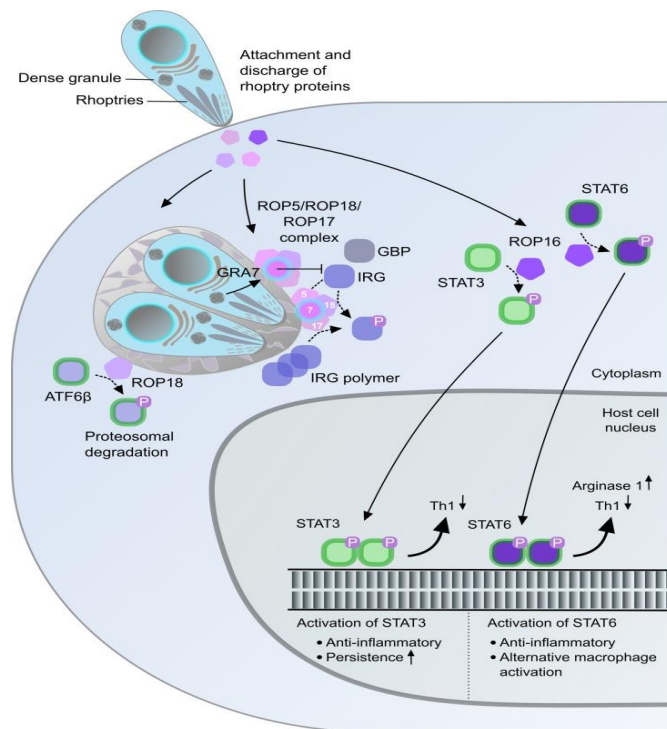
Figure 15–Function of ROP proteins in modulation of the host cell (Hakimi et al., 2017). After adhesion of the parasite to the host cell and formation of the moving junction, ROP proteins are secreted into the cytoplasm of the host cell and associate with the PV or are translocated to the host cell's nucleus. TgROP5, TgROP17, and TgROP18 function as a complex in order to phosphorylate IRGs and prevent their accumulation at PVM. TgGRA7 can either function alone or with the TgROP5/17/18 complex in order to inhibit IRGs. TgROP18 phosphorylates transcription factor ATF6β and TgROP16 phosphorylates STAT3 and STAT6 in order to trigger anti-inflammatory responses.

Certain secreted rhoptry proteins constructing the PV have an important role in the parasite's virulence. Among these rhoptry proteins is TgROP5, a pseudokinase that interacts and activates two kinases, TgROP17 and TgROP18 forming a complex that enhances *T. gondii*'s virulence activity (Figure 15). TgROP17 and TgROP18 target and phosphorylate immunity related GTPases (IRGs) that function in innate immunity in mice (Etheridge et al., 2014). In addition, the deletion of TgROP17 in Type I parasites led to a slight attenuation of virulence. The same phenotype was observed when deleting TgROP18. However, a double knock-out of TgROP17 and TgROP18 resulted in total attenuation of virulence *in vivo* in mice (Etheridge et al., 2014). Furthermore to this, TgROP18 targets ATF6β

by phosphorylation , a member of the unfolded protein which has an influential role in adaptive immunity (Figure 15) (Yamamoto et al., 2011).

Once the nascent parasitophorous vacuole has been formed, separating the parasite from the host cell cytoplasm, and consequently separating the parasite from nutrients located in the host's cytoplasm and organelles, the PV is converted into a dynamic structure in order to obtain the required nutrients for the parasite's survival. This transformation step of the PV is known as a maturation step where several GRA proteins are implicated within 10-20 minutes after the initiation of invasion (Sibley et al., 1995). TgGRA17 localizes at the PVM and has an important role in maintaining the morphology of the PV. Mutant parasites in which TgGRA17 was knocked-out resulted in a substantial number of PVs that were abnormally enlarged (Gold et al., 2015). The abnormal PV morphology in TgGRA17-deficient parasites was able to be rescued by complementing the TgGRA17 knock-down strain with TgGRA17-related protein PfEXP2 which has an important role in mediating the export of proteins across the PVM and into the cytosol of the red blood cell (de Koning-Ward et al., 2009; Gold et al., 2015). In addition, mutant parasites lacking TgGRA17 led to PVs which were extremely dynamic and unstable. TgGRA17 was proven to have an important role in small molecule passage from the PV to the host cell. TgGRA23 was also suggested to function synergistically with TgGRA17 in small molecule permeability (Gold et al., 2015). Furthermore, TgGRA17 and TgGRA23 function in a synergistic manner to ensure normal parasite growth and affect the parasite's virulence *in vivo* (Gold et al., 2015).

GRAs are known to be secreted primarily right after invasion within the forming PV followed by a continuous secretion of GRAs during the entire development cycle of the parasite (Carruthers et al. 1997).

Some GRAs are located at the TVN. The TVN is made up of an intricate network of tubules which stands for the tubulo-vesicular network also termed as the intravacuolar network (IVN) and is built within the PV. These tubular structures are around 30 nm in diameter (de Souza & Attias, 2015; Magno, Lemgruber, et al., 2005). The TVN network enlarges by incorporation of host lipids (Caffaro & Boothroyd, 2011; Nolan et al., 2017). The maturation of the TVN is associated with the secretion of dense granule proteins (GRAs), these proteins accumulate at the posterior end of the parasite within an invaginated pocket. Overall, the TVN functions as an obtainer of necessary nutrients from the host cell as well as a protector of the parasite within the confinements of the PV and therefore decreases the exposure of parasite antigens to the host.

In addition to the TVN, the PV contains vesicles which consist of actin filaments connecting the PVM to the TVN and the parasites in between. The tubules have an important role in controlling synchronicity in the division of the parasites within the parasitophorous vacuole as well as material transfer between the parasites (Frénal, Jacot, et al., 2017; Periz et al., 2017). The PV is also characterized by modifications at the level of the host cell organelle. After invasion, mitochondria and endoplasmic reticulum (ER) of the host cell encircle

the developing PV and remain within its proximity during the intracellular development of the parasite, at a conserved distance between the PV and each of the two organelles of around 12 nm for the mitochondria and 18 nm for the endoplasmic reticulum (Sinai et al., 1997; Magno, Straker, et al., 2005). The mechanism by which host organelles are allocated towards the PVM remains to be identified, yet the anchoring of the mitochondria of the host cell to the PVM of type I and III strains is achieved through MAF1b, a dense granule protein termed 'mitochondria association factor 1' (Pernas et al., 2014).

5.5 Cell cycle and intracellular replication

Modes of division across Apicomplexa

Apicomplexans are known to have peculiar cell cycles compared to other model eukaryotes. Asexual cell division among apicomplexan members is a means by which the parasite ensures expansion of its biomass within its host cells. Members of the apicomplexan phylum exhibit a variety of distinctly different division modes (Figure 16) (Gubbels et al., 2020). However, all division modes conclude with the production of invasive zoites which possess an apical complex region consisting of secretory organelles in addition to cytoskeletal components (Gubbels et al., 2021). The main division modes in Apicomplexa include schizogony which has been extensively studied in *Plasmodium*, endodyogeny which has been studied in *Toxoplasma*, endopolygeny with karyokinesis which occurs in *T. gondii* merozoites and endopolygeny without karyokinesis which occurs in *Sarcocystis neurona*. Another mode of division that occurs in apicomplexans is binary fission which is known to be carried out by *Babesia*.

A recent review written by Gubbels et al. (2021) nicely portrays the various asexual division modes stating that each division mode consists of a number of 'modules' which represent distinct events that occur during division. Four modules were identified and include the replication and segregation of DNA (D&S), karyokinesis, budding of the daughter cells (zoite assembly), and the disassembly of the mother cytoskeleton (Gubbels et al., 2021). The main feature that differentiates between the different division modes is whether the assembly of the mother cytoskeleton is the initial or final step during division and this gives rise to either external budding or internal budding, respectively (Gubbels et al., 2021). Yet another distinguishable feature between the division modes is whether the karyokinesis module occurs after the DNA replication and segregation module. This is due to the synchronous budding of nuclei situated in the same cytoplasm and necessitates a synchronizing process in the case if the nuclear division is asynchronized. Overall, all the division modes (almost always) result in an even number of progenies (Gubbels et al., 2021).

The variability of the asexual cell division modes among apicomplexans is attributed to differences in budding through the membrane skeleton assembly which lies beneath the plasma membrane. The assembly of the cytoskeleton is initiated from the centrosomes and the three main conserved elements of the cortical cytoskeleton (alveolar vesicles, the alveolar meshwork, and the subpellicular microtubules) are assembled in a concerted fashion following a

direction from the apex to the basal end of the parasite (Gubbels et al., 2020). A further common characteristic is the linking of budding to a round of S and M phase (Francia & Striepen, 2014; Suvorova et al., 2015).

The specific replication scheme where daughter parasites are formed internally entails endodyogeny and endopolygeny whereas daughter parasite budding from the periphery (externally) entails schizogony and binary fission.

Schizogony meaning 'multi-fission' is usually attributed to modes of division that generate more than two daughter parasites from a single round of division (Gubbels et al., 2020). This process is characterized by the formation of daughter parasites from the periphery of the parasite. For example, the best studied system in which schizogony occurs is within the *Plasmodium* species. After the *Plasmodium* sporozoites invade the liver cells, they undergo a single cycle of schizogony in order to form tens of thousands of progeny cells following the schizogony scheme. The same scheme is followed by *Plasmodium* during asexual division within the red blood cells (Gubbels et al., 2021). The defining trait of external budding is that right after the parasite invades the host cell, the mother cytoskeleton starts to disassemble (Gubbels et al., 2020). Breaks in the IMC appear in the middle near the nucleus. This is followed by the bulging of the cytoplasm in an outwards direction. The IMC is seperated from the plasma membrane and the sporozoite distal ends disappear within 24 hours-time all the while the zoite rounds up in appearance (Jayabalasingham et al., 2010). This is followed by the re-organization of the alveolar cytoskeleton and the degradation of the micronemes and rhoptries. The microtubules remain with the IMC while it is being broken down during the initial phases (Verhave & Meis, 1984). The resulting cell undergoes multiple rounds of DNA replication and nuclear division which occurs devoid of budding. In this case, nuclear division is asynchronous, and it is only the last round of S phase and mitosis which is synchronous and is followed by a synchronized budding step (Ferguson et al., 2008; Kono et al., 2016; Rudlaff et al., 2019). Prior to external budding, the centrosomes' inner and outer cores are activated yet the exact timing entailing the initiation of budding remains to be elucidated (Gubbels et al., 2020).

Endopolygeny is an internal budding process which results in the production of more than two daughter parasites simultaneously. These daughter parasites are produced within the cytoplasm and not from the periphery of the parasite which is the case in *Plasmodium* schizogony. The main distinguishable feature of this mode of division is that the mother cytoskeleton is retained throughout the division process and is only disassembled right before the daughter cells emerge at the end of the cell cycle. In fact, in *T. gondii* and *Cystoisospora suis* endopolygeny, the timing of emergence of daughter cells from the mother parasite overlaps with the mother cytoskeleton's destruction (R. Dubey et al., 2017; Gubbels et al., 2020).
This type of asexual division consists of two sub-types: Endopolygeny with karyokinesis and in this case the mother cell is multi-nucleated. The second sub-type involves endopolygeny with no karyokinesis and in this case the mother cell

consists of one large polyploid nucleus. The two subtypes of internal budding are adopted by tissue cyst forming Coccidia, particularly Sarcocystidae.

Another internal budding process is endodyogeny which results in the production of two daughter cells within the mother cell. This type of asexual division is carried out by *T. gondii* tachyzoites and bradyzoites. This division mode is also used by several genera belonging to Sarcocystidae which includes *Hammondia*, *Neospora*, *Besnotia*, and Sarcocystis neurona during the stages of tissue cyst development. In this case, the mother cytoskeleton is not disrupted right after the invasion of the host cell, and it is exclusively at the very final steps of cell division where the parental cytoskeleton is disrupted, and the plasma membrane is delivered to the two budding daughter cells. This process is mediated by the recruitment of the glideosome to the IMC , and is responsible for suturing the daughter IMC outer membrane and the plasma membrane following a direction from the parasite's apex to its basal pole (Frénal et al., 2014; Gaskins et al., 2004).
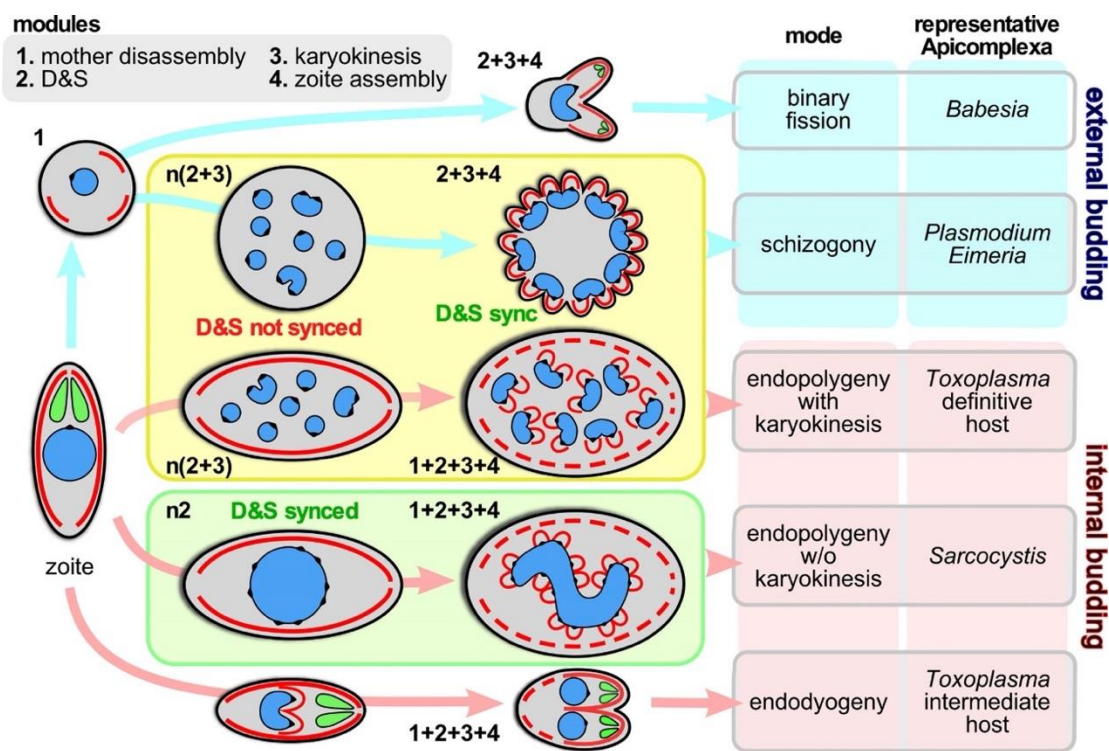
Figure 16-Schematic representation of the different modes of division present among apicomplexans (Gubbels et al., 2021). The division modes of Apicomplexa are categorized into internal and external budding. The yellow box contains division modes where karyokinesis occurs after D&S whereas the green box contains a division mode in which karyokinesis does not take place after D&S. 'D&S' stands for DNA replication and segregation. 'n' demonstrates that the modules are repeated. Blue represents the nucleus. The black dot on the nucleus represents the centromere cluster present at the centrocone. The red lines represent the IMC/cytoskeleton. The rhoptries are represented in green.

Modes of division vary not only between species but also between the different developmental life stages of a single species and this variation can be due to a number of genetic and environmental factors (Gubbels et al., 2021). For example, the number of daughter parasites varies from one mode of division to another ranging from two daughter cells produced from *T. gondii* endodyogeny to several thousands of daughter cells generated from *Plasmodium* schizogony. The host cell environment can be manipulated by the parasite to accommodate for the number of progenies produced by host cell expansion. The host liver cell of *Plasmodium* can expand to accommodate up to 90,000 merozoites from the infection of one lone sporozoite (Vaughan & Kappe, 2017). Another example is the parasite's ability to respond to certain environmental factors such as phosphatidic acid (PA) and the decrease in the parasite's pH level which results in the egress of the parasite (Bisio et al., 2019; Roiko et al., 2014).

Overall, the in-depth study of asexual cell division in apicomplexans has allowed for laying out a distinct set of guidelines or rules which are characteristic of this phylum and are applicable to all modes of asexual division. Hence, in the case when the replication and segregation of DNA is not followed by karyokinesis, DNA replication and segregation cycles of nuclei present in the same cytoplasm are asynchronous. Another rule is that although the parasite can harbor multiple rounds of DNA replication and karyokinesis, it is necessary to have a final round of karyokinesis after DNA replication in order to activate the formation of daughter zoites. Furthermore, budding is always synchronized across the cell cycle and almost nearly all modes of division result in an even number of offspring (Gubbels et al., 2021).

Atypical cell cycle across the Apicomplexa phylum

Contrary to the conventional eukaryotic cell cycle, the Apicomplexan cell cycle lacks a G2 phase and is composed of distinct phases that transition in a precise order and include: G1, S, and M (J. Radke, 2001). In *T. gondii*, the tachyzoite cell cycle is initiated by a gap phase, G1 which is dedicated to the biogenesis of protein and RNA constituents, this first half of the G1 phase is termed 'G1a'. After this, another phase follows and is characterized by the production of components needed for the production of DNA. This phase occurring in the second half of the G1 phase is termed 'G1b' (Behnke et al., 2010). The following S phase includes replication of the chromosomes followed by their segregation during the M (mitosis) phase (White & Suvorova, 2018) (Figure 17, following page).

Apicomplexans perform a closed mitosis and possess the core machinery necessary for the synthesis of DNA which is highly conserved among eukaryotes and includes all of the MCM helicase subunits as well as specific DNA polymerases (Naumov et al., 2017). The initiation of the G1 phase in Apicomplexans is most likely triggered by the transduction of signaling cascades through the phosphorylation functions of various kinases (Brown et al., 2017). These signaling pathways are responsible for the ordered biogenesis cascade (Behnke et al., 2010; Bozdech et al., 2003).
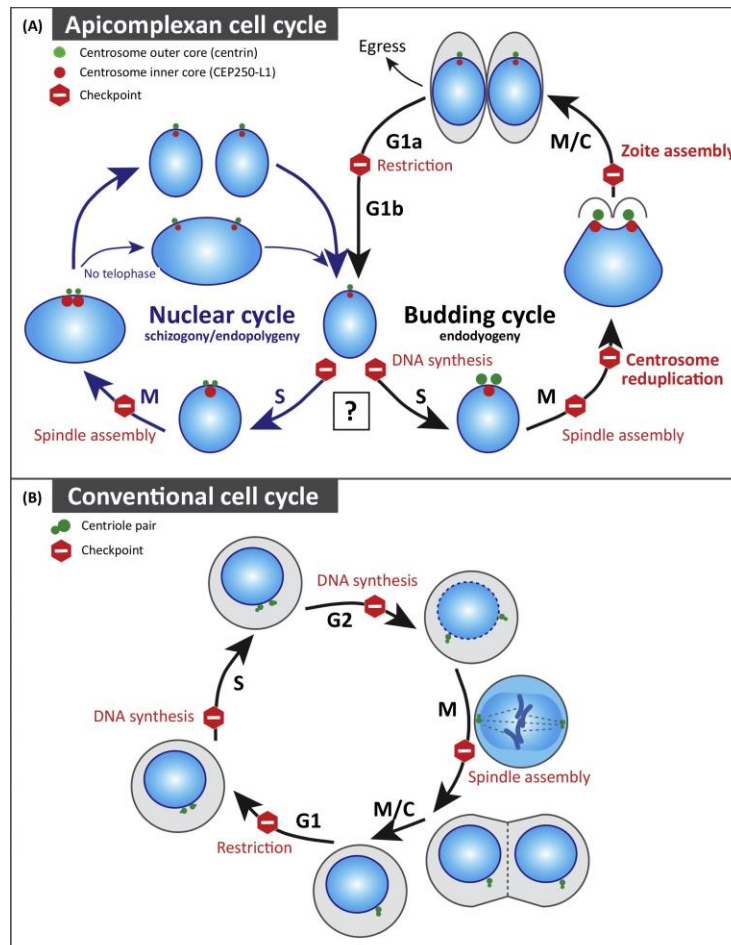
Figure 17 - Schematic representation of the cell cycle comparing (A) Apicomplexan cell cycle phases to (B) conventional ones and their associated checkpoints (White & Suvorova, 2018). In the conventional cell cycle, there exists two separate growth phases (G1 and G2). Chromosome replication within the cell cycle is conducted by the 'once only' rule. In opposition to the Apicomplexan cycle which is a more complex cycle and has many regulatory points. In Apicomplexa, the parasites either undergo a separate nuclear cycle represented by blue arrows characterized by a dissociation of the nuclear segregation from the budding cycle or a nuclear cycle accompanied with the budding cycle represented by black arrows and chromosome replication is segregated in synchronization with the formation of the daughter parasites.

5.6 Cellular division in *Toxoplasma gondii*

T. gondii tachyzoites and bradyzoites replicate through an internal budding system known as endodyogeny. This division is characterized by an intertwined connection between mitosis and cytokinesis. Asexual division in *T. gondii* involves a haploid genome (1N) with the parasite's DNA content accommodated within 13 chromosomes (Bunnik et al., 2019). The nuclear cycle occurs within the nuclear envelope and mitosis is closed.

During nuclear replication, the chromosomes remain minimally condensed with the centromeres clustered at the periphery (White et al., 2004). Chromosome replication pauses during the late S phase and a dominant sub-population

possessing 1.8 N emerges. In accordance with the emergence of the 1.8 N subpopulation, the assembly of the spindle poles and spindle is carried out. This is then followed by nucleation of the two developing buds close to the centrosomes (J. Radke, 2001; White et al., 2004).

Centrosome division and regulation

The *T. gondii* centrosome plays a major role during cell division (mitosis, karyokinesis and cytokinesis). The centrosome is considered to be a centriole-associated organizing center or MTOC (Microtubule Organizing Center) in *T. gondii*. After the association of the centrosome with the Golgi organelle and its division via lateral elongation which occurs during the G1 phase (Hartmann et al., 2006; Nishi et al., 2008; Pelletier et al., 2002), the centrosome duplicates at the basal end of the nucleus which is then followed by migration of the replicated centrosomes towards the apical end of the nucleus during the S phase (Hartmann et al., 2006). The centrosomes have a particular bipartite structural organization and are composed of an inner core and an outer core (Suvorova et al., 2015).

At the G1 phase, the parasite possesses a condensed centrosome which augments in size through the progression of G1 and is associated with the nuclear envelope. This is followed by the expansion and replication of the outer core centrosome during the late G phase. At the same time, the inner core centrosome partitions from the outer core centrosome yet remains connected to the centrocone which is a specialized conical-shaped structure with an important role during mitosis in members of the Apicomplexan phylum (Suvorova et al., 2015; Ferguson et al., 2008). These centrocones are situated close to the location of chromosome tethering at the interphase stage (Anderson-White et al., 2012; Francia et al., 2014; Brooks et al., 2011). In addition, centrocones are structures through which spindle fibers pass through to gain access into the nucleus in order to carry out the separation of chromosomes during the mitosis stage (Francia et al., 2014). After the outer core replication, the inner core centrosome duplicates all the while the spatial orientation remains intact with the inner core in proximity to the nucleus and the outer core distal from the nucleus. Super-resolution microscopy exhibited that the outer cores, inner cores, and centromeres are aligned in a linear fashion (Suvorova et al., 2015). During the final stage of mitosis, the centrocone which consists of the TgMORN1 protein is segregated into two distinct entities. At the end of daughter parasite formation, each daughter parasite is equipped with one core of each centrosome type (Figure 18, following page).
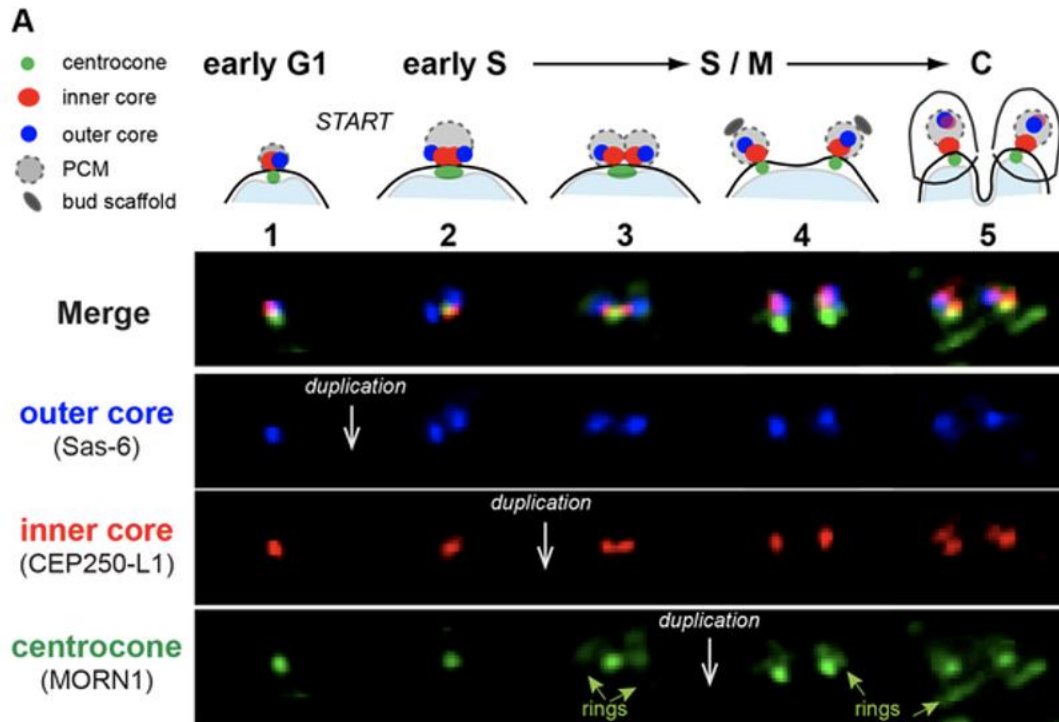
Figure 18 - Development of *T. gondii* centrosome during cell division (Suvorova et al., 2015). There are five states which the centrosome transitions through throughout the different stages of the cell cycle. During the S phase, centrosome replication is initiated by division of the outer core which is represented in blue (TgSas-6). This is then followed by division of the inner core which is represented in red (TgCEP250-L1). Finally, the centrocone represented in green (TgMORN1) is duplicated.

Several proteins have been found to localize at the inner or outer centrosome. TgSfi1 is an outer core centrosome protein and the corresponding temperature sensitive mutant displayed growth arrest at an elevated temperature of 40°C. At this temperature, the mutant parasites exhibited a severe defect in parasite budding with the capacity of nuclear replication. This resulted in unequal distribution of DNA and nucleus and even tachyzoites that were devoid of a nucleus (Suvorova et al., 2015). TgSfi1 is closely associated to TgCentrin1 at the outer core and the absence of TgSfi1 resulted in a severe decrease in TgCentrin1 associated cores at 40°C (Suvorova et al., 2015). In addition, the TgCep250-L1 protein associated with the inner core centrosomes resulted in the over amplification of TgCep250-L1 associated inner cores and were localized in an independent manner to the remaining outer core centrosomes.

The outer core and inner core structures are uncoupled from each other (Surovora et al., 2015). The two regions of the centrosome have distinct functions. The inner core of the centrosome has a principal role in karyokinesis whereas the outer core functions in driving cytokinesis and has an important role in the formation of daughter parasites (Suvorova et al., 2015).

The duplication of the centrosome cores requires the presence of regulatory mechanisms. Several kinases are involved in the division of the centrosome such as TgNek1(NIMA related kinase) (C.-T. Chen & Gubbels, 2013), TgArk1/2/3 (Auorora Kinase) and TgMAPK-L1 (Mitogen-activated protein kinase L1)(Berry et al., 2018; Suvorova et al., 2015), and TgCDPK7 (Morlon-Guyot et al., 2014). TgMAPK-L1 was demonstrated to have an important role in the coupling of mitosis and cytokinesis. Temperature-sensitive TgMAPK-L1 mutant parasites demonstrated severe defects in coordination between mitosis and budding and resulted in multiple buds and nuclei. TgMAPK-L1 is a kinase which has a key role in the regulation of the nuclear replication and normal budding of the parasite by ensuring the proper duplication of the centrosome occurs (Suvorova et al., 2015) Another kinase with an important role in regulating centrosome replication is TgNek1 (C.-T. Chen & Gubbels, 2013). Mutant parasites with a temperature sensitive mutant V-A15 which consists of a point mutation in TgNek1 displayed a defect in parasite budding. The mutant parasites harbor centrosomes which have two linked globular structures with a dumbbell-shape. In these mutants, the centrosomes replicate but there is a defect in their separation (C.-T. Chen & Gubbels, 2013). Furthermore, TgArk3 which is localized at the centrosome and partially associated with TgCentrin1 at the outer core was demonstrated to have an important role in regulating centrosome division (Berry et al., 2016). Mutant parasites depleted of TgArk3 displayed a defect in daughter cell formation with a normal nuclear cycle but an impaired budding and cytokinesis (Berry et al., 2016). By contrast, TgArk2-deficient parasites did not display any notable phenotype (Berry et al., 2016). Calcium-dependent protein kinase 7, TgCDPK7 exhibits a role in maintaining the integrity of the centrosome by having a key role in the proper positioning and segregation of the centrosomes (Morlon-Guyot et al., 2014).

During mitosis, Striated-Fiber Assemblin proteins termed TgSFA2 and TgSFA3 emerge from centrosomes with the goal of tethering the forming apical complex of future daughter cells to the centrosomes. Loss of either SFA proteins results in subsequent loss of daughter cell formation (Francia et al., 2012).

Daughter cell formation

The *T. gondii* tachyzoite internal budding process is propelled by the formation of the daughter parasite's cytoskeleton (Striepen et al., 2007) (Figure 19). The formation of nascent parasite cytoskeletons is initiated at the centrosomes (Hu, 2008) The cytoskeleton grows as mitosis and cytokinesis occur concurrently following an apical to basal direction of growth. After migration of the centrosomes to the apical side of the nucleus and their alignment with the centrocone, the first feature of the daughter cytoskeletons to appear are small hazy entities that form close to the centrosomes and can be labelled with TgMORN1 (Gubbels, 2006; Hu, 2008; Hu et al., 2006). These TgMORN1 bodies develop into basal complexes. TgMORN1 rings are found in mature parasites at both apical and basal ends. With the progression of division, the TgMORN1 rings move towards the basal end of the developing parasites aided by the polymerization of microtubules (Gubbels, 2006). The apical complex including the conoid are formed after MORN1 rings are made (Hu, 2008). This is then followed by the localization of the conoid towards the apex and the migration of the basal ring longitudinally across the nucleus.

The formation of the IMC involves two subsequent steps. The IMC is assembled *de novo* during the elongation of the IMC of the daughter cells present within the mother cell. This is then followed by recycling the mother cell's IMC membranes after the daughter cells emerge from the mother cell (Ouologuem & Roos, 2014). The assembly of IMC proteins follows a temporal sequence and a spatial pattern, they are expressed in a 'just in time' cell-cycle dependent manner exactly at the time when they are required for assembly (Anderson-White et al., 2011).

In the final steps of internal budding, TgCentrin2 starts to accumulate at the basal edge of the MORN1- ring and has an important role in its constriction designating the basal region of the daughter cells (Gubbels, 2006; Hu, 2008).
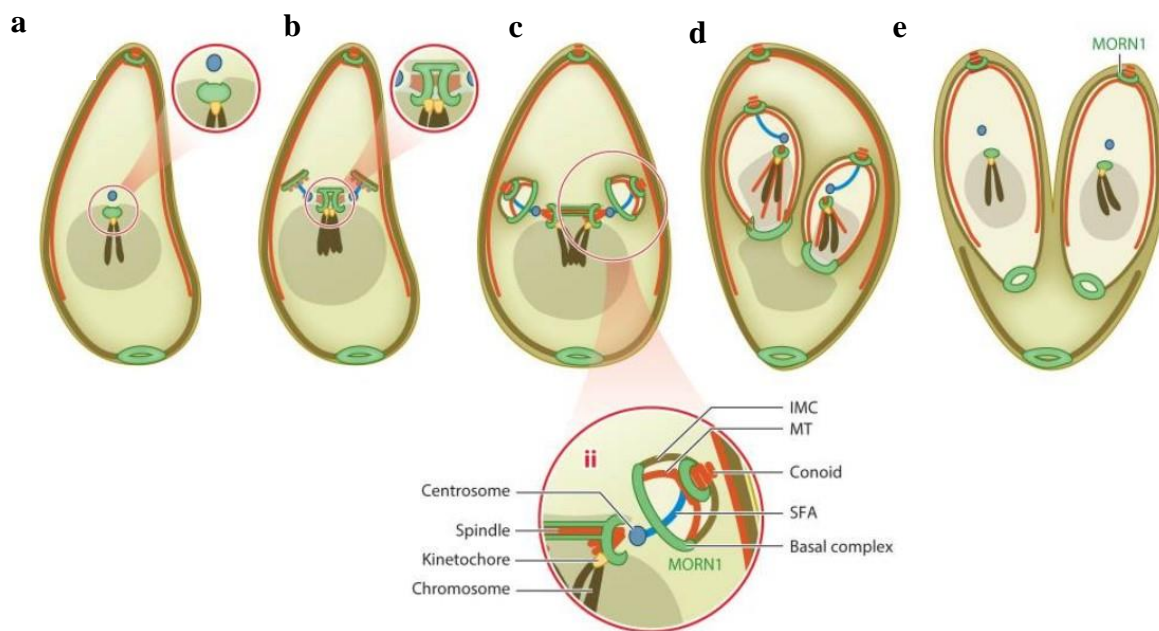
Figure 19 – Schematic representation of the tachyzoite's cortical cytoskeleton during cell division (Blader et al., 2015). (a, b) Closed mitosis occurs without the condensation of chromosomes which cluster at the centrosomes and are anchored by the kinetochore at the centrocone. (c) Construction of the cortical cytoskeleton of the two daughter cells with formation driven from the apical pole to the basal end. (d) The nucleus of the mother cell is anchored to the forming daughter cells by the centrosome which is connected to the conoid by SFA. (e) Daughter cells are separated when the basal complex becomes constricted during the late stages of the cell cycle.

The various organelles are divided and segregated in the forming daughter parasites in a tightly coordinated manner (Nishi et al., 2008). The division of the organelles follows a precise order and is initiated by the division of the Golgi and the centrosome (Figure 20). This is then followed by apicoplast division. The division of the apicoplast occurs concurrently with the parasite's nuclear division (Striepen et al., 2000). During division, the ends of the apicoplast are linked to the centrosomes of the mitotic spindle. Time-lapse video microscopy allowed to

visualise the progression of apicoplast division which occurs at the apical end of the nucleus (Striepen et al., 2000). At the beginning of the parasite's cell division, the apicoplast retains an ovoid shape, which then elongates to form a U-shaped intermediate with its ends pointing towards the apical tip of the parasite. This is then followed by fission allowing for the complete segregation of the plastid into two daughter plastids. The fission of the apicoplast occurs right before the daughter parasites emerge from the mother cell (Striepen et al., 2000). In fact, during endodyogeny the plastid does not only associate with the centrosomes but also associated with the spindle and the inner membrane complex (Striepen et al., 2000).

Electron microscopy of the tachyzoite apicoplast has allowed for the observation of division rings suggesting that there may potentially be ring-forming proteins that mediate apicoplast fission (Matsuzaki et al., 2001). Fission occurs exactly at the base of the U shape within the intermediate apicoplast form with TgDrpA having a direct role in apicoplast fission (van Dooren et al., 2009). Apicoplast division is followed by the division of the endoplasmic reticulum, which is followed by mitochondria division (Gubbels, White et al., 2008; Nishi et al., 2008).
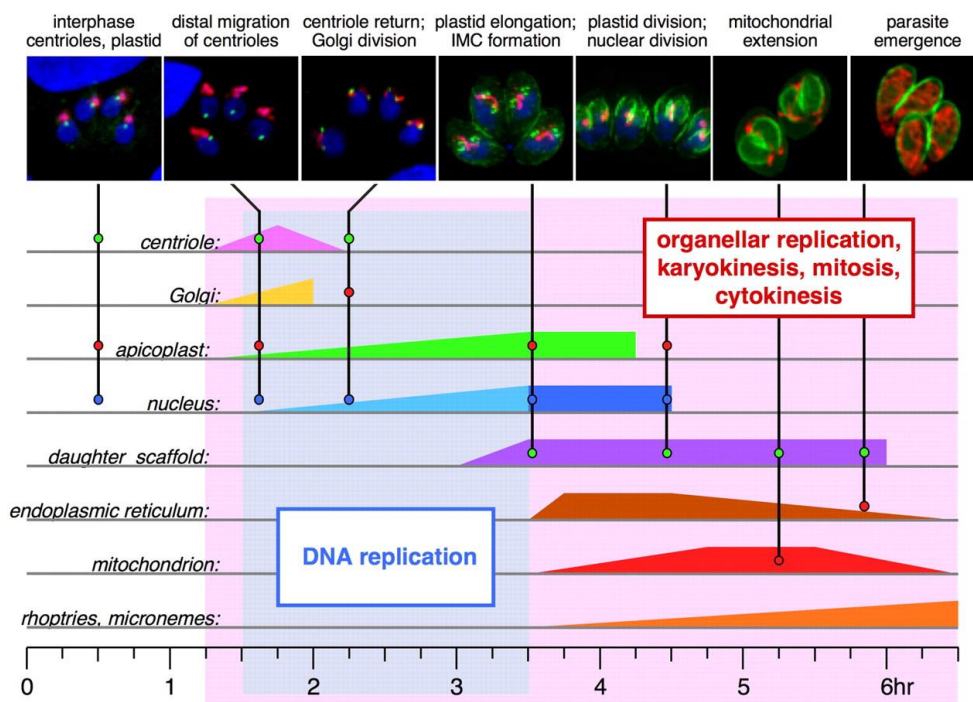
Figure 20 – Schematic representation of the organellar replication cell cycle timeline (Nishi et al., 2008). The coordination of organellar replication is depicted with the duration of replication of each organelle represented along the timeline. Images corresponding to the morphological replication events representing the precise timepoint at which each organelle divides are represented in the upper most panel.

Rhoptries and micronemes, the secretory organelles of the parasite are synthesized *de novo* within each daughter parasite cell rather than being inherited from the mother parasite (Nishi et al., 2008). After the formation of the

rhoptries and micronemes, they associate with the apical complex at the apex of the parasite. This process is thought to be dependent on cytoskeletal components which function as paths for molecular motors by carrying these organelles to the apical tip of the daughter parasites (Francia & Stripen, 2014). The mitochondrion divides late during the cell cycle and is integrated into the daughter cells at the very end of the cell cycle when the daughter parasites are almost completely emerged from the mother parasite (Nishi et al., 2008). This is then followed by the acquisition of the plasma membrane from the mother cell during the cytokinesis phase (Gubbels et al., 2008). Once the organelles have been assembled within the developing daughter parasites, the daughter cells start to emerge from the mother cell leaving behind remnants which consist of degraded mother cell secretory organelles and parts of the mother cell mitochondrion in form of the residual body (Attias et al., 2019; Muñiz-Hernández et al., 2011; Nishi et al., 2008). The formation of daughter parasites requires approximately 6-7 hours to complete in a type I strain. Once the daughter cells completely emerge from the mother cell, they can initiate another cycle of division (Figure 20).

5.7 Host cell lysis and parasite egress

After the tachyzoite replicates intracellularly, it actively egresses by rupturing the host cell. To date, the signals that trigger the parasite's egress are not very well comprehended. Egress of the parasites occurs after they detach from the IVN, the rosette becomes disrupted, and the PVM becomes displaced towards the nucleus of the host cell (L. A. Caldas & de Souza, 2010). The PVM is then destroyed, and the parasites glide freely within the host cell's cytoplasm and eventually rupture the host cell plasma membrane. Among the signals that trigger the egress of the parasites from the host cell is a drop in the pH level, a reduction in the concentration of potassium ions and phosphatidic acid build-up in the PV (Bisio et al., 2019; Roiko et al., 2014; L. Yang et al., 2019).

The accumulation of ABA during the development of the parasite functions as a quorum sensing mechanism for the parasite's egress. ABA concentrations increase immediately before tachyzoites exit from the host cell whereas ABA concentrations stay decreased during the replication process. ABA triggers the release of parasites from the host cell through activation of the release of intracellular calcium, this coincides with microneme secretion and motility of the parasite leading to its egress (Nagamune et al., 2008). A prior study on the causes of egress linked the permeability of the host cell membrane to the sudden decrease in potassium concentration describing that the host cell membrane becomes permeable exactly 2-3 minutes before actual egress. After analyzing the specificity of the ion concentration, it was found that the decrease in cytoplasmic potassium ions triggers parasite release (Moudy et al., 2001). In another independent study, the activation of nucleoside triphosphate hydrolases (NTPases) was demonstrated to promote parasite egress by effectively depleting the PV of ATP necessary for the release of Ca^{2+} ions that are ATP dependent (Stommel et al., 1997). In addition, cysteine proteases such as calpain most likely play an important role in PVM and host cell membrane disruption, therefore contributing to parasite egress. Calpain activation is most likely achieved as an end-result of the parasite's perforin function (Chandramohanadas et al., 2009).

Acidification of the PV activates microneme secretion and promotes the activity of perforin-like protein 1 (*Tg*PLP-1) (Roiko et al., 2014). The secretion of TgPLP-1 is dependent on calcium secretion and is necessary for the permeabilization of the PVM. Additionally, *Tg*PLP-1 forms pores of ~100 Å in diameter within the host cell's membrane consequently leading to its disruption and therefore facilitating the exit of the parasites from the host cell. Studies on *Tg*PLP-1 depleted parasites demonstrated that the mutant parasites were not able to exit and remained entrapped within the host cell (Kafsack et al., 2009; Kafsack & Carruthers, 2010).
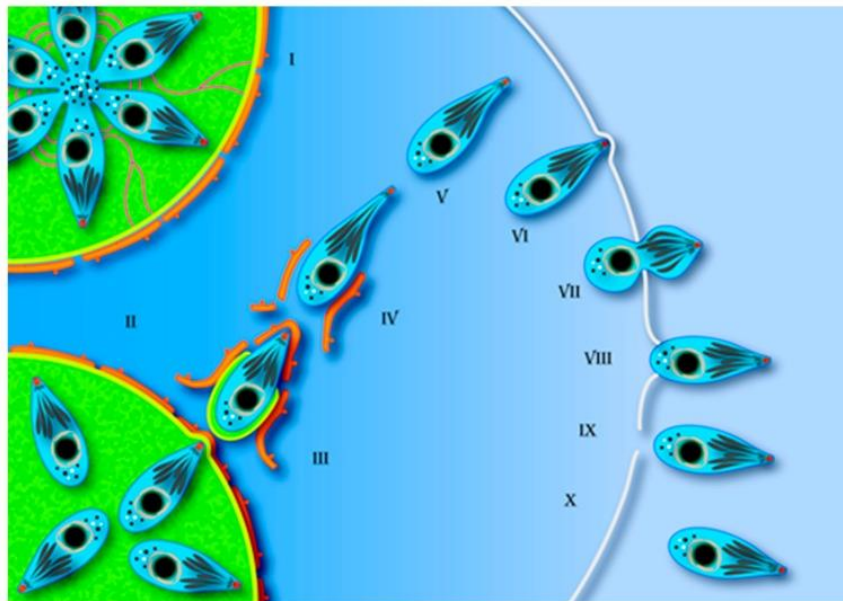
Figure 21 – Schematic representation of tachyzoite egress in *Toxoplasma gondii* (L. Caldas & De Souza, 2018). (**I**) Rosette organization of the tachyzoites after several cycles of asexual replication. (**II**) Parasites become motile after egress signaling takes place and rosette conformation is disrupted. Permeabilization of the PVM is achieved which allows for the tachyzoites to emerge within the host cell's cytosol. PV membrane and ER host cell remnants are dragged along with the tachyzoite and are represented in red. (**III**) and (**IV**) The tachyzoite's cell body can either become stretched or constricted (**V**) the tachyzoite releases the host cell remnants as it moves through the cytosol (**VI**) and (**VII**) the parasite conforms to an hourglass form as it traverses the host cell plasma membrane. During the final steps of the egress process (**VIII**), the host cell plasma can become either disrupted which occurs during collective egress (**IX**) or re-seal as in (**X**).

In addition, egress of parasites can be provoked by the host's immune system through the involvement of lymphocytes. T-cells that affect infected *T. gondii* cells via death ligand or perforin/granzyme-dependent cytotoxicity result in host cell destruction triggering the egress of the infectious parasites within the host with the capacity of infecting the surrounding neighboring cells (Persson et al., 2007).

6 Gene Regulation in *Toxoplasma gondii*

The *T. gondii* parasite utilizes main transcriptional machinery to regulate the expression of genes coding for proteins. This machinery involves RNA polymerase II and its corresponding general transcription factors (GTFs). An in-depth analysis of GTFs and the nuclear polymerases suggest the conservation of the transcriptional machinery within eukaryotes (Ranish & Hahn, 1996).

6.1 The parasite transcriptome and transcriptional regulation
a) General mechanisms of transcription

In eukaryotes, transcription requires several coregulatory complexes working simultaneously to ensure that RNA of a specific genomic locus is transcribed in a correct manner. *Toxoplasma* possesses homologs of RNA polymerases required in other well-studied eukaryotes, RNA polymerase I which synthesizes ribosomal RNA (rRNA), RNA polymerase II which synthesizes transcripts encoding for proteins (mRNA), and RNA polymerase III which synthesizes small RNAs (tRNA) (Meissner & Soldati, 2005). *Cis*-acting promoter elements are bound by activating transcription factors (ATFs). These ATFs are responsible for recruiting chromatin remodelling enzymes which modify chromatin near the cis-element area by relaxing it. In addition, a multi-subunit Mediator complex, which is recruited by the chromatin remodelling enzymes, activates the RNA polymerase II preinitiation complex (PIC) (Blazek et al., 2005). There are a variety of factors that dictate whether the cis-elements are accessible to the ATFs such as their interaction with the chromatin remodelling enzymes, the condition of the chromatin at the cis-element regions, and the cell cycle stage (Fry, 2002). As soon as the chromatin relaxes, the PIC is established at the core promoter elements in accordance with the Mediator, RNA polymerase II, and GTFs.

The largest subunit of RNA polymerase II (TgRPB1) is characterized by the presence of a carboxy-terminal domain (CTD), which is progressively phosphorylated during the progression of transcription. Phosphorylation of TgRPB1 occurs at two serine residues, serine 5 and serine 2 (Deshmukh et al., 2016,2018). The CTD of TgRPB1 consists of nine heptapeptide YSPxSPx sequences with a high conservation of serine 5 and serine 2 residues (Deshmukh et al., 2016). The phosphorylation of the serine 5 residue of TgRPB1 is mediated by cyclin-dependent kinase, TgCdk7 (Deshmukh et al., 2016). Additionally, activated Cdk-related kinase, TgCrk9 phosphorylates the CTD of TgRPB1 since the impairment of the kinase activity of TgCrk9 results in reduced phosphorylation of TgRPB1 serine 2 residue (Deshmukh et al., 2018).

Promoters of class II genes which are protein encoding genes include core promoter elements (CPE) which are composed of a TATA box, an initiator (INR), and downstream promoter elements (DPE) (Lemon, 2000; Shandilya & Roberts, 2012). In *Toxoplasma*, particular components remain absent such as the TATA-box, the CAAT box, and SP1-motifs.

Downstream promoter elements are recognized by several GTFs and which include TATA binding proteins (TBPs), TFIIA, TFIIB, TFIID, TFIIE, TFIIF, and

TFIIH (Blazek et al., 2005; Featherstone, 2002; Ranish & Hahn, 1996) which allow for binding of RNA Pol II to DNA. In *Toxoplasma*, some GTFs and TAFs (TBP associated factors) were not found by homology searches (Meissner & Soldati, 2005). However, two TBP homologues were identified, and chromatin immunoprecipitation experiments were carried out by Hakimi *et al* (data available on toxodb.org).

A recent study was carried out by the Lourido lab in which transcription initiation at *T. gondii* promoters in acute and chronic stages were analysed in-depth at nucleotide resolution (Markus et al., 2020). 5' end RNA-sequencing was used in order to generate a genome-wide map of transcription initiation during acute tachyzoite and chronic bradyzoite stages (Markus et al., 2020). This allowed for assigning transcription start sites (TSSs) for 7603 protein-encoding genes (~91%). However, 66% of the TSS predictions differed from the gene models that were available on ToxoDB by a length of more than 40 nucleotides. Additionally, this analysis demonstrated the presence of stage specific alternative TSSs that produce mRNA isoforms with specific 5' ends (Markus et al., 2020). 26 genes were validated to have alternative TSSs after manual inspection. Among these 26 genes, 16 demonstrated a shift in stage-specific usage whereas the remaining 10 genes possessed alternative TSSs which were used at similar levels in a stage-independent manner. For example, *TGME49_200250* illustrated *bona-fide* alternative stage-dependent usage, with a shift leading to an extension of 649 nucleotides (Markus et al., 2020).

In *T. gondii*, the TSS is positioned deep within the +1 nucleosome located at approximately 41 bp from its upstream end (Markus et al., 2020). This model of nucleosome internally located TSS is similar to that found in yeast (Albert et al., 2007). *T. gondii* 5' leaders which represent the entry point for the ribosome during translation that is cap-dependent are one of the longest in eukaryotes reaching up to a length of ~800 nucleotides (Markus et al., 2020).

b) DNA motifs in promoters

T. gondii is also characterized by the presence of specific regulatory elements localized upstream of the target promoter.

The promoter that codes for the main surface antigen, SAG1 contains a cis-element consisting of 6 tandem repeats of 27 bp. The tandemly repeated repeats have an important role in directing the start of transcription (Soldati & Boothroyd, 1995) and is characterized by the presence of a central heptamer motif (A/TGAGAGC) (Bohne et al., 1997; Matrajt et al., 2004; Mercier et al., 1996; Nakaar et al., 1998). When studying promoters controlling the expression of MIC proteins, two conserved sequences were identified: 5'GCGTCDCW also known as the MICA motif and 5'SMTGCAGY also known as the MICB motif. The MICA motif is similar, in reverse orientation, to the conserved cis-acting element in the promoter of TgSAG1 (Mullapudi et al., 2009).

In addition, specific regulatory cis elements were found to be dependent on the parasite's developmental stage. A study on the promoters regulating bradyzoite-specific genes demonstrated that the presence of cis-regulatory elements is

necessary for gene transcription (Behnke et al., 2008). The promoter of bradyzoite-specific gene *TgB-NTPase*, consisted of two regulatory motifs: TGTGTG and CAGC. Another bradyzoite-specific gene *TgBAG1*, possesses a promoter containing a regulatory motif: TACTGG (Behnke et al., 2008). In a study regarding the binding profile of a myb-like TF, TgBFD1 which represents a master regulator of bradyzoite differentiation (Waldman et al., 2020), in which the CUT & RUN method was used (Skene & Henikoff, 2017), TgBFD1 was demonstrated to bind to 509 genes and the binding sites are preferentially located close to TSSs (Waldman et al., 2020). Analogous motifs (CACTGG) were identified by carrying out motif enrichment analysis. These motifs were found to be positioned upstream of bradyzoite-specific genes. Additionally, they were found upstream of TgBFD1's own promoter, and early bradyzoite marker AP2 TF, TgAP2IX-9 (Waldman et al., 2020)

Furthermore, nucleotide resolution TSS data allowed for the identification of a novel motif gCATGCa which was identified to be present in 44% of *T. gondii* promoters and located at approximately 82 nucleotides upstream of TSSs (Markus et al., 2020).

c) transcriptome

The *Toxoplasma* genome has been proven to possess a scarcity of gene clusters with a few virulence gene clusters characterized (Adomako-Ankomah et al., 2014; Blank & Boyle, 2018) indicating that the regulation of transcription is performed at the promoter level.

Initial studies on the *T. gondii* transcriptome resulted in the construction of a limited cDNA microarray that studied tachyzoite-bradyzoite transitions as well as gene expression in strains with impaired bradyzoite differentiation. Results from these studies demonstrated that developmental life stages of the parasite relied on transcriptional regulation. In addition, a strong correlation between the mRNA levels of parasites in the bradyzoite stage and bradyzoite-specific proteins was found and this suggested a hierarchical induction of gene regulation during bradyzoite differentiation (Cleary et al., 2002; Singh et al., 2002). Additionally, the analysis of the *T. gondii* transcriptome by SAGE (Serial Analysis of Gene Expression) at different developmental stages of the parasite demonstrated that gene expression mechanisms are associated with the transitions of the different developmental stages of the parasite (J. Radke et al., 2005).

During the tachyzoite cell cycle, several transcripts encoding for basal metabolic mechanisms and subcellular structures are expressed by the parasite solely when required during growth and development (Behnke et al., 2010). This is similar to the 'just-in-time' concept initially described in *Plasmodium* (Bozdech et al., 2003). In *T. gondii* tachyzoites, the expression of more than one third of genes which is equivalent to 2833 genes have been shown to be tightly regulated with peaks of expression at specific time-points during the cell cycle (Behnke et al., 2010). The analysis of synchronous tachyzoite culture indicated the presence of two major transcriptional waves. These two waves represent two functionally distinct sub-transcriptomes. The G1 sub-transcriptome includes the expression of conserved eukaryotic genes that are essential for main biosynthesis activity and metabolic

functions. However, the S/M sub-transcriptome is characterized by the expression of genes which are apicomplexan-specific and essential for parasite development, the development of specific apicomplexan organelles (rhoptries and micronemes), and parasite exit from host cells (Figure 22).

A closer look at the S/M sub-transcriptome revealed that mRNA transcripts encoding for Apicomplexan-specific proteins are expressed in a precise and sequential order, with plastid genes being expressed first followed by the rhoptry genes and then those for micronemes (Behnke et al., 2010). This order of mRNA transcription reflects the sequential order of organelle division during the tachyzoite cell cycle (Nishi et al., 2008).
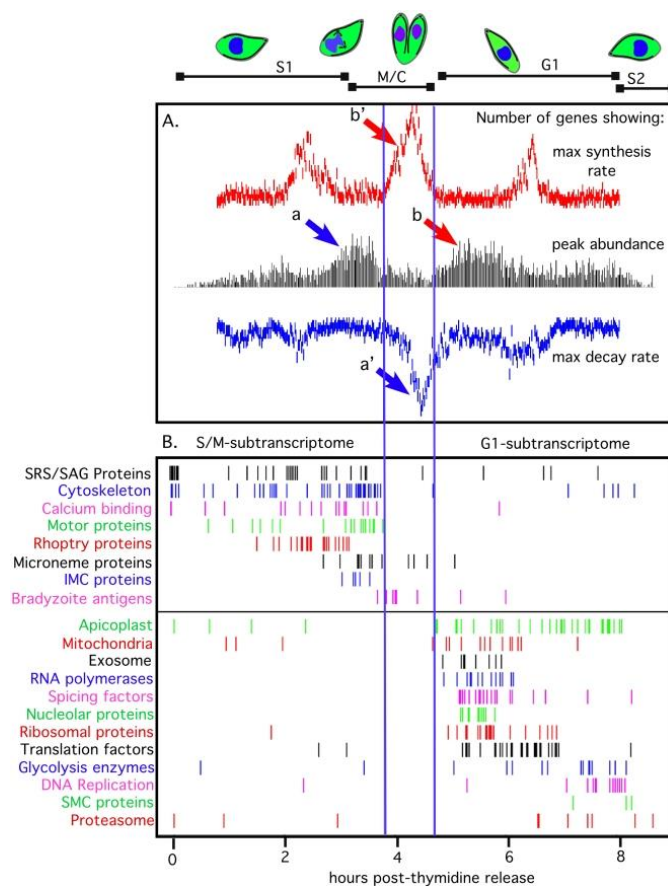
Figure 22- Representation of the two functional sub-transcriptomes of the tachyzoite cell cycle (Behnke et al., 2010). **(A)**Two main waves are present during RNA abundance peak times. These two waves correlate to the S/M and G1 sub-transcriptomes which are separated by a transition phase in which RNA is actively synthesized and decayed. The number of genes is represented by histograms. The maximum net increase in mRNA is in red, the maximum RNA abundance is in black, and the maximum net rate of RNA decrease is in blue and represented by an inverted scale during a complete *T. gondii* tachyzoite replication cycle for 8.7 hours post-thymidine release. RNA abundance peaks demonstrate the presence of two main waves of the two sub-transcriptomes. Genes labelled 'a' (black S/M histogram peak) demonstrate maximum net decrease in mRNA levels in the later transition phase peak in blue and which is labelled 'a'. Genes labelled 'b' (black G1 histogram peak) are mostly derived from the prior transition phase red peak of

maximum net increase in mRNA levels labelled 'b'`. Highly rapid increases and decreases in the expression levels of various transcripts occurs in the transition phase and this coincides with budding, initiation of the cell cycle, and decay of the mother cell. **(B)** Peaks of expression of mRNAs categorised according to their functional groups are dispersed among the two sub-transcriptomes. Genes implicated in the basal development of the parasite peak during the G1 wave whereas genes associated with Apicomplexan-specific functions peak during the S/M wave.

Single cell RNA sequencing (scRNA-seq) of tachyzoites and tachyzoites grown in alkaline bradyzoite conditions confirmed the findings of Behnke et al. (2010). In these single cell RNA sequencing studies, the presence of clusters of gene expression corresponding to the different cell cycle phases (G1a, G1b, S, M and C) was demonstrated (Waldman et al., 2020; Xue et al., 2020). The presence of bradyzoites was mostly dominant during the G1b phase (Xue et al., 2020). In addition, it was demonstrated that there is a strong correlation between the gene expression of specific proteins and the cell cycle (Waldman et al., 2020; Xue et al., 2020). Single cell RNA-sequencing carried out on tachyzoite, tachyzoite-induced cells and TgBFD1 KO cells demonstrated that cell difference was based on the cell cycle or state of differentiation (Waldman et al., 2020). Overall, these results demonstrate that in-depth study of the cell cycle by using scRNA-seq allows to establish a link between the cell cycle and bradyzoite differentiation.

6.2 Superfamily of specific transcription factors

Transcription in eukaryotes is a highly regulated process which involves a large number of proteins interacting with each other. In model eukaryotes, the basic mechanism by which transcription is controlled is by sequence-specific binding of transcription factors with DNA elements of an approximate length of ~ 5-25 bp (Wingender, 1993). These specific transcription factors regulate the transcriptional process by either activating or repressing gene expression. The Transcription Factor Database: TRANSFAC is a database containing data associated with transcriptional level gene expression and includes data on different TFs, their targeted genes, and the specific sequences to which they bind. TRANSFAC allowed for the categorization of specific TFs into five distinct super classes, and which include: TFs with basic domains (Class I), TFs with zinc-coordinating DNA-binding domains (Class II), TFs with helix-turn-helix domain (Class III), TFs with ß -scaffold factors with minor groove contacts (Class IV), and other TFs (Class V) (Coulson, 2003; Wingender, 1996). Analysis of Apicomplexan genomes such as *Plasmodium* and *Cryptosporidium* demonstrated that there are much less transcription factors in these Apicomplexa species compared to yeast or other eukaryotes (Templeton, 2004). This difference hinted towards the apicomplexans adopting different mechanisms of gene regulation. The presence of ApiAP2 TFs in apicomplexans which bind specific DNA sequences and control gene expression has been demonstrated (Balaji et al., 2005; Silva et al., 2008).
In addition, a thorough inspection of the *Plasmodium* genome indicated that there is an absence of specific transcription factors which contain a homeodomain, basic domains, and FKH domains (Aravind et al., 2003). A more recent bioinformatic-aided study suggests that the genome of *Plasmodium* species is characterized by

an absence of any basic domain and winged-helix TFs (Sardar et al., 2019). The analysis also suggested the presence of new families of TFs not previously described in Apicomplexans such as the TUB, NAC, BSD, HTH, Cupin/Jumonji, winged-helix and FHA families of TFs (Sardar et al., 2019). In *T. gondii*, no TUB proteins have been identified. Two NAC proteins (TGME49 strain) have been identified in addition to 1 BSD protein, 3 HTH proteins, 5 Cupin/Jumonji proteins, 2 winged-helix proteins, and 9 FHA proteins (Sardar et al., 2019) (Table 2).

Gene Family	Number of TFs	Gene IDs
AP2	67	TGME49_203050, TGME49_203690, TGME49_203710, TGME49_205650, TGME49_208020, TGME49_211720, TGME49_214840, TGME49_215150, TGME49_215570, TGME49_215895, TGME49_216220, TGME49_217700, TGME49_218960, TGME49_220530, TGME49_224230, TGME49_225110, TGME49_233120, TGME49_247700, TGME49_247730, TGME49_251740, TGME49_253380, TGME49_255220, TGME49_262000, TGME49_264485, TGME49_267460, TGME49_269010, TGME49_271030, TGME49_272710, TGME49_280460, TGME49_280470, TGME49_282210, TGME49_282220, TGME49_285895, TGME49_290180, TGME49_290630, TGME49_299020, TGME49_299150, TGME49_306000, TGME49_306620, TGME49_310900, TGME49_310950, TGME49_315760, TGME49_318610, TGME49_320700, TGME49_252370, TGME49_320680, TGME49_211720, TGME49_264485, TGME49_288950, TGME49_289710, TGME49_240460, TGME49_240900, TGME49_244510, TGME49_202490 TGME49_262420, TGME49_229370 TGME49_233120, TGME49_273660, TGME49_271200, TGME49_227900 TGME49_224050, TGME49_237090, TGME49_237425, TGME49_214960 TGME49_215340, TGME49_246660 TGME49_249190, TGME49_250800
CUPIN/Jmc	5	TGME49_212110, TGME49_226840, TGME49_240840, TGME49_259210, TGME49_283890
bZIP_1	1	TGME49_305220
Myb/SANT	14	TGME49_200385, TGME49_203380, TGME49_203950, TGME49_211010, TGME49_213890, TGME49_217050, TGME49_259860, TGME49_262420, TGME49_264120, TGME49_275480, TGME49_286920, TGME49_306320, TGME49_321440, TGME49_321450
HTH	3	TGME49_215950, TGME49_233160, TGME49_278530
NAC	2	TGME49_205558, TGME49_257090
HMG	5	TGME49_210408, TGME49_217500, TGME49_219828, TGME49_263720, TGME49_281900
FHA	9	TGME49_201790, TGME49_202840, TGME49_203830, TGME49_208310, TGME49_221420, TGME49_228040, TGME49_262780, TGME49_267600, TGME49_287980
Winged Helix	2	TGME49_281950, TGME49_286920

Table 2 – Different specific transcription factors present in *T. gondii* (TGME49 strain) based on an *in-silico* study (Sardar et al., 2019).

a) <u>Basic domain TFs (Class I)</u>

Basic region: leucine zipper (bZIP) proteins represent a major class of conserved transcription factors within eukaryotes and are characterized by binding to specific target DNA sites either as homodimers or heterodimers. bZIP proteins have a critical role in gene regulation. Distinct palindromic sequences are recognized by members of the bZIP family. The study of an enhancer binding protein α (C/EBP α), demonstrated that the DNA binding domain of bZIP TFs possesses a positively charged portion known as the basic region of the TF which is connected to a 'leucine zipper' consisting of a heptad repeat sequence of leucine amino acids (Landschulz et al., 1988). The peptides of these bZIP proteins bind to their associated DNA complexes inheriting a dimer formation of uninterrupted α helices. The structure formed is like a 'chopsticks-like' structure. The leucine zipper segments are the region of the protein which drive dimerization resulting in the formation of two parallel coiled-coil intertwined α helices and are situated at a perpendicular angle to the DNA helix. Each one of the basic regions of the bZIP TF remains in contact with one half of the DNA's major groove palindromic segment. The binding of bZIP to DNA leads to stabilization of the dimer and induces helical folding of the protein (Miller, 2009). In *T. gondii*, one single putative bZIP TF (TGME49_305220) has been identified based on the recent *in silico* study carried out by Sardar et al. (2019) but no other data are available on the function of this protein.

b) <u>Zinc-coordinating DNA-binding domain TFs (Class II)</u>

Specific transcription factors with zinc-coordinating domains are abundant within eukaryotic genomes. The superfamily of zinc-coordinating DNA-binding domains include the family of C_2H_2 zinc finger domain proteins, characterized by a compact globular structure and the presence of a zinc ion (Zn^{2+}) which is essential for the proper folding of the protein and is bound by two cysteine and two histidine ligands. The backbone of the polypeptide consists of an α helix and two hairpin-arranged β strands (M. Lee et al., 1989). An *in-silico* analysis of C_2H_2 zinc-coordinating TFs in eukaryotes indicated that these TFs make up for ~2,8 % of all genes in *diptera* (Chung et al., 2002), ~ 3% of all genes in mammals (Mistry et al., 2021), 0,8 % of genes in *Saccharomyces cerevisiae* (Bohm et al., 1997) and 0.7% in *Arabidopsis thaliana* (Englbrecht et al., 2004). C_2H_2 zinc finger proteins do not only have active roles in transcriptional regulation but also have functions in RNA metabolism, as well as other cellular pathways that require interaction with zinc finger proteins. For example, in *Arabidopsis*, zinc-finger domains have an important role in the regulation of floral organogenesis, gametogenesis, and leaf formation (Takatsuji, 1999). C_2H_2 zinc finger proteins do not only bind to DNA but also RNA and interact with other proteins. The differential use of the two cysteine and histidine residues gives rise to the various types of zinc finger domains ($C_2H_2,$ C_2HC, C_2C_2, C_2HC C_2C_2, C_2C_2 C_2C_2). 133 species of C_2H_2 zinc-finger proteins have been found within the human brain alone. The general concept of zinc-finger

protein function is that the greater the number of fingers, the greater the number of different ligands the fingers have specific affinity to (Iuchi, 2001). In addition to the presence of C_2H_2 domain zinc finger proteins, other zinc finger proteins are existent within the *Toxoplasma* genome such as B-box (1 putative protein) and CW zinc finger proteins (2 putative proteins).

Disruption of the locus of zinc finger protein TgZFP1, which contains a CCHC motif led to an impaired bradyzoite differentiation phenotype (Vanchinathan et al., 2005). Furthermore, many zinc finger proteins consisting of various domains (C_2H_2, MYND, B-box) were upregulated during alkaline stress in *Toxoplasma* (Naguleswaran et al., 2010). Another C_2H_2 zinc-finger protein TgZNF2 which is conserved among eukaryotes was characterized to have an important role in nuclear translocation of polyadenylated mRNA from the nucleus towards the cytoplasm. Inducible knock-down mutants of TgZNF2 demonstrated a cell cycle arrest during the G1 stage. Overall, TgZNF2 is essential for the survival of the parasite (Gissot et al., 2017). A more recent study revealed that zinc-finger protein TgZFP2 results in cell cycle arrest. The conditional knock-out of TgZFP2 demonstrated that the nuclear cycle remains unaltered yet the budding cycle is severely affected (Semenovskaya et al., 2020). Most interestingly, TgZNF2 and TgZFP2 were not shown to bind to DNA but are most likely binding to RNA.

   c) Helix-turn-helix domain TFs (Class III)

The HTH superfamily consists of 5 different types of HTH domain proteins and which include: Homeo, Forkhead, Heat Shock, Tryptophan, and TEA (Harrison & Aggarwal, 1990). The structure of the HTH domain can vary slightly according to the type of HTH domain. Most HTH domains consist of two α-helices which consist of 20 amino acids connected by the turn. In other cases, HTH domains consist of three α-helices where the core of the domain consists of an open tri-helical bundle. The HTH domain binds DNA through its third α-helix. The HTH domain is a simple fold which forms a right-handed helical bundle characterized by a partially open structure. The three helices of the HTH domain appear to have a triangular form when placing the third helix in front horizontally. The defining structural feature of the HTH domain is the sharp turn and is located between helix 2 and helix 3. The third helix is termed the recognition helix and interacts with DNA by insertion into the DNA's major groove. Conserved hydrophobic residues within the structure of the HTH domain localize towards the interior and give rise to a hydrophobic core which contributes to domain stability. HTH domains participate in a variety of functions which are not solely limited to transcriptional regulation but are also involved in other functions such as DNA repair and RNA metabolism (Aravind et al., 2005).

Myb proteins are HTH domain TFs with three α-helices and three repeats of around 50 residues which include three tryptophan residues positioned between repeats. A large number of Myb proteins have been shown to specifically bind DNA and have important roles in regulating genes responsible for cell differentiation and growth control (Lipsick, 1996; Kanei-Ishii et al., 1996). For example, in *Plasmodium*, PfMyb1 an HTH domain TF was demonstrated to have a role in the regulation of genes that have an important role in the pre-erythrocytic stage of the parasite's life cycle (Gissot et al., 2005). Additionally, in a more recent study, a myb-like TF designated TgBFD1 has been characterized (Waldman et al., 2020).

This myb-like TF was demonstrated to have a key role in the regulation of differentiation (Waldman et al., 2020). Mutant parasites lacking TgBFD1 resulted in complete ablation of parasite differentiation *in vitro*. Furthermore, mutant parasites lacking TgBFD1 lost their brain tissue cyst formation capability in mice (Waldman et al., 2020).

A recent *in-silico* study carried out by Sardar et al. (2019) identified 3 novel putative HTH proteins in the *T. gondii* Me49 strain which are predicted to localize to the chromatin of the nucleus based on the recent hyperLOPIT data (Barylyuk et al., 2020).

Overall, the indication of these novel HTH TFs in the *T. gondii* genome could give novel insight into their potential role in regulating gene expression by their further characterization. Nonetheless, their precise role and mechanism of action remain to be elucidated.

d) β- scaffold architecture domain TFs (Class IV)

Contrary to the name used to classify this type of DNA binding TFs, not all TFs categorized under Class IV contain a "β-scaffold" architecture. Members of this superfamily which possess a β-scaffold architecture interact with DNA through minor groove contacts. HMG (High Mobility Group) domain TFs are a type of DNA binding domain TFs belonging to the "β-scaffold" superfamily and only consist of α helices. (Stegmaier et al., 2004). However, the mechanism of interaction with DNA is very similar to all the other members of this superfamily and consists of insertion into the minor groove, resulting in a sharp kink of the DNA helix (A. Lebrun & Lavery, 1999).

In *T. gondii*, it has been shown that there are three orthologs of the protein HMGB1 (High Mobility Group Box-containing protein). A phylogenetic and bioinformatics study revealed that all three orthologs (HMGB1a, HMGB1b, HMGB1c) have an HMG box domain. One of the orthologs termed TgHMGB1a, was demonstrated to have an implication in the regulation of gene expression. The generation of a transgenic strain over-expressing TgHMGB1a resulted in an increase in virulence factor expression (H. Wang et al., 2014).

e) Other transcription factors (Class V)

Studies carried out on eukaryotic lineages, which branch out of the crown group of the eukaryotic domain of life demonstrate a lack of specific TFs, this pattern of specific TF scarcity is also the case in Apicomplexans despite the presence of all of the expected basal transcription factors (Aravind et al., 2003; Templeton, 2004). The presence of rare representatives of the 5 specific TF superfamilies was predicted to be explained by two main factors. The first one being that the genome of Apicomplexans might comprise of genes coding for specific transcription factors which have not been previously identified and most likely consist of domains which are distantly related or unrelated to the previously characterized DNA binding domains. The second factor involves the possibility of alternative methods being responsible for the regulation of gene transcription such as chromatin level regulation as well as post-transcriptional regulation (Balaji et al., 2005).

Analysis of predicted apicomplexan nuclear proteins resulted in the identification of a novel family of DNA binding proteins (Balaji et al., 2005). These proteins consist of AP2 (Apetala-2) domains characterized by their ability to bind specific

sequences of DNA (Balaji et al., 2005; Silva et al., 2008) and control the expression of genes.

6.3 AP2 transcription factors

AP2 transcription factors in plants

AP2 transcriptions factors were identified for the first time in plants in *Arabidopsis* and were shown to play a crucial role in several regulatory mechanisms related to plant growth such as the establishment of the floral meristem, the development of organ identity , and most importantly the control of gene expression (Jofuku & Laboratories, 1994). Transcription factors containing AP2 domains were assumed to be only present in plants (Krizek, 2003; Riechmann & Meyerowitz, 1998). AP2 domains are widely conserved given the presence of AP2 homologs in several non-plant species; for example AP2 domains are present in cyanobacterium, ciliates, and viruses (Magnani et al., 2004; Wuitschick et al., 2004). These homologs were found to possess another domain encoding for a homing endonuclease which is a mobile genetic element able to make a single or double break in DNA initiating the transposition of DNA elements from one locus to another. This process is termed 'homing' and is completed by repairing the break in DNA (Chevalier et al., 2001; Koufopanou et al., 2002). It was hypothesized that plant AP2/ERF (ethylene response factor) originated from the homing endonucleases belonging to the HNH-AP2 family found in bacteria and viruses. This was then followed by the incorporation of the HNH-AP2 domains within plants through horizontal gene transfer or perhaps incorporation through endosymbiosis with a cyanobacterium. However, it is most likely that the role of the homing endonuclease has been lost with time in plants and the AP2 DNA-binding domain has become the one to be responsible for controlling gene expression to ensure proper plant development (Magnani et al., 2004). ApiAP2 TFs within apicomplexan genomes may have originated from a similar endosymbiotic origin (Balaji et al., 2005).

The family of AP2/ERF transcription factors (AP2/EREBP) within *Arabidopsis* consists of numerous proteins and includes a total of 145 distinct transcription factors, classified into 5 sub-families: 1) **DREB** subfamily (Dehydration Responsive Element Binding) (56 proteins), 2) **ERF** subfamily (65 proteins): comprise one AP2 domain and a WLG domain, 3) **AP2** subfamily (14 proteins) consisting of two AP2 domains, 4) **RAV** subfamily (6 proteins) comprises of two AP2 domains in addition to a B3 binding domain, 5) subfamily of **other** proteins (4 proteins): comprise of one AP2 domain and a WLG domain (Sakuma et al., 2002). The determination of the structure of members of AP2 proteins in *Arabidopsis* and *Plasmodium* allowed for providing discernment regarding the mechanism followed in which the AP2 domain binds specific DNA motifs. By using nuclear magnetic resonance (NMR), a structural analysis of AtERF1 demonstrated that the secondary structure of the AP2 domain consists of a three-stranded antiparallel β-sheet and an α-helix present in a parallel fashion to the β- sheet. The AP2 domain structure depicted that DNA interacted with 11 highly conserved residues, among them 7 maintain a specific association with the consensus DNA sequence AGCCGCC which is more commonly known as the GCC box.

From this structural study, the residues of the AP2 domain interacting directly with DNA were identified in the ß-sheet. These residues included four arginine residues whose guanidyl groups were in direct contact with DNA (R150, R152, R162, R170) in addition to the interaction of two tryptophan residues (W154 and W172). The 6 interacting residues were demonstrated to be in direct contact with the cytosine and guanine bases of the GCC box. This specific interaction results in the AP2 domain binding to the major groove of the DNA (Allen et al., 1998). The target DNA-binding sequence is slightly altered according to which subfamily the transcription factor containing the domain belongs to. For example, the DREB subfamily recognized the DRE sequence TACCGACAT which is slightly different from the ERF one (Sakuma et al., 2002). Within the subfamily RAV, the protein AtRAV1 interacts with CAACA and CACCTG through its two domains AP2 domain and B3 domain, respectively (Kagaya et al., 1999). AtANT (AINTEGUMENTA), a member of the AP2 subfamily, has been demonstrated to specifically bind to DNA via the consensus site gCAC(A/G)N(A/T)TcCC(a/g)ANG(c/t) *in vitro* (Nole-Wilson & Krizek, 2000). A further study demonstrated that transcription factors such as AtANT which possess two AP2 DNA-binding domains have a complex scheme of DNA binding (Krizek, 2003).

AP2 transcription factors in Apicomplexans

The identification of AP2 TFs in Apicomplexans (ApiAP2) has paved the road towards having a better understanding of the regulation of gene expression within this phylum. All members of the apicomplexan family possess ApiAP2 TFs. For example, *Theileria* consists of 19 ApiAP2 TFs, *Cryptosporidium* possesses 19 ApiAP2 TFs, and *Plasmodium* comprises of 27 ApiAP2 TFs. *Toxoplasma* possesses about more than double the number of ApiAP2 TFs identified in *Plasmodium* and includes 67 ApiAP2 TFs (toxodb.org). There are up to four repeats of the AP2 domain in each AP2 TF in apicomplexans (Balaji et al., 2005).

In *T. gondii*, ApiAP2 TFs were initially named according to their chromosome location. However, the naming is most likely in need of revision due to the most recent study of the 3D organization of the nucleus which specifically demonstrated that there are 13 chromosomes within *T. gondii* rather than 14 (Bunnik et al., 2019).

A total of 22 genes of the 26 encoding for ApiAP2 TFs in *P. falciparum* were demonstrated to be expressed during different stages of the intraerythrocytic developmental cycle and named according to the specific phase at which they are expressed. Nine members of the ApiAP2 family are conserved across members of the apicomplexan family. Evolutionary studies indicate that since *Cryptosporidium* and *Plasmodium* diverged from each other at an early time point within Apicomplexa, it is most likely that the common ancestor of Apicomplexa already acquired a minimum of nine ApiAP2 proteins (Balaji et al., 2005).

6.4 Structure of the AP2 domain and function of ApiAP2 proteins

a) Structure

ApiAP2 domains comprise of about 60 amino acids and are found within the folds of ApiAP2 proteins. When comparing the sequence and structural characteristics of 211 ApiAP2 domains from the AP2 family derived from Apicomplexans (*Plasmodium*, *Theileria*, and *Cryptosporidium*) with those from plants, and bacteria, 12 residues were shown to be highly conserved in 241 representatives of the 285 AP2 domains included in the study, and which included different AP2 domain representatives. The conserved residues have an important role in the formation of important stabilizing hydrophobic interactions (Balaji et al., 2005). Most members of the ApiAP2 family consist of one single globular AP2 domain. In addition, in Apicomplexa, there are existent AP2 proteins possessing 2-4 AP2 domains. Furthermore, there is solely one other motif that is characterized by DNA-binding and is associated with the AP2 domain in some proteins in Apicomplexan members, this motif is termed AT-hook (Aravind, 1998).

DNA binding studies of two AP2 *P. falciparum* proteins, PF14_0633 and PFF0200c, demonstrate that these two ApiAP2 proteins interact with DNA by specific binding to the following DNA sequences TGCATGCA and GTGCAC, respectively (Silva et al., 2008). Further studies involving the crystal structure determination of the ApiAP2 domain from *P. falciparum* (PF14_0633) allowed for insight regarding the function of the ApiAP2 domain. Comparing the crystal structure of the ApiAP2 domain of *P. falciparum* (PF14_0633) to the plant AP2 domain of *A. thaliana* indicated that ApiAP2 retain several canonical characteristics which are found in the plant *A. thaliana* (Allen et al., 1998) yet, there are important key variations. *P. falciparum* AP2 domains dimerize through a domain-swapping mechanism, contrary to plant AP2 domains which function as a monomer. Domain-swapping of the ApiAP2 domains is characterized by the swapping of α-helices between the two monomers in order to form the dimer (Lindner et al., 2010). The dimerization model that was developed suggested that the binding of the ApiAP2 domain to DNA initiates a stabilizing effect on the homodimer or that the binding of AP2 to DNA as a monomer triggers a conformational change which then triggers the binding of the second monomer (Figure 23).

The dimerization of ApiAP2 domains in the specific case of PF14_0633 has been suggested to have an important role in uniting distant loci of DNA to facilitate regulating sporozoite-specific gene expression (Lindner et al., 2010).
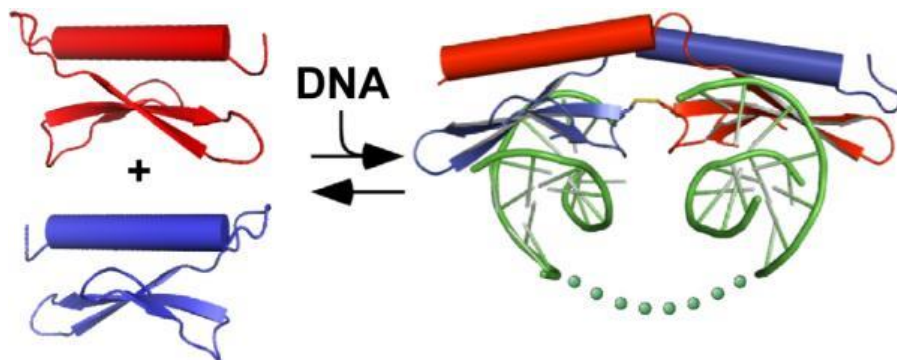
Figure 23 – Schematic representation of ApiAp2 domain-swapping (Lindner et al., 2010). DNA binding of ApiAP2 domain stimulates dimerization and domain-swapping leading to looping by exempting all the DNA that intervenes between the binding location. DNA looping is represented by green dots.

b) ApiAP2 TFs in *T. gondii* bradyzoites

Overall, *T. gondii* consists of 67 putative ApiAP2 TFs which are categorized as follows: 24 ApiAP2 TFs are cell-cycle regulated, 27 are constitutively expressed in the tachyzoite, 11 are bradyzoite-specific and the remaining are expressed in other stages of the parasite's development (Behnke et al., 2010). To date, there is a total of 12 ApiAP2 TFs that have been characterized in *Toxoplasma*. The key developmental change of the *T. gondii* parasite associated with human disease is the inter-conversion of the parasite between the rapidly replicating tachyzoite stage and the latent mature bradyzoite stage. This developmental switch requires differential expression of genes specific to each stage (White et al., 2014).

One of the first ApiAP2 TFs to be characterized in *Toxoplasma* is AP2XI-4. This TF was shown to have an essential role in the bradyzoite with a peak of expression during G1/S phase (Walker et al., 2013). High expression levels of TgAP2XI-4 transcripts in bradyzoite containing cysts compared to tachyzoites implied that TgAP2XI-4 has a role in the bradyzoite stage. The direct knock-out mutant of TgAP2XI-4 in a type II Pru *T. gondii* strain resulted in a downregulation of bradyzoite-specific genes *in vitro* and *in vivo*. In addition, the absence of TgAP2XI-4 resulted in a lower cyst burden in mice compared to cyst burden in mice infected with the wildtype strain (Walker et al., 2013).

Furthermore, *Tg*AP2XI-4 was demonstrated to bind to the specific DNA sequence "CACACAC" which is the same sequence to which the homologs of *Tg*AP2XI-4 bind to in *Plasmodium* (Walker et al., 2013). The specific DNA motif to which *Tg*AP2XI-4 binds to is found to be present in more than half of the promoters of the genes regulated by this particular TF (Campbell et al., 2010; Walker et al., 2013).

A second ApiAP2 TF was then characterized: *Tg*AP2IX-9 was proven to be a bradyzoite repressor after studying the effect of its overexpression and depletion *in vitro*. *Tg*AP2IX-9 overexpression resulted in significantly low cyst formation under alkaline stress conditions whereas the depletion of *Tg*AP2IX-9 resulted in cyst formation in vitro. *Tg*AP2IX-9 was found to bind in cis to promoters of bradyzoite-specific genes such as *Tg*BAG1 and TgB-NTPase. Protein binding microarrays allowed for determination of the DNA sequence motif "CAGTGT" to which *Tg*AP2IX-9 binds to (J. B. Radke et al., 2013).

TgAP2IV-3 is another activator of bradyzoite differentiation. The overexpression of TgAP2IV-3 led to an increase in the expression of bradyzoite-specific genes. TgAP2IV-3 directly binds to the promoter of the bradyzoite-specific gene TgBAG1. Comparing the bradyzoite-specific genes that were upregulated by TgAP2IV-3 to those that were downregulated by TgAP2IX-9, allowed for the confirmation that indeed TgAP2IX-9 is a bradyzoite repressor (Hong et al., 2017).
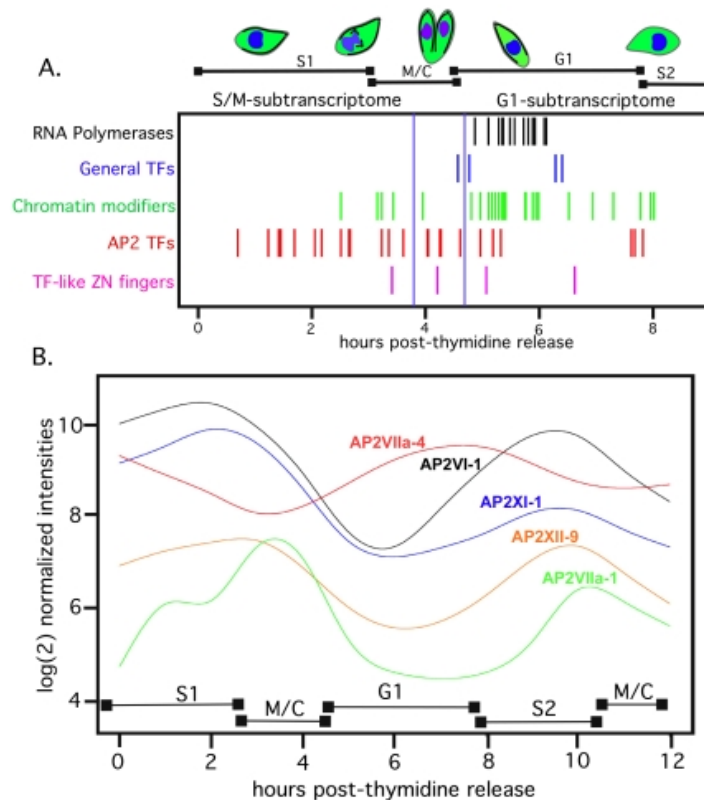
Figure 24 – Schematic representation of putative Toxoplasma transcription factors expressed during the cell cycle (Behnke et al., 2010). **(A)** mRNA abundance of RNA polymerases, general TFs, chromatin modifiers, AP2 TFs, and TF-like Zn fingers during the cell cycle of a synchronized tachyzoite cell culture. **(B)** Spline model curves for specific AP2 mRNAs which are cell cycle regulated indicating relative mRNA abundance and time shifts. The expression of the selected factors follows a serial order with peaks at different cell cycle stages.

Additional ApiAP2 TFs were shown to have a repressing effect on bradyzoite differentiation such as TgAP2IV-4 which peaks in the tachyzoite during the S/M phase. Type I parasites lacking TgAP2IV-4 displayed expression of bradyzoite-specific genes. In addition to this, mice inoculated with type II parasites deficient in TgAP2IV-4 were unable to form cysts and establish chronic infection of the disease *in vivo* (J. B. Radke et al., 2018). Yet another ApiAP2 TF that peaks during the S/M phase of the cell cycle is TgAP2IX-4. The knock-out of TgAP2IX-4 renders the parasite uncapable of forming cysts *in vitro* and *in vivo* (Huang et al., 2017). The two repressors of bradyzoite differentiation TgAP2IV-4 and TgAP2IX-4 are exclusively expressed at a specific timepoint during the S/M phase of the tachyzoite cell cycle. The existence of ApiAP2 TFs that are solely expressed at a single timepoint during the S/M phase of the tachyzoite cell cycle such as TgAP2IV-4 and TgAP2IX-4 imply that 'just in time' expression of ApiAP2 TFs has a major role in striking the balance between activation and repression of bradyzoite differentiation in order to establish successful chronic infection of the parasite (Figure 24).
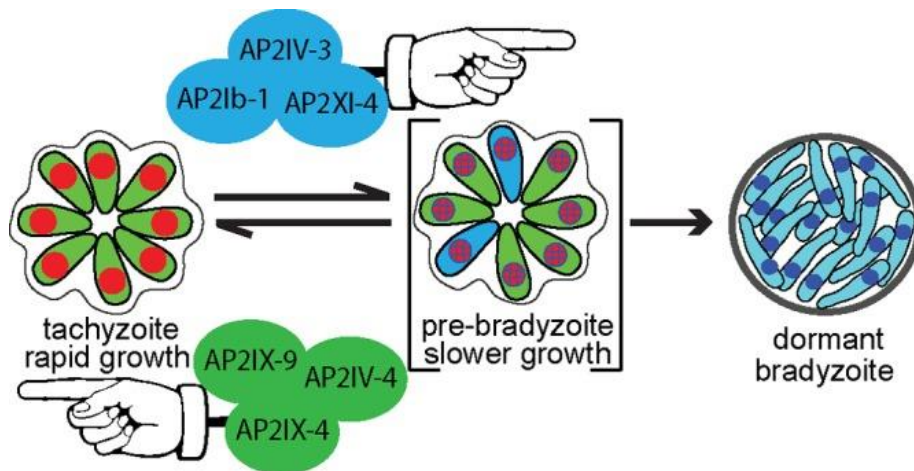
Figure 25 – Schematic representation of ApiAP2 regulation of bradyzoite differentiation (Hong et al., 2017a). The model represents the ApiAP2 TFs identified to have a role in bradyzoite development. To date, three ApiAP2 TFs have been described as activators of bradyzoite differentiation (TgAP2IV-3, AP2Ib-1, AP2XI-4) and three other ApiAP2s have been described as bradyzoite repressors (TgAP2IX-9, TgAP2IV-4, and TgAP2IX-4).

Furthermore, when studying the transcriptome associated with bradyzoite differentiation using scRNA-seq, a few bradyzoite BAG1+ cells belonged to either S, M, or C clusters suggesting that this small group of cells is replicating and proceeding with the cell cycle (Xue et al., 2020). Particular AP2 TFs (TgAP2Ib-1, TgAP2IX-1, TgAP2IX-6, and TgAP2VI-2) were found to be over-expressed in cluster P1 which was enriched for bradyzoite-specific genes. This observation suggested that these particular AP2 TFs may have potential roles in the transition of the parasite to the bradyzoite stage (Xue et al., 2020).

Moreover, gene expression profiles during *T. gondii* parasite bradyzoite differentiation were studied by carrying out RNA-seq on infected *in vitro* brain cell culture in the laboratory. The parasites infecting the *in vitro* brain cell culture proved to produce mature bradyzoites (Mouveaux et al., 2021). When examining the expression profiles of AP2 TFs during differentiation of the parasite infecting this brain cell culture, they were found to vary during the bradyzoite differentiation process, and several clusters were observed. Two bradyzoite clusters were present, the first cluster of bradyzoite genes were expressed at the very initial stages of bradyzoite differentiation and this cluster included TgAP2IX-9 whereas the second bradyzoite cluster consisted of genes that were expressed during the later stages of bradyzoite differentiation, and this second cluster included AP2XI-4. Nevertheless, a third cluster consisting of tachyzoite-specific genes was also observed and consisted of TgAP2IX-5 and TgAP2X-5 (Mouveaux et al., 2021). To conclude, AP2 TFs present in the bradyzoite clusters may control bradyzoite differentiation.

Eight ApiAP2 TFs have been characterized to have a role in tachyzoites, three of which have been proven to form complexes with chromatin remodeling enzymes. TgAP2IX-7 and TgAP2X-8 have been proven to interact with TgGCN5b (J. Wang et al., 2014). TgGCN5b is a member of the lysine acetyltransferase (KAT) family and is responsible for the acetylation of histone H3 at specific lysine residues (J. Wang et al., 2014). A dominant negative mutant of TgGNC5b resulted in the blockage of parasite replication, a reduction in histone H3 acetylation, and decreased expression of genes being targeted by TgGCN5b. Interaction of TgGCN5b with proteins containing AP2 domains was demonstrated via proteomics studies and indicates that TgGBN5b has a central role in regulating gene expression in concordance with ApiAP2 TFs (J. Wang et al., 2014). Therefore suggesting that ApiAP2 TFs play an important role in recruiting TgGCN5b to the promoters of targeted genes since TgGCN5b are void of any DNA-binding motifs Wang et al., 2014). A recent study describes the TgGCN5b complex by carrying out a more rigorous investigation in which multiple AP2 TFs were demonstrated to interact with TgGCN5b (Harris et al., 2019).

Identification of the TgAP2IX-7 interactome by carrying out co-immunoprecipitation and proteomic analysis demonstrated that TgAP2IX-7 interacts with TgGCN5b,TgADA2a, and TgAP2X-8 in addition to only five other proteins which were also identified in the TgGCN5b interactome (four hypothetical proteins and a kinase) (Harris et al., 2019). Co-immunoprecipitation followed by proteomic analysis demonstrated that TgAP2XII-4 interacts with TgGCN5b and TgADA2a (Harris et al., 2019). Furthermore, a fourth AP2 TF was identified to most likely function in concordance with TgGCN5b and TgAP2XII-4 which is TgAP2VIIa-5 (Harris et al., 2019). It is also worthy to note that the association of TgGCN5b with AP2 TFs is lost under alkaline stress conditions.

Therefore, these results confirm that TgGNC5b is a member of several complexes in the tachyzoite. It is plausible that specific AP2 TFs have a role in recruiting the TgGCN5b core complex in order to regulate genes (Harris et al., 2019).

TgAP2VIII-4, initially identified as TgCRC-350, and a component of the *T. gondii* repressor complex, TgCRC which forms a complex with histone deacetylase (TgHDAC3), has been demonstrated to be crucial for the repression of transcription by means of TgHDAC3 activation (Saksouk et al., 2005).

Furthermore, TgAP2XI-5, an ApiAP2 transcription factor constitutively expressed during the tachyzoite stage plays an important role in the regulation of virulence genes (rhoptry and microneme genes) (Walker, Gissot, Huot, Alayi, Hot, Marot, Schaeffer-Reiss, et al., 2013). By carrying out a Chip-on chip experiment, it was demonstrated that TgAP2XI-5 binds to hundreds of promoters of genes including those of genes which are apicomplexan-specific and involved in the virulence of parasites and the invasion of hosts The specific DNA motif to which TgAP2XI-5 binds to was identified: GCTAGC by carrying out a binding analysis using the RSAT computational program (Walker, Gissot, Huot, Alayi, Hot, Marot, Schaeffer-Reiss, et al., 2013).

By carrying out protein co-immunoprecipitation experiments, TgAP2XI-5 was demonstrated to interact and form a complex with TgAP2X-5 (Lesage et al., 2018). TgAP2X-5 is a cell-cycle regulated TF mainly expressed during the S/M phases (Lesage et al., 2018). The depletion of TgAP2X-5 resulted in downregulation of 153 genes and the upregulation of 70 genes. Most of the genes that were deferentially regulated peaked during the S/M phases of the cell cycle among them were multiple virulence genes (rhoptry and microneme genes). In addition, the depletion of TgAP2X-5 led to a severe defect in virulence in *vivo*. ChIP-chip experiments using the tagged strain of TgAP2X-5 failed to demonstrate that TgAP2X-5 binds to promoters. However, Chip-chip experiments performed with the aim of assessing whether TgAP2XI-5 binds to any promoters in the absence of TgAP2X-5, demonstrated that 92 promoters exhibited a decrease in TgAP2XI-5 binding in the absence of TgAP2X-5 (Lesage et al., 2018). In the presence of TgAP2X-5, TgAP2XI-5 was found to bind to promoters of virulence genes that were downregulated when TgAP2X-5 was depleted whereas in the absence of TgAP2X-5, a portion of genes that TgAP2XI-5 binds to when TgAP2X-5 is present exhibited decreased binding by TgAP2XI-5. Thus, demonstrating that for certain promoters of genes, TgAP2XI-5 binding is dependent on TgAP2X-5 (Lesage et al., 2018). Overall, these results identify that AP2 TFs have the capacity to function in a cooperative manner in order to regulate virulence factors in *T. gondii*.

TgAP2IX-4 is a cell cycle regulated TF which is expressed mainly during the S/M phase of the cell cycle. Mutant parasites exhibiting a knocked-out *TgAP2IX-4* gene displayed no defect in tachyzoite growth rendering TgAP2IX-4 dispensable for the growth of the parasite *in vitro* (Huang et al., 2017). The depletion of TgAP2IX-4 led to a decrease in the frequency of tissue cyst formation *in vitro*. The loss of TgAP2IX-4 led to the dysregulation of the expression of genes during bradyzoite-inducing stress conditions *in vitro*. Enhanced expression of bradyzoite genes such as TgBAG1, TgLDH2, and TgENO1 among others in the TgAP2IX-4 knock-out was observed.
When studying the effect of the loss of TgAP2IX-4 on the formation of tissue cysts in vivo, it was demonstrated that TgAP2IX-4 depletion resulted in a modest virulence impairment and a decrease in the formation of tissue cysts which is consistent with what was observed *in vitro* (Huang et al., 2017).

In a recent study on TgAP2IX-4 in order to further characterize this TF, TgAP2IX-4 was found to interact with multiple AP2 TFs such as TgAP2XII-2 and TgAP2VIIa-3. TgAP2IX-4 was also identified to interact with components of the MORC complex and this shed light regarding the transcriptional repressor activity of TgAP2IX-4 suggesting that several AP2 TFs recruit MORC in order to regulate the expression of genes (Farhat et al., 2020; Srivastava et al., 2020). TgAP2IX-4 was verified to strongly interact with TgAP2XII-2 and immunofluorescence assays demonstrated that the two AP2 TFs are co-expressed (Srivastava et al., 2020). Mutant parasites depleted of TgAP2XII-2 demonstrated a defect in parasite replication. The loss of AP2XII-2 resulted in a delayed S phase and thus delayed replication of the tachyzoite and an increase in the frequency of bradyzoite differentiation (Srivastava et al., 2020).

One of the AP2 TFs proved to have an effect on the surface antigens of the tachyzoite. TgAP2IX-1 was demonstrated to have a key role in controlling the switch of surface antigens (Xue et al., 2020). This was determined based on the observation of a SAG1- single tachyzoite observed in scRNA-seq experiments of RH Type I strain. The single tachyzoite devoid of SAG1 revealed a transcriptome characterized by the absence of usually abundant genes which are tachyzoite-specific and bradyzoite-specific (Xue et al., 2020). This gene expression is very similar to that of the sexual stage where SRS22C is abundantly expressed. TgAP2IX-1 was expressed in the SAG1- tachyzoite and a transient transfection of TgAP2IX-1 demonstrated that this AP2 TF is responsible for the decrease of SAG1 antigen on the tachyzoite's surface whereas RT-PCR demonstrated a significantly increased expression of genes which were upregulated in the SAG1- parasite including SRS22C (Xue et al., 2020). These results clearly demonstrated that TgAP2IX-1 has the capacity to alter the expression of the parasite's antigens.

The most recent transcription factor to be characterized, TgAP2IX-5 is a key regulator of the asexual cell cycle in the tachyzoite and also has an impact on the bradyzoite stage. Overlap of RNA-seq and ChIP-seq experiments demonstrated that TgAP2IX-5 directly binds to genes necessary for daughter parasite formation such as IMC genes as well as other ApiAP2 TFs necessary for the continuation of the cell cycle (Khelifa et al., 2021; C. Wang et al., 2021).

6.5 Epigenetic Control of Gene Expression

Epigenetics is a term meaning heritable modifications that are not encoded in the genetic composition (DNA sequence) of an organism and thus affects the expression of genes. Many mechanisms of epigenetic regulation exist: 1) mechanisms which influence the accessibility of factors to chromatin, and which include methylation of DNA, modification of histones, and localization of nucleosomes. 2) mechanisms which utilize noncoding RNA to affect several processes which take place in the nucleus or cytoplasm. The recent models of transcriptional activation include a larger number of cofactors than was initially identified more than ten years ago with chromatin remodelers being the facilitating factors to enhance gene transcription and thus transform chromatin into a forefront position when studying epigenetic control of gene expression.

The basic components of chromatin are histone proteins of which exist four different types: H2A, H2B, H3, and H4. These four sorts of histone proteins form an octamer in complex with 146 bp of DNA wound twice around the octamer forming the nucleosome. The tails of histones undergo a myriad of modifications which result in different outcomes regarding gene transcription (Peterson & Laniel, 2004). In *Toxoplasma*, histone proteins are highly conserved which is the case in all eukaryotes. Conserved histone proteins include H3 and H4 proteins. The residues of each N-terminal tail of each histone are highly likely to be subject to chemical modification (Nardelli et al., 2013; Sullivan, 2003). Furthermore, there are two distinguishable lineages of H2B: *Tg*H2B.Z which is associated with parasites and TgH2Ba and TgH2Bb which represent a stage-regulated lineage (Dalmasso et al., 2006). *Tg*H2A also has multiple variants: *Tg*H2A1, *Tg*H2AZ and *Tg*H2AX. *Tg*H2AZ forms a dimer with *Tg*H2B.Z, this dimer is localized at promoters of actively transcribed genes (Dalmasso et al., 2009). Furthermore,

ChIP-chip experiments carried out on a tagged orthologous variant of H3, TgCenH3 demonstrated that TgCen3 localizes to an apical region within the nucleus mapping to centromeres, and remaining in close proximity to the nuclear envelope (Brooks et al., 2011).

The N-terminal tails of histones are rich in basic, positively charged residues that bind strongly to DNA which is negatively charged leading to a condensed state. The default state of chromatin is represented by the construction of genomic DNA into histone nucleosomes which is then compacted into a chromatin structure. The default state of chromatin correlates to the repression of transcription and is termed "silenced" chromatin or heterochromatin. After the replication of DNA, chromatin adopts this silenced conformation (Ehrenhofer-Murray, 2004). Alternatively, the relaxed form of chromatin allowing DNA to be accessible by cofactors in order to carry out gene transcription is termed: 'euchromatin' (Li et al., 2007).

In *T. gondii,* it was demonstrated by carrying out co-immunoprecipitation experiments that TgH2BZ and TgH2AZ interact with each other forming a dimer. However, TgH2BZ does not interact with TgH2AX (Dalmasso et al., 2009). In addition, ChIP experiments followed by qPCR revealed that TgH2AZ and TgH2BZ are enriched at promoters of genes that are transcriptionally active as opposed to TgH2AX which is enriched upstream of genes that are transcriptionally repressed (Dalmasso et al., 2009). In addition, TgH2AX was shown to associate with TgIRE which is a repeat element located at the end of chromosomes (telomeres) since TgH2AX was observed to be highly enriched at TgIRE as opposed to TgH2AZ and TgH2BZ (Dalmasso et al., 2009). In *T. gondii*, histone proteins were found to have an association with the bradyzoite stage of the parasite. TgH2AX had an increased expression in bradyzoites induced *in vitro*. These results were further confirmed by microarray. Furthermore, TgH2BZ, the partner of TgH2AZ, has a similar expression pattern as its partner and both histone proteins' expression remains unchanged whereas TgH2Ba which interacts with TgH2AX has an increased expression in induced bradyzoites (Dalmasso et al., 2009). A subsequent study carried out on tissue cysts obtained from mice demonstrated that *H2AX* and *H2AZ* transcripts were present within the mature bradyzoite stage (Dalmasso et al., 2009).

Overall, chromatin structure is implicated in DNA-related processes which include DNA transcription, DNA replication, DNA reparation, in addition to many others. The most studied process is transcriptional regulation, a process that is possible by altering the chromatin structure in order to attain active transcription of genes.

6.5.1 Chromatin Remodeling and modification
There are two existent mechanisms used to regulate the structure of chromatin through the alteration of its compaction state. Chromatin structure can be altered chemically through the covalent modification of histones or by using ATP in order to reposition nucleosomes. These two sorts of chromatin-modifying mechanisms are conserved among eukaryotes and are existent in *Toxoplasma* as well.

In *Toxoplasma*, apicomplexan N-terminal histone tails are susceptible to a wide range of covalent modifications such as acetylation, methylation, succinylation, phosphorylation, ubiquitination, and SUMOylation (Braun et al., 2009; Dixon et al., 2010; El Bissati et al., 2016; Jeffers & Sullivan, 2012; Nardelli et al., 2013; Silmon de Monerri et al., 2015). These post-translational modifications constitute a 'histone code' representing the set of modifications in activation and inactivation of particular genes (Jenuwein et al., 2001; Nardelli et al., 2013). Contrary to the case in other eukaryotes, methylation of DNA cytosines is absent in *Toxoplasma* and *Cryptosporidium* (Gissot et al., 2008). However, cytosine methylation remains controversial in *Plasmodium*. In two studies carried out by Choi et al. (1996) and before that Pollack et al. (1982), cytosine methylation appeared to be absent in the *P. falciparum* genome (Choi et al., 2006; Pollack et al., 1982). Strikingly, a more recent study identified the presence of cytosine methylation in *Plasmodium* (Ponts et al., 2013). This was achieved by using highly sensitive mass spectrometry and formic acid (Ponts et al., 2013). C5-DNA methyltransferase activity was detected in *P. falciparum* in addition to the generation of a genome-wide map of cytosine loci which are methylated during the intra-erythrocytic cycle (Ponts et al., 2013).

Histone Acetylation

Histone acetylation involves the acetylation of lysine residues present in the N-terminal tails of histones rendering highly positively charged histones negatively charged. Acetylation relaxes the chromatin structure and is correlated with gene activation. In opposition, the removal of acetyl groups is linked to the repression of transcription. In eukaryotes, there exists several histone acetyltransferases (HATs) and histone deacetylases (HDACs) that have been characterized and that regulate the acetylation condition of histones associated with the nucleosome. HATs and HDACs are specific enzymes with important roles in the epigenetic control of gene transcription (Sterner & Berger, 2000; Thiagalingam et al., 2003).

In *Toxoplasma*, there are around seven HATs and seven HDACs present within the parasite's genome. Recently, these enzymes have been termed KATs and KDACs (lysine acetyltransferases and lysine deacetyl transferases). The renaming of these enzymes was based on these chromatin remodeling enzymes having substrates which are not histones (Allis et al., 2007; Jeffers & Sullivan, 2012). KATs in *T. gondii* belong to two families, the GCN5 family and the MYST family. *Tg*MYST-A and *Tg*MYST-B are homologous KATs and members of the MYST family. *Tg*MYST-A and *Tg*MYST-B are essential to the parasite's survival (Smith et al., 2005). TgGCN5a and TgGCN5b are two homologous members of the GCN5 family of KATs. In eukaryotes, members of the GCN5 family have a preference towards acetylating histone 3 and specifically lysine 14 (K14). Purified recombinant TgGCN5a protein preferentially targets H3K18 while TgGCN5b selects H3K9, H3K14, and H3K18 (Bhatti et al., 2006; Saksouk et al., 2005). TgGCN5a plays a major role in transcriptional regulation since microarray studies demonstrated that mutant parasites in which TgGCN5a was knocked-out demonstrated their inability to upregulate ~ 75% of bradyzoite-specific genes that should be usually expressed during alkaline induced stress (Naguleswaran et al.,

2010). Several unsuccessful attempts to generate a knock-out strain of TgGCN5b suggests the essentiality of this particular KAT in the tachyzoite (J. Wang et al., 2014). GCN5 KATs provide promising drug targets since garcinol, a pharmacological drug targeting TgGCN5b has a critical effect on the parasite's survival (Jeffers et al., 2016).

Analysis of the *Toxoplasma* genome indicates that there are potentially seven KDACs categorized into three different classes (I, II, and III), with only a single HDAC characterized so far TgHDAC3. TgHDAC3 is a component of the TgCRC complex and has been proven to have histone lysine deacetylation activity that can be inhibited by a selection of HDAC inhibitors (butyrate, aroyl-pyrrole-hydroxy-amides, and trichostatin A) (Saksouk et al., 2005). In addition, when treating *T. gondii* parasites with the FR235222 inhibitor and by carrying out ChIP on ChIP experiments, it was demonstrated that the upstream regions of 369 genes were characterized by hyperacetylated nucleosomes. These genes are mainly expressed during the bradyzoite or sporozoite stages. In addition, upon treatment with the FR235222 drug, histone 4 (H4) is hyperacetylated inducing bradyzoite differentiation (Bougdour et al., 2009).

TgHDAC and TgMORC were demonstrated to co-purify with each other and function in gene silencing (Saksouk et al., 2005). The association between TgMORC and TgHDAC3 was verified by carrying out reverse immunoprecipitation and mass spectrometry experiments in which a strain consisting of a tagged version of TgMORC was used to confirm this association (Farhat et al., 2020). In addition, TgMORC was found to interact with 10 AP2 TFs and machinery necessary for chromatin remodeling (Farhat et al., 2020). Furthermore, ChIP-seq experiments exhibited that the binding sites of TgMORC and TgHDAC3 overlapped extensively with more than 90% of peaks situated at intergenic regions. More specifically, TgMORC and TgHDAC3 were found to associate with each other at regions where chromatin was hypoacetylated which is most probably a consequence of TgHDAC3 deacetylation activity. Overall, TgMORC associates with TgHDAC3 and together these proteins play a major role in the silencing of a distinct set of genes via histone deacetylation in the tachyzoite stage.

Besides TgHDAC3, other HDACs exist within the *Toxoplasma* genome and those of type I are predicted to be essential for tachyzoite replication whereas this is not the case for type III HDACs (TgSIR2 and TgSIR2b), and this is based on the genome-wide CRISPR/Cas9 screen carried out on the tachyzoite (Sidik et al., 2016).

The acetylation of histones H3 and H4 represent classical gene activation markers (H4ac and H3K9ac) (Kim, 2018). By carrying out chromatin immunoprecipitation (ChIP) experiments, it was demonstrated that the acetylation of H3K9 and H4 co-localize and form a complex pattern at specific loci within the parasite's genome with identified peaks located near the 5' end of genes (Gissot et al., 2007). Thus, these modified histones are enriched at promoter regions hence, the acetylation of these histones marks the promoters of genes which are actively transcribed (Gissot et al., 2007). Furthermore, acetylation of H3 and H4 was observed for

tachyzoite-specific promoters yet not for bradyzoite-specific promoters in tachyzoite-stage parasites (Saksouk et al., 2005). However, in bradyzoite-induced conditions, tachyzoite-specific promoters become hypoacetylated and bradyzoite-specific promoters become acetylated (Saksouk et al., 2005). Moreover, differential association of TgGCN5 and TgHDAC3 on stage-specific promoters was demonstrated by carrying out ChIP assays. TgGCN5 was found to be associated with tachyzoite-specific promoters such as SAG2A whereas TgHDAC3 was found to be associated with bradyzoite-specific promoters (Saksouk et al., 2005).

To conclude, this association of different chromatin modifying enzymes to stage-specific promoters contributes to overall gene regulation by the acetylation/deacetylation of genes.

Histone methylation

Histone methylation is a process consisting of the addition of methyl groups to lysine (K) and arginine (R) residues. The methylation of theses specific residues results either in the activation or repression of gene transcription (Zhang et al., 2001). Arginine and lysine residues can become either mono-, di-, or trimethylated. Methyltransferases are divided into 2 classes: protein arginine methyltransferases (PRMT) and histone lysine methyltransferases (KMT). There are five PRMT homologs within *Toxoplasma* and are referred to as TgPRMT1-5. Two protein arginine methyltransferases have been characterized via *in vitro* histone methyltransferase assays using recombinant proteins of TgCARM1, the equivalent of TgPRMT4 and TgPRMT1. TgPRMT1 was identified to methylate arginine residue 3 on histone 4 (H4R3) whereas TgCARM1 was identified to methylate arginine residue 17 on histone 3 (H3R17) (Saksouk et al., 2005). TgPRMT1 has 68 potential substrates which include AP2 TFs and regulatory RNA binding proteins (Yakubu et al., 2017).

TgSET8 belongs to a novel family of histone lysine methyltransferases which is highly related to human SET8 (Sautel et al., 2007). TgSet8 was demonstrated to have the capacity to methylate H4 at lysine residue 20. TgSet8 does not only mono-methylate lysine residue 20 but can also di-methylate and tri-methylate this specific residue present on histone 4 (Sautel et al., 2007). Additionally, TgSet8 was found to be mostly enriched in intergenic regions (Sautel et al., 2007). Moreover, based on ChIP-on-chip data, TgSet8 was found to bind to rRNA gene regions specifically. rRNA gene loci were found to be mono- and tri-methylated at H4K20 in addition to the presence of TgSet8 at these specific sites. Additionally, TgSet8 was discovered to bind to multiple DNA repeats close to telomeres (Sautel et al., 2007). In a following experiment in which ChIP was carried out, H4K20me1 and H4K20me3 were found to be enriched at heterochromatic DNA regions (heterochromatic loci) in addition to the presence of H3K9 methylation as another heterochromatic marker. These results indicate that H3K9 and H4K20 methylation function in synergy in silencing chromatin.

Another post-translational modification site in *T. gondii* is H4K31 which is located on the lateral surface of histone 4 and is situated at the dyad axis of the protein-DNA interception site at the nucleosome where the K31 residue is present (Sindikubwabo et al., 2017). By carrying out ChIP-seq experiments, H4K31me1

was found to display enrichment at large genes which span from the start codon to the whole body of the gene. H4K31me1 was found to be missing from intergenic regions alternatively to H4K31ac which was enriched in intergenic regions aligning with *in situ* euchromatin localization (Sindikubwabo et al., 2017). Therefore, this data suggests that H4K31me1 distribution is restricted to the gene bodies (Sindikubwabo et al., 2017).

The *Toxoplasma* genome encodes seven demethylating enzymes which belong to the JmjC family and consist of Jumonji demethylating domains (Bougdour et al., 2014; Chang et al., 2007). However, further studies are needed to characterize these demethylases although the genome-wide CRISPR screen has suggested the presence of two homologs of lysine dimethyl-transferases which deem important for the overall fitness of the tachyzoite (Sidik et al., 2016).
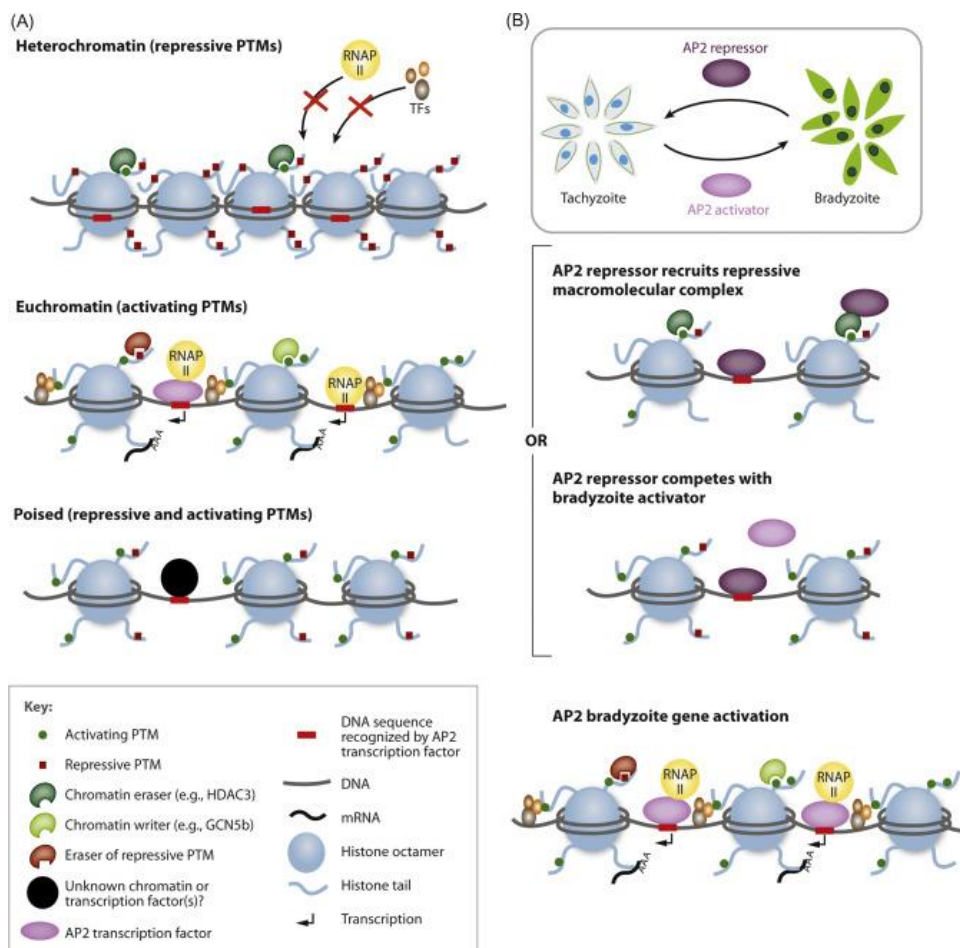
Figure 26 – Schematic representation of ApiAP2 regulation of bradyzoite differentiation (Kim et al., 2020). (A) Heterochromatin and euchromatin are the two states of chromatin. Heterochromatin is a compact structure characterized by posttranslational modifications of histones such as the methylation of H3K9 in order to prevent access to cofactors crucial for gene transcription. For the sake of simplicity, all factors participating in the remodeling of chromatin are designated

as histone modifying enzymes (ATP-dependent factors, enzymes modifying histones, and other complexes). HDAC3 is used as an example of a histone modifying enzyme which leads to gene transcription repression through modifying the state of chromatin to a compact state. Euchromatin is the relaxed chromatin state and GCN5b is used as an example of an acetyl transferase associated with active genes. GCN5b also interacts with ApiAP2 TFs. Poised genes represent an intermediate state consisting of marks for both heterochromatin and euchromatin and has been suggested to have a role in gene regulation as well. **(B)** AP2 TFs have a major role in gene regulation, and several have been identified as either activators or repressors of bradyzoite differentiation.

b) <u>ATPase based chromatin remodeling</u>

Chromatin remodeling by using DNA-dependent ATPases represents the second mechanism by which the chromatin structure is altered. SWI/SNF2 DNA-dependent ATPases form complexes which have important roles in the activation or repression of genes (Mohrmann & Verrijzer, 2005). The energy generated from hydrolysis of the ATP molecule results in a change in the placement and conformation of the nucleosome since the contacts between the histones and DNA becomes changed (Lusser & Kadonaga, 2003). The complexes that participate in ATPase dependent chromatin remodeling contain members belonging to the SWI/SNF2 family which are characterized by the presence of a unique ATPase domain. ATPase domains possess a DEXDc region at the N-terminal end and a HELICc region located at the C-terminal end. The SWI/SNF2 family is categorized into 4 classes according to homology of sequence and particular structural characteristics. There are members that possess bromodomains and are termed Snf2, other members consist of a SANT domain and are designated as ISWI, while others contain a chromodomain and are termed Mi-2. In addition, there exists a fourth class consisting of a long insert located between the N-terminal region and the C-terminal HELICc region, this class is termed Ino80/SRCAP/p400 (Kingston et al., 1999). SWI2/SNF2 members are present in Apicomplexans. There is a homolog of ISWI in *Plasmodium* termed SNF2L (Ji & Arnot, 1997). Additionally, there is a SCRAP (Sbf2-related CREBBP activator protein) homolog present in the genomes of most Apicomplexans including *Toxoplasmosis*, *Plasmodium* and *Cryptosporidium* (Sullivan et al., 2003). A yeast two-hybrid screen allowed for investigation of the function of SRCAP in *Toxoplasma* by using the *Tg*SRCAP protein as 'bait'. Proteins identified to interact most strongly with *Tg*SRCAP were identified as parasite-specific proteins without them having any eukaryotic homologs. Interacting proteins identified through this study are predicted to function in DNA processes such as transcription (Nallani & Sullivan, 2005). Furthermore, *Toxoplasma* contains 15 other homologs of SWI2/SNF2 with at least one member representing each of the four classes mentioned previously. Among them, there is a predicted member of the SWI2/SNF2 family that contains a chromodomain, belongs to the *Tg*CRC complex, and is most likely an ortholog of Mi-2 (Saksouk et al., 2005). Interestingly, *Toxoplasma* contains two SWI2/SNF2 members homologous to snf2 with one of them containing a bromodomain which have characteristic features specific to *T. gondii* and represent potential drug targets (Jeffers et al., 2017).

6.6 Other factors involved in regulating gene expression

In addition to enzymes with chromatin remodeling capacities, there are other factors that exist within *Toxoplasma*, and which take an active part in regulating the expression of genes.

Glycolytic enzymes such as TgENO1 expressed within the bradyzoite and TgENO2 expressed within the tachyzoite localize to the nucleus and are suggested to have a role in the regulation of gene expression within the parasite. Bradyzoite-specific TgENO1 promoter represented bait in an affinity chromatography experiment in order to determine nuclear factors that control stage-specific promoters such as TgENO1. A total of 35 nuclear proteins were identified as proteins interacting with the bradyzoite-specific promoter and among them was TgNF3, a novel nucleolar chromatin associated protein. TgNF3 was demonstrated to bind specifically to nucleosome associated histones leading to a major role in transcriptional regulation through transcription silencing (Olguin-Lamas et al., 2011). A following study reported that TgENO1 and TgENO2 which localize preferentially to the nucleus of intracellular replicating tachyzoites interact with chromatin resulting in differential expression of genes (Mouveaux et al., 2014). TgENO1 mutant knock-out parasites resulted in decreased cyst burden *in vivo*. Moreover, the deletion of TgENO1 had a direct effect on the regulation of gene transcription. By using qRT-PCR, it was demonstrated that the expression of eight genes targeted by TgENO2 was differentially expressed at a magnitude of 2- to 5-fold between the knock-out TgENO1 mutant and the parental intracellular tachyzoites (Mouveaux et al., 2014). However, in *in vitro* induced bradyzoites, the TgENO1 knock-out mutant parasites exhibited a constant decrease in the transcript levels of seven of the eight TgENO2-targeted genes (Mouveaux et al., 2014). Overall, the deletion of TgENO1 has an immediate effect on gene regulation.

In addition to the enolase enzymes, there were many other glycolytic enzymes which were determined to be constituents of complexes involved in transcription, such as LDH and GAPDH suggesting a role in controlling gene transcription (Zheng et al., 2003).

7 Protein phosphatases in *Toxoplasma gondii*

7.1 Phosphorylation and cell cycle regulation

Reversible phosphorylation is an abundantly utilized regulatory mechanism that employs specific protein kinases and phosphatases which interact in opposing manners in order to ensure the regulation of the phosphorylation process. Phospho-proteomics studies recently carried out in eukaryotes have clearly demonstrated that about 50% of the entire amount of proteins in humans, mice, and yeast are subject to phosphorylation and thus are designated as phosphoproteins (Vlastaridis et al., 2017).

Kinases are enzymes which possess a mechanism of action involving the shift of a phosphoryl group belonging to an ATP molecule to a hydroxyl group present in the substrate. The hydroxyl group belongs to either a serine, threonine, or tyrosine residue of the substrate. Substrates of kinases are widely variable ranging from small molecules to proteins and peptides. In addition, kinases can be auto-phosphorylated (Gaji et al., 2021). Phosphorylation of substrates is considered as a post-translational modification and can have further downstream effects such as activation, repression, targeting modification, and initiation of signaling cascades (Manning, 2002).

A total of 159 genes coding for kinases which is equivalent to ~2% of total genes (~8000 genes total) are present within the *Toxoplasma* genome (Gaji et al., 2021). These genes encode 108 true kinases and 51 pseudokinases elicited from genomic analysis of the conserved KEDD signature motif of kinases (Lorenzi et al., 2016; Peixoto et al., 2010).

In *T.gondii*, a phospho-proteome analysis of enriched peptides in intracellular and purified tachyzoite samples was carried out (Treeck et al., 2011). The analysis of *T. gondii* intracellular samples which consisted of tachyzoites, and the invaded host cells identified 11,822 phospho-peptides exhibiting 12,793 phosphorylation sites associated to 2,793 proteins (Treeck et al., 2011). When analyzing the phospho-peptides of purified tachyzoite samples, a 2-fold increase in the number of phospho-peptides was observed (21,498 phospho-peptides) exhibiting 24,298 phosphorylation sites associated to 3,506 phosphoproteins. The most abundantly phosphorylated residue in *T. gondii* is the serine residue (pS), which is followed by the threonine residue (pT), and finally the least abundantly phosphorylated residue is the tyrosine residue (pY). The phosphorylation sites were found at regions of disorder and are apparently enriched in coil secondary structures (Treeck et al., 2011).

Mass spectrometry analysis of phosphopeptides and flow-through which consists mainly of non-phosphorylated peptides was carried out in attempt to identify which classes of proteins are phosphorylated in *Toxoplasma*. 50.9% of the whole *T. gondii* proteome was identified among them 63.9% of the analyzed proteins were phosphorylated. In *T. gondii*, representation of the phospho-proteome in comparison to the entire proteome demonstrated that surface, mitochondrion, and apicoplast proteins are significantly under-represented as opposed to a significantly overrepresented kinome (Treeck et al., 2011). Moreover, several IMC proteins as well as proteins involved in host cell invasion designated in the study as the 'invasome' were phosphorylated yet not significantly over-represented.

Comparing the phospho-proteome and the proteome of the intracellular and purified tachyzoites allowed to identify proteins that are secreted and phosphorylated within the host cells. Among them were proteins previously identified to be phosphorylated within the infected host cell such as TgGRA7 and TgROP2 (Treeck et al., 2011). The cytosol of the *T. gondii* parasite is where most phosphorylation events take place since only around 14% of phosphoproteins possessed a signal peptide as opposed to about 20% of the predicted proteome

proteins. Furthermore, about 40% of proteins encoding for rhoptry and dense granule proteins exhibited a signal peptide, these proteins demonstrated a decreased phosphorylation in the purified tachyzoite samples and were designated as outliers. These results suggested that these proteins are phosphorylated in the PV or the host cell cytosol (Treeck et al., 2011).

A sub-type of kinase genes code for Cyclin-dependent kinases (CDKs). Within higher eukaryotes, CDKs represent the backbone of cell cycle regulation and are known to associate to specific proteins which are temporarily expressed and termed cyclins. Once cyclins are associated to CDKs, they activate CDKs and issue substrate specificity to the CDK they are bound to. CDKs belong to the serine/threonine family of kinases and are only fully active when they form heterodimers. CDKs represent the kinase unit whereas the associated cyclins represent regulatory units. The activity of CDKs is tightly regulated during the cell cycle which is ensured by the continuous expression of CDKs and the temporal expression of the cyclins (L. Liu et al., 2019).

The *Toxoplasma* genome encodes a total of 10 genes which consist of a kinase domain and a sequence to which cyclins bind to termed as the C-helix. These 10 genes are designated as CDK-related kinases (Crks) (Alvarez & Suvorova, 2017). *T. gondii* tachyzoite and bradyzoites host the expression of eight TgCrks designated TgCrk1-8 whereas the remaining two TgCrks designated TgCrk2-L1 and TgCrk5-L1 are expressed in merozoites and sporozoites. TgCrks are expressed in a cyclical manner as opposed to the constitutively expressed CDKs in superior eukaryotes. Contrary to the conventional eukaryotic cell cycle which consists of canonical cyclins designated cyclins A to E, *Toxoplasma* consists of atypical cyclins designated cyclins P, H, L and Y. Most of the atypical cyclins are strikingly constitutively expressed (Alvarez & Suvorova, 2017; White & Suvorova, 2018).
Reverse genetics involving the conditional knock-down of TgCrks allowed for the characterization of the TgCrks within *T. gondii*. TgCrks were demonstrated to have an important role in the regulation of cell division by regulating the different checkpoints of the cell cycle in order to guarantee smooth progression of the cell cycle. Five of the TgCrks were identified to be involved in the different *T. gondii* cell checkpoints. TgCrk2 associates with The P cyclin also known as TgPHO80. The complex TgCrk2/P cyclin is responsible for controlling the START checkpoint in the G1 phase specifically the transition from the G1a phase to the G1b phase. This is then followed by the DNA licensing checkpoint during the S phase carried out by TgCrk5. TgCrk4 is responsible for controlling the replication of the centrosome and segregation during the M phase. TgCrk1 is essential for controlling cytoskeleton assembly of the daughter cells and TgCrk6 is crucial for the transition of the dividing parasite from the Anaphase stage to the Metaphase stage. Moreover, many TgCrks do not have to interact with cyclins such as the case in higher eukaryotes and can normally carry out their regulatory functions without necessary association to any cyclins (Alvarez & Suvorova, 2017; Naumov et al., 2017).
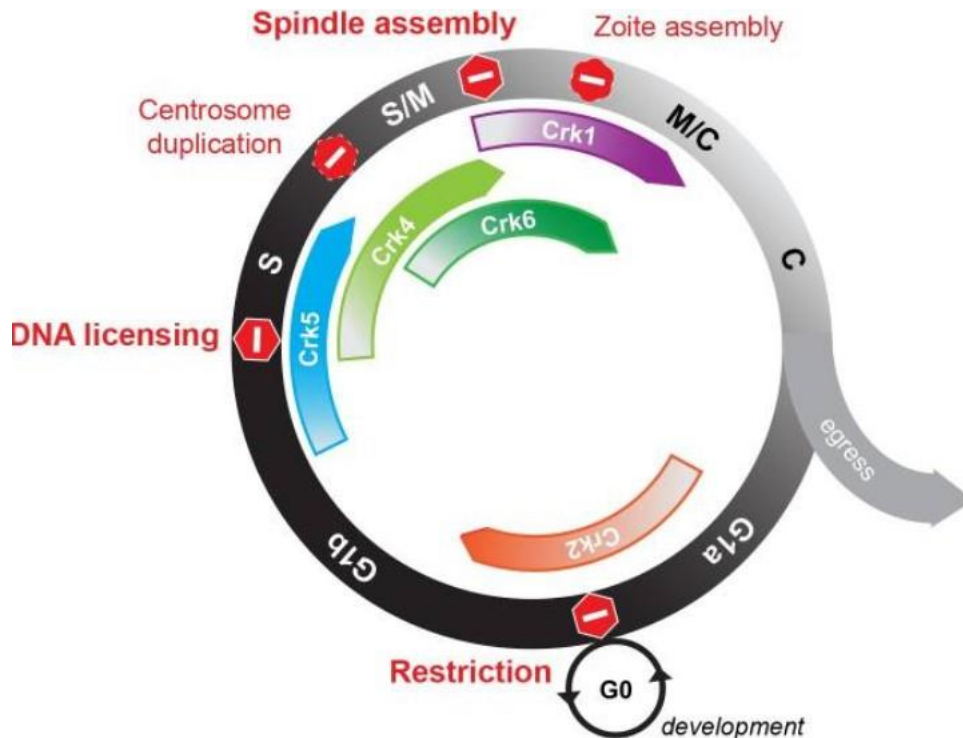
Figure 27: Schematic representation of the cell cycle check points in *T. gondii* tachyzoites (Alvarez & Suvorova, 2017). The cell cycle consists of several checkpoints to ensure that cell division proceeds correctly. The cell cycle in *T. gondii* consists of three conserved checkpoints. The G1 checkpoint is associated with cell differentiation and dormancy and is regulated by the TgCrk2/TgPH080 cyclin complex (orange arrow). TgCrk5 controls DNA replication licensing (blue arrow). TgCrk4 controls the checkpoint necessary for controlling proper centrosome stoichiometry (light green arrow). TgCrk1 controls the bud assembly checkpoint (purple arrow), and TgCrk6 is suggested to control the spindle formation checkpoint during metaphase (dark green arrow).

Nevertheless, protein phosphatases exist within the *Toxoplasma* genome as well. However, none have been implicated to have a role in the cell cycle and thus the role of *T. gondii* protein phosphatases remain to be elucidated.

7.2 Protein Phosphatases

There are three main types of protein phosphatases categorized according to the type of amino acid targeted: serine/threonine phosphatases, tyrosine phosphatases, and dual specificity phosphatases (target all three residues).

Protein serine/threonine phosphatases (PSPs) consist of three families: phosphoprotein phosphatases (PPPs), protein phosphatases that are Mg^{2+}/Mn^{2+} dependent (PPMs), and aspartate-based phosphatases (Shi, 2009). The PPP and PPM subfamilies have been extensively studied in eukaryotes. In apicomplexans, *P. falciparum* and *T. gondii* were shown to possess PPP subfamilies such as PP1

and PP2A in addition to the presence of PPMs such as PPM2 and PPM5 which have an important role in the sexual stages of *P. falciparum* and ookinete formation, respectively (Guttery et al., 2014). However, not much is known about the aspartate-based phosphatases which include FCP (FIIF-associating carboxyl-terminal domain) phosphatases in addition to small CTD phosphatases which are collectively known as the FCP/SCP family of phosphatases (C. Yang & Arrizabalaga, 2017). Furthermore, apicomplexans possess phosphatases with characteristic Kelch-like domains (PPKL), which are found in plants and alveolates as well as Shewanella-like phosphatases (SLP) only present in bacteria (Kutuzov & Andreeva, 2008).

a) <u>Phosphoprotein phosphatase subfamily (PPPs)</u>

The PPP family contains protein phosphatase 1 (PP1), PP2A, PP2B (calcineurin), PP4, PP5, PP6, and PP7 subfamilies. For most of the members of the PPP family, a single catalytic subunit can associate with several substrates. However, this is not the case for members of other families such as PPM which do not possess regulatory subunits but rather additional domains and conserved motifs that communicate the specificity of the protein phosphatase. When comparing the eukaryotic genome to that of the four apicomplexan genomes (*T. gondii, P. falciparum, C. parvum,* and *B. bovis*) *P. falciparum* and *T. gondii* possess an entire set of the PPP subfamilies with at least one member of each of its seven subfamilies with the exception of PP2A since *T. gondii* possesses two of these protein phosphatases (C. Yang & Arrizabalaga, 2017). However, in the case of each of *Cryptosporidium* and *Babesia*, there are subfamilies that are absent in their respective genomes. These missing families include PP6 and PP7 from *C. parvum* and PP2B and PP6 from *B. bovis*. Members of the PPP family are highly conserved in apicomplexans and possess conserved consensus sequences and includes GDxHG, GDxVDRG, RG, GNHE, HGG and H (C. Yang & Arrizabalaga, 2017)

PPPs are crucial for the viability of cells. However, it is most likely presumed that in eukaryotic cells lethality is evaded since there are several isoforms within the PPP subfamily that possess overlapping functions and can compensate for absence of certain PPP members (Brautigan & Shenolikar, 2018).

PPP family members possess a high level of identity across species (~ 80%). Members of the PPP family do not exhibit the same mechanism of subunit association. The direct binding of subunits by means of the RVxF motif in addition to other sequences is a mechanism adopted by PP1. However, PP2A, PP4, and PP6 adopt a different manner of binding their respective subunits and use scaffold subunits as intermediate bridges in order to bind the catalytic and regulatory subunits together (Brautigan, 2013). Regarding phosphatase regulation of the cell cycle, protein phosphatase 2A (PP2A) has been demonstrated to have a role in cell cycle control. For example, in yeast, PP2A regulates the cell cycle at the transition point between the G2 phase and the M phase. Loss of the phosphatase activity of PP2A results in delayed progression throughout the cell cycle. In addition to this, the loss of PP2A function disrupts the spindle assembly checkpoint and leads to

an irregular mitotic exit. Furthermore, PP2A controls the G1/S transition and the cytokinesis stage (Jiang, 2006). Overall, PP2A has multiple roles and contributes to the regulation of nearly most of the cell cycle progression in mammals and higher eukaryotes but despite the presence of PP2A within *Toxoplasma*, its specific characterization remains to be elucidated. Additionally, *T. gondii* does not possess a Cdc25 phosphatase ortholog which is known to also have an important role in regulation of cell cycle progression in higher eukaryotes and is responsible for removing the phosphorylation in CDKs (Shen & Huang, 2012).

b) <u>Protein phosphatases Mg^{2+} /Mn^{2+} dependent subfamily (PPMs)</u>

This family includes members that are metal-dependent protein phosphatases. PPMs carry out their phosphatase roles as one subunit enzyme with either bound Mn^{2+} or Mg^{2+} ions and are extremely conserved throughout eukaryotes and prokaryotes (M. J. Chen et al., 2017; Kamada et al., 2020). PPM phosphatases have differed to a great extent throughout evolution giving rise to specificity in functions in higher eukaryotes. For example, in yeast there are 8 different PPM isoforms yet in mammals there are 20 PPM isoforms. A thorough phylogenetic analysis of PPM phosphatases, including the analysis of more than 50% of sequences in the most conserved domain of the catalytic region, demonstrated that the majority of conserved residues lie within the catalytic core and are crucial for phosphatase function (Kamada et al., 2020).

In Apicomplexans, members of the PPM family are found in all four apicomplexan genomes. Similar to other organisms, there is great difference in the number of PPM homologs in each apicomplexan species. There are 13 PPMs in *P. falciparum*, 33 in *T. gondii*, 14 in *C. parvum*, and 4 in *B. bovis*. A phylogenetic analysis clustered apicomplexan PPMs into 10 main groups designated from I-X. Clusters II and X are one of the most important. Group II is predicted to consist of PDPs, a subtype of PPM phosphates whereas Group X includes *Pf*PPM3 and 8 homologs of TgPPM3 (A-H), of which six include localization signal peptides suggesting that these TgPPM3s are likely targeted to the PV or host cell (Yang & Arrizabalaga, 2017). The function of several PPM phosphatases in *Plasmodium* and *Toxoplasma* have been elucidated. PPM2 in *P. falciparum* possesses two catalytic cores characterized by phosphatase activity (Mamoun et al., 1998). Two PPMs have regulatory roles in translation in *P. falciparum*. *Pf*PPM2 is involved in translational regulation since one of its substrates is translation elongation factor 1- beta (*Pf*EF-1ß) (Mamoun & Goldberg, 2001). PfUIS2 is another *Pf*PPM phosphatase with an implication in translation and carries out dephosphorylation of an important translational factor eIF2α-P (M. Zhang et al., 2016). Direct knockouts of PPMs targeted in a genome-wide functional analysis were obtained where mutants of knocked-our PfPPM2 and knocked-out PfPPM5 exhibited the most detrimental defects. For example, mutant parasites in which PfPPM2 was knocked-out demonstrated a significant decrease in the number of macrogametes as well as a defect in ookinete formation rates whereas parasites depleted of PfPPM5 displayed a defect in ookinete size and number (Guttery et al., 2014).

In *T. gondii*, TgPPM13 plays an important role in phosphorylation regulation of an actin binding protein, Toxofilin. TgPPM13 functions in combination with casein

kinase II (CKII) in order to modulate the phosphorylation of Serine residue 53 of Toxofilin. The coordinated function of PPM13 and CKII controls binding of Toxofilin to G-actin and sequestration of actin monomers contributing to the overall actin dynamics of the parasite which has a role in gliding motility (Delorme et al., 2003; Jan et al., 2007). *T. gondii* PPM protein, TgPPM20 which is a rhoptry protein secreted during invasion, is important during parasite growth (Gilbert et al., 2007).

Furthermore, plasma membrane PPM phosphatase, TgPPM5C has an implication in the parasite's lytic cycle (C. Yang et al., 2019). Vacuolar protein TgPPM3C has an important role in GRA16 export. Furthermore, parasites depleted in TgPPM3C exhibited a major defect in virulence *in vivo* (Mayoral et al., 2020).

c) <u>Aspartate-based phosphatases subfamily (FCP/SCP)</u>

Members of this family are different from those of the PPP and PPM families by their characteristic aspartate-based catalysis. A great majority of aspartate-based phosphatases possess a conserved catalytic motif DxDT/V. There are eight aspartate-based phosphatases in humans and five in yeast. Within apicomplexans, there exists five putative aspartate-based phosphatases in *C. parvum*, eight within *T. gondii*, *P. falciparum* possesses four and *B. bovis* consists of six. Among all the phosphatases existent in this subfamily, there is only a single member that has been mostly studied and that is FCP1 also termed as CTDP1. Studies carried out in humans and yeast demonstrate that FCP1 plays an important role in the dephosphorylation of the CTD of RNA polymerase II large subunit. The CTD region has a consensus sequence YSPTSPS, all residues contained within the consensus sequence can be phosphorylated with the exception of the two prolines (Stiller & Cook, 2004; C. Yang & Stiller, 2014). CTD has a role in gene expression and serves as a docking platform and has been investigated in yeast yet the characterization of the role of CTD in RNA polymerase activity within apicomplexans remains to be elucidated (Corden, 2013).

Apicomplexans consist of two orthologs of FCP1 within their respective genomes, contrary to humans and yeast which have only one FCP1 gene. *T. gondii* has a peculiar CTD region compared to the CTD of other apicomplexans. *T. gondii* consists of only two heptapeptides which are tandemly repeated and the remaining 8 heptapeptides are randomly distributed. This suggests that the single distributed heptapeptides possibly lack the conventional CTD functions since it is based on heptapeptide pairs (Stiller & Cook, 2004).

7.3 Protein phosphatase 1 (PP1) in the eukaryotic cell
Protein phosphatase 1 (PP1) was the first phosphatase to be discovered belonging to the PPP family and was initially characterized as an enzyme that dephosphorylates glycogen phosphorylase (Cori & Cori, 1945). As of today, it has been demonstrated that PP1 plays a central role in several biological mechanisms involving cellular division, metabolism, transcription, translation, and apoptosis, in addition to many others (Ceulemans & Bollen, 2004).

PP1 is described as a holoenzyme consisting of a catalytic and regulatory subunit. The regulatory subunit of PP1 are designated proteins that associate with the catalytic subunit and are termed as phosphatase type 1- interacting proteins (PIPs). The highly conserved catalytic subunit consists of specific residues (3 histidine residues, 2 aspartic acid residues, and 1 asparagine residue) that coordinate Mn^{2+} and Fe^{2+} metal ions (Shi, 2009). PP1 catalytic subunit (PP1c) consists of one polypeptide that has an active enzymatic domain (Berndt et al., 1987). Within humans, PP1 carries out around a third of total dephosphorylation events. Furthermore, there is about 200 proteins that are PP1 regulatory subunits and contribute to specificity to the very limited number of PP1 catalytic subunits present in humans (Rebelo et al., 2015).

PP1c has an essential role in cell viability and disturbing its function can have deadly consequences. Furthermore, the disruption of the normal interaction of PP1c with PIPs has an important implication in multiple human diseases (Ferreira et al., 2019).

Many isoforms of PP1c exist within eukaryotes save for yeast which only harbors a single PP1c isoform encoded for by the Glc7 gene (Stark, 1996). In humans, three different genes code for PP1c, PPP1CA, PPP1CB, and PPP1CC leading to the existence of three distinct PP1c isoforms, PP1-A, PP1-B, and PP1-C (Yates et al., 2017).

The first crystal structures of PP1 complexes were resolved for PP1A/microcystin and PP1-G/tungstate providing the initial hints regarding the catalytic domain PP1c (M.-P. Egloff et al.,1995 ; Goldberg et al., 1995). Structural studies have revealed that the catalytic domain consists of a central ß-sandwich. Its active core consists of divalent metal ions. The cations bind to oxygen atoms present in the substrate's phosphate molecule in order to carry out dephosphorylation. Despite that several isoforms of PP1c exist, the structure is highly conserved and rarely changes when bound to other molecular entities (M. P. Egloff et al., 1997). PP1c also has grooves on its surface which are employed by the catalytic subunit as anchoring regions for interacting proteins (PIPs). Mostly all of the interacting proteins exhibit a specific docking motif termed as 'RVxF-type docking motif' known to bind to PP1c by associating with a hydrophobic pocket on the surface of the catalytic subunit far away from its core active site (Figure 28) (Felgueiras et al., 2020; Heroes et al., 2013).

T. gondii, P. falciparum, C. parvum, and B. bovis, present one PP1 catalytic subunit which are extremely similar to homologs of higher eukaryotes in both length and sequence (C. Yang & Arrizabalaga, 2017).
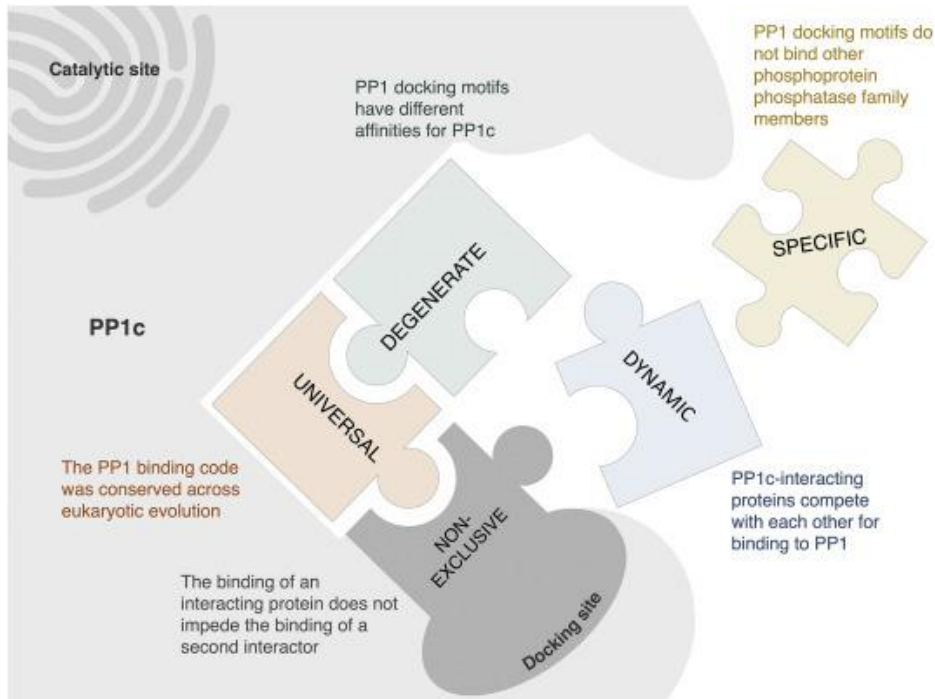
Figure 28 – Schematic representation PP1c-PIP interaction following the PP1c binding code (Felgueiras et al., 2020). PP1c binds to regulatory subunits by means of the multiple grooves present on its surface. PIPs bind to PP1c docking sites and form the PP1 holoenzyme. The binding follows a code introduced by Heroes et al. (2013) which is specific, universal, degenerate, nonexclusive, and dynamic.

7.4 Protein phosphatase 1 (PP1) in *Toxoplasma gondii*

In *T. gondii*, PP1 activity was initially discovered by carrying out experiments which involved the exposure of tachyzoites to PP1 inhibitors such as okadaic acid (OA) and tautomycin (TAU), respectively. These experiments resulted in the impairment of tachyzoite invasion by 50% suggesting that PP1 activity in *T. gondii* is important during the invasion process of the host cell (Delorme et al., 2002). *T. gondii* tachyzoite invasion is inhibited when parasites are exposed to 2µM of OA. However, exposure to concentrations below 100 nM has no impact on tachyzoite invasion. Furthermore, TAU possesses a greater selectivity for PP1 compared to OA (Delorme et al., 2002).

Phosphatase assays carried out on *T. gondii* extracts involving the de-phosphorylation of ^{32}P-phosphorylase α indicate that *T. gondii* indeed possesses PP1 activity, which is sensitive to OA and human I-2, a specific inhibitor of PP1 (Delorme et al., 2002). Since PP1c is known to always be associated to regulatory subunits, a monoclonal antibody against human PP1c was used to precipitate *T. gondii* PP1c and all the polypeptides to which it is associated to. Immunoprecipitated peptides verified the presence of phosphorylase α dephosphorylation activity. When adding the OA inhibitor, there was a single polypeptide which competed against OA in binding to PP1c. Furthermore, several proteins were identified as targets of PP1 in *T. gondii* via *in-vitro* phosphate labelling assays. The immuno-depletion of PP1c from a fraction containing the *T. gondii* cytosol was carried out initially followed by the phosphate-labelling assays.

An increase in the phosphate signal of multiple polypeptides was observed whereas there was a decrease in phosphate signal in other polypeptides (Delorme et al., 2002).

The subcellular localization of TgPP1 within the tachyzoite and bradyzoite forms of *T. gondii* was investigated via immunofluorescence assays using polyclonal antibodies (Daher et al., 2007). Within the tachyzoite, TgPP1 localizes within the nucleus. In addition to co-localization when using anti-ROP1 anti-bodies. In bradyzoites, TgPP1 seemed to localize more within the cytoplasm rather than the nucleus.

This was followed by further immunofluorescence assays in order to investigate TgPP1 localization in tachyzoites by carrying out a c-Myc tagged PP1 transient transfection which demonstrated a strong cytoplasmic signal in addition to partial overlap with the nucleus yet no localization at the rhoptry was observed in this case (Daher et al., 2007). Moreover, the unsuccessful attempt to maintain stable transgenic parasites suggested that the over-expression of TgPP1 possibly impacts the growth of the parasites (Daher et al., 2007).

Within the nuclear sub-compartment of the *T. gondii* tachyzoite, TgPP1 interacts with TgLRR1, an identified homolog of sds22 in yeast with an important role in PP1 activity regulation. This results in the formation of a TgPP1-TgLRR1 complex (Daher et al., 2007). The formation of a TgPP1-TgLRR1 complex was identified through affinity pull-down and immunoprecipitation assays. The presence of both TgPP1 and TgLRR1 proteins in eluates of tachyzoite proteins was demonstrated by immunoblot analysis of tachyzoite protein eluates which bind to microcystin beads with anti-PP1 or anti-TgLRR1 antibodies. This interaction was further confirmed by carrying out immunoprecipitation in which anti-TgLRR1 antibodies were used (Daher et al., 2007).

Further investigation of the role of TgLRR1 indicated that it most likely inhibits the activity of TgPP1. Inhibition of TgPP1 by TgLRR1 was further confirmed by studying the inhibitory function of TgLRR1 on TgPP1 by using a *Xenopus* oocyte model. Within the *Xenopus* oocyte model, microinjection of OA or anti-bodies against PP1 results in germinal vesicle breakdown (GVBD) (Swain et al., 2003). When microinjecting oocytes with TgLRR1 cRNA, it resulted in more than 90% of oocytes undergoing GVBD (Daher et al., 2007).

A recent study functionally characterizing Inhibitor-2 (I2) in *T. gondii* demonstrated that it has a similar effect as its homolog in *P. falciparum* on PP1 phosphatase activity via an inhibitory effect (Deveuve et al., 2017). TgI2 has a total of three conserved motifs, a SILK-like motif, an RVxF motif, and a third FKK/HYNE motif. The SILK-like motif is present only in the I2 protein of *T. gondii* when compared to other apicomplexan I2 proteins. TgI2 exhibited binding to TgPP1 through the RVxF motif mainly whereas SILK-like and HYNE motifs contribute towards TgPP1 binding minimally (Deveuve et al., 2017).

However, despite these findings, many questions regarding PP1 in *Toxoplasma* remain unanswered. Whether PP1 is essential in *Toxoplasma*, what specific proteins are targeted and de-phosphorylated by TgPP1, the specific mechanism of action of this protein phosphatase, and what downstream pathways PP1 is implicated in within *T. gondii* are a few questions of many.

Objectives

Chapter II-Objectives

The *T. gondii* cell cycle is a highly regulated event and its successful completion depends on both transcriptional and post-transcriptional regulation mechanisms. The highly dynamic nature of transcriptional regulation during the tachyzoite cell cycle has been illustrated by the transcriptome of synchronized parasites expressing the Thymidine kinase (Behnke et al., 2010). This comprehensive study showed that at least 2000 transcripts were dynamically regulated during the tachyzoite cell cycle. This implies a tight control of transcriptional expression of these genes. However, how this regulation is orchestrated at the molecular level was an outstanding question at the beginning of this PhD.

Based on the accumulated knowledge on the function of ApiAP2 TFs in both *T. gondii* and *Plasmodium spp.*, we reasoned that these proteins may play an important role in controlling the cell-cycle dependent expression profiles. More than 65 ApiAP2 encoding genes are present in the *T. gondii* genome and at least 20 of them are dynamically regulated during the cell cycle. We therefore aimed at characterizing these TFs. We identified among these the most promising candidates based on their cell cycle expression profiles and their fitness score (Sidik et al., 2016). This led to the identification of the TgAP2IX-5 protein as a promising target to control the cell-cycle specific expression program. We therefore aimed at identifying the phenotypes caused by an inducible knock-down mutant of this gene and also the pathways regulated by this TF during the cell-cycle. Through the characterization of its regulation network, we aimed at better understanding the mechanisms controlling the transcriptional regulation of the cell cycle.

The tachyzoite cell cycle is also controlled by a number of phosphorylation events (Treeck et al., 2011). However, most of the knowledge accumulated so far is based on the characterization of kinases (Gaji et al., 2021). The enzymes controlling the de-phosphorylation events, that are described in other eukaryotes as crucial for the cell cycle regulation (Manning, 2002), are poorly investigated in *T. gondii*. By contrast, genome wide targeting studies have illustrated the crucial role of these enzymes in *Plasmodium spp.* (Guttery et al ., 2014) in multiple pathways controlling its life cycle. We decided to investigate the *T. gondii* homolog of PP1 since its crucial role in controlling the cell cycle has been described in a number of organisms including *P. falciparum* and *P. berghei* (Zeeshan et al., 2021; Paul et al., 2020). The objective of this study entailed determining the role of TgPP1 in *Toxoplasma gondii*. Other objectives of this study included aiming for the determination of potential TgPP1 substrates. The final objective of this study was to identify the mechanism of action of TgPP1 and link it to any potential defects which may be observed upon TgPP1 depletion.

Finally, cell cycle and differentiation are intertwined in *T. gondii*. For example, a specific cell-cycle arrest has been shown to happen during the differentiation process (Waldman et al., 2020; Xue et al., 2020). We therefore attempted to

understand this link through the characterization of two other ApiAP2 TFs, TgAP2X-10 and TgAP2III-1. These transcripts were originally identified as dynamically regulated during the spontaneous differentiation of tachyzoites into bradyzoites in brain cell culture *in vitro* (Mouveaux et al., 2021). The specific objectives of this part of the PhD study included determining the functional role of these ApiAP2 TFs and to determine the precise role of TgAP2X-10 and TgAP2III-1 in the developmental differentiation process of the parasite.

Contributions

Chapter III - Contributions

This section is introduced to clarify the respective contribution of Asma Sarah Khelifa and the work performed in collaboration with previous students within the lab as well as external collaborators.

Regarding the first project of the PhD (role of TgAP2X-10 and TgAP2III-1 during *T. gondii* differentiation), I generated all direct knock-out mutant strains as well as characterized both direct knock-out mutants by carrying out growth assays, bradyzoite differentiation studies using the HFF cell model at a pH 7.0 and pH 8.2. I also carried out bradyzoite differentiation studies using the brain cell culture model with primary brain cell culture that were initially produced in the lab of Jean-Charles Lambert. In addition, I carried out the *in vivo* experiments with the help of Thomas Mouveaux. I generated all the RNA samples used for studying the gene expression studies. I also constructed the RNA libraries for Type II WT and direct Knock-out parasites in both pH conditions of pH 7.0 and pH 8.2 which were sent for sequencing.

Regarding the second project of the PhD study (role of TgAP2IX-5 in asexual cell cycle division), the iKD mutant of TgAP2IX-5 was generated by previous PhD student Kevin Lesage and previous Masters student Cecilia Gomez-Sanchez. I carried out a confirmation of the growth and proliferation phenotype including the growth and plaque assay. I carried out all experiments regarding the characterization of the iKD TgAP2IX-5 mutant with the exception of the electron-microscopy preparation and image acquisition that was performed by Nicolas Barois. I also generated the complementation strain of the iKD TgAP2IX-5 strain and carried out all of the characterization experiments of the complemented strain. I carried out the TgAP2IX-5 re-expression experiments where the parasite was left to grow in the presence of auxin before washing out auxin for different durations of time. The video-microscopy experiments were performed by Mathieu Gissot. RNA-seq and ChIP-seq experiments included in the manuscript were performed by Kevin Lesage, Cecilia Gomez-Sanchez, Thomas Mouveaux and Ludovic Huot. The bioinformatics analysis and integration of both datasets was performed by Pierre Pericard under the supervision of Helene Touzet and Guillemette Marot.

I carried out all complementary experiments where I prepared all the RNA samples of the iKD TgAP2IX-5 mutant treated with auxin for 1 hour, 2 hours, and overnight. RNA library construction of all the samples was also carried out by me. Molecular biology experiments in order to generate the plasmids with deleted domain 1 and AP2 domain were generated by me. I also carried out the transfections to generate mutant strains in which the deletions of the different regions of the TgAP2IX-5 protein were carried out including domain1 and the AP2 domain. I also characterized these mutant strains with the deleted domain1 and the AP2 domain by carrying out plaque assays, nucleus per parasite counts and a growth assay. All graphs regarding counts were generated by me as well as all associated statistical analysis. Heat maps for the complementary experiments gene expression studies were generated and analyzed by me.

Regarding the third and final project, the iKD TgPP1 mutant was generated previously by Mathieu Gissot. All phenotype characterization experiments were carried out by me. Electron microscopy experiments were carried out in collaboration with Wanderley De Souza and Tatiana Araújo in Brazil at the Federal University of Rio de Janeiro. The phosphoproteomics analysis was performed by Chiarra Guerrera and Cerina Chluon at the Imagine Institute at Necker Hospital in Paris.

Materials & Methods

Chapter IV – Materials and Methods

1 Cell Culture

1.1   Maintenance of *T. gondii* parasite cell culture

Tachyzoites were grown in monolayers of human foreskin fibroblast (HFF) cells *in vitro*. Cells were maintained in culture in the presence of Dulbecco's Modified Eagles Medium (DMEM) GlutaMAX-1 (GibcoLife Technologies) which was supplemented with 10% of Fetal Bovine Serum (FBS) (GibcoLife Technolgies) and 1% Penicillin-Streptomycin (GibcoLife Technologies).

Strains	Genotype
KO TgAP2III-1 (Type I)	Direct knock-out (KO) RH Δhxgprt∆ku80; DHFR
KO TgAP2X-10 (Type I)	Direct knock-out (KO) RH Δhxgprt∆ku80; DHFR
KO TgAP2III-1 (Type II)	Direct knock-out (KO) Pru Δhxgprt∆ku80; DHFR
KO TgAP2X-10 (Type II)	Direct knock-out (KO) Pru Δhxgprt∆ku80; DHFR
iKD TgAP2IX-5-AID-HA	Inducible knock-down (iKD) RH Δhxgprt∆ku80 Tir1; HXGPRT
iKD TgAP2IX-5-AID-HA KI IMC3 mCherry	Knock-In (KI) RH Δhxgprt∆ku80 Tir1; AP2IX-5 AID-HA, HXGPRT IMC3-mCherry, DHFR (Tubulin promoter)
iKD Tg AP2IX-5-AID-HA KI SFA2-myc	Knock-In (KI) RH Δhxgprt∆ku80 Tir1; AP2IX-5 AID-HA, HXGPRT SFA2-Myc, DHFR
iKD TgAP2IX-5 AID-HA KI IMC29-myc	Knock-In (KI) RH Δhxgprt∆ku80 Tir1, AP2IX-5 AID-HA, HXGPRT IMC29-Myc, DHFR
iKDc TgAP2IX-5-AID-HA	Complemented strain (iKDc) RH Δhxgprt∆ku80 Tir1 ; AP2IX-5 AID-HA, HXGPRT AP2IX-5-myc, UPRT
iKDc TgAP2IX-5 AID-HA Δdomain1	Complemented strain (iKDc) RH Δhxgprt∆ku80 Tir1, AP2IX-5 AID-HA, HXGPRT AP2IX-5 Δdomain1-Myc , UPRT
iKDc TgAP2IX-5-AID HA ΔAP2 domain	Complemented strain (iKDc) RH Δhxgprt∆ku80 Tir1, AP2IX-5 AID-HA, HXGPRT AP2IX-5 ΔAP2domain-Myc , UPRT
iKD TgPP1-AID-Ty	Inducible Knock-down (iKD) RH Δhxgprt∆ku80 Tir1, PP1 AID-Ty-HXGPRT

Table 3 – Compilation of *T. gondii* parasite strains used in the study

Parasite strains were grown in T25 ventilated flasks containing a monolayer of HFF cells which were maintained in an incubator at 37°C and 5% CO_2. Parasite

culture was maintained by successive passaging of parasites once lysed out from the HFF host cells. Certain experiments required the collection of *T. gondii* tachyzoites prior to their lysis from the HFF cells. In this case, *T. gondii*-infected HFF cells were first scraped and then this was followed by the mechanical lysis of the parasites by passing scraped cells using a syringe sequentially. First, a 17-guage needle was used and then a 26-guage needle. The lysate was then filtered through a 3 μm Whatman membrane. The filtered parasites were then centrifuged for 15 minutes at 2400 rpm either at 4°C or at room temperature according to the experiment carried out and then washed with 1XPBS.

Parasite strains used to carry out this study include Type I and Type II parasites. Three *T. gondii* strains were used to carry out transfections and produce mutants. These strains can be designated as 'parental' strains and include: RHΔhxgprtΔku80, this Type I strain has the *Ku80* gene deleted in order to promote homologous recombination (Huynh & Carruthers, 2009). PruΔhxgprtΔku80, this Type II strain is devoid of the *Ku80* gene in order to promote homologous recombination as well. RH ΔhxgprtΔku80Tir1 strain, is a Type I strain which has a deleted *Ku80* gene and expresses the Tir1 protein which combines an increased rate of homologous recombination with an Auxin-inducible degradation (AID) system (Brown et al., 2018). The different transgenic parasite strains generated for the purpose of this study are summarized in Table 3.

2 Molecular Biology

2.1 *T. gondii* genomic DNA extraction

Genomic DNA (gDNA) was extracted from purified Type I and Type II *T. gondii* tachyzoites by using the Wizard Genomic DNA Purification Kit (Promega).
The pellet of filtered tachyzoites was re-suspended in 200 μL of Nuclei Lysis Buffer. 1 μL of RNase A was added and the re-suspended pellet was incubated at 37°C in a water bath for 15 minutes. This was the followed by the addition of 200 μL of Protein Precipitation Solution. Once the solution had cooled down to room temperature, it was vortexed and incubated on ice for 5 minutes. This was then followed by a centrifugation step at 13000g for 4 minutes at 4°C. After this, the supernatant was separated from the pellet and pipetted into a new tube which already contained 600 μL of room temperature isopropanol in order to precipitate the genomic DNA. The solution was then inverted gently and centrifuged again at 13000g for 30 minutes at 4°C. After this, the supernatant was removed from the tube and 600 μL of 70% ethanol was added to the pellet and centrifuged at 13000g for 30 minutes at 4°C. After the centrifugation step, the supernatant was removed and the pellet was left to airdry for 10 minutes until the ethanol had fully evaporated. Once the pellet had dried, 20 μL of DNA rehydration solution was added to each tube and incubated for 10 minutes at 65 °C. Once the gDNA was completely dissolved and cooled to room temperature, its concentration was measured by using a NanoVue Plus spectrophotometer (GE Healthcare). The gDNA was then stored at -20°C until required for use.
Extracted gDNA was used to test for the obtention of direct Knock-out mutants.

2.2 RNA sample preparation and extraction

RNA samples were prepared by infecting T175 flasks containing a monolayer of HFF cells with different *T. gondii* strains and under different conditions. Four different strains were used to prepare RNA samples required for this study (Pru WT, Pru TgAP2X-10 KO, Pru TgAP2III-1 KO, and iKD TgAP2IX-5) each of which were grown under a particular set of conditions prior to extraction of RNA (Type II strains were grown in normal pH (pH 7.0) as well as bradyzoite-inducing conditions (pH 8.2 and no CO_2), iKD TgAP2IX-5 parasites were grown in the absence of auxin (control) as well as the presence of auxin for different periods of time (1 hour, 2 hours, and 6 hours of auxin treatment). Parasites were collected by mechanical lysis and filtered prior to RNA extraction.

RNA extraction was carried out by re-suspending the collected parasite pellet in cold Trizol (Invitrogen). After this, Chloroform (4 °C) was added to the RNA samples which allowed for the separation of the RNA-containing aqueous phase and the protein-containing organic phase. The solution was then centrifuged at room temperature for 10 minutes. This was followed by transferring the aqueous phase into a new tube which contained cold isopropanol in order to precipitate the RNA by centrifugation at 4°C for 20 minutes at top speed. The precipitated pellet was then washed with 70% ethanol, dried, and re-suspended in RNase-free milliQ water (Gibco). This was then followed by a purification step in order to remove genomic DNA and clean the RNA samples by using the RNase-free DNase I Amplification Grade Kit (Sigma).

The last step was an RNA quality verification step in which the extracted RNA was verified by using an RNA 6000 Nano (Agilent) chip read by an Agilent 2100 Bioanalyzer. RNA samples which had an integrity score equal to or greater than 8 were used to prepare RNA libraries. RNA samples were stored at -80°C before RNA-seq library preparation.

2.3 RNA-seq Library Preparation

RNA library samples were prepared by using the TruSeq Stranded mRNA Sample Preparation Kit (Illumina). This kit was used to prepare RNA libraries according to the manufacturer's protocol. After RNA library samples were prepared, the libraries were validated by passing the samples on a DNA high-sensitivity chip using an Agilent 2100 Bioanalyzer. This was followed by a qPCR library quantification step using the KAPA library quantification kit (Illumina) by using a 12K QuantStudio thermocycler.

2.4. Different Strategies used to generate mutant parasites in this study

a) Direct Knock-out using CRISPR/Cas9 technology

In this strategy, two gRNAs were used in order to target the 5' and 3' ends of the of the gene of interest (*TgAP2X-10* gene and *TgAP2III-1* gene). This is to promote the insertion of the dihydrofolate reductase (DHFR) selection cassette flanked by 35 bp homology regions at the 5' and 3' ends. The transfection of the two Cas9 plasmids targeting the two gene ends with the PCR product containing the DHFR cassette allowed for the replacement of the entire gene of interest by the DHFR selection cassette. This resulted in a clean Knock-out mutant parasite achieved via homologous recombination.
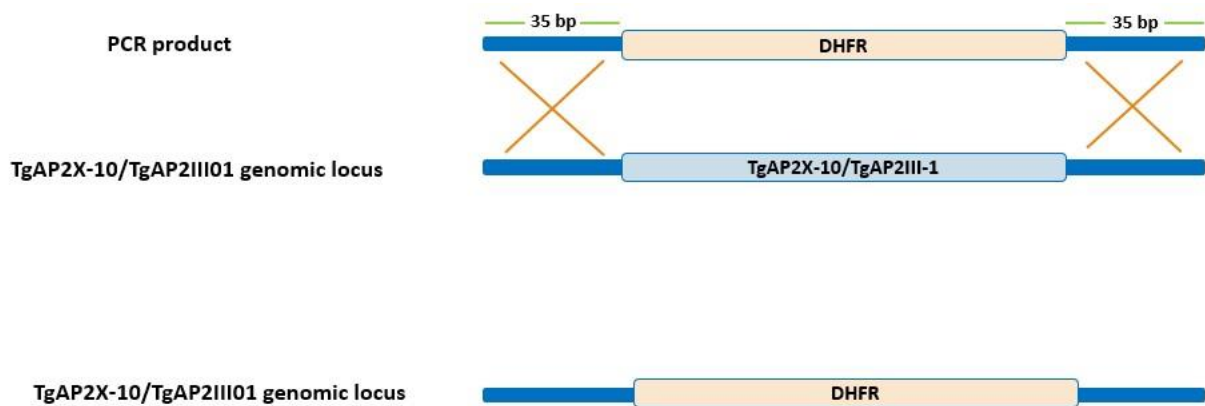
Figure 29 – Schematic representation of the direct Knock-out strategy used to generate TgAP2X-10 and TgAP2III-I knock-out strains.

Integration of the DHFR cassette was verified by PCR by amplifying the 3' and 5' ends of the genomic locus of the gene of interest that was replaced by the DHFR cassette. The pairs used to test DHFR cassette integration are illustrated in the schematic below:

Figure 30- Schematic representation of the primers used to verify DHFR cassette integration in the direct knock-out mutants.

b) Inducible Knock-down using the Auxin-induced degron (AID) system

This system was used to generate the iKD TgAP2IX-5 mutant strain by using gRNA to target the 3' end of the *TgAP2IX-5* gene after the STOP codon. A PCR product consisting of an AID-HA -HXGPRT cassette flanked by short homology arms was used in combination with the 3' targeting Cas9 plasmid in order to carry out the transfection to generate the mutant parasite. AID-HA-HXGPRT was added to the 3' end of the endogenous *TgAP2IX-5* gene. The transfected strain expresses Transport Inhibitor Response (Tir1) protein which has a role in targeted protein degradation upon the addition of the plant hormone Auxin (indole-3-acetic acid (IAA)).

In order to generate the iKD TgPP1 strain, a similar AID system was utilized. However, tagging of the endogenous gene was carried out at the 5' end of the gene instead of the 3' end due to the many complications that were demonstrated when initially attempting to generate iKD TgPP1 strain by targeting the 3' end of the *TgPP1* gene. In this case and for 5' targeting of the TgPP1 gene, a CRISPR/Cas9 plasmid consisting of a gRNA targeting the 5' end of the gene was generated. A PCR product with 30 bp homology containing an HXGPRT selection cassette (HXGPRT-T2A-AID-Ty) was transfected with the gRNA plasmid in order to tag the N-terminal of the gene of interest. The Skip peptide (T2A) present within the PCR product allowed for dual protein expression under a single promoter. The SKIP peptide is also characterized by cleavage properties and is responsible for the cleavage of the PP1 protein from the HXGPRT protein so that the TgPP1 protein can get degraded by the proteasome upon addition of the plant hormone Auxin.

A
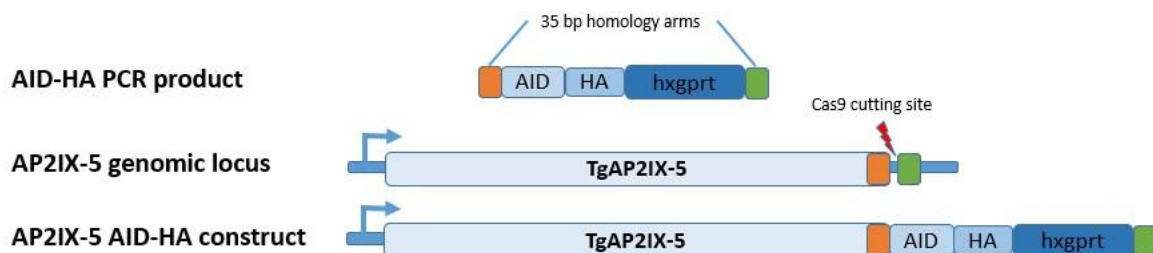
B
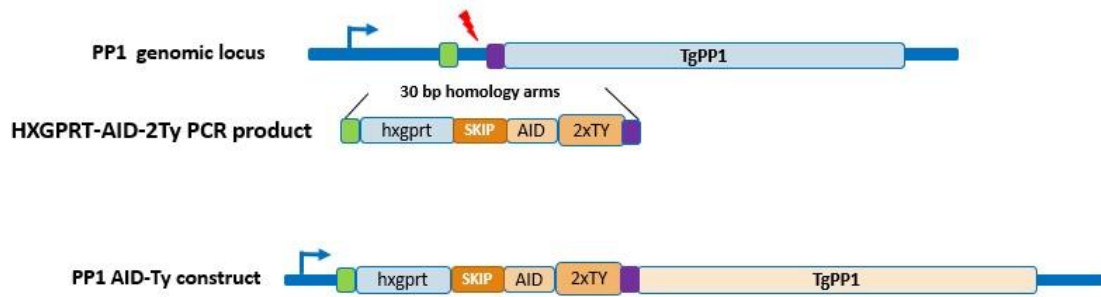
Figure 31 -Inducible Knock-down strategies using the AID system **(A)** Schematic representation of iKD TgAP2IX-5 mutant generation strategy. **(B)** Schematic representation of iKD TgPP1 mutant generation strategy.

c) Knock-In using the CRISPR/Cas9 strategy

Knock-In mutants were generated in the laboratory by targeting the 3' end of the gene of interest using a gRNA within CRISPR/Cas9 plasmid. PCR product was amplified by using the pLIC-Myc-DHFR plasmid as a template. Upon successful transfection of the amplified PCR product and the CRISPR/Cas9 PCR product, the gene of interest becomes tagged with the Myc tag at the C-terminal end of the gene. In this study, two genes were separately targeted TgSFA2 and TgIMC29.

Figure 32- Schematic representation of the strategy used to generate knock-in (KI) mutants using the 3' Cas9 strategy.

d) TgAP2IX-5 complementation and domain 1 and AP2 domain deletions

The complementation plasmid was synthesized by the GeneWiz company. A ~6.9 kb fragment coding for the TgAP2IX-5 gene which is myc-tagged in addition to a 3kb fragment corresponding to the promoter region were synthetically inserted

132

into a UPRT plasmid which consists of 2kb homology sequences for the UPRT gene. Upon transfection, integration of the TgAP2IX-5 gene at an exogenous locus (UPRT locus) was carried out since the UPRT gene is non-essential for the growth of the parasite and allows for counter selection of mutant parasites by FUDR treatment. In order to delete the AP2 domain and domain1 from the exogenous myc-tagged TgAP2IX-5 gene contained within the pUPRT plasmid, inverse primers were used for amplification and the complementation plasmids consisting of the deleted domains were constructed by using the Q5 mutagenesis kit (NEB) according to the manufacturer's protocol. The primers used to construct pUPRT plasmids with deleted domains are summarized in Table 4.

Deleted domain

AP2 domain/domain1
deletion from UPRT
plasmid
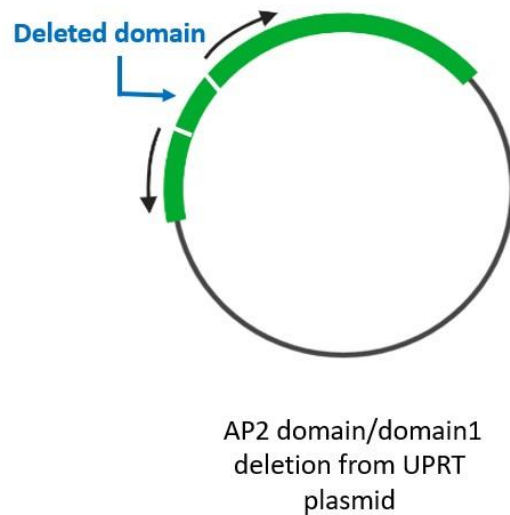
Figure 33–Schematic representation of strategy used to delete domain1 and AP2 domain from the pUPRT plasmid.

2.5 Cloning Techniques

Primers used to generate transgenic parasites used for this study are listed in the following table:

Name	5' Primer sequence 3'
KO TgAP2X-10 F	CAGAAGCCAGTTCACGAACTGTCCGTATTGATGTAAGCCGGATCCATTATGCGTGA
KO TgAP2X-10 R	GATTCAGAAAAGCGTAAACTGCTGTTTATTGCCTTTACTAGTGGATCGATCCCCCG
KO TgAP2III-1 F	GTTAAATAAGCTCCGCTCCAAACTAGGTCGCAACCAGCCGGATCCATTATGCGTGA
KO TgAP2III-1 R	ACTTCTCCATCGGTTACAGCCTATCGCATCTCTTGTACTAGTGGATCGATCCCCCG
iKD TgAP2IX-5 F	GGTACGGACGAAACCAAGTTGACGACTCCAGTGGATATCGGgctagcAAGGGCTCGG
iKD TgAP2IX-5 R	CTTCTGTGTCCATTTCTCCCCTTGGCTCCCGAGACCCCTTTGAATACGACTCACTATAGG
KI TgIMC29 F	CGCTCAGGCAGCAGTACCCCGGACACGGCCTCAATAAAATTGGAAGTGGACGG
KI TgIMC29 R	GTCACATCCGTATACACGGTTCTATGAGCAGATTCCGAATTGGAGCTCCACCGC
KI TgSFA2 F	CCTTACAGAAGGGCCTTCGAAATATAACAAGTCGCAAAATTGGAAGTGGAGGACGG
KI TgSFA2 R	ATACCGTGCTGATTCTTCTCTGAGAATCATCAACACGAATTGGAGCTCCACCGC
iKD TgPP1 F	TCTCAGGTTTCGCCAAAGCGCGCATGCATTCGGCAGATGGCGTCCAAACCCATTGA
iKD TgPP1 R	ATGACGGCGTCGACATCGACGTCTAATGACACCATATCGAGCGGGTCCTGGTT
5' Cas9 KO TgAP2X-10 F	GAAACGGTGGATACGAGCCGGTTTTAGAGCTAGAAATAGCAAGTTAAA
3' Cas9 KO TgAP2X-10 KO F	GCCTGACACGGACACACCGAGTTTTAGAGCTAGAAATAGCAAGTTAAA

5' Cas9 KO TgAP2III-1 F	CTGAAGCGCGGAAGGCGAGGGTTTTAGAGCTAGAAATAGCAAGTTAA
3' Cas9 KO TgAP2III-1 F	TGTGCCATCGAGCAGACGAAGTTTTAGAGCTAGAAATAGCAAGTTAAA
3' Cas9 iKD TgAP2IX-5 F	GGAGCGTAGAAAAGAAAGCGGTTTTAGAGCTAGAAATAGCAAGTTAA
3' Cas9 KI IMC29 F	AGCAGCATGATTACGTATTCGTTTTAGAGCTAGAAATAGCAAGTTAAA
3' Cas9 KI SFA2 F	CGTACTGCACGCCCATGCAAGTTTTAGAGCTAGAAATAGCAAGTTAAA
5' Cas9 iKD PP1 F	TATCTACATGTGATACAATGGTTTTAGAGCTAGAAATAGCAAGTTAAA
Cas9 generic reverse	AACTTGACATCCCCATTTAC
Q5-AP2IX-5 del_dom1-F	TGCGGAGCCAAGGGCGAG
Q5-AP2IX-5 del_dom1-R	GTCGCTATTCGCCGGGGC
Q5-AP2IX-5 del_AP2dom-F	ATCCGGTCGCCAGGCAATTC
Q5-AP2IX-5 del_AP2dom-R	AGGCGTCGGGTAACGCGC
Deletion screen domain 1- F	TGCAGAGCGCGCGGGCGA
Deletion screen domain 1 -R	CCACTCGGATCCTGCACG
Deletion screen AP2 domain- F	GTCGAAGAACGCGAAGCC
Deletion screen AP2 domain - R	CCCGACGTCTGGCGCGGC
TgAP2X-10 5' F KO screen	AAGCGTAGACGGCTTGGTTT
TgAP2X-10 3' R KO screen	AGGACTCGGTCGTCTCCTTT
TgAP2III-1 5' F KO screen	CTCCGTGGCTCTGTCTCATC
TgAP2III-1 3' R KO screen	CCGCTGCTCAATTACCTTGC

Table 4- Table of primers used to generate mutant parasites for this study

Plasmid name	Corresponding mutants
pLIC-DHFR	KO TgAP2X-10 and KO TgAP2III-1
pLIC-MYC-DHFR	KI TgIMC29 and KI TgSFA2
pAID-HXGPRT-3XHA	iKD TgAP2IX-5
pHXGPRT-2TA-AID-Ty	iKD TgPP1

Table 5- Table of plasmids used as templates to generate PCR products

2.5.1 Generation of PCR products

In order to generate the PCR products for the transfections, forward and reverse primers indicated in Table 4 were used. Plasmids indicated in Table 5 were used as templates to generate appropriate PCR products. gDNA mentioned previously in section 2.1 was used as a template in the case of testing for dhfr integration. Phusion High-Fidelity DNA Polymerase (NEB) enzyme was used according to the manufacturer's recommendations and using the following thermocycler protocol:

Initial Denaturation	→	95 °C (5 min)	
Denaturation	→	95 °C (30 sec)	
Annealing	→	primer-specific (58°C -65°C)	35 cycles
Elongation	→	72°C (30 sec/Kb)	
Final Elongation	→	72 °C (10 min)	
Storage	→	4 °C (∞)	

Amplified PCR product bands were visualized on agarose gels in order to confirm PCR product amplification. After this, PCR products were purified by using NucleoSpin Gel and PCR Cleanup Kit (Machery Nagel). The concentration of the PCR products was measured using the NanoVue Plus spectrophotometer (GE Healthcare).

2.5.2 CRISPR/Cas9 Plasmid Construction

The CRISPR/Cas9 plasmids were generated within the laboratory by directed mutagenesis in order to modify the gRNA region of the plasmid (pSAG1:Cas9-U6::sgUPRT) obtained from Dr Sibley and following the method described by Shen et al. (2014).

2.6 Chromatin Immunoprecipitation (ChIP)

Chromatin immunoprecipitation experiments were carried out on iKD TgAP2IX-5 mutant parasites. Parasites were grown intracellularly for 40 hours. This was followed by a fixation step for 10 min at room temperature by adding 1% formaldehyde in order to ensure that the DNA and proteins are covalently linked. The parasites were then filtered and re-suspended in lysis buffer which consists of 50mM Tris-HCl pH8, 10 mM EDTA, and 1% SDS. After this, parasites were sonicated in a Bioruptor sonicator for 10 minutes at 4°C (30 sec on/off per cycle). Protein-DNA associated complexes were diluted using IP dilution buffer which consists of 16.7 mM Tris-HCl pH8, 167 mM NaCl, 1.2 mM EDTA, 0.01% SDS, 1.1% Triton, and 0.5 mM PMSF. Then, an overnight incubation step was carried out in the presence of IgG agarose beads (Amersham Biosciences). The following day, the IgG beads were washed five times using ChIP wash buffer consisting of 50 mM Tris-HCl pH8, 250 mM NaCl, 1% NP-40, 1% desoxycholic acid, and 0.5 mM PMSF followed by two elution steps using 75 μL of ChIP elution buffer which consists of 50 mM NaHCO$_3$ and 1% SDS. This experiment was realized in duplicates (biological replicate of immunoprecipitation and input samples). This was followed by ChIP-seq library preparation where 1 ng of purified DNA was used as a template. The Nugen Ovation® Ultralow System V2 kit was used, and the preparation of libraries was carried out according to the manufacturer's instructions. The validation of the libraries was carried out using Fragment Analyzer and qPCR was used to quantify the libraries (ROCHE LightCycler 480).

3   Cell Biology

3.1   Parasite transfection

Parasite transfection was carried out by using 10^6 freshly lysed and purified tachyzoites for each transfection by electroporation. In order to generate the direct KO strains (KO TgAP2X-10 and KO TgAP2III-1), 30 µg of Cas9 plasmids targeting the 3' and 5' ends of the *TgAP2X-10* and *TgAP2III-1* genes and ~ 10 µg of PCR product consisting of the DHFR selection cassette flanked by homology sequences were electroporated into the parental RH*Δku80* (Type I) and Pru*Δku80* (Type II) strains.

In order to generate the iKD TgAP2IX-5 strain, the parental RH*Δku80* Tir1 strain was transfected with 30 µg of Cas9 plasmid targeting the 3' end of the TgAP2IX-5 gene after the stop codon and ~10 µg of PCR product consisting of the AID-HXGPRT-HA cassette flanked by homologous arms. In order to generate the KI TgIMC29 and KI TgSFA2 strains, the iKD TgAP2IX-5 strain was transfected with 30µg of Cas9 plasmid targeting the 3' UTR of each gene and 10 µg of PCR product consisting of a DHFR cassette and Myc tag.   For the iKD complementation transfection, 60µg of synthetically produced plasmid consisting of the 3-kb upstream region of the start codon of the *TgAP2IX-5* gene, the full length *TgAP2IX-5* gene and full-length c-Myc tag flanked by 2 kb of homology sequence for the *UPRT* gene was co-transfected with the pSAG1::Cas9-U6::sgUPRT plasmid to ensure the insertion into the UPRT locus. A similar approach was carried out for generating iKD complementation parasites with deleted domain1 and AP2domain sequences where 60 µg of pUPRT plasmid consisting of a myc-tagged *TgAP2IX-5* gene with either a deleted domain1 or deleted AP2domain was co-transfected with 30µg of Cas9 plasmid targeting the *UPRT* gene. In order to generate the iKD TgAP2IX-5 strain expressing TgIMC3-mCherry, the iKD TgAP2IX-5 strain was transfected with a TgIMC3-mCherry expressing plasmid with a *tubulin* promoter.

Plasmids and PCR products were precipitated by using sodium acetate and re-suspended in a cytomix solution which consisted of 120mM KCl, 10mM K2HPO4/KH2PO4 pH7.4, 25mM HEPES pH7.6, 2mM EGTA pH7.6, 5mM MgCl2, and 0.15mM CaCl2; pH 7.6. The filtered parasites were re-suspended in a cytomix solution complemented with 2mM ATP and 5mM GSH (reduced glutathione). Re-suspended parasites and precipitated DNA were mixed and placed within an electroporation cuvette to carry out electroporation by using a BTX Electro Cell Manipulator 600 at 1.5 kV.cm^{-1}, 25µF capacitance, and 24Ω resistance. After electroporation, the parasites were put into a T25 flask and left to grow for 24 hours before adding the appropriate selection drug. For DHFR cassette transfections, 2 µM pyrimethamine (Sigma) was added. For HXGPRT selection, 25 µg/mL of mycophenolic acid (Eurogentech), and 50µg/mL of Xanthine (Sigma) was added. For UPRT counter-selection, 5µM of 5-fluorodeoxyuridine (FUDR) (Sigma) was used.

Regarding direct knock-out strains, mixed population parasites were verified for integration of the DHFR cassette by PCR. All other transfections were verified by

IFA for the presence of either the HA-tag or c-Myc tag. Clonal lines were generated by limiting dilution by cloning them into a 96-well plate and then transferring single parasite clones to 24-well plates for further validation either by IFA or integration PCR.

3.2 Intracellular growth assays

Growth assays were carried out by inoculating 8×10^4 parasites of parental and mutant parasites on a monolayer of HFF cells grown on 24-well plate coverslips for 24 hours. In the case of iKD TgAP2IX-5 and iKD TgPP1 growth assays, parasites were left to grow for 24 hours in the presence and absence of 0.5 mM of auxin. Infected coverslips were fixated using 4% paraformaldehyde (PFA). Parasites were stained with anti-TgEno2 and anti-TgIMC1 antibodies. The number of parasites per vacuole was counted for a total of 100 vacuoles for each biological replicate. A total of three biological replicates were included for each growth assay experiment.

3.3 Plaque assays

For the plaque assays, a total of 200 parental and mutant parasites were inoculated on a monolayer of HFF cells grown in a 6-well plate in normal media or media treated with auxin. Parasites were left to grow for 7 days before fixation with 100% ethanol. Plaques were stained with Crystal Violet in order to visualize the proliferation.

3.4 *In-vitro* bradyzoite differentiation assays

All pre-bradyzoite formation assays were carried out using Type II Pru Δku80 WT and KO TgAP2X-10 and KO TgAP2III-1 strains. Parasites were inoculated on HFF cells grown on coverslips in a 24-well plate for either 24 hours or 48 hours in normal media at a pH of 7.0 or RPMI media (RPMI 1640) supplemented with 1% FBS and 10mM HEPES at a pH of 8.2. Parasites grown in alkaline conditions were incubated at 37°C without CO_2. After fixation with 4% PFA, *Dolichos biflorus agglutinin* also known as DBA (Vector Laboratories), a bradyzoite-specific lectin that binds a major cyst wall protein CST1, was used to label pre-bradyzoite cyst walls at a dilution of 1:500. The percentage of parasites exhibiting pre-bradyzoite formation (*Dolichos* positive) was measured in both pH conditions.

3.5 Bradyzoite formation in brain cell culture assay

An *in vitro* primary brain cell culture was used to study mature bradyzoite formation in brain cells extracted from the hippocampus of rat pup brains. Brain cells grown on coverslips of 24-well plates were infected with 5×10^3 parasites of Type II PruΔku80 WT and TgAP2X-10 KO and TgAP2III-1 KO strains for 7 days before fixation with 4% PFA. Labelling was carried out using DBA at a dilution of 1:500. The percentage of parasites with a DBA- positive cyst wall was measured.

3.6   Organelle and IMC labelling

Parental and mutant parasites (iKD TgAP2IX-5 and iKD TgPP1) were inoculated on a monolayer of HFF cells grown on coverslips of a 24-well plate.

iKD TgAP2IX-5 organelle labelling: For nucleus labelling, parental and mutant parasites were left to grow for 24 hours prior to addition of auxin for 3 hrs, 6hrs, and 12 hrs. Parasites were then fixated with 4% PFA and nuclei were stained with anti-TgEno2 and the number of nuclei per parasite was counted. For labelling of the Inner Membrane Complex (IMC), parental and mutant parasites were left to grow for 24 hours on HFF cells grown on coverslips. Then, auxin was added for 6 hours prior to fixation. Parasites were labelled with anti-TgIMC1 and anti-TgISP1. The outer and inner core of the centrosomes were labelled after parental and mutant parasite growth overnight followed by addition of auxin for 6 hours. Anti-TgCentrin1 and anti-TgChromo1 were used to label the outer core and inner core, respectively. For Golgi, plastid, and mitochondria labelling, parasites were grown overnight in the presence of auxin before fixation and labelling with the following antibodies: anti-TgSort, anti-TgACP, and anti-TgTom40, respectively.

iKD TgPP1 organelle labelling: Parental Tir 1 and iKD TgPP1 mutant parasites were left to grow in the presence of Auxin for 24 hours, 48 hours, and 72 hours prior to fixation and labelling. The IMC was labelled using anti-TgIMC1, anti-TgISP1, and anti-TgGAP45. Golgi, plastid, and Centrin1 were labelled using the following antibodies: anti-TgSort, anti-TgACP, and anti-TgCentrin1, respectively.

3.7   Immunofluorescence Assays

All immunofluorescence assays (IFAs) were carried out by fixating intracellular parasites with 4% PFA for 30 minutes. The coverslips were then washed 3 times with 1x PBS and permeabilized using the following solution (1x PBS; 0.1% Triton 100x (Sigma); 0.1% glycine (Sigma); 5% FBS (Gibco Life Technologies)) for 30 minutes. Coverslips were then incubated in primary antibodies (Table 6) for 1 hour diluted in the same IFA buffer used previously for permeabilization. Coverslips were then washed 3 times using 1x PBS and then incubated in secondary antibodies coupled to either Alexa-594 or Alexa-488 (Invitrogen) for 1 hour. Host cell and parasite nuclei were stained with DAPI (Euromedex). After incubation with secondary antibodies and DAPI, coverslips were washed with 1x PBS and mounted onto microscope slides using Moviol (Sigma). IFA quantification was carried out manually by counting the appropriate signal by visual observation. Signal was counted for 100 parasites for each replicate. Each experiment was carried out 3 times independently (triplicate).

Antibody Name	Dilution	Origin
Anti-TgEno2 (rabbit)	1:1000	Dzierszinski et al., 2001
Anti-TgIMC1 (mouse)	1:500	Prof. Ward, U. Vermont
Anti-TgISP1 (mouse)	1:500	Beck *et al*, 2010

Anti-TgGAP45 (rabbit)	1:10000	Dr Soldati
Anti-TgCentrin1 (rabbit)	1:500	Prof. Gubbels, Boston College
Anti-TgChromo1(mouse)	1:500	Gissot et al., 2012
Anti-TgSort (rat)	1:500	Sloves et al., 2012
Anti-TgACP (mouse)	1:500	Dautu et al., 2008
Anti-TgTom40	1:500	van Dooren et al., 2016
Anti-myc (rat)	1:200	abcam
Anti-HA (rabbit)	1:500	Sigma-Aldrich

Table 6- List of antibodies and their corresponding dilutions used in IFAs.

3.8   TgAP2IX-5 re-expression experiments

iKD TgAP2IX-5 mutant parasites were inoculated on HFF cells grown on 24-well plate coverslips and left to grow for 16 hours in the presence of auxin. This was followed by washing out auxin from the media and leaving the parasite to grow in normal media for 3 hrs, 6hrs, and 16 hrs before fixation with 4% PAF. Auxin washout consisted of changing the media treated with auxin to normal media 3 times with 5-minute incubation periods at 37°C between each media change.

Anti-TgEno2 was used to label the nuclei of the parasites in order to count the number of nuclei per parasite. In parallel, the IMC was labelled with TgISP1 and TgIMC3 in order to measure the percentage of daughter parasite formation. Furthermore, the plastid was labelled with anti-TgACP in order to measure the ratio of plastid to nucleus. Each experiment was carried out in biological triplicates.

3.9   *In Vivo* cyst burden counts experiment

Ten balb/c mice were intraperitoneally injected with $2x10^3$ parasites of either the wildtype PruΔku80, TgAP2X-10 KO or TgAP2III-1 KO strains. The mice were left infected with the Type II wildtype and KO strains for 4 weeks before dissecting and isolating the brains of the mice. After the collection of mice brains, they were mechanically homogenized and one fifth of each mouse brain was labelled with *Dolichos biflorus Agglutinin* (DBA) overnight in order to count the number of tissue cysts formed within each individual brain.

A second subsequent experiment was carried out where ten balb/c mice were injected intraperitoneally with $2 x10^3$ parasites of either the Type II Pru wildtype, TgAP2X-10 KO, or TgAP2III-1 KO strains. These mice were then left for 8 weeks before isolating the brains and counting the total number of tissue cysts formed within the brain using DBA labelling.

4 Microscopy

4.1 Confocal microscopy

Imaging of immunofluorescence assay experiments was carried out by using a confocal microscope (ZEISS LSM880 confocal microscope or Apotome Microscope).

A magnification of 63x was used. Processing of images was carried out by using the Carl Zeiss Zen software.

4.2   Electron microscopy

iKD TgAP2IX-5 parasites were inoculated on a monolayer of HFF cells and were grown for 24 hrs either in normal media or media treated with auxin in T25 flasks. iKD TgPP1 parasites were inoculated on a monolayer of HFF cells and were grown for 48 hrs either in the presence or absence of auxin. Parasite samples were then fixated overnight with 1% glutaraldehyde in 0.1M sodium cacodylate pH 6.8 at 4°C. This was then followed by a post-fixation step using 1% osmium tetraoxide and 1.5% potassium ferricyanide followed with 1% uranyl actetate. Post-fixation steps were carried out in distilled water, in the dark, and at room temperature for the duration of 1 hour. Samples were then washed and dehydrated using increasing ethanol-concentration solutions. Then, samples were infiltrated by using epoxy resin and cured at 60°C for 24 hrs. 70-80 nm- thick sections were deposited in grids coated with formvar and were observed at 80 kV using a Hitachi H7500 TEM (Milexia, France). Image acquisition was carried out by using a 1 Mpixel digital camera (AMT, Milexia, France).

4.3   Live-imaging re-expression experiments

iKD TgAP2IX-5 parasites expressing IMC3-mCherry were inoculated on HFF cells grown in an 8-well chamber for 7 hours before adding 0.5mM auxin overnight (16 hrs). The next day, auxin was washed out from the media by changing the media three times with 5-minute incubation times at 37°C between each medium change. Signal corresponding to TgIMC3-mCherry was collected every 13 minutes (4 lines average and zoom factor between 2-4). Images obtained were 512x512 pixels in size, and 8 bits in resolution (256 gray levels). Image J (NIH) was used to treat images and Z-stack acquisition allowed for 3D fluorescent signal visualization. The movie was created at a rate of 2 frames per second. Representative images collected at 5 different time points (T_0= baseline for auxin washout, T_1= 43 min after washing out auxin, T_2 =1.5 h after auxin washout, T_3 = 1.73 h after auxin washout, and T_4 =3.9 h after auxin washout) were used to illustrate the phenotype.

5 Biochemistry

5.1 Protein extraction and Western Blotting

For western blots, $2x10^6$ parasites of the parental Tir1 strain were grown in normal media for 24 hrs and iKD TgAP2IX-5 strain parasites were grown for 24 hours in normal media or media treated with auxin for different durations of time for 1 hour, 3 hours, and 6 hours. Parasites were purified by filtration, centrifuged, and the pellet obtained was re-suspended in the following loading buffer (240mM Tris-HCl pH 6.8; 8% SDS, 40% saccharose; 0.04% bromophenol blue, and 400 mM DTT). WB samples were then incubated for 10 minutes at 95°C. Denatured protein extracts were then separated on a 6% polyacrylamide electrophoresis gel and then transferred onto a nitrocellulose membrane (GE Healthcare). Protein transfer was carried out for around 2 hours at 100V. Western blot membranes were then blocked by using a blocking buffer consisting of 5% milk in TNT buffer (100mM Tris pH8; 150 mM NaCl and 0,1% Tween). This was followed by incubating the

membranes in primary antibody for 1 hour, washing the membrane 4 times, and then incubation in secondary antibody for another hour. Antibodies were diluted in 5%milk dissolved in TNT buffer. Protein band revelation was carried out by using Super Signal West Femto Maximum Sensitivity Substrate (Thermo Scientific). Band visualization was carried out by using the ChemiDoc™ XRS+ (Biorad).

Western blots for re-expression of TgAP2IX-5 were carried out using a similar Western blotting protocol. However, preparation of parasite samples for re-expression consisted of leaving the iKD TgAP2IX-5 parasite to grow overnight in the presence of auxin before washing auxin out for different durations of time for 3 hrs, 6 hrs, and overnight.

Antibodies used: anti-HA mAb (rabbit) (Sigma-Aldrich) used at a dilution of 1:500, anti-TgSortilin (rat) at a dilution of 1:400 (Sloves *et al.* 2012). The secondary antibodies used are species-specific and conjugated to HRP.

5.2 Phospho-proteome extraction and analysis

Mutant iKD TgPP1 parasites were left to grow in T175 flasks consisting of confluent HFF cells before Auxin treatment for 2 hours. Mutant parasites grown without Auxin treatment were used as a control. Parasites were filtered and the pellet was re-suspended in 8M Urea solution containing Protease and Phosphatase Inhibitor Cocktail (Thermo Fisher Scientific) to a final concentration of 35 million parasites/50 µL of re-suspension buffer. Parasite samples were always kept on ice in between different steps of the extraction. Then, samples were sonicated by using a Bioruptor sonicator at 4°C for 10 cycles (30 sec on/off per cycle). Samples were then centrifuged at 4°C for 20 minutes at 4000 rpm. After centrifugation, the supernatant was transferred into a new tube. Extracted proteins concentration was quantified by using the Pierce ™ BCA Protein Assay (Life Technologies). Samples were then stored at -80°C until sent for analysis.

Titansphere TiO_2 was used to carry out phosphopeptide enrichments (GL Sciences Inc). 20 µL of solution A which consists of 80% acetonitrile and 0.4% TFA was used to condition the TiO_2 Spin tips. This was followed by a 2-minute centrifugation step at 3000g. The tips were then equilibrated with 20 µL of solution B which consists of 75% acetonitrile, 0.3% TFA, and 25% lactic acid. Then, a 2-minute centrifugation step was carried out at 3000 g. 20 µL of solution A was used to dissolve the peptides. 100 µL of solution B was added and mixed with the peptides followed by centrifuging for 10 minutes at 1000g. Phosphopeptide adsorption was increased by spinning the tips two more times followed by sequential washing using Solutions A and B. Elution of the peptides was carried out by adding 50 µL of 5% NH_4OH and 5% pyrrolidine. This was followed by a centrifugation step for 5 minutes at 1000g. The phosphopeptides were then purified using GC Spin tips (GL Sciences Inc.). After elution from the GC Spin tips, the phosphopeptides were vacuum dried.

In order to analyze the phosphoproteome, phosphopeptides were resuspended in 42 µL of 0.1% TFA dissolved in HPLC-grade water. Injection of 5 µL of each individual sample into the mass spectrometer was carried out. Loading of the samples was done on a µ-precolumn (Thermo Scientific). This was followed by separation on a 50 cm reversed-phase liquid chromatographic column (Thermo Scientific). The solvents used for chromatography were solvent A which was

composed of 0.1% formic acid dissolved in water, and solvent B which consists of 80% acetonitrile and 0.08% formic acid. The gradient used to elute the samples from the column is as follows: 5% to 40% B for 120 minutes, 40% to 80% for 6 minutes, 5% re-equilibrium for 20 minutes before the proceeding injection. Sample carry-on was prevented by running a blank in between each two samples. Data dependent MS/MS analysis was carried out in order to analyze the eluted samples. The MaxQuant software version 1.5.8.3 was used to process the MS files. Statistical analysis and heatmaps were generated using the Perseus software (version 1.6.0.7).

6 Bio-informatics Analysis

6.1 RNA-seq analysis

RNA libraries were sequenced as 50 bp reads on a HiSeq 2500 using the technique known as the sequence by synthesis technique. Image analysis was carried out by using HiSeq control software and real-time analysis component. Demultiplexing was carried out by using the bcl2fastq 2.17 conversion software (Illumina). Raw sequencing datasets including a total of 110 M reads were checked for quality using the FastQC v0.11.8-0. The sequencing adapters were treated with Cutadapt v1.18. Trimmomatic v0.38.1 was used to filter out reads shorter than 50 bp and low-quality bases.

After datasets were cleaned and aligned with HiSAT2 v2.1.0 against the *T. gondii* ME49 genome from ToxoDB. The quantification of annotated gene expression was carried out by using htseq-count belonging to the HTSeq suite v0.9.1. Differential expression analysis between mutant parasites treated with auxin (1 hr, 2 hrs, and 6 hrs) and control mutant parasites not treated with auxin was carried out by using DESeq2 v1.22.1 using the SARTools framework v1.6. and this was performed after adding raw counts from technical replicates. The Benjamin-Hochberg method was used to adjust the p-values. Differentially expressed genes with an adjusted p-value less than 0.05 and a log2 fold change greater than 2 were kept.

6.2 ChIP-seq analysis

Alignment of cleaned datasets consisting of 14 M reads was carried out by using Bowtie2 v2.3.4 against the *T. gondii* ME49 genome (ToxoDB). This was followed by merging alignments from biological and technical replicates using SAMtools v1.9. Picard MarkDuplicates v2.18.20 were used to identify duplicates. DeepTools suite v3.1.3 was used to verify ChIP quality and dataset consistency. MAC2 v2.1.2 was used to identify peaks.

6.3 AP2 domain sequence alignment

A Basic Local Alignment Search Tool (BLAST) (Altschul et al., 1990) analysis was performed and used to align the TgAP2IX-5 protein sequence with the protein sequences of other proteins in the genomes of apicomplexan members. This allowed for the identification of a novel conserved domain (domain 1).

6.4 Statistical analysis

Graph Pad Prism software version 8 (San Diego, California, USA) was used to analyse all data. A student t-test was used in order to indicate significant differences between means. In all cases, $p < 0.05$ was considered as significant. All experiments consisted of using biologically independent replicates with a minimum of 100 parasites counted per independent experiment.

Results and Discussions

Chapter V – Results

V-1- Role of AP2X-10 and AP2III-1 during *T. gondii* differentiation

This PhD study consisted of three different projects. In the first part of the study, an attempt to functionally characterize two ApiAP2 transcription factors, TgAP2X-10 and TgAP2III-1 was carried out.

INTRODUCTION

T. gondii exhibits a unique and complex life cycle shared between the warm-blooded intermediate host and the definitive felid host correlating to asexual and sexual division, respectively. *T. gondii* asexual division consists of two separate stages of growth contingent on whether the infection is in the acute or chronic phase. The tachyzoite stage present during the acute phase of the infection is known for its rapid growth whereas the bradyzoite stage present during the chronic phase of the infection is a dormant form of the parasite with slow replicating properties (MW Black, JC Boothroyd, 2000).

Replication of the tachyzoites occurs within a membrane-bound compartment known as the parasitophorous vacuole (PV); this compartment can develop into a cyst wall during the conversion of the rapidly replicating tachyzoites to latent bradyzoite cysts (Sullivan WJ,Jr,Jeffers V, 2012). Tissue cysts were found to appear 7 to 10 days post infection in animals (MW Black, JC Boothroyd, 2000) having the ability to develop within the central nervous system (CNS) as well as within the fibers of muscle tissues across the body. Bradyzoites present within a tissue cyst are protected by a prominent thick wall structure also known as the cyst wall which can be visualized by electron microscopy (JP Dubey, 1998). The 'cyst wall' is heavily glycosylated and is easily stained with *Dolichos biflorus lectin* (DBA) (JP Dubey et al, 1998; Sims et al, 1988; Boothroyd et al, 1997) and is rich in glycoproteins such as PPG1 (Craver et al., 2010) and CST1 which is the specific target for binding of DBA (Tomita et al., 2013). The modifications of carbohydrates present on the cyst are suggested to have a role in allowing the cyst wall to remain undetected by the host immune system leading to life-long persistence of the chronic infection.

Interconversion between the tachyzoite and bradyzoite form is a key characteristic of the *T. gondii* parasite. The importance of this phenomenon lies in ensuring parasite pathogenesis and transmission.

Tachyzoite to bradyzoite interconversion has been studied *in vitro* using stress-inducing alkaline conditions in addition to other stimuli such as starvation from nutrients, heat shock, and the utilization of specific drugs (Cerutti et al., 2020). The pH stress bradyzoite-inducing *in vitro* model has been extensively used to study bradyzoite differentiation. However, it remains with certain limitations as

mature bradyzoite development is not achieved and only early bradyzoite markers are expressed in addition to the expression of some tachyzoite markers (Soete et al., 1994).

The transition from tachyzoites to bradyzoites has been demonstrated to involve significant transcriptomic changes. The significant differential expression of hundreds of genes has been shown to occur in *in vivo* cysts isolated from the host 3-4 weeks post-infection (Buchholz et al., 2011; Pittman et al., 2014). A full understanding of how the regulation of genes associated with tachyzoite to bradyzoite interconversion remains to be elucidated. Albeit this, previous studies have demonstrated that gene expression regulation associated with tachyzoite/bradyzoite transitions involves epigenetic modification of histones (Bougdour et al., 2009; Naguleswaran et al., 2010; Saksouk et al., 2005). A Myb-like transcription factor designated as TgBFD1 has been recently characterized and has proven to have an essential role in the differentiation of bradyzoites in tissue cell culture and *in vivo* in mice by binding to the promoters of several stage-specific genes (Waldman et al., 2020). Moreover, this Myb-like transcription factor has been shown to be sufficient for driving the differentiation of bradyzoites (Waldman et al., 2020). Furthermore, genetic studies in *T. gondii* have demonstrated that several ApiAP2 TFs control cyst formation, by either activating or repressing bradyzoite differentiation. For example, TgAP2XI-4 and TgAP2IV-3 are known bradyzoite activators and co-regulate TgBAG1 and TgLDH2 bradyzoite- specific genes. In a similar fashion, TgAP2IV-4 and TgAP2IX-9 were identified as bradyzoite repressors regulating bradyzoite-specific genes such as TgBPK1 and TgB-NTPase (Walker et al., 2013a; Hong et al. 2017; Huang et al., 2017; Radke et al. 2013; Radke et al., 2018). Despite previous studies in which a number of ApiAP2 TFs have been characterized, none of these ApiAP2 TFs have demonstrated to be exclusively responsible for the control of bradyzoite development. Therefore, the identification of other ApiAP2 TFs that could have a potential role in controlling bradyzoite development remains to be explored. Here, we took advantage of a novel primary brain cell culture model that has been recently developed in which bradyzoites can be maintained for up to 2 weeks (Mouveaux et al., 2021). In this study, it was demonstrated that several ApiAP2 TFs are preferentially expressed during differentiation, indicating their potential involvement in this process.

We therefore attempted to characterize two ApiAP2 TFs, TgAP2X-10 and TgAP2III-1, both of which are expressed preferentially late during differentiation kinetics (Mouveaux et al., 2021).

In order to characterize TgAP2III-1 and TgAP2X-10 TFs, direct Knock-out mutant parasites were generated. Mutant parasites lacking TgAP2X-10 and TgAP2III-1 did not display any growth defect. Studying the effect of TgAP2X-10 and TgAP2III-1 on bradyzoite differentiation in pH-stress bradyzoite-inducing *in vitro* models using HFF cells yielded unsignificant results. However, when studying the effect

of TgAP2X-10 and TgAP2III-1 on bradyzoite differentiation using the novel brain cell culture *in vitro* model, TgAP2X-10 was demonstrated to have a role in bradyzoite differentiation. Additionally, the role of TgAP2X-10 and TgAP2III-1 was studied *in vivo* by measuring cyst burden counts in mice suggesting that both TFs could have a role in bradyzoite differentiation *in vivo*.

1.1   Role of TgAP2X-10 and TgAP2III-1 in parasite growth

With the goal of characterizing the function of the two ApiAP2 TFs, TgAP2X-10 and TgAP2III-1, Type I RH ΔKu80 and Type II PruΔKu80 transgenic parasites were generated in which a direct Knock-out strain of either TgAP2X-10 or TgAP2III-1 was produced via homologous recombination (Figure 1A). Transfections were carried out on the Type I RH ΔKu80 strain since it is a rapidly growing strain and thus easy to handle. However, transfections were carried out on the Type II PruΔKu80 strain to study differentiation. This system consisted of replacing the gene of interest's locus by a DHFR selection cassette and integration of the DHFR cassette at 3' and 5' ends was verified by PCR (Figures 1B and 1C). Growth assays in which the Type I RH ΔKu80 wildtype and the two Type I knock-out mutants were left to grow for 24 hours followed by counting the number of parasites per vacuole did not demonstrate any growth defect (Figure 1D). Similar unsignificant results were obtained when studying the growth of the Type II PruΔKu80 wildtype and the two Type II knock-out mutants (Figure 1E).

A
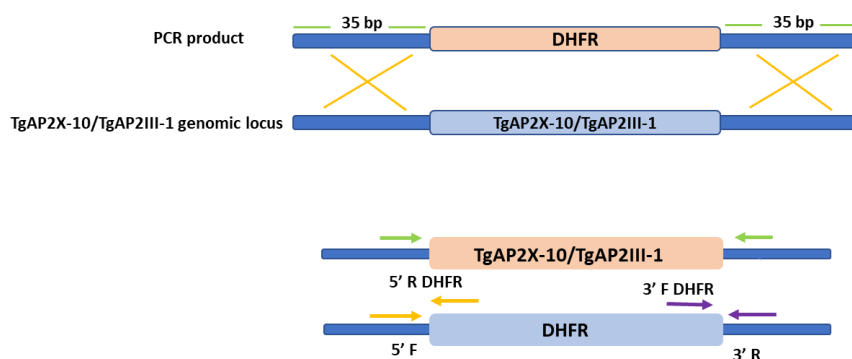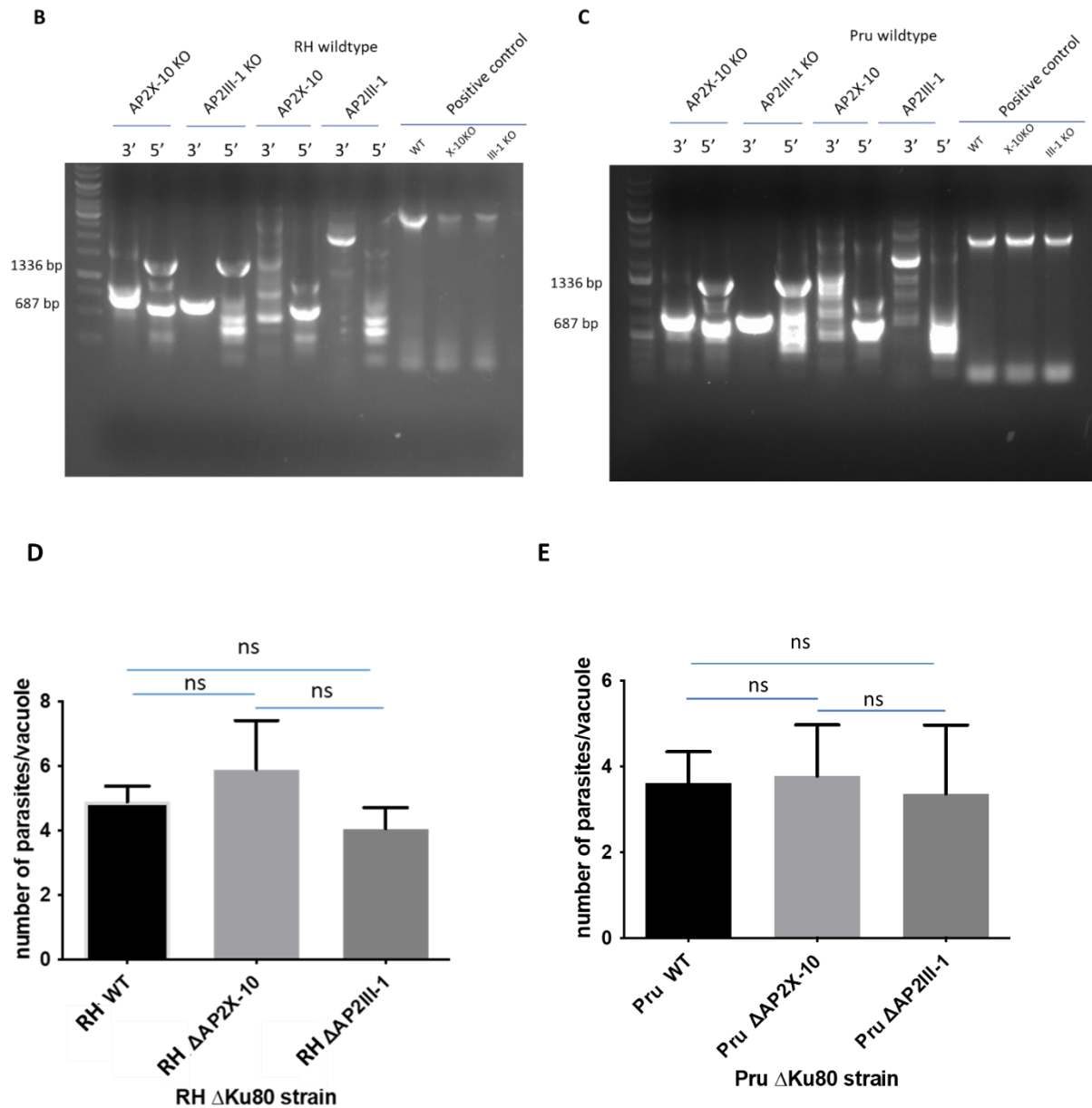
Figure 1: **(A)** Schematic representation of the Knock-out strategy utilized to generate transgenic parasite lines used for the study. **(B)** PCR image of the dhfr cassette integration test at 3' and 5' ends of the genomic locus in Type I RHΔKu80 WT and Knock-out strains. **(C)** PCR image of the dhfr integration test at 3' and 5' ends of the genomic locus in the Type II Pru ΔKu80 WT and transgenic strains **(D)** Bar graph representing the growth assay of Type I RH RHΔKu80 TgAP2X-10 and TgAP2III-1 Knock-out parasites. **(E)** Bar graph representing the growth assay of Type II Pru ΔKu80 TgAP2X-10 and TgAP2III-1 Knock-out parasites. 'ns' stands for nonsignificant. A two-tailed Student's t-test was performed, two tailed p-values: ns p>0.05; mean ± s.d. (n=3 independent experiments).

1.2 TgAP2X-10 and TgAP2III-1 deletions do not affect expression of early bradyzoite markers in the alkaline stress differentiation model.

In order to study bradyzoite differentiation in the mutant type II TgAP2X-10 and TgAP2III-1 Knock-out parasites, labelling of the bradyzoite-specific lectin *Dolichos Biflorous* Agglutinin (DBA) was carried out in normal pH conditions of 7.0 as well as bradyzoite-inducing alkaline conditions. Under normal conditions (pH 7.0) and after 24 or 48 hours post-infection, no significant difference between the percentage of DBA positive pre-bradyzoite cysts was observed between the wildtype PruΔKu80 mutant parasites and the Knock-out mutant parasites (Figures 2A, 2C). Similarly, at 24 or 48 hours post-infection in alkaline bradyzoite inducing conditions, (pH 8.2), no significant difference between the percentage of DBA positive pre-bradyzoite cysts in the wildtype and the two Knock-out mutant parasites was identified (Figures 2B, 2D). These results suggest that TgAP2X-10 and TgAP2III-1 do not impact the expression of early bradyzoite markers.

However, when comparing the pH 7.0 *Dolichos* positive counts to the pH 8.2 counts, we notice that the cyst counts increased by about 2-fold in pH 8.2 conditions 24 hours post infection as well as 48 hours post infection. Thus, validating that the *in vitro* pH-stress inducing model is functioning and promotes the formation of pre-bradyzoite cysts in HFF cells.
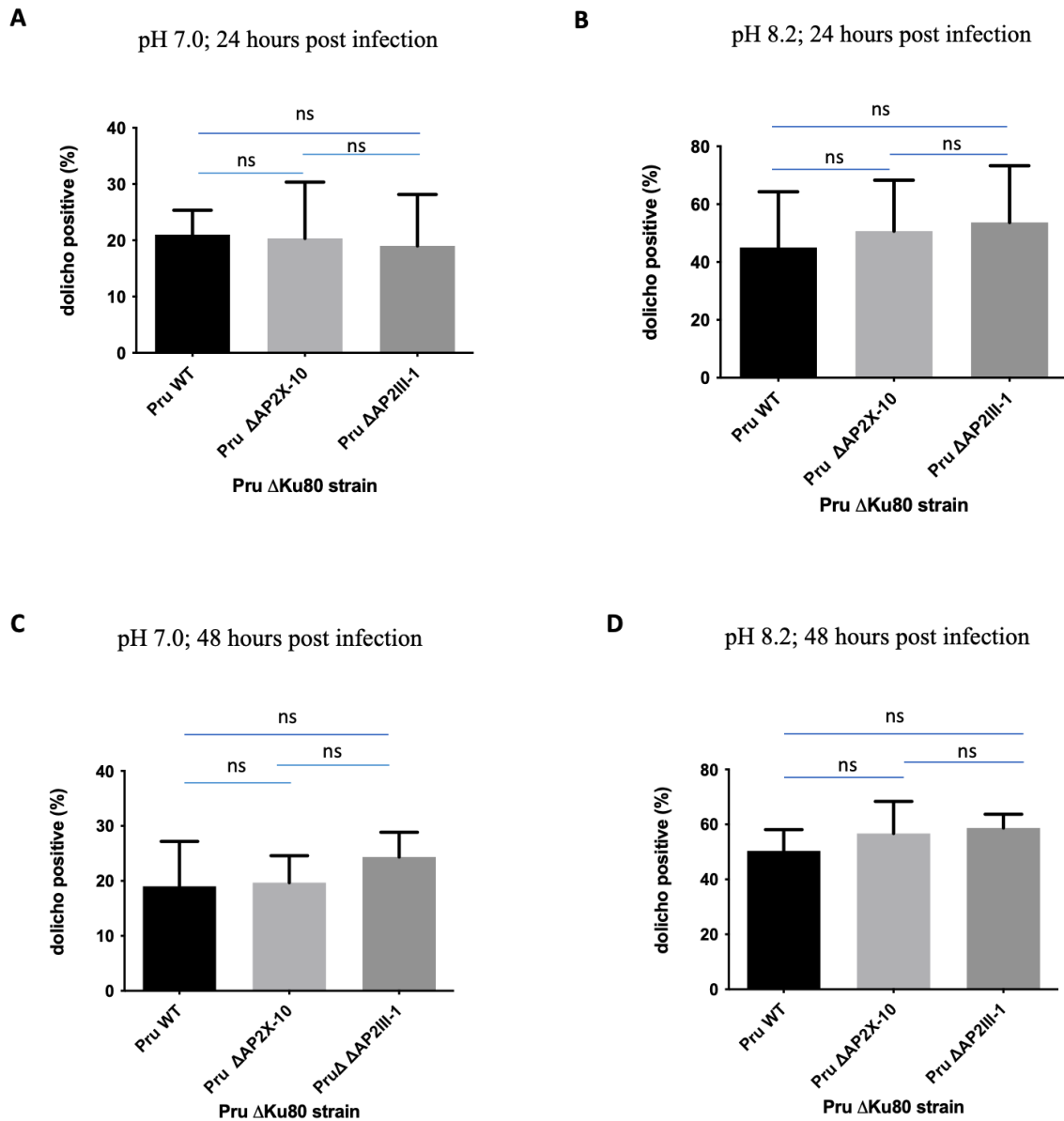
Figure 2: (A) Bar graph representing the percentage of *Dolichos* positive cysts in Type II Pru ΔKu80 strains 24 hours post-infection in normal conditions (pH 7.0). **(B)** Bar graph representing the percentage of *Dolichos* positive cysts in Type II Pru ΔKu80 strains 24 hours post-infection in alkaline conditions (pH 8.2). **(C)** Bar graph representing the percentage of Dolichos positive cysts in Type II Pru ΔKu80 strains 48 hours post infection grown in normal media pH 7.0 **(D)** Bar graph representing the Type II Pru ΔKu80 strains 48 hours post infection grown in alkaline conditions (pH 8.2). In all cases, a student's t-test was performed, two tailed p-values: ns p>0.05; mean ± s.d. (n=3 independent experiments).

1.3 TgAP2X-10 is a potential bradyzoite repressor in *in vitro* brain cell culture

A more biologically relevant *in vitro* brain cell model was developed by Dr Gissot and used to carry out bradyzoite differentiation studies (Mouveaux et al., 2021). The primary brain cell culture was infected with Type II Pru ΔKu80 and Knock-out TgAP2X-10 and TgAP2III-1 mutant strains and was left to grow for 7 days before labelling with DBA. There was a slightly significantly increased percentage of DBA positive cysts in the PruΔKu80 ΔAP2X-10 strain compared to the PruΔKu80 wildtype strain (Figure 3), thus suggesting that TgAP2X-10 might possibly play a role in bradyzoite differentiation in this model.
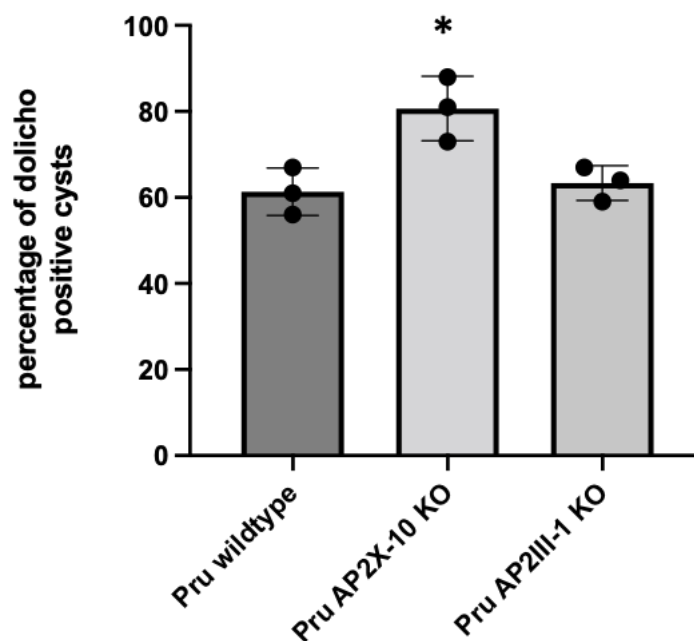
Figure 3: Bar graph representing the percentage of *Dolichos* positive cysts in Type II Pru ΔKu80 and mutant Knock-out parasites grown in a primary brain cell culture for 7 days. A Student's t-test was performed, two tailed p-values: ns p>0.05 (Pru ΔKu80 ΔAP2III-1 compared to PruΔKu80 wildtype), *p< 0.05 (PruΔKu80 ΔAP2X-10 compared to PruΔKu80 wildtype); mean ± s.d. (n=3 independent experiments).

1.4 TgAP2X-10 and TgAP2III-1 play a role in differentiation *in vivo*

Type II PruΔKu80 wildtype and mutant Knock-out parasites PruΔKu80 ΔAP2X-10 and PruΔKu80 ΔAP2III-1 were injected into ten Balb/c mice intra-peritoneally. Cysts in the brains of mice infected with the wildtype and mutant strains were identified using DBA staining. Significantly lower tissue cyst counts in the brain of mice infected with PruΔKu80 ΔAP2X-10 and PruΔKu80 ΔAP2III-1 were

observed suggesting that TgAP2X-10 and TgAP2III-1 most likely have a role in differentiation *in vivo* (Figure 4A). These results were verified in a subsequent *in vivo* experiment. In this case, the parasites were left to form tissue cysts in the injected mice's brains for 8 weeks rather than 4 weeks (due to the COVID19 lockdown in 2020). Three mice infected with PruΔKu80 ΔAP2III-1 did not survive the infection. Cyst burdens were significantly lower in the brains of mice infected with PruΔKu80 TgAP2X-10 and TgAP2III-1 Knock-out parasites compared to that of the wildtype (Figure 4B). Thus, the results obtained follow a similar trend to the initial *in vivo* experiment. Overall, these results indicate that TgAP2X-10 and TgAP2III-1 most likely have a role during the process of parasite differentiation into cysts *in vivo* in mice.

A

B
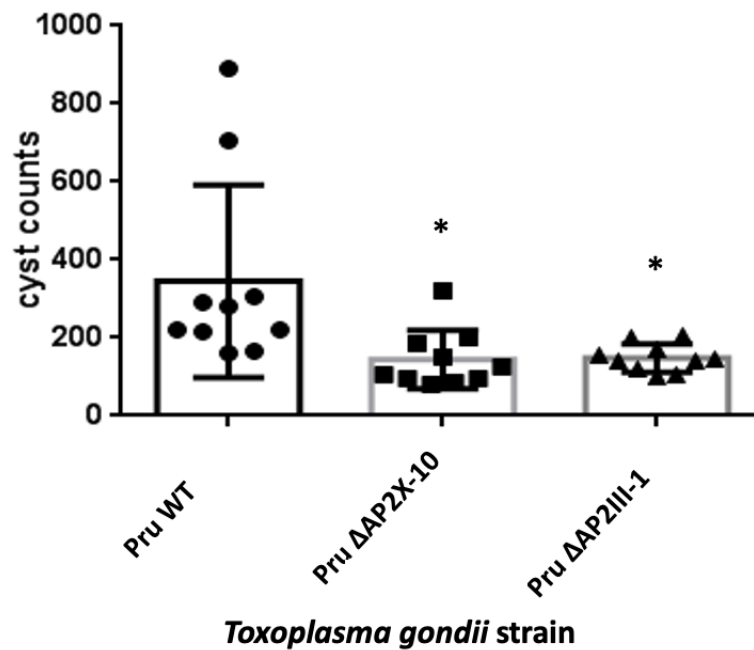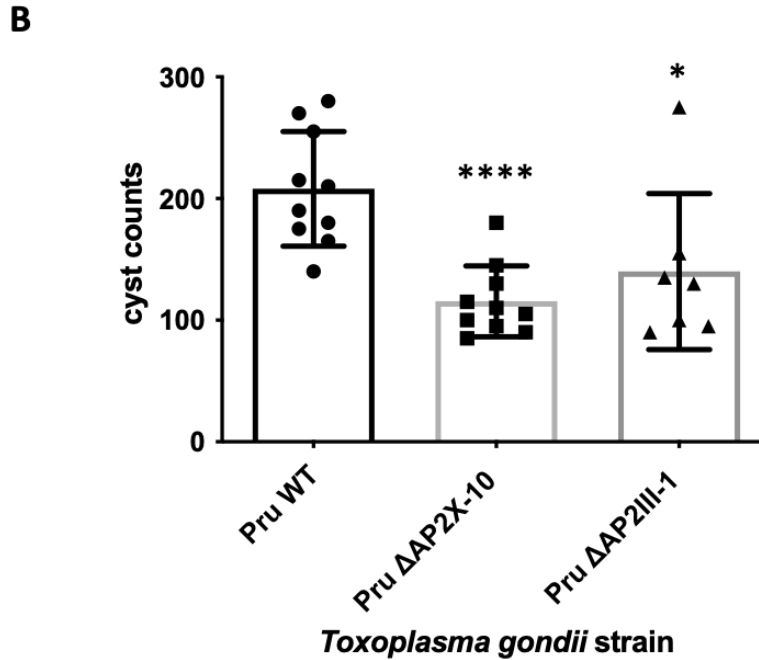
Figure 4: **(A)** Bar graph representing cyst burden counts in isolated brains of mice infected with Type II PruΔKu80 wildtype and PruΔKu80 ΔAP2X-10 and PruΔKu80 ΔAP2III-1 parasites. Mice were left for 4 weeks before isolating the brains. **(B)** Bar graph representing cysts burden counts in isolated brains of mice infected with Type II PruΔKu80 wildtype and PruΔKu80 ΔAP2X-10 and PruΔKu80 ΔAP2III-1 parasites. Mice were left for 8 weeks before brain isolation. A Student's t-test was performed, *p<0.05, ****p<0.0001; mean ± s.d. (n=10).

1.5 Study of gene expression in TgAP2X-10 and TgAP2III-1 Knock-out mutant parasites

In order to study the expression of genes within the Knock-out mutant parasites, RNA-seq was carried out. Type II PruΔKu80 mutant parasites which were collected to study gene expression were either grown on HFF cells in normal media at a pH of 7.0 or alkaline bradyzoite-inducing media at a pH of 8.2. Wildtype PruΔKu80 parasites were used as a control. By carrying out this experiment, we anticipated to observe a downregulation and/or upregulation of certain genes. However, expression studies by RNA-seq did not demonstrate differential gene expression upon loss of either the *TgAP2X-10* or *TgAP2III-1* gene when compared to the PruΔKu80 wildtype parasites in both conditions. These results coincide with the results obtained from infecting HFF cells with wildtype and mutant parasites where there was no significant difference in DBA staining counts. Overall, gene

expression studies were not able to provide any further information regarding the genes that are potentially targeted by these two transcription factors.

DISCUSSION

The *T. gondii* life cycle is characterized by its complexity with a sexual cycle in the definitive host and an asexual cycle in the intermediate warm-blooded host. Within the asexual cycle, tachyzoites differentiate into the latent bradyzoite state and tissue cyst formation is achieved within the host mainly within brain and muscle tissue (Cerutti et al., 2020). Tissue cysts consisting of the bradyzoite form of the parasite are life-long persistent in the host cell thus deeming the bradyzoite as a central component in the life cycle of the *T. gondii* parasite.

Striking the correct balance between the proliferation of the tachyzoite ensuring parasite dissemination throughout the host and bradyzoite formation in order to warrant transmission of the parasite to other hosts, remains a necessary process during the development of the parasite in the intermediate host. Thus, this leaves the bradyzoite with a pivotal role in the parasite's life cycle. Given the central role of the *T. gondii* bradyzoite, studying tachyzoite-bradyzoite differentiation remains a critical topic to fully understand. More particularly, the factors controlling bradyzoite formation are of interest in this study. Previously, a number of ApiAP2 TFs have been demonstrated to have a role in either activating or repressing bradyzoite differentiation. With the intention of continuing along with the trail of characterization of ApiAP2 TFs in terms of bradyzoite development control, an attempt to characterize two never-before studied ApiAP2 TFs was carried out in the first portion of this PhD study.

First, direct knock-out mutant parasites of the *TgAP2X-10* and *TgAP2III-1* genes were generated with the aim of gaining insight into the biological role of these two ApiAP2 TFs. When studying the growth capacity of the parasites, we were able to determine the non-essentiality of the two ApiAP2 TFs for the replicating tachyzoites since no significant growth defect was identified despite the fitness scores of the genome-wide CRISPR screen of -2.98 and -0.82 corresponding to the TgAP2III-1 and TgAP2X-10 genes, respectively (Sidik et al., 2016).

The development of bradyzoites consists of a stepwise process involving the formation of a pre-bradyzoite form before mature bradyzoite formation. Following experiments focused on studying the effect of TgAP2X-10 and TgAP2III-1 on bradyzoite differentiation by using the pH stress bradyzoite-inducing *in vitro* method in HFF cells. However, since we were not able to detect any effect of TgAP2X-10 and TgAP2III-1 on bradyzoite differentiation in HFF cells, we used the primary brain cell culture model and were able to identify a significant increase in the percentage of cysts in primary brain cell culture infected by

TgAP2X-10 KO mutant parasites compared to the wildtype parasites. The *in vitro* brain cell model which we used remains a closer approach to mimicking the *in vivo* environment and is a more ideal model since fully mature bradyzoites can be achieved. The discrepancy between the results of experiments carried out using the two different *in vitro* models, the *in vitro* model utilizing alkaline stress induced differentiation and the one utilizing brain cells, to study bradyzoite differentiation could be due to the nature of the cells.

Furthermore, ApiAP2 TFs were demonstrated to have variable expression profiles during the bradyzoite differentiation process (Mouveaux et al., 2021) and given that the deletion of TgAP2X-10 results in differential bradyzoite formation, TgAP2X-10 might be regulated by other ApiAP2 TFs during developmental transition.

In addition, in a previous study, it has been shown that primary neurons which are a major component of the brain cell culture exhibit high rates of bradyzoite differentiation compared to the pH-stress induced model (Halonen et al., 1996). This could be an impacting factor rendering the brain cell culture model as a more reliable *in vitro* model to study the effect of TgAP2X-10 loss compared to the pH-stress induced model. Moreover, since the increase in the number of mature cysts developed in the case of the TgAP2X-10 KO strain was of a moderate level compared to the number of cysts developed in the wild-type counterpart, we hypothesized that perhaps this increase was not observable in the pH-stress differentiation model.

Transcriptome analysis of TgAP2X-10 and TgAP2III-1 KO parasites grown under alkaline stress did not detect altered expression of genes and not much light was shed on the biological role of the two ApiAP2 TFs. Consistent with the presumed lack of a role of TgAP2X-10 and TgAP2III-1 in tachyzoite cell division, was the lack of significant difference in the transcriptomes of the two knock-out strains grown in normal media (pH 7.0) compared to wild-type tachyzoites grown at pH 7.0. Since there was a slightly significant increase in the number of DBA-positive cysts in TgAP2X-10 KO parasites in the brain cell model, one would assume that transcriptome changes might be detectable and therefore it would be of interest to investigate further and study gene expression of the mutant parasites infected in brain cell culture. This might provide further insight into which genes TgAP2X-10 is responsible for targeting.

In vivo experiments demonstrated a significant decrease in tissue cyst production in brains of mice infected with the two knock-out mutants, this opposes what was observed in the case of TgAP2X-10 knock-out mutant in brain cells where an increase in tissue cysts was observed. Thus, in the absence of TgAP2X-10 *in vivo*, there might be a dysregulation of tachyzoite to bradyzoite differentiation that may result in an unbalanced expression of bradyzoite-associated genes leading to an increase in the elimination of bradyzoites by the immune-system. Perhaps this

155

may be due to an increased recognition of bradyzoite antigens by the host's immune system resulting in a more prominent immune response. A previous study on ApiAP2 TF, TgAP2IV-4 showed that the absence of this single transcription factor can significantly alter the host's immune response. This was illustrated by demonstrating that inflammatory monocytes have a major function in contributing towards the protective immune response when TgAP2IV-4 is absent (J. B. Radke et al., 2018). It is likely that the loss of TgAP2X-10 and TgAP2III-1 might have a similar effect on the host's immune system. However, further studies must be carried out in order to validate that TgAP2X-10 and TgAP2III-1 loss can lead to a more protective immune response.

Additionally, the different effects of TgAP2X-10 and TgAP2III-1 on tissue cyst development *in vitro* and *in vivo* might depend on the type of host tissue environment since the *T. gondii* parasite senses different host cell environments and this contributes to mechanisms controlling tachyzoite to bradyzoite developmental transitions (White et al., 2014). Hence, it would be useful to investigate the effect of TgAP2X-10 absence on bradyzoite differentiation in other tissue types such as skeletal muscle (Swierzy et al., 2014).

The results obtained here could also be confirmed by complementing the mutant strains by a WT copy of the targeted genes.

Overall, this study sheds light on never-before characterized ApiAP2 TFs that might be potential regulators of bradyzoite development adding to the reservoir of ApiAP2s that have been studied so far and have been demonstrated to control the development of bradyzoites.

V-2 – Role of TgAP2IX-5 in asexual cell cycle division

For the second part of the PhD project, TgAP2IX-5, an AP2 TF which is expressed in a cell-cycle dependent manner was studied. Initial experiments in the laboratory carried out by previous PhD and Masters students Kevin Lesage and Cecilia Gomez-Sanchez, respectively consisted of generating an iKD TgAP2IX-5 mutant using the AID system. The iKD TgAP2IX-5 mutant demonstrated a severe division defect and thus TgAP2IX-5 was demonstrated to be essential for the growth and proliferation of the parasite. For this part of the PhD study, the main goal was to continue the characterization of TgAP2IX-5 in order to determine the biological role of TgAP2IX-5. More specifically, two main objectives were intended; studying the effect of TgAP2IX-5 on the cell cycle and the identification of the precise time point of division at which the division defect of TgAP2IX-5 appears. During this study, the iKD TgAP2IX-5 mutant parasite's mutli-nucleated phenotype was further characterized. We were able to identify the exact timepoint of the division defect of the iKD TgAP2IX-5 mutant during the progression of the

cell cycle and which was determined to be precisely after elongation of the plastid and before its segregation. Transfections consisting of generating KI mutants in which IMC and centrosome markers were labelled in the iKD TgAP2IX-5 strain allowed for studying the effect of TgAP2IX-5 depletion on the subcellular structures of the parasite. In addition to this, RNA-seq experiments in which TgAP2IX-5 was depleted for different durations of time revealed that TgAP2IX-5 regulates several genes localized to the IMC and apical complex in addition to regulating other AP2 TFs. Furthermore, overlap of ChIP-seq and RNA-seq allowed to identify genes that are directly targeted by TgAP2IX-5. TgAP2IX-5 re-expression experiments allowed to demonstrate that the *T. gondii* parasite cell cycle modes of division are flexible where the iKD TgAP2IX-5 mutant parasites completely changed their mode of division from endodyogeny to endopolygeny following re-expression of the TgAP2IX-5 protein.

Additional experiments were carried out in order to elucidate the role of different domains of the TgAP2IX-5 protein. Complemented iKD TgAP2IX-5 mutants with deleted domains of the protein were produced and characterized. Overall, TgAP2IX-5 was proven to be a key regulator of asexual cell cycle division in *Toxoplasma gondii*.

This study resulted in a recent publication in the Nature Communications journal entitled "**TgAP2IX-5 is a key transcriptional regulator of the asexual cell cycle division in *Toxoplasma gondii*.**" The introduction, main results, and discussion that were obtained from this study are presented here as published in the article:

INTRODUCTION

Apicomplexa is a phylum consisting of unicellular, obligate, intracellular protozoan parasites, which includes various human pathogen species such as *Plasmodium* spp. (causative agent of malaria), *Toxoplasma* (cause of toxoplasmosis) and *Cryptosporidium* spp. (cause of cryptosporidiosis).

Apicomplexan parasites trigger disease associated with an uncontrollable expansion of parasite biomass resulting in inflammation and host cell destruction (Francia & Striepen, 2014). Although, apicomplexan parasites present a sexual cycle within the definitive host, the pathogenesis of these parasites results from the ongoing asexual replication cycles within the host's cells. All Apicomplexa possess complex life cycles consisting of parasite propagation controlled by the tight regulation of the cell cycle and result in the formation of new daughter cells containing one nucleus and a complete set of organelles. (Gubbels, White, et al., 2008). Apicomplexa have evolved the ability to independently divide their nucleus (nuclear cycle) and produce the parasite body through a process that is termed budding (budding cycle). This allows flexibility in order to produce a suitable number of offspring in a single cell cycle while allowing the parasite to cope with

the different host-cell environments (C.-T. Chen & Gubbels, 2015). Apicomplexa have evolved efficient and distinctive strategies for intracellular replication (Francia & Striepen, 2014). How the division pattern is chosen to ensure parasite expansion during host-cell infection remains unanswered. However, it has been clear that the mode of division is dependent on the timing and coordination of the nuclear and budding cycles (Francia et al., 2012; Sheffield & Melton, 1968).

Plasmodium falciparum and *Toxoplasma gondii* represent two modern branch points of the Apicomplexa phylum, a divergence that occurred several hundred million years ago (Escalante & Ayala, 1995). This divergence has led to changes in the usage of different cell division patterns. For instance, in its intermediate host, *P. falciparum* replicates through schizogony, a division pattern which produces a multinucleated intermediate (schizont) where the daughter parasites bud from the periphery at the closure of the division process to produce infective merozoites. By contrast, in its intermediate hosts, *T. gondii* undergoes endodyogeny, a division pattern that consists of the formation of two daughter parasites within the mother cell. In this case, the formation of new daughter cells occurs within the cytoplasm rather than from the periphery (Francia & Striepen, 2014) and is coordinated to arise simultaneously with nuclear division. In addition to endodyogeny, which is the simplest form of internal budding, *T. gondii* asexually divides within its definitive host through a division scheme that closely resembles schizogony and is known as endopolygeny. It consists of the production of multiple nuclei and a final step of daughter cell formation where parasites perform internal budding in the cytoplasm, unlike schizogony (Ferguson et al., 2007). Furthermore, *Babesia spp.* divide by a binary form of schizogony, where nuclear and budding cycle are linked, with the difference that they bud from the periphery rather than internally (Gubbels et al., 2020). These distinct replication patterns (endodyogeny, schizogony and endopolygeny) rely on the coordination of the timing of the budding and nuclear cycles. Apicomplexa, such as *T. gondii* which exhibit endodyogeny and endopolygeny, are able to employ several division patterns depending on the cellular microenvironment and the developmental stage of the parasite's lifecycle. Such a flexibility suggests overlapping mechanisms in control of the cell cycle independent of the division pattern used.

Apicomplexa show a peculiar cell cycle with a closed mitosis that is divided into three phases (G1, S and M) while the G2 phase is apparently absent (Gubbels, Lehmann, et al., 2008). Centrosomes play a central role in controlling the cell cycle in Apicomplexa. Division and maturation of the centrosome controls the progression and the coordination of the nuclear and budding cycle (Alvarez & Suvorova, 2017; C.-T. Chen & Gubbels, 2013; Francia et al., 2012; Gubbels, Lehmann, et al., 2008; Suvorova et al., 2015). Evidence suggests that soon after centrosome division, centrosome maturation through kinases is key to the activation of daughter cell formation (Alvarez & Suvorova, 2017; Suvorova et al., 2015).

During the Apicomplexa cell cycle, division and segregation of organelles is a highly ordinated process in order to ensure that each daughter parasite acquires the proper complement of organelles (Nishi et al., 2008). This highly controlled process implies a tight regulation of the gene expression during the cell cycle. This was illustrated by the transcriptomic analysis of synchronous cell cycle populations indicating that *T. gondii* may have adapted a "just in time" mode of expression whereby transcripts and proteins are produced right when their function is needed (Behnke et al., 2010). This suggests that transcriptional regulation of gene expression may exert a centralized control on both centrosome activation and the expression of proteins needed for daughter cell formation.

 However, little is known on the potential regulators that may control this transcriptional switch. Apicomplexan genomes encode a family of putative transcription factors that are characterized by the possession of one or more DNA binding AP2 domains (Balaji et al., 2005). ApiAP2 transcription factors were shown to control expression profiles during *T. gondii* differentiation (Hong et al., 2017; J. B. Radke et al., 2018; Walker et al., 2013a). ApiAP2s were also shown to cooperatively control the expression of virulence factors (Lesage et al., 2018; Walker et al., 2013b) in *T. gondii* indicating that this family of transcription factors may control cell cycle dependent expression profiles as also suggested for *P. berghei* (Modrzynska et al., 2017). Moreover, *T. gondii* ApiAP2s were shown to bind to promoters and regulate cell-cycle specific activity, indicating that they play an active role in regulating cell cycle specific expression patterns in this parasite (Lesage et al., 2018; Walker et al., 2013b). In this study, we functionally characterize a cell cycle dependent ApiAP2 transcription factor, TgAP2IX-5. We show that it controls cell cycle events downstream of centrosome duplication including organelle division and segregation. TgAP2IX-5 binds to the promoter of hundreds of genes and controls the activation of the S/M-specific cell cycle expression program. Reversible destabilization of the TgAP2IX-5 protein showed that its expression is sufficient for activation of the budding cycle in multinucleated parasites. Therefore, controlled TgAP2IX-5 expression allows for the switching from endodyogeny to endopolygeny division patterns. TgAP2IX-5 acts as a master regulator controlling the budding cycle and therefore, asexual cell cycle division patterns in this parasite.

2.1 TgAP2IX-5 is a cell-cycle regulated transcription factor essential for parasite growth and proliferation

To find specific regulators of the cell cycle dependent expression program, we identified potential transcriptional regulators whose expression was cell cycle regulated (Behnke et al., 2010). Among these regulators, we focused on the ApiAP2 family of transcription factors and discovered that the *tgap2ix-5* transcript was dynamically expressed with a peak of expression within the S phase (toxodb.org).

TgAP2IX-5 AP2 domain is conserved among apicomplexan parasites (eupathdb.org). To confirm that the TgAP2IX-5 protein was also cell cycle regulated, we produced a *T. gondii* strain that had an epitope-tagged version of this gene at its endogenous locus. Immuno-fluorescence assays using cell-cycle markers demonstrated that TgAP2IX-5 is a nuclear protein mostly expressed during the early S phase (Figure 1A). TgAP2IX-5 expression was detected at the G1/S transition and early S phase when centrosomes are divided but remained in close proximity of each other (as identified by TgCentrin1; a marker of the outer core of the centrosome, Figure 1A upper panel, Supplementary Figure 1A). TgAP2IX-5 was detected before centromere division (as identified by TgChromo1; a marker of pericentromeric chromatin (Gissot et al., 2012), Figure 1A middle panel, Supplementary Figures 1B-1C) but not after (late S phase), indicating that TgAP2IX-5 was only present during the G1/S transition and early S phase. TgAP2IX-5 was no longer detected when parasites enter the S/M phase (as indicated by an early budding marker TgISP1, (Figure 1A, lower panel). Therefore, TgAP2IX-5 protein expression is tightly controlled during the cell cycle.

To identify the biological role of TgAP2IX-5, an inducible knock down (iKD) mutant of TgAP2IX-5 was generated using the AID system which allowed for the conditional depletion of the TgAP2IX-5 protein (Figure 1B). For this purpose, we produced a strain that presented an AID-HA insert at the 3' end of the *TgAP2IX-5* gene using a CrispR/Cas9 strategy (Supplementary Figure 2A). The correct locus of integration of this insert was confirmed by PCR (Supplementary figure 2B). The AID system allows for the conditional depletion of the target protein after addition of auxin (indoleacetic acid) (Figure 1B). A single detectable band at the expected protein size (251 kDa) was present in absence of auxin in the iKD TgAP2IX-5 strain as verified by Western-Blot (Figure 1C). Rapid depletion of the TgAP2IX-5 protein (as early as 1 hour) was obtained in iKD TgAP2IX-5 mutant strain grown in media containing auxin (Figure 1C).
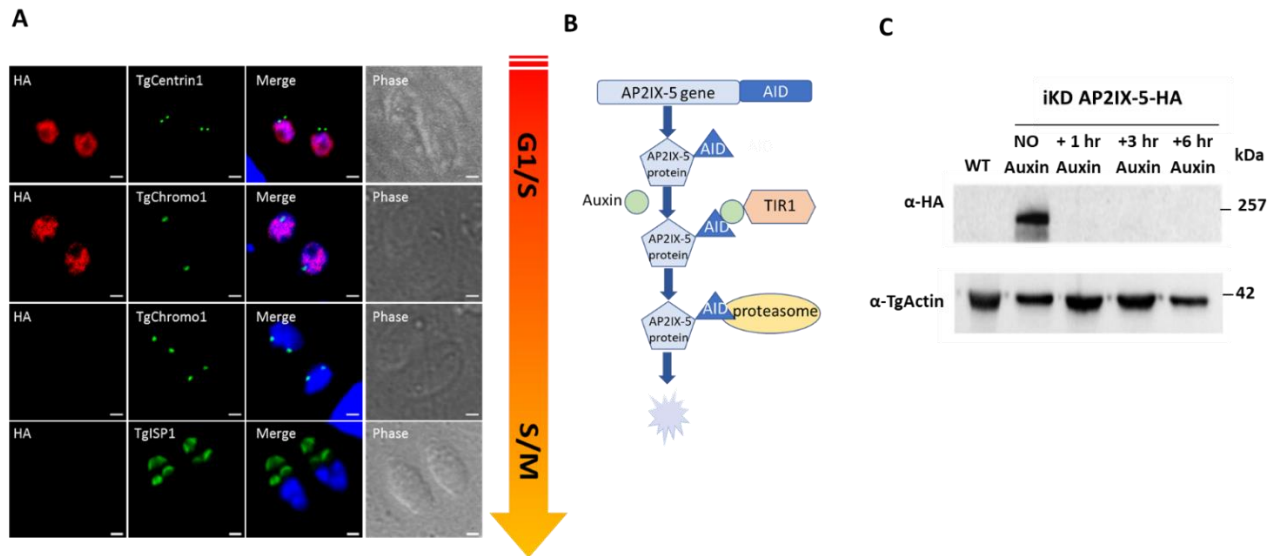
Fig. 1: TgAP2IX-5 is a cell-cycle-regulated protein. (A) Confocal imaging demonstrating the expression of the TgAP2IX-5 protein using anti-HA antibody during the tachyzoite cell cycle. Anti-TgCentrin1, anti-TgChromo1, and anti-TgISP1 were used as cell cycle markers. The schematic cell cycle phase is indicated on the right side of the figure and the scale bar (1 µm) is indicated on the lower right side of each confocal image. **(B)** Schematic representation of the AID system used to degrade the TgAP2IX-5 protein. This system consists of introducing a recognition sequence into the gene of interest, which expresses a protein fused to the recognition sequence and in the presence of Auxin, will be recognized by the TIR1 protein and degraded by the proteasome. This system was used to produce an inducible knockdown parasite in which the expression of TgAP2IX-5 can be controlled. **(C)** Western blot of total protein extract from the parental and iKD TgAP2IX-5 strains treated with Auxin for different durations of time validating the AID system. Western blots were probed with anti-HA to detect the presence of TgAP2IX-5 protein (upper panel), anti-TgActin was used as a control for normalization (lower panel).
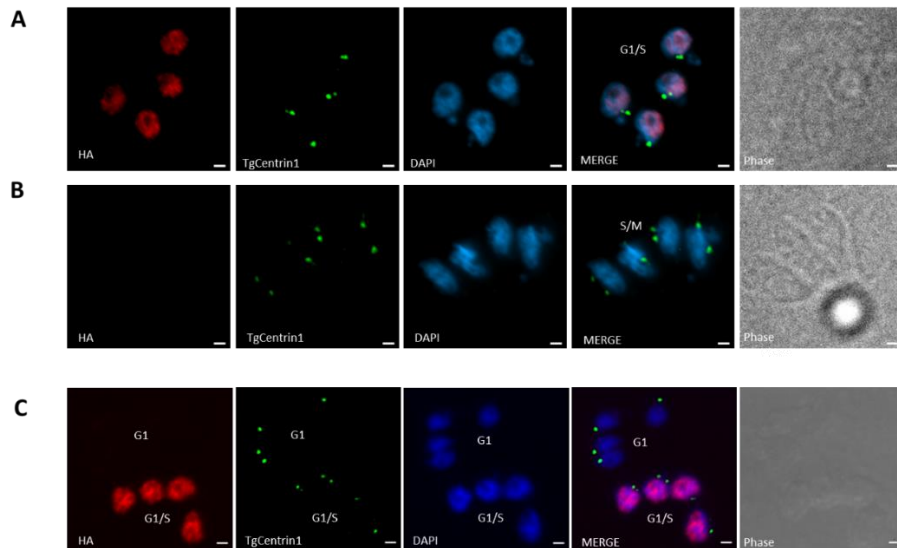
Supplementary Figure 1. Cell cycle expression of the TgAP2IX-5 protein.
Confocal imaging demonstrating the expression of TgAP2IX-5 protein during different stages of the tachyzoite asexual cell cycle using anti-TgCentrin1 as a marker of the cell cycle. Expression of TgAP2IX-5 is indicated in red (HA-tag) and TgCentrin1 is indicated in green. DAPI was used to stain the nucleus. Scale bar is indicated at the lower right side of each image. (**A**) TgAP2IX-5 expression during the G1/S phase. (**B**) TgAP2IX-5 expression during the S/M phase. (**C**) TgAP2IX-5 expression of parasites within two separate vacuoles at different stages of the cell cycle G1/S and G1.
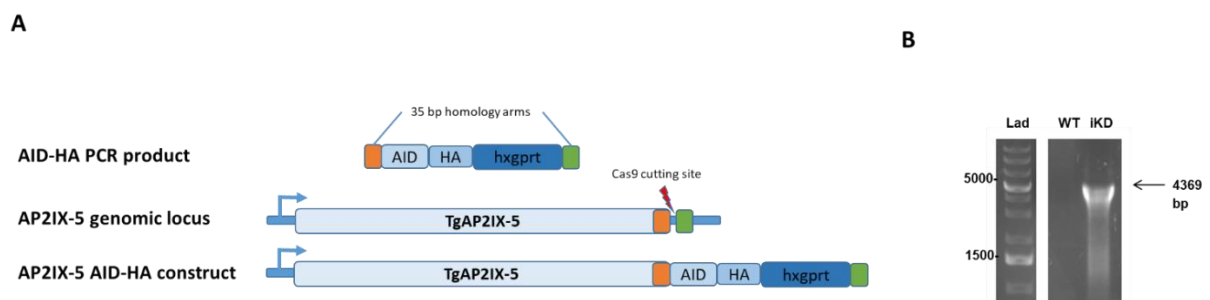
Supplementary Figure 2. Production of an iKD TgAP2IX-5 mutant strain.
(**A**) Diagram showing the strategy used to generate *Toxoplasma gondii* parasites expressing AP2IX-5 tagged with AID-HA-HXGPRT at the C terminus. The location of the primers used for integration PCR is indicated by arrows. (**B**) PCR confirming the insertion of AID-HA-HXGPRT insert at the endogenous locus coding for TgAP2IX-5.

2.2 iKD TgAP2IX-5 mutant displays a defect in daughter parasite formation

To phenotypically characterize the iKD TgAP2IX-5 mutant, a standard growth assay was carried out. The growth capacity of the iKD TgAP2IX-5 mutant in the presence of auxin was tested and we observed that the iKD TgAP2IX-5 mutant growth ability was drastically decreased in the presence of auxin (Figure 2A). In fact, growth was completely abrogated in the iKD TgAP2IX-5 mutant in presence of auxin with a calculated mean of 1.22 parasites per vacuole while the parental strain (in presence and absence of auxin) and the iKD TgAP2IX-5 mutant in absence of auxin grew at a mean of 2.5 parasites per vacuole. This demonstrated a complete blockage of the proliferation capacity of the parasite in the absence of TgAP2IX-5 (Figure 2A). A plaque assay, that measured the ability of the parasite to grow and invade over a period of seven days confirmed the phenotype with the absence of lysis plaques in the iKD TgAP2IX-5 strain treated with auxin contrary to the control used (parental strain in presence of auxin) where lysis plaques were observed (Supplementary Figure 3A). These results suggest that TgAP2IX-5 expression is essential for the parasite's growth and proliferation.

To better assess the growth phenotype, we examined the parasite by IFA using a nucleus marker (TgENO2) and an inner membrane complex (IMC) marker (TgIMC1), a network of flattened vesicles lying beneath the plasma membrane (Figure 2B). It was apparent that the parasite accumulated nuclei and did not form daughter cells in absence of TgAP2IX-5 while exhibiting normal daughter cell formation in presence of the protein. To confirm the inability of the parasite to form daughter cells in presence of auxin, we performed transmission electron microscopy and observed that in absence of auxin the iKD TgAP2IX-5 mutant was able to produce daughter cells, while in presence of auxin, the parasite accumulated nuclei associated with lack of apparent daughter cell formation (Figure 2C). To confirm these observations, we measured the number of nuclei per parasite (Figure 2D and Supplementary Figures 3B-C). Depending on the timing during the cell cycle, the parasites exhibit either one nucleus (80 % of the total parasite population) or two nuclei (20 % of the total parasite population) (before or after cytokinesis) for the parental strain (in absence or in presence of auxin) and for the iKD TgAP2IX-5 strain in absence of auxin (Figure 2D and Supplementary Figures 3B-C). By contrast, the percentage of parasite exhibiting more than 2 nuclei increased overtime in the iKD TgAP2IX-5 strain in presence of auxin (Figure 2D and Supplementary Figures 3B-C). The observation of multi-nucleated parasites in presence of auxin suggests that the iKD TgAP2IX-5 mutant displays a defect in daughter parasite formation but not in the ability of the parasite to multiply and segregate its nuclear material. To assess the capacity of the iKD TgAP2IX-5 mutant to produce daughter cells, we recorded the number of

163

parasite cells that were in the process of producing daughter cells through internal budding (Figure 2B and E and Supplementary Figures 4A-B), therefore measuring the parasite's ability to produce daughter cells at an early stage of internal budding. Using two different markers, we were able to show a drastic decrease of the number of parasites undergoing budding in the iKD TgAP2IX-5 strain after 6h of auxin treatment (Figure 2E and Supplementary Figures 4A-B). These results indicate that TgAP2IX-5 plays an important role during the early stages of internal budding and is necessary for daughter cell formation.
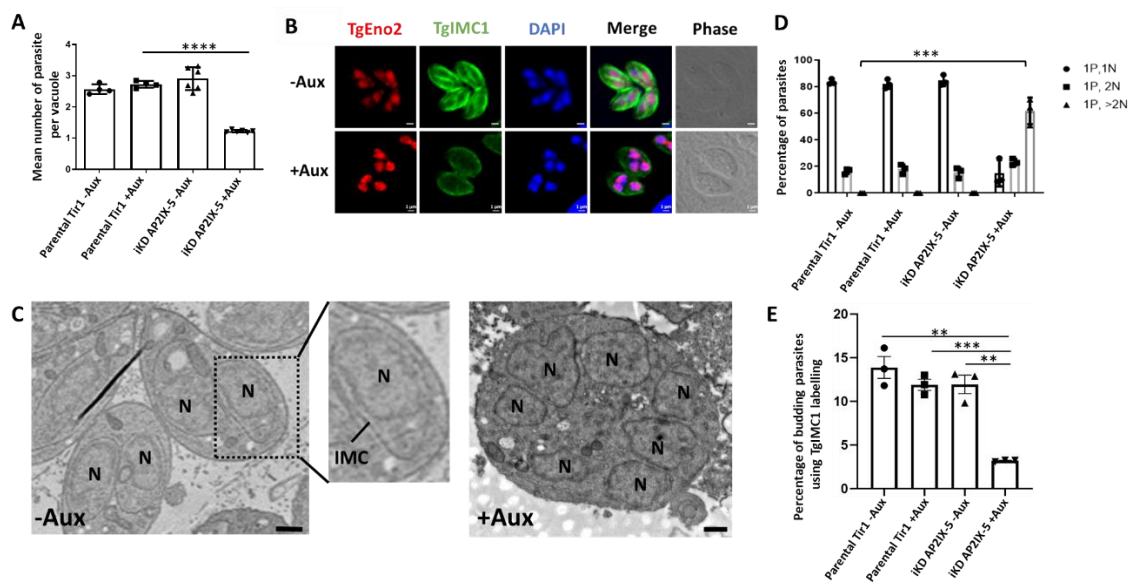
Fig. 2: Characterization of TgAP2IX-5 iKD parasite. (**A**) Growth assay for parental and iKD TgAP2IX-5 strains in the absence and presence of auxin treatment for 24 h. The number of parasites per vacuole was measured and the average number of parasites is represented within the graph. A total of 100 vacuoles were counted for each replicate. A Student's t-test was performed; two-tailed p-value: ****$p < 0.0001$; mean ± s.d. ($n = 4$ independent experiments). (**B**) Confocal imaging of iKD TgAP2IX-5 labelled with TgEno2 (red) and TgIMC1 (green) in the presence and absence of auxin treatment. Auxin was added 24 h post-infection. DAPI was used to stain the nucleus. Scale bar is indicated at the lower right side of each image. (**C**) Electron microscopy scans demonstrating the structural morphology of the nucleus in iKD TgAP2IX-5 parasite in the absence and presence of auxin. (N) represents the nucleus. Two daughter parasites are formed within each mother parasite in absence of auxin. Multinucleated parasites are visible in presence of auxin. Scale bar (500 nm) is indicated at the lower right side in the TEM images. (**D**) Bar graphs representing

nucleus per parasite counts for parental and iKD TgAP2IX-5 strains in the absence and presence of auxin (12 h treatment). P stands for parasites and N stands for nuclei. A Student's *t*-test was performed comparing mean percentage of multinucleated parasite between the control (Parental in absence of auxin) and iKD TgAP2IX-5 in the presence of auxin, two-tailed *p*-values: ***$p = 0,0004$; mean ± s.d. ($n = 3$ independent experiments). **(E)** Bar graph representing the percentage of daughter parasite formation in the absence and presence of 6 h of auxin treatment using TgIMC1 labelling, A Student's *t*-test was performed, two-tailed *p*-values: ***$p = 0.0002$, **$p = 0.0012$; mean ± s.d. ($n = 3$ independent experiments).
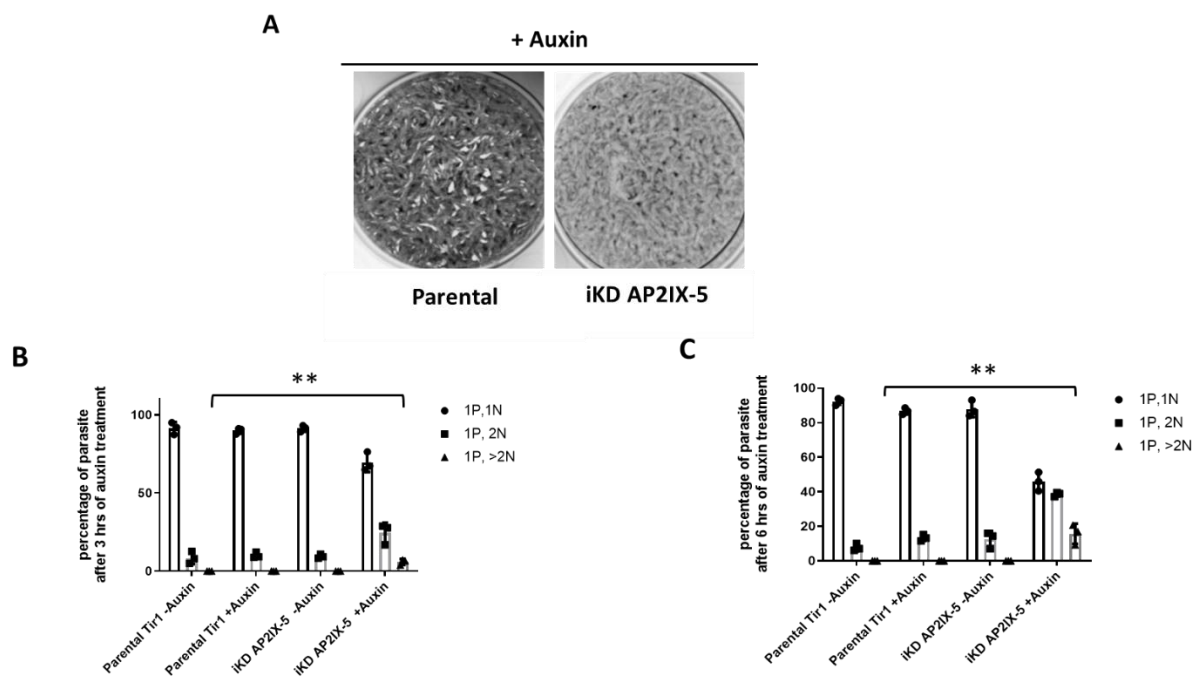
Supplementary Figure 3. Phenotype of the iKD TgAP2IX-5 strain.
(A) Plaque assay for the parental and iKD TgAP2IX-5 strains in the presence of auxin treatment for 7 days. **(B)** Bar graph representing nucleus per parasite counts for parental Tir1 and iKD TgAP2IX-5 strains in the absence and presence of 3 hours of auxin treatment. A Student's t-test was performed to compare between the mean percentage of multinucleated parasites between the control (Parental Tir1 -auxin) and the iKD TgAP2IX-5 mutant strain. Two-sided p-values: **: p=0.0049; mean ± s.d. (n=3 independent experiments). **(C)** Bar graph representing nucleus per parasite counts for the parental and iKD TgAP2IX-5 strains in the absence and presence of 6 hours of auxin treatment. Student's t-test was performed to compare between the mean percentage of multinucleated parasites between the control (Parental Tir1 -auxin) and the iKD TgAP2IX-5

mutant strain. Two-sided p-values: ** P=0.0097; mean ± s.d. (n=3 independent experiments).
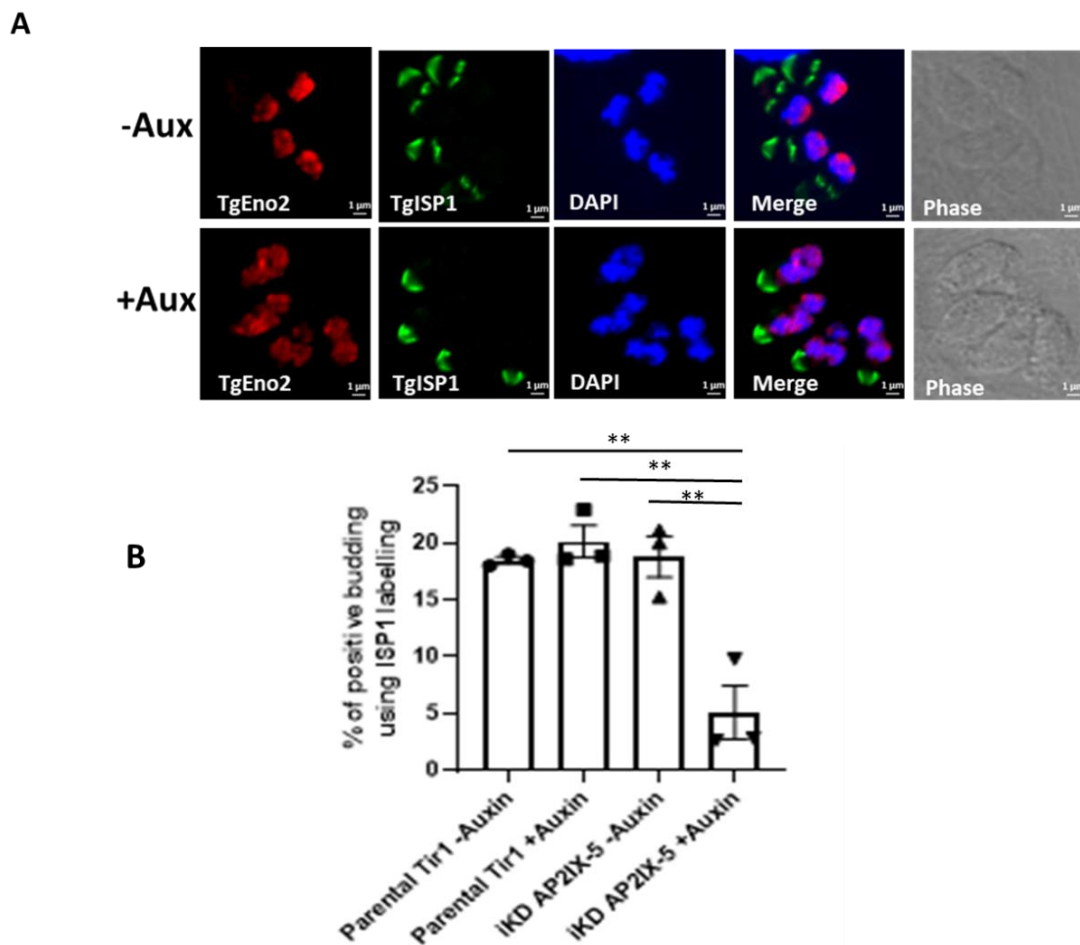
Supplementary Figure 4. Production of daughter cells is severely impaired in absence of TgAP2IX-5
(A) Confocal imaging of iKD TgAP2IX-5 labelled with TgEno2 (red) and TgISP1 (green) in the presence and absence of auxin treatment. DAPI was used to stain the nucleus. Scale bar is indicated at the lower right side of each image. (B) Bar graph representing the percentage of daughter parasite formation in the absence and presence of 6 hours of auxin treatment 24 hours post-infection using TgISP1 labelling, A Student's t-test was performed, Two-sided p-values: **p=0.0048 (iKD TgAP2IX-5 +auxin compared to Parental Tir1 – auxin),
**: p=0.0054 (iKD TgAP2IX-5 +auxin compared to Parental Tir1 +auxin),
**: p=0.0098 (iKD TgAP2IX-5 +auxin compared to iKD TgAP2IX-5 -auxin); mean ± s.d. (n=3 independent experiments).

2.3 TgAP2IX-5 is required at a precise timepoint of the cell cycle

The *T. gondii* cell cycle has been described precisely and presents a well-organized time line for the division of the subcellular structures of the parasite (Nishi et al., 2008) establishing the following sequence of organelle duplication and segregation: first the centrosome is duplicated and divided and then the Golgi complex, the apicoplast, the nucleus, the cytoskeleton (e.g. the IMC), the endoplasmic reticulum and eventually the mitochondrion. To identify the exact timepoint at which TgAP2IX-5 affects daughter parasite formation, a study of the effect of TgAP2IX-5 on organelle duplication and segregation was carried out.

During division, the centrosome (outer core) divides first and then the centromere (as well as the inner core centrosome) follows. We measured the ability of the centrosome and centromere to divide within the iKD TgAP2IX-5 strain using TgCentrin1 and TgChromo1 as a centrosome and centromere marker, respectively. For the parental and the iKD TgAP2IX-5 strains, the centrosome to nucleus and centromere to nucleus ratio were recorded after 6 hours of auxin treatment (Figure 3A-C). The recorded ratios of centrosome to nucleus and centromere to nucleus are close to 1 in both the presence and absence of auxin (Figure 3B-C) despite that the Student's t-test carried out for statistical analysis shows a significantly lower number for both centrosome to nucleus and centromere to nucleus ratios. These results suggest that TgAP2IX-5 does not have a drastic effect on the replication of the centrosome. Similarly, the centromere division is minimally affected, a result that is in line with the multiplication of nuclei observed in the iKD TgAP2IX-5 strain in presence of auxin, as confirmed by the labelling of TgSFA2, another centrosome marker (Supplementary Figures 5A-B).
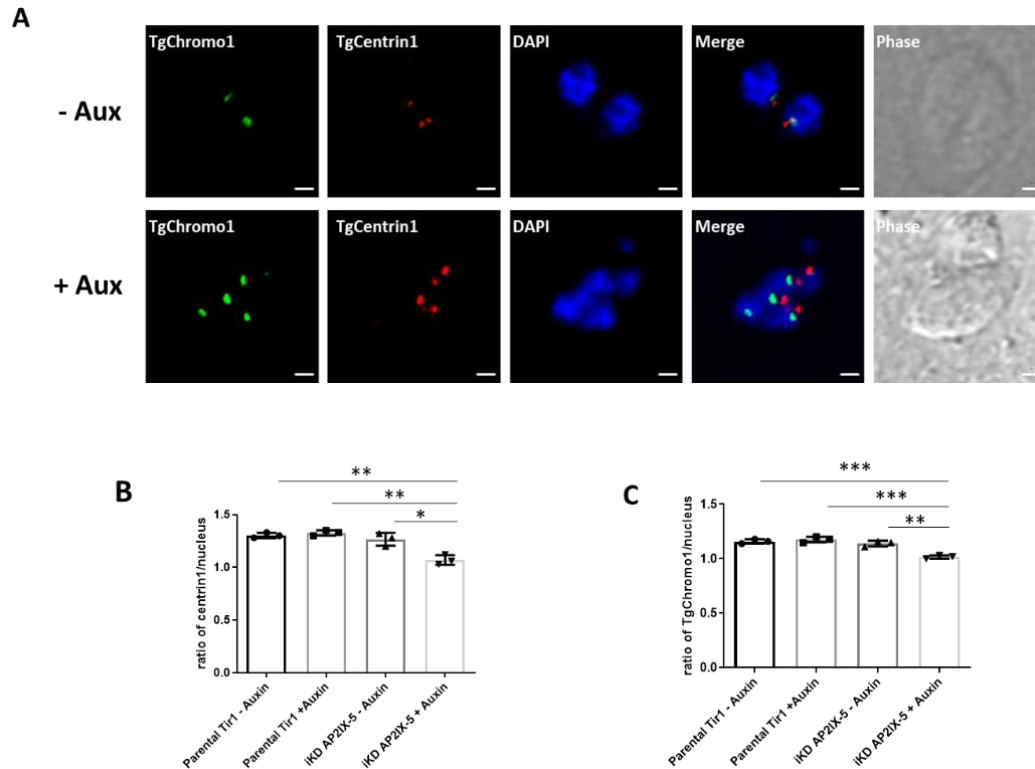
Fig. 3: Centrosome division is mostly unaffected in the absence of TgAP2IX-5.
(A) Confocal imaging of iKD TgAP2IX-5 labelled with TgChromo1 and TgCentrin1. TgChromo1 is indicated in green. TgCentrin1 is indicated in red. DAPI was used to stain the nucleus. Scale bar is indicated at the lower right side of each image. Occasional disconnection between centromere and outer centrosome was observed but does not represent the majority of cases. (B) Bar graph representing TgCentrin1: nucleus ratio using the parental and iKD TgAP2IX-5 strains in the absence and presence of auxin treatment for 6 h. A Student's t-test was performed, two-tailed p-values: **$p = 0.0015$ (iKD TgAP2IX-5 +auxin compared to Parental Tir1 -auxin), **$p = 0.001$ (iKD TgAP2IX-5 +auxin compared to Parental Tir1 +auxin), **$p = 0.0112$ (iKD TgAP2IX-5 +auxin compared to iKD TgAP2IX-5 −auxin); mean ± s.d. ($n = 3$ independent experiments). (C) Bar graph representing chromo1: nucleus ratio using the parental and iKD TgAP2IX-5 strains in the absence and presence of auxin treatment for 6 h; A Student's t-test was performed, two-tailed p-values: ***$p = 0.0006$ (iKD TgAP2IX-5 +auxin compared to Parental Tir1 −auxin), ***$p = 0.0007$ (iKD TgAP2IX-5 +auxin compared to Parental Tir1 +auxin), **$p = 0.0022$ (iKD TgAP2IX-5 +auxin compared to iKD TgAP2IX-5 −auxin); mean ± s.d. ($n = 3$ independent experiments).
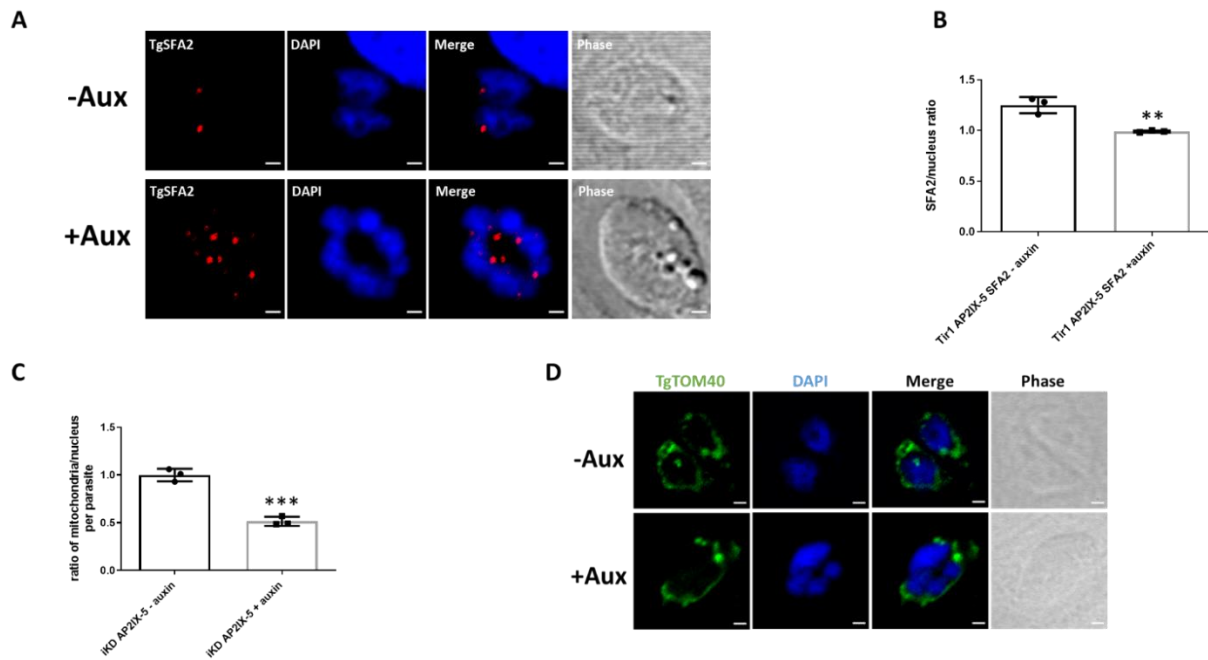
Supplementary Figure 5. Effect of TgAP2IX-5 on TgSFA2 and mitochondrion replication in absence of TgAP2IX-5. (A) Confocal imaging of iKD AP2IX-5 TgSFA2-myc. TgSFA2 is labelled in red and the nucleus is stained with DAPI. Scale bar is indicated in the lower right of each image. **(B)** Bar graph representing the ratio of SFA2: nucleus in the absence and presence of overnight auxin treatment. A Student's t-test was performed, Two-sided p-values: **: p=0.0017; mean ± s.d. (n=3 independent experiments). **(C)** Bar graph representing the ratio of mitochondria: nucleus in the absence and presence of overnight auxin treatment. A Student's t-test was performed; two-sided p-values: ***: p=0.0005; mean ± s.d. (n=3 independent experiments). **(D)** Confocal imaging of iKD TgAP2IX-5 labelled with TgTom40 (mitochondria) in green in the presence and absence of overnight auxin treatment. DAPI was used to stain the nucleus. Scale bar is indicated in the lower right side of each image.

Since centrosome division remained minimally affected by TgAP2IX-5, a study of the proceeding organelles to divide in the *T. gondii* organellar cell cycle division timeline was carried out (Figure 4A). The Golgi complex was labelled in parasites and the ratio of Golgi to nucleus was calculated (Figure 4B). We observed no significant difference between the ratios of Golgi to nucleus in the presence or absence of auxin, therefore suggesting that TgAP2IX-5 depletion does not impact Golgi division and segregation (Figure 4C). We then observed plastid division and segregation (Figure 4B) and measured the plastid to nucleus ratio. This ratio is significantly lower in the iKD TgAP2IX-5 strain in presence of auxin (Figure 4D),

suggesting that plastid division is blocked in the mutant. The plastid division is a multistep process where it first elongates before the completion of scission and segregation (Blanchard & Hicks, 1999). To determine the exact timepoint at which plastid division is affected, the number of parasites with an elongated plastid was recorded in the presence and absence of TgAP2IX-5. We observed a significantly high number of elongated plastid in the absence of TgAP2IX-5 (Figure 4E), suggesting a critical role for TgAP2IX-5 after elongation and before plastid division. This short time frame corresponds to TgAP2IX-5 protein cell cycle dependent expression. As expected, the mitochondria division (the last step during the cell cycle, before cytokinesis) is also affected in the iKD TgAP2IX-5 mutant (Supplementary Figure 5C and 5D), confirming that the blockage during the cell cycle precedes mitochondria division.
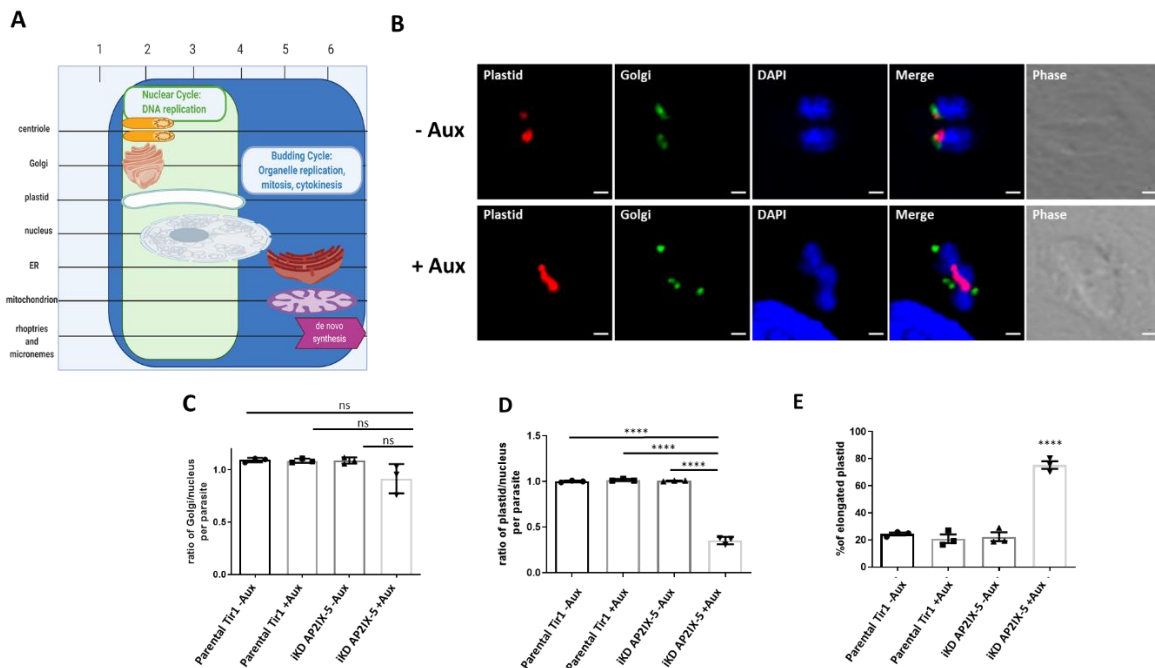
Fig. 4: Organelle replication in iKD TgAP2IX-5 throughout the tachyzoite asexual cell cycle. (A) Schematic representation of the chronological order of organellar division throughout a normal *Toxoplasma gondii* cell cycle. Nuclear cycle is indicated in green and budding cycle is indicated in blue. Timeframe of each organelle division is represented by length of representative organelle. (B) Confocal microscopy of iKD TgAP2IX-5 parasite with labelled plastid (red) and Golgi (green) in the presence and absence of overnight auxin treatment. The lower panel clearly represents the elongated plastid phenotype. DAPI was used to stain the nucleus. Scale bar is indicated at the lower right side of each image. (C) Bar graph representing the ratio of Golgi: nucleus using the

parental and iKD TgAP2IX-5 strains in the absence and presence of overnight auxin treatment. A Student's *t*-test was performed, two-tailes *p*-values: $p = 0.0948$ (iKD TgAP2IX-5 +auxin compared to Parental Tir1 −auxin), $p = 0.1039$ (iKD TgAP2IX-5 +auxin compared to Parental Tir1 +auxin), $p = 0.1030$ (iKD TgAP2IX-5 +auxin compared to iKD TgAP2IX-5 −auxin); mean ± s.d. ($n = 3$ independent experiments). **(D)** Bar graph representing the ratio of plastid to nucleus using the parental and iKD TgAP2IX-5 strains in the absence and presence of overnight auxin treatment. A Student's *t*-test was performed, two-tailed *p*-values: ****$P < 0.0001$; mean ± s.d. ($n = 3$ independent experiments). **(E)** Bar graph representing the percentage of parental and iKD TgAP2IX-5 parasites with an elongated plastid in the absence and presence of overnight auxin treatment. A Student's *t*-test was performed, two-tailed *p*-values: ****$P < 0.0001$; mean ± s.d. ($n = 3$ independent experiments).

2.4 TgAP2IX-5 impacts the expression of cell-cycle regulated genes

Since TgAP2IX-5 is a potential transcription factor, we examined the changes in the transcriptome after depletion of the TgAP2IX-5 protein using RNA-seq. Total RNA was purified from tachyzoites of the iKD TgAP2IX-5 strain grown with or without auxin for 6 hours (three biological triplicates). Data analysis using Deseq2 allowed us to identify significant changes in the iKD TgAP2IX-5 transcriptome with an adjusted p-value cutoff of 0.05 and a minimum fold change of 2 (Figure 5A). We identified more than 600 transcripts that were downregulated and around 300 transcripts (Supplementary Data 1) that were upregulated in the iKD TgAP2IX-5 mutant when treated with auxin (Figure 5A). We examined the cell-cycle expression of the downregulated genes and represented their expression using a heat-map (Figure 5B). We discovered that most of them showed an expression peak during the late S and M phase with a few of them exhibiting a peak during the cytokinesis phase (Figure 5B) while the upregulated genes showed mostly peaks of expression that are quite heterogenous along the cycle with low expression peaks corresponding to the S/M and cytokinesis phase. Additionally, an expression peak during the G1 phase was present (Supplementary Figure 6A).

In the list of downregulated transcripts, we were struck by the number of annotated genes corresponding to proteins targeted to the IMC and to the apical complex both structures that are the first to appear when the daughters bud within the mother cell. To better assess the potential localization of the proteins that correspond to downregulated transcripts, we used a HyperLopit proteomic dataset that predicts with high confidence the localization of proteins in the parasite (Barylyuk et al., 2020). We showed that a high proportion of the downregulated transcripts present in the dataset (331 genes) encode proteins predicted to localize to the IMC or to the apical complex (a total of 30% of the

downregulated transcripts present in the HyperLopit dataset; Supplementary Figure 6B). Moreover, these two localizations are overrepresented (16% and 14 %, respectively) when compared to the whole proteome localization (3% for each; 2487 proteins). Based on this dataset, the downregulated genes represent 64 % of the IMC proteome (52/81) and more than 70 % (45/63) of the predicted apical complex proteome. These results suggest that TgAP2IX-5 may act mainly as an activator of genes whose expression shows a cell cycle regulated profile with a peak at the late S and M phases. These genes represent a high proportion of the IMC and apical complex proteome. We also examined the upregulated gene list using the same dataset (Barylyuk et al., 2020). While no upregulated genes are predicted to encode proteins that localize to the IMC or the apical compartment, a majority of the upregulated proteins may localize to the nucleus, ER and rhoptry (Supplementary Figure 6C).

By RNA-seq, we were able to identify that TgAP2IX-5 either activates directly or indirectly the expression of genes. In order to identify what promoters are directly targeted by TgAP2IX-5, we carried out a ChIP-seq analysis. Biological duplicates were produced and processed for sequencing (Supplementary Figure 7A). The MACS2 software was used to identify the significant peaks (p-value < 0.05) that were in intergenic regions close to an annotated gene. This analysis revealed that TgAP2IX-5 directly binds to 696 gene promoters among which key genes are involved in parasite formation (Figure 5C and Supplementary Figures 7A-D) such as genes encoding proteins targeted to the IMC such as TgIMC1 and TgIMC4 (Figure 5Ci), TgGAPM3 (Figure 5Cii) and TgIMC29 (Figure 5Ciii). Interestingly, we also identified that TgAP2IX-5 was able to bind to the promoters of other ApiAP2 encoding genes (Figure 5Civ and Supplementary Figures 7C-D). We examined the cell cycle expression of the genes whose promoter was targeted by TgAP2IX-5 and found that a majority of these genes were showing an expression peak during the S and M phase, although a cluster of genes showed a strong expression during C and early G1 phase (Supplementary Figure 7E). These data confirm the ability of TgAP2IX-5 to act as a bona-fide transcription factor by directly binding to promoters of genes encoding essential proteins for the establishment of the daughter cells.

Since RNA-seq does not enable the identification of the genes that are solely directly controlled by TgAP2IX-5, we overlapped the RNA-seq and ChIP-seq dataset. For that, we identified within the differentially regulated genes list whether they were downregulated or upregulated (as initially identified from RNA-seq), and compared this list with the genes identified to be targeted by TgAP2IX-5 from ChIP-seq analysis using the MACS software. Overall, 117 genes were recorded from the overlap of RNA-seq and ChIP-seq data representing a 17% overlap (Figure 5D). A closer study of the overlap between RNA-seq and ChIP-seq genes identified that 10% of upregulated genes are directly targeted by TgAP2IX-5 whereas 14% of downregulated genes are directly targeted by

TgAP2IX-5. We examined the cell cycle regulation of the downregulated transcripts directly controlled by TgAP2IX-5 and found that these genes exhibit a cell-cycle regulated expression peak during the late S and early M phases (Figure 5E). These results suggest that TgAP2IX-5 directly controls genes expressed during the S phase and beginning of the M phase. Examples of genes that were found to be directly activated by TgAP2IX-5 included a number of IMC proteins such as TgIMC1, TgIMC4, TgIMC3, TgIMC29 and TgGAPM3 (Supplementary Data 2 and Figure 5C). Since TgAP2IX-5 was shown to directly activate genes that are mainly involved in daughter parasite formation, TgIMC29 was myc-tagged within the iKD TgAP2IX-5 strain and we observed a significant decrease in the TgIMC29 expression in the absence of TgAP2IX-5 as confirmed by Western blot (Supplementary Figure 8A).

Considering the difference between the RNA-seq and ChIP-seq dataset, we searched the RNA-seq dataset for potential regulators that might be directly regulated by TgAP2IX-5 and therefore may in turn perturb the expression of genes not directly targeted by TgAP2IX-5. Interestingly, 8 ApiAP2 TFs were downregulated (TgAP2III-1, TgAP2III-2, TgAP2IV-4, TgAP2VIIa-1, TgAP2X-11, TgAP2XI-4, TgAP2XII-9, and TgAP2XII-2) and 4 upregulated (AP2IX-5, AP2IX-1, AP2VI-3 and AP2X-9) following the depletion of TgAP2IX-5 as measured by RNA-seq (Supplementary Data 1). Among these genes, 5 (TgAP2IV-4, TgAP2III-2, TgAP2XII-9, TgAP2X-9 and TgAP2XII-2) had their promoters directly bound by TgAP2IX-5 (Supplementary Figure 8B, underlined). Interestingly, much like other genes directly regulated by TgAP2IX-5 (Figure 5E), these genes showed an expression peak during the late S phase (Supplementary Figure 8B) with the exception of TgAP2X-9 which peaks in early S phase and whose expression is likely directly repressed by TgAP2IX-5 (upregulated in absence of TgAP2IX-5 and its promoter bound by TgAP2IX-5). TgAP2IV-4, a known repressor of developmentally regulated genes, is expressed during the S/M phase (J. B. Radke et al., 2018). Since TgAP2IV-4 is involved in differentiation, we examined the expression of the upregulated genes expression profile during the parasite life cycle (Supplementary Figure 8C). Interestingly, TgAP2IX-5 depletion induced the expression of transcripts that are preferentially expressed in bradyzoites and also during the sexual stages that occur in the definitive host (Supplementary Figure 8C). Genes preferentially expressed in bradyzoite include MAG1 a known cyst matrix protein (Parmley et al., 1994). Interestingly, a cluster of genes upregulated in absence of TgAP2IX-5 is strongly expressed in the early days of sexual development where division by endopolygeny occurs (Supplementary Figure 8C, EES1 and EES2). These data suggest that TgAP2IX-5 directly controls other TFs during the S phase that may in turn activate the late S and M expression program but also coordinate developmental choices (such as differentiation into bradyzoite). Surprisingly, we found that TgAP2IX-5 was enriched at its own promoter (Supplementary Figure 7D, boxed) and the TgAP2IX-5 transcript was found to be

173

upregulated in the presence of auxin based on RNA-seq. These data indicate that TgAP2IX-5 may directly regulate its own transcript expression suggesting that TgAP2IX-5 expression may be under the direct regulation of a possible negative feedback loop.
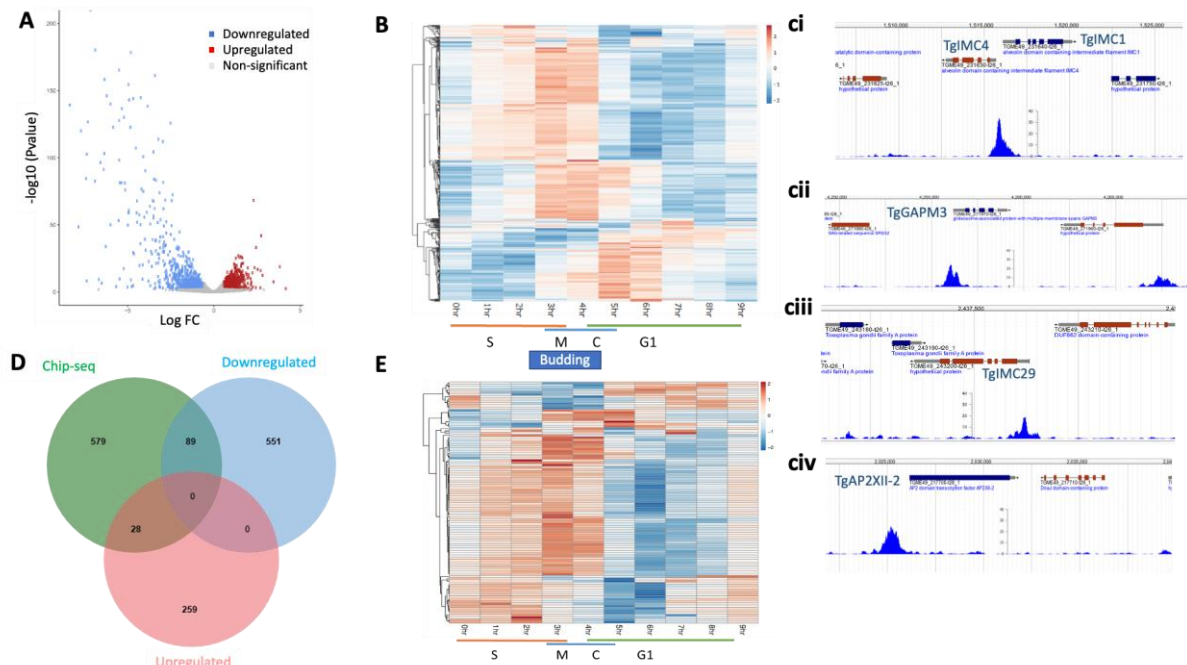
Fig. 5: TgAP2IX-5 controls the expression of key genes involved in daughter parasite formation. **(A)** Volcano plot of differentially expressed genes analyzed from RNA-sequencing of TgAP2IX-5 parasites treated with auxin for 6 h. Downregulated genes are represented in blue, upregulated genes are represented in red. Statistically nonsignificant genes are represented in gray. The differential expression analysis (DE) was based on three independent biological experiments. **(B)** Heatmap showing the cell cycle expression of all individual transcripts that are downregulated in the iKD AP2IX-5 strain in the presence of 6 h of auxin treatment. The cell cycle phases are represented at the bottom as well as the timing when budding occurs. **(C)** ChIP-seq data representing the direct targeting of TgAP2IX-5 to the promoters of TgIMC4 (i), TgIMC1 (i), TgGAPM3 (ii), TgIMC29 (iii), and TgAP2XII-2 (iv) genes. MACS2 generated tracks are represented together with the annotated genes (top). **(D)** Venn diagram of overlapping downregulated genes, upregulated genes from RNA-seq, and identified promoters of genes directly interacting with TgAP2IX-5. DEseq2 and MACS2 software were used to analyze RNA-seq and ChIP-seq data, respectively. **(E)**Heatmap of 89 downregulated genes directly activated by TgAP2IX-5. The cell cycle phases are represented at the bottom.
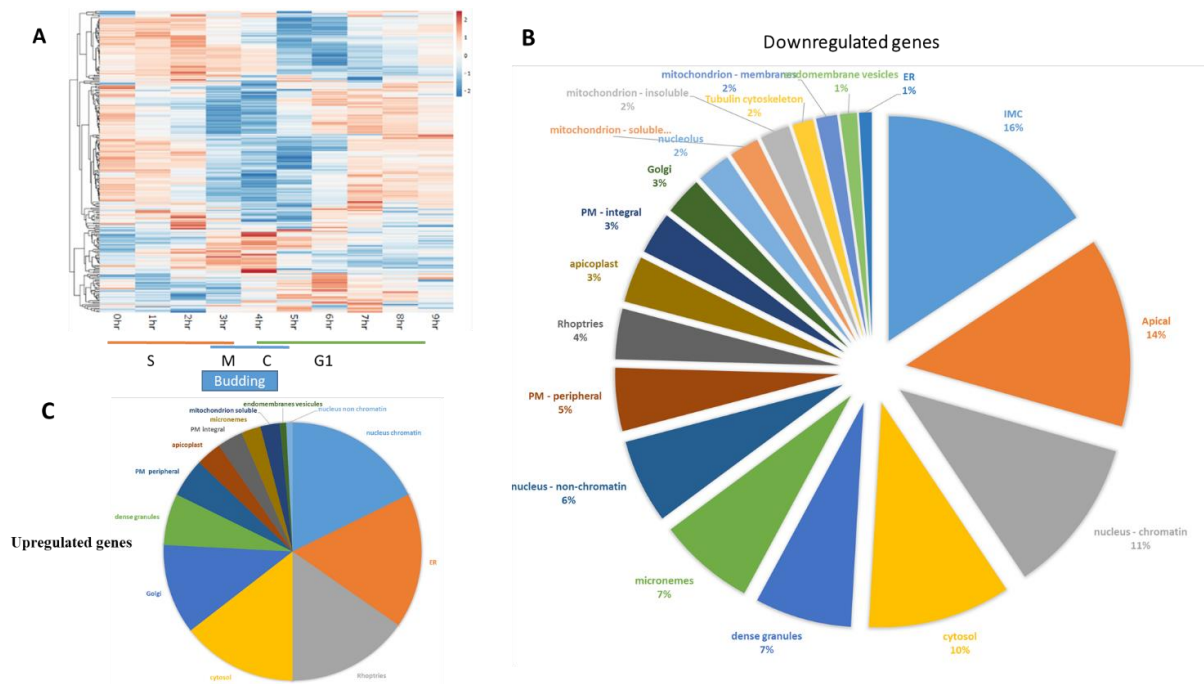
Supplementary Figure 6. Cell cycle expression and putative localization of differentially expressed genes.
(**A**) Heat map of the cell cycle expression profile for all individual transcripts that are upregulated in the iKD AP2IX-5 strain in the presence of 6 hours of auxin treatment. Scale of expression is color-coded with highly expressed genes in orange and less expressed genes in blue according to cell cycle phase indicated at the bottom of the heat map (S-M-C-G1). The cell cycle phases are represented at the bottom as well as the timing when budding occurs. Although the majority of up-regulated genes are not expressed in S/M phase, a cluster of genes shows a strong expression during this phase. (**B**) Pie chart representing the distribution of the putative localization, according to Barylyuk *et al.*, of the proteins encoded by downregulated transcripts. (**C**) Pie chart representing the distribution of the putative localization, according to Barylyuk *et al.*, of the proteins encoded by upregulated transcripts.

175
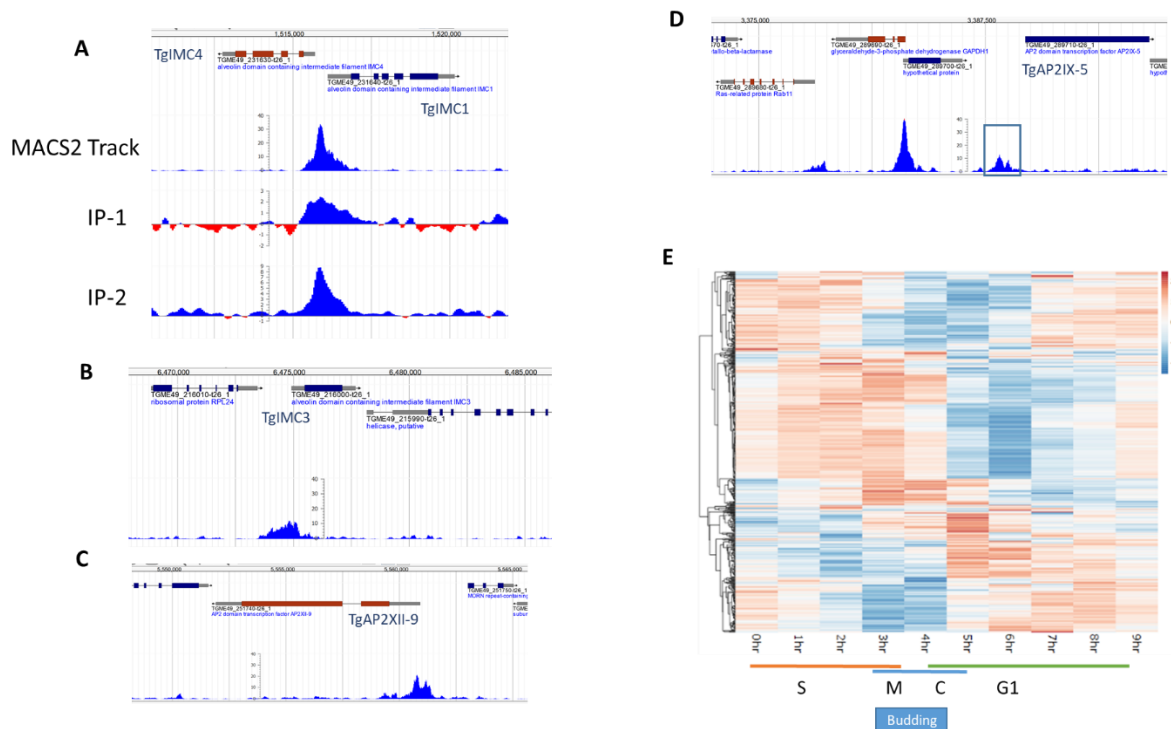
Supplementary Figure 7. ChIP-seq data analysis represented by peaks targeting the promoter of several genes. (**A**) MACS2 generated track and individual ChIP tracks (background subtracted) representing the direct targeting of TgAP2IX-5 to the promoter of downregulated gene TgIMC1 and TgIMC4. (**B**) MACS2 track representing the direct targeting of TgAP2IX-5 to the promoter of downregulated gene TgIMC3. (**C**) MACS2 track representing the direct targeting of TgAP2IX-5 to the promoter of downregulated gene TgAP2XII-9. (**D**) ChIP-seq data peak indicated by blue box demonstrating the targeting of TgAP2IX-5 towards upregulated gene TgAP2IX-5 (boxed). (**E**) Heat map representing the cell cycle expression of all individual transcripts that are targeted by TgAP2IX-5 based on ChIP-seq analysis. Phases of the cell cycle are indicated at the bottom of the figure. The approximate timing for the budding cycle is indicated at the bottom.
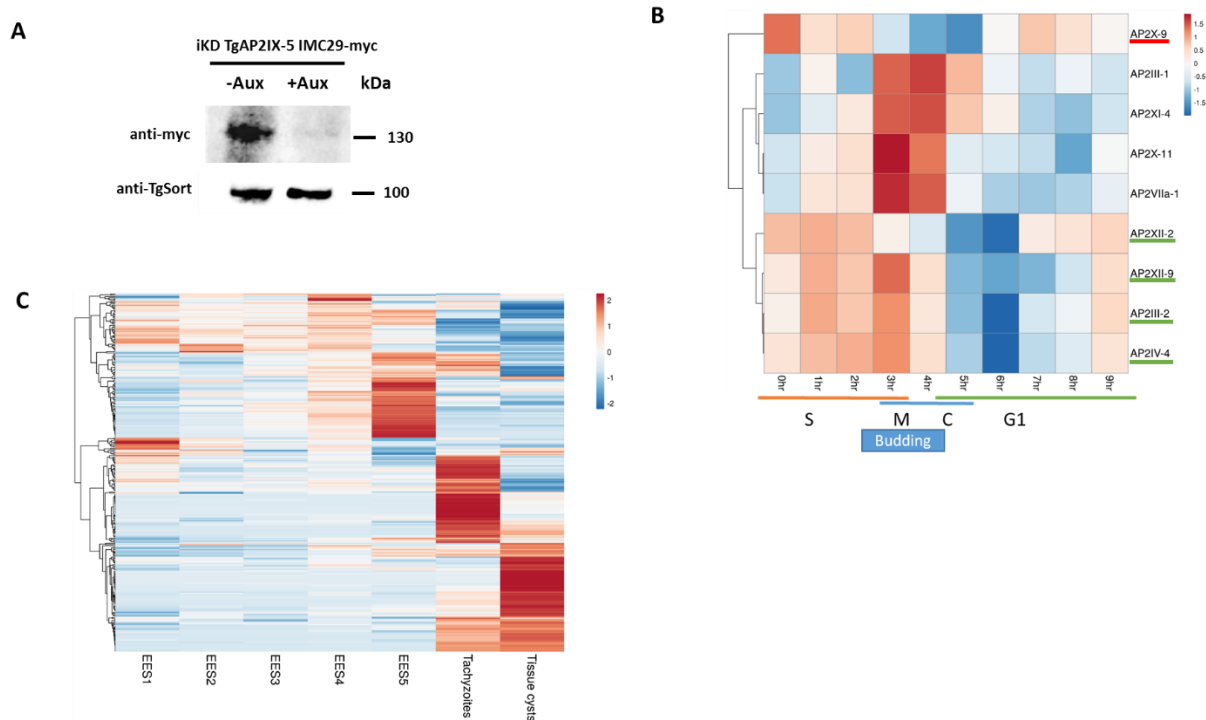
Supplementary Figure 8. Characterisation of genes differentially regulated in the iKD TgAP2XI-5 mutant. (A) Western blot depicting the total protein extract of iKD TgAP2IX-5 IMC29-myc strain treated with or without auxin for 24 hours. Western blots were probed with anti-myc to detect the presence of the TgIMC29 protein (upper panel), anti-TgSortilin was used as a control for normalization (lower panel). **(B)** Heat map of 9 individual TgApiAP2 TF transcripts that are downregulated and upregulated during 6 hours of TgAP2IX-5 depletion. Cell cycle phases are indicated at the lower bottom (S-M-C-G1). Downregulated ApiAP2 TF that are directly bound to promoters are underlined. The downregulated ApiAP2 TFs are underlined in green. The upregulated ApiAP2 TF is underlined in red. **(C)** Heat map of upregulated transcripts that are expressed during the parasite life cycle (cat sexual stages, tachyzoite and bradyzoite stages). EES stands for enteroepithelial developmental stages.

2.5 Complementation demonstrates TgAP2IX-5 is responsible for the phenotypes observed.

We generated a complemented strain (iKDc TgAP2IX-5) by inserting a myc-tagged version of the TgAP2IX-5 gene (under the control of its own promoter) into an exogenous locus (*uprt*; Supplementary Figure 9A). The expression and localization of the exogenous TgAP2IX-5-myc in the complemented strain was verified by immunofluorescence (Supplementary Figure 9B) and the percentage of positively labelled parasite with myc-tag was compared to the expression of the endogeneous HA-tagged copy. A similar number of parasites (30 % of the asynchronous parasite

population) were shown to express the myc-tagged copy in the complemented strain rather than the parental iKD TgAP2IX-5 strain (Figure S9C-D). In order to determine whether the iKD TgAP2IX-5 strain phenotype can be complemented by the ectopic expression of TgAP2IX-5, the number of nuclei per parasite was recorded in the iKDc TgAP2IX-5 strain in the absence and presence of auxin. We observed that the maximum number of nuclei per parasite did not exceed 2 nuclei per parasite (Supplementary Figure 9E). These results demonstrated that the multi-nucleated phenotype of iKD TgAP2IX-5 is due to the absence of the TgAP2IX-5 protein. Similarly, Golgi to nucleus and plastid to nucleus ratios were recorded. Calculated ratios of around 1:1 were recorded and we therefore inferred that each parasite contains one Golgi as well as one plastid (Supplementary Figures 9F-G). These results demonstrate that the TgAP2IX-5 protein was indeed responsible for the phenotypes observed.
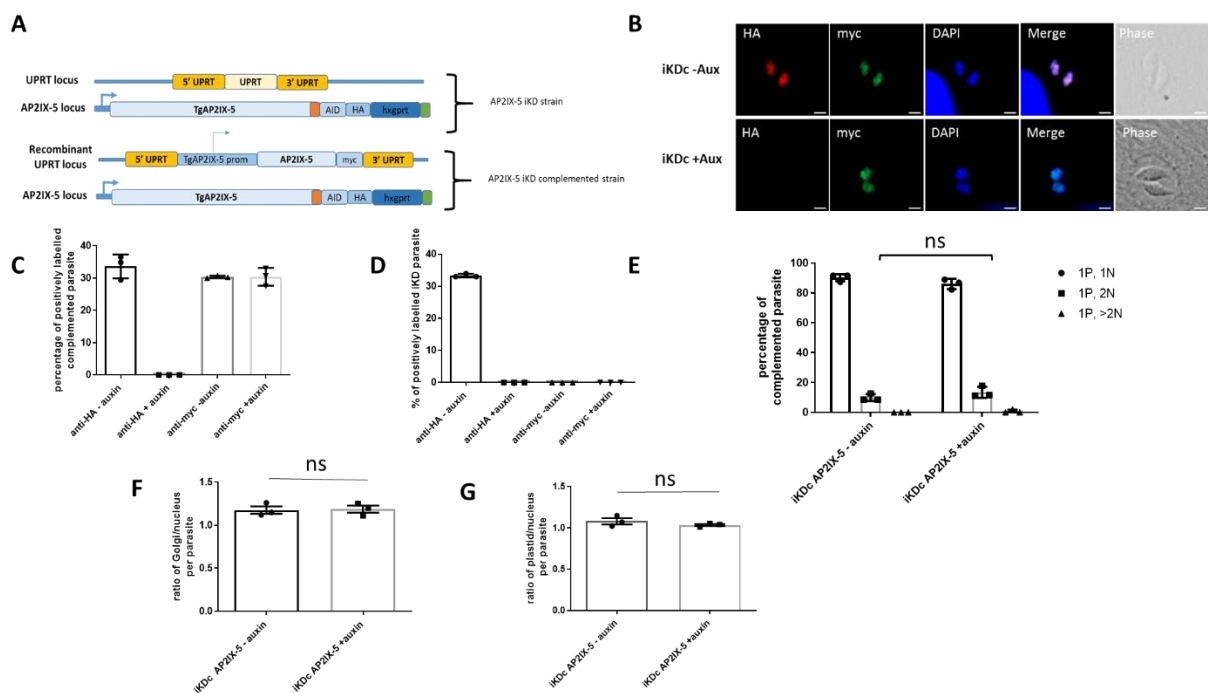
Supplementary Figure 9. Complementation of the iKD TgAP2IX-5 demonstrate that the TgAP2IX-5 protein is responsible for the phenotypes observed in the mutant (**A**) TgAP2IX-5 iKD complementation schematic representation demonstrating the strategy used for generating the complemented TgAP2IX-5 iKD strain by targeting the UPRT locus and replacing it with exogenous myc-tagged TgAP2IX-5 under the control of its own specific promoter. (**B**) Confocal imaging of ciKD TgAP2IX-5 strain. Endogenous TgAP2IX-5 tagged with HA is represented in red while exogenous TgAP2IX-5 tagged with myc is represented in

green. (**C**) Bar graph representing the expression of TgAP2IX-5 using anti-HA and anti-myc antibodies in the complemented strain. mean ± s.d. (n=3 independent experiments). (**D**) Bar graph representing the expression of iKD TgAP2IX-5 using anti-HA antibody and anti-myc antibody as a negative control; mean ± s.d. (n=3 independent experiments). (**E**) Bar graph representing nucleus per parasite counts in the iKDc TgAP2IX-5 strain in the presence and absence of overnight auxin treatment. A Student's t-test was performed to compare mean percentage of multinucleated parasite in the iKDc TgAP2IX-5 strain (-auxin) and iKDc TgAP2IX-5 strain (+auxin). Two-sided p-values: ns: p=0.3739; mean ± s.d. (n=3 independent experiments). (**F**) Bar graph representing Golgi: nucleus ratio in the iKDc TgAP2IX-5 in the presence and absence of overnight auxin treatment. A Student's t-test was performed, two-sided p-values: ns: p=0.9387; mean ± s.d. (n=3 independent experiments). (**G**) Bar graph representing plastid: nucleus ratio in the iKDc TgAP2IX-5 in the presence and absence of overnight auxin treatment. A Student's t-test was performed, two-sided p-values: ns: p=0.1630; mean ± s.d. (n=3 independent experiments).

2.6 TgAP2IX-5 regulates cell cycle pattern flexibility from endodyogeny to endopolygeny

The timing of daughter cell formation is key to define the cell division pattern employed by the parasite at any given time of its life cycle. Since we established that TgAP2IX-5 is the master regulator controlling the production of daughter cells during endodyogeny, we reasoned that controlling the expression of TgAP2IX-5 may be sufficient to switch from one division pattern to another. *T. gondii* undergoes endopolygeny, during its asexual reproduction in the definitive host, where multiple nuclei are formed before a final phase of internal budding. We created a strain of the iKD TgAP2IX-5 mutant expressing a marker of the IMC (TgIMC3-mCherry) to be able to follow the daughter cell formation using live imaging. We treated this strain with auxin to deplete the TgAP2IX-5 protein and obtain parasites that presented around 4 nuclei per parasite (over-night treatment with auxin, Supplementary Figure 10A). Using this treatment and after auxin washout, TgAP2IX-5 re-expression was apparent after 3 hours (Supplementary Figures 10B and 10C). By time-lapse microscopy, we were able to visualize the fate of these parasites after washing auxin out from cell culture media and inducing the re-expression of the TgAP2IX-5 protein. At T_0 (parasites grown for 16 hours with auxin and 3 hours without auxin) we observed enlarged multinucleated parasites. At T_1 (43 mins after T_0), we started to observe multiple daughter cells emerging from within the initial multinucleated mother parasite labeled with TgIMC3. The emergence of parasites continued throughout T_2 (1.5 hrs after T_0) and T_3 (1.7 hours after T_0). At T_4 (3.9 hours after T_0), we observed individual parasites each separately labelled with TgIMC3 mCherry that had

completely emerged from the mother parasite (Figure 6A). After removing auxin from the media, the multinucleated parasites where daughter cell budding was inhibited by the absence of TgAP2IX-5, continued their division in a similar way to endopolygeny. Multiple daughter parasites were observed to internally bud within the cytoplasm of the mother cell leading to the release of multiple daughters from an initial multi-nucleated parasite (Supplementary Movie 1). This forced endopolygeny was due to the re-expression of TgAP2IX-5 in these parasites. These data indicate that expression of TgAP2IX-5 controls the initiation of the budding process and that parasites initially depleted from TgAP2IX-5 were still division competent.

To quantify the ability of the parasite to restart division after an initial depletion of TgAP2IX-5, we designed a protocol producing parasites with around 4 nuclei and then observed the effect of the re-expression of TgAP2IX-5 on the number of nuclei per parasite. For that, we counted the number of nuclei per parasite by immunofluorescence at different time points after auxin washout. While this number increased with longer auxin treatment (Figure 6B), we observed that the number of nuclei per parasite decreases as the duration of auxin washout increases (Figure 6C) indicating that the parasites formed by the "forced" endopolygeny are competent for the next cycles of division. However, we noticed a small percentage of parasites with multiple nuclei after overnight auxin washout, indicating that some parasites did not recover from the original depletion of the TgAP2IX-5 protein. In order to study the effect of auxin removal on daughter parasite formation, we recorded the ability of the initial budding capability of the parasite by labelling TgISP1 and TgIMC3 during auxin washout and compared it with the parasite's budding capability when continuing the auxin treatment. We observed a significant increase in the daughter parasite's budding ability when removing auxin that increased as the duration of auxin washout increased (Figure 6D-6G, Supplementary Figure 10D). To assess if the parasites were able to divide and segregate the apicoplast after depletion and re-expression of TgAP2IX-5, we monitored the fate of the plastid during auxin washout by recording the ratio of plastid to nucleus. While we observed a steady decrease of the number of plastid per nucleus in presence of continuing auxin treatment (Figure 6H), we recorded an increase in the ratio of plastid to nucleus per parasite as the duration of auxin washout increased (Figure 6I) demonstrating that the plastid was competent for replication. These results demonstrate that the timing of TgAP2IX-5 expression is the sole determinant of the creation of daughter cells in the parasite. It may therefore determine the cell division pattern flexibility from endodyogeny to endopolygeny observed in this study. In order to determine whether the parasites generated after re-expression of TgAP2IX-5 (auxin wash-out) and produced by forced endopolygeny remain viable, we carried out plaque assays. For that, the parasites were left to grow in the presence of auxin for 16 hours, 24 hours, and 48 hours before auxin washout and removal. They were then grown without auxin for

several days. Plaques were visible after 16hr and 24hr auxin treatment and subsequent washout. Residual plaques were visible after 48hr auxin treatment (Supplementary Figure 11). This indicates that the parasites emerging from a division cycle by forced endopolygeny were viable.
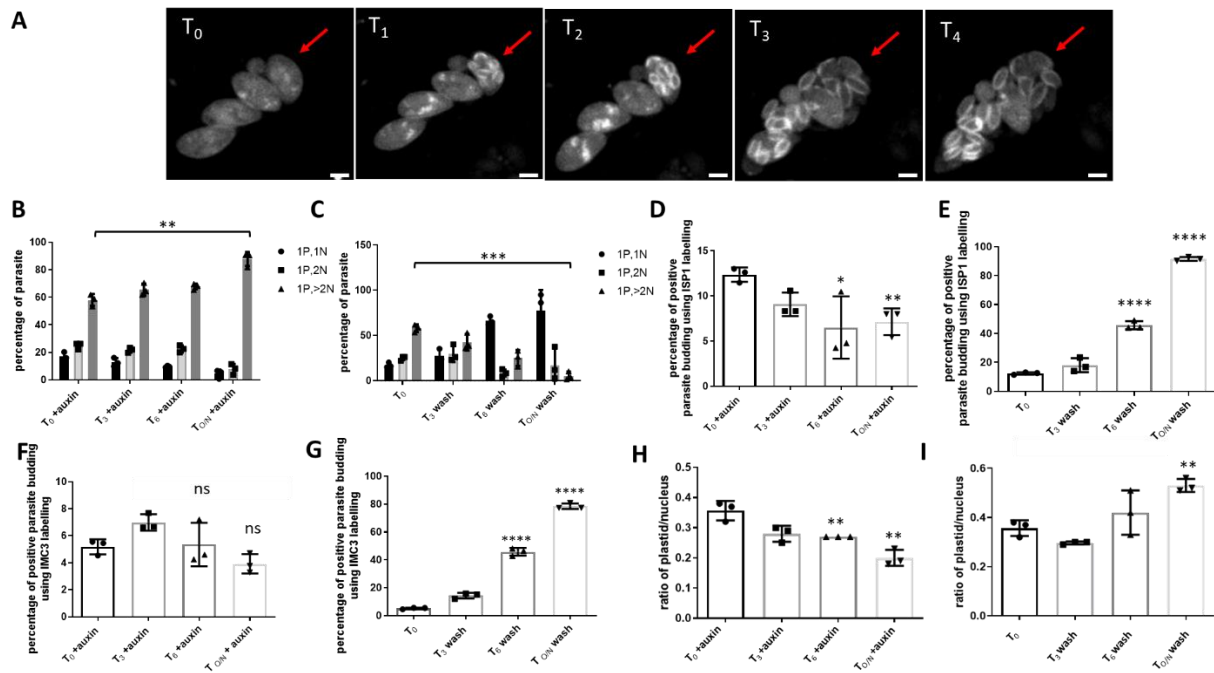
Fig. 6: iKD TgAP2IX-5 parasites treated with auxin resume cell division and daughter parasite formation mimicking endopolygeny. (A) Video-microscopy images of iKD TgAP2IX-5 parasites at different timepoints after auxin washout. The budding vacuole and the emergence of parasites is indicated with a red arrow. The IMC of the parasite is labelled with IMC3-mCherry. The scale bar is indicated at the bottom right of each panel. (B) Bar graph representing nucleus per parasite ratio. Timepoint $T_0 = 0$ min is equal to start of auxin wash. Two-tailed p-values: $**p = 0.0015$; mean ± s.d. ($n = 3$ independent experiments). (C) Bar graph representing iKD TgAP2IX-5 nucleus per parasite counts during different timepoints of auxin washout treatments; 3 h, 6 h, and overnight (O/N) washout. Two-tailed p-values: $**p = 0.0001$; mean ± s.d. ($n = 3$ independent experiments). (D) Bar graph representing parasite budding in the iKD TgAP2IX-5 strain during overnight auxin treatment using ISP1 labelling. Two-tailed p-values: $*p = 0.0457$, $**p = 0.0057$; mean ± s.d. ($n = 3$ independent experiments). (E) Bar graph representing parasite budding in the iKD TgAP2IX-5 strain using TgISP1 labelling during different timepoints of auxin washout treatments; 3 h, 6 h, and overnight (O/N) washout. Two-tailed p-values: $****p < 0.0001$; mean ± s.d. ($n = 3$ independent experiments). (F) Bar graph

representing parasite budding in the iKD TgAP2IX-5 strain using TgIMC3 labelling during overnight auxin treatment. Two-tailed p-values: ns: $p > 0.05$; mean $\pm$ s.d. ($n = 3$ independent experiments). **(G)** Bar graph representing parasite budding in the iKD TgAP2IX-5 strain using TgIMC3 labelling during different timepoints of auxin washout treatments; 3 h, 6 h, and overnight (O/N) washout. Two-tailed p-values: ****$p < 0.0001$; mean $\pm$ s.d. ($n = 3$ independent experiments). **(H)** Bar graph representing the ratio of plastid to nucleus in the iKD TgAP2IX-5 strain during overnight auxin treatment. Two-tailed p-values: **$p = 0.0029$ ($T_{O/N}$ + auxin compared to T_0), **$p = 0.0095$ (T_6 + auxin compared to T_0); mean $\pm$ s.d. ($n = 3$ independent experiments). **(I)** Bar graph representing the ratio of plastid to nucleus in the iKD TgAP2IX-5 strain during different timepoints of auxin washout treatments; 3 h, 6 h, and overnight (O/N) washout. Two-tailed p-values: **$p = 0.0020$; mean $\pm$ s.d. ($n = 3$ independent experiments).
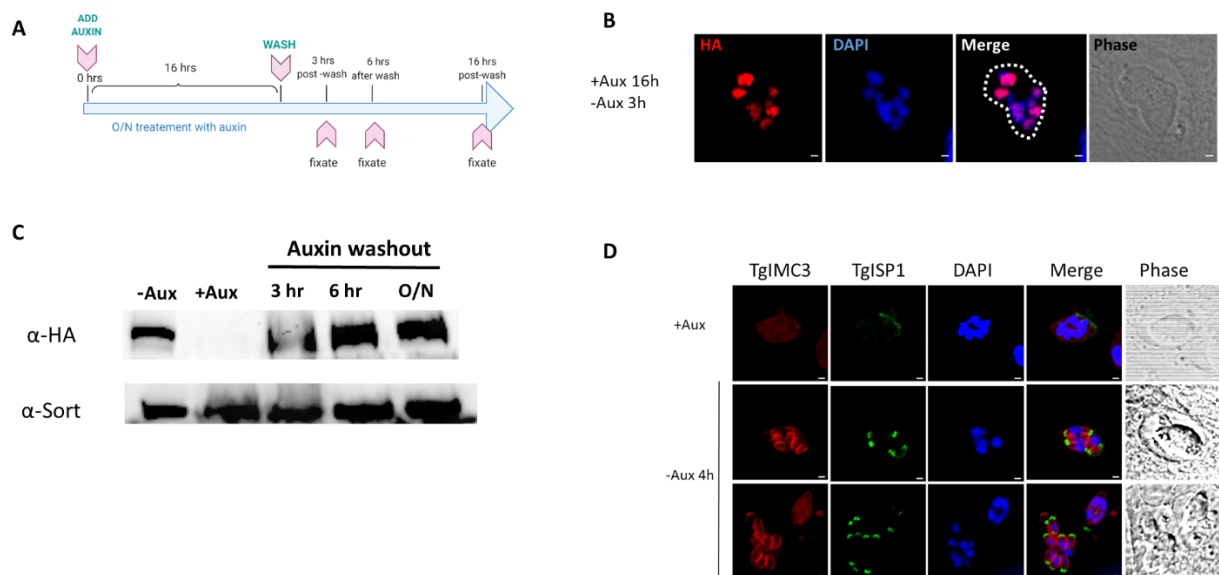
Supplementary Figure 10. Auxin washout allows the re-expression of TgAP2IX-5
(a) Schematic representation of auxin treatment and washout times used to carry out re-expression experiments of TgAP2IX-5. **(b)** Immunofluorescence assay of iKD TgAP2IX-5 parasites treated with auxin for 16 hours and re-expressing TgAP2IX-5 after auxin washout and culture without auxin for 3 hours. TgAP2IX-5 is indicated in red (HA-tagged). DAPI was used to stain the nucleus. Scale bar is indicated in the lower right side of each image. **(c)** Western-blot depicting the total protein extract of iKD TgAP2IX-5-HA strain treated with (+Aux) or without (-Aux) auxin for 16 hours. Parasites extracts were also produced after a 16 hours auxin treatment and then cultured for 3h, 6h or over-night without auxin (Aux washout, 3h, 6h and O/N, respectively). Western blots were probed with anti-HA

to detect the presence of the TgAP2IX-5 protein (upper panel), anti-TgSortilin was used as a control for normalization (lower panel). (**d**) Immunofluorescence assays of iKD TgAP2IX-5 parasites before auxin washout and after auxin washout for a duration of 4 hours. TgIMC3 is labelled in red. TgISP1 is labelled in green. DAPI was used to stain the nucleus. Scale bar is indicated at the lower right side of each image.
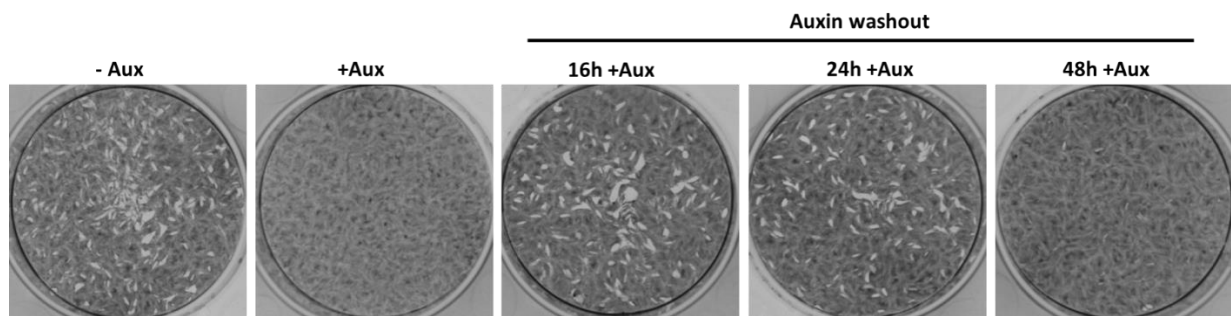
Supplementary Figure 11. Parasites are viable after a cycle of forced endopolygeny.
Plaque assay images representing the viability of iKD TgAP2IX-5 parasites after auxin washout. Parasites were treated with auxin for 16 hours, 24 hours, and 48 hours prior to washout.

Discussion

TgAP2IX-5 depletion was found to completely halt the formation of daughter cells (budding cycle) while nuclear division seemed unaffected. When auxin was added at the time of parasite invasion, daughter cell budding was stopped in the first cell cycle, indicating a direct relationship between budding and the expression of TgAP2IX-5. This led to the accumulation of multinucleated parasites without any signs of daughter cell formation. To our knowledge, such a stark phenotype was observed before in a collection of temperature sensitive cell cycle mutants (Gubbels, Lehmann, et al., 2008), overexpressing a dominant negative version of TgRAb11b (Agop-Nersesian et al., 2010) and when mutating the specific fibers (SFA2 and 3) that connect the centrosome (outer core) to the forming daughter cells (Francia et al., 2012). However, this is the first report demonstrating the importance of transcriptional control in the timing and assembly of daughter cell formation.

After TgAP2IX-5 depletion, the cell cycle stops at a specific time-point after plastid elongation and before its segregation. This time-point corresponds to the onset of daughter cell formation. Surprisingly, the nuclear cycle proceeds while the

apicoplast remains elongated and is not segregated. This underlines the absence of a checkpoint to ensure proper apicoplast segregation as was observed for other mutants (Jacot et al., 2013). A similar effect on plastid division was observed upon depletion of MORN1 (Lorestani et al., 2010) or in a TgDrpA mutant (van Dooren et al., 2009) although they were able to form daughter cells.

Flexibility between the nuclear and budding cycle is thought to be controlled in this parasite by the dual core centrosome with the inner core controlling the nuclear cycle and the outer core controlling the budding cycle (Suvorova et al., 2015). A detailed study of the effect of TgAP2IX-5 on the subcellular structures of the parasite revealed that nuclear and bi-partite centrosome division remain mainly unaffected by TgAP2IX-5 depletion. Given the lack of daughter parasite formation observed after TgAP2IX-5 depletion, it is surprising that the outer core centrosome (as represented by TgCentrin1) is duplicated but remains inactivated by the parasite's kinases, such as TgMAPK-L1(Suvorova et al., 2015). In addition, TgAP2IX-5 may participate in the regulation of the expression of TgFBOX1 because it is found present at its promoter. However, TgFBOX1 transcript (which has a transient expression during the cell cycle) is not present in the RNA-seq dataset. TgFBOX1 localizes early at the daughter cell bud and may organize the daughter cell scaffold (Baptista et al., 2019). Depletion of FBOX1 does not lead to such a dramatic effect on budding like those observed in the iKD TgAP2IX-5 strain. Other components of the outer core, such as the SFA fibers that were shown to be involved in the emergence of daughter cells (Francia et al., 2012), but were present at the centrosome after TgAP2IX-5 depletion. Indeed, SFA fiber expression was also unchanged in the mutant as measured by RNA-seq. This indicates that the outer core centrosome functionality is probably intact in the mutant but centrosome activation and maturation is lacking to proceed with the budding cycle. Therefore, it is most likely that depletion of TgAP2IX-5 hinders normal centrosomal activity despite its successful division. The experiments inducing re-expression of TgAP2IX-5 after its depletion further illustrate the undamaged function of the centrosome in absence of the TF, since daughter cell formation re-started after several cycles of unproductive budding. TgAP2IX-5 is therefore the determinant factor for centrosome activation and the control of the budding cycle.

The phenotype observed after TgAP2IX-5 depletion illustrates the independence of the nuclear and budding cycles in this parasite. Using inducible degradation of the TgAP2IX-5 protein, we have established that the tachyzoites are able to divide by endopolygeny *in vitro.* These experiments also underline the ability of the centrosome to duplicate and maintain its functionality in absence of daughter cell formation. This is a key aspect of the parasite centrosome biology that allows to accumulate nuclei and then activate the budding cycle as seen for division patterns such as endopolygeny or schizogony. Although tachyzoites divide by endodyogeny, they retained the ability to divide by endopolygeny. This simple

mechanism of control which allows multiple nuclear cycles to happen before cytokinesis is also dependent on TgAP2IX-5. The presence of the TgAP2IX-5 transcript during asexual division in the intermediate host in the tachyzoite and bradyzoite stage (endodyogeny) or asexual division in the definitive host (Ramakrishnan et al., 2019) (endopolygeny) may indicate that the same mechanisms are shared for both division patterns, although global expression profiles are profoundly different. Regulation of the timing of expression of TgAP2IX-5 may be sufficient to switch from one division pattern to another. Alternatively, the absence of TgAP2IX-5 may be a signal that promotes endopolygeny. In this line, it is interesting to note that the artificial depletion of TgAP2XI-5 induced the expression of a set of specific transcripts that are normally expressed in the first days of the sexual cycle when endopolygeny occurs. Strikingly, two ApiAP2 (AP2IX-1 and AP2VI-3) TFs upregulated after depletion of TgAP2IX-5 are normally expressed in the sexual stages, indicating that in absence of TgAP2IX-5 part of a sexual specific expression program may be promoted. Interestingly, PF3D7_0613800, the AP2 domain containing protein that is homologous to AP2IX-5 is expressed at the end of the red blood stage (schizont stage) when parasites are budding after multiple round of DNA synthesis. The molecular mechanisms that count the rounds of DNA synthesis and provide the proper timing for parasite budding may be linked to the proteins that activate the expression of TgAP2IX-5

We have established that TgAP2IX-5 controls the timing of activation of the centrosome and therefore creation of daughter cells. However, the molecular mechanisms leading to centrosome activation remain unknown. This key event permits the production of daughter cells at the right timing irrespective of the division pattern used. We reasoned that TgAP2IX-5 may directly control the expression of the proteins in charge of centrosome activation. Although expression of the SFA fibers or other known centrosome markers were unaffected in the mutant, we noticed that the expression of a key centrosomal protein, TgCep530, was directly under the control of TgAP2IX-5 (downregulated in RNA-seq and its promoter bound in ChIP-seq). This protein was shown to be targeted to a centrosomal region situated between the inner and outer core (Courjol & Gissot, 2018). It is essential for the coordination of the nuclear and budding cycle although budding seemed to occur (Courjol & Gissot, 2018). However, its depletion leads to the accumulation of outer core centrosome (Courjol & Gissot, 2018), a phenotype that is not observed with TgAP2IX-5 expression. This protein may therefore have other functions in the maturation or activation of the outer core centrosome that were not identified previously. Another possibility leading to lack of centrosome activation is a plausible downstream effect of non-transcriptional origin, targeting either a kinase or phosphatase with an important role in the centrosome activation cascade. Key serine/threonine kinases such as MAPK-like protein kinases have been identified within *T. gondii* and have been shown to ensure proper formation

of new daughter parasites (Gubbels, Lehmann, et al., 2008; Suvorova et al., 2015). We found that expression of kinases and phosphatases were downregulated after TgAP2IX-5 depletion, but in our ChIP-seq analysis, TgAP2IX-5 was not found to bind their promoters. One obvious candidate, that is directly regulated by TgAP2IX-5, was the TgCDC48AP protein but it was shown to be involved in apicoplast protein import (Fellows et al., 2017). TgAP2IX-5 directly activates the expression of several proteins of unidentified function in *T. gondii*; these hypothetical proteins may serve as direct centrosome activators and the characterization of their function may lead to the discovery of new centrosome activators.

We have also established that TgAP2IX-5 directly activates key components of the daughter cell scaffold. In particular, it regulates the expression of components to be targeted early to the forming daughter buds, such as TgISP1 (Beck et al., 2010), TgIMC1, TgIMC3, TgIMC4 and TgIMC10 (B. R. Anderson-White et al., 2011). Apical cap component, such as TgAC2 and TgAC7 may also be loaded early on the forming buds. Similarly, TgGAPM3 expression is directly dependent on TgAP2IX-5 and its invalidation provokes IMC collapse (Harding et al., 2016). However, TgIMC15, a protein known to be loaded early on the centrosome before reaching the forming buds is not affected by TgAP2IX-5 depletion. TgIMC15 may have a limited role in daughter cell formation or centrosome activation as suggested by the mild phenotype exerted by its mutant (R. Dubey et al., 2017). This suggests that TgAP2IX-5 may activate the centrosome but also directly regulates the expression of key components of the daughter cell scaffold that will be needed in a short time frame to proceed with daughter cell formation (Figure 7).
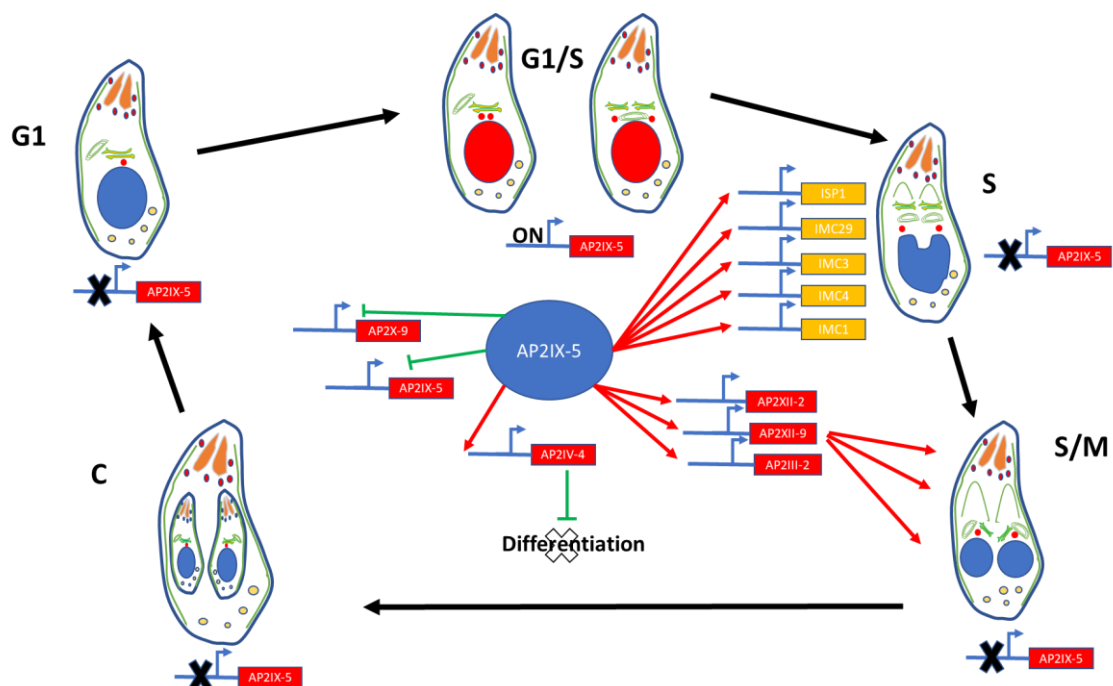
Fig. 7: Schematic representation of the effect of TgAP2IX-5 depletion on daughter cell formation according to the different phases of the cell cycle. Absence of TgAP2IX-5 leads to the blockage of the cell cycle within the G1/S phase. This is associated with the direct targeting of key inner membrane complex proteins such as TgISP1, TgIMC1, TgIMC29, TgIMC3, and TgIMC4 as well as other key TFs (TgAP2XII-2, TgAP2XII-9, TgAP2III-2, TgAP2IV-4, TgAP2X-9). TgAP2IV-4 is a known repressor of differentiation. TgAP2X-9 may be repressed by TgAP2IX-5. The TgAP2IX-5 transcript may also be regulated by a negative feedback loop.

We observed that RNA-seq and ChIP-seq datasets only partially overlapped. We reasoned that indirect effects on gene expression may be identified using RNA-seq even at a short timing after TgAP2IX-5 depletion (6 hours). The cell-cycle expression profile of the genes that are directly controlled by this TF and downregulated in its absence showed that regulated transcripts are expressed during the S phase before the budding occurs. Among these genes, we identified 4 other ApiAP2 transcription factors (TgAP2III-2, TgAP2IV-4, TgAP2XII-2 and TgAP2XII-9) that were directly controlled by TgAP2IX-5. These TF may be responsible for the expression of the transcripts that were identified as downregulated in RNA-seq and that peak during the late S and M phase. Although no data is available for TgAP2III-2, TgAP2XII-2 and TgAP2XII-9, TgAP2IV-4 was shown to be a repressor of the bradyzoite differentiation expression program (J. B. Radke et al., 2018). Interestingly, depletion of TgAP2IX-5 leads to the upregulation of transcript preferentially expressed in bradyzoites, such as MAG1, indicating that the absence of TgAP2IX-5 promotes the differentiation pathway. The control of the expression of a repressor of differentiation by a TF that also controls the continuation of cell cycle may provide the missing link between cell cycle and differentiation. It has been shown that the cell cycle is linked to bradyzoite differentiation (J. R. Radke et al., 2003). In particular, the developmental switch toward the latent bradyzoite is made during S phase and/or mitosis (J. R. Radke et al., 2003). It seems convenient for the parasite to link the choice of continuing the tachyzoite cell cycle (by starting the budding cycle) with the expression of a repressor of differentiation. Therefore, expression of TgAP2IX-5 may serve as a molecular check point for the choice between proliferation or differentiation. TgAP2IX-5 may act as a limiting factor for this developmental choice at each round of the cell cycle (Figure 7).

We also observed that TgAP2IX-5 may act as a repressor since it was found at the promoter of genes whose transcript was up-regulated after depletion of this protein. It was striking to see that the TgAP2IX-5 transcript was overexpressed after TgAP2IX-5 depletion. We also found that TgAP2IX-5 was bound to its own

promoter indicating that a direct negative feedback loop may be present to limit the expression of TgAP2IX-5. This might explain the short timeframe when TgAP2IX-5 is expressed during the cell cycle since its expression might be self-limiting. Another ApiAP2 TF expression (AP2X-9) may be directly repressed by TgAP2IX-5. AP2X-9 transcript peaks at the G1/S boundary, just before the expression peak of TgAP2IX-5. Therefore, TgAP2IX-5 may repress the expression of the TF that control the cell cycle expression program preceding the budding phase. In summary, TgAP2IX-5 serves as a platform for the repression of the G1/S expression program (through AP2X-9 repression), the promotion of the S/M expression program (through the activation of TgAP2III-2, TgAP2XII-2 and TgAP2XII-9) and limiting differentiation (through AP2IV-4 activation).

In other eukaryotes, TFs associate with each other and form complexes to either activate or repress gene expression (Nakagawa et al., 2018). ApiAP2s are known to associate with each other (Lesage et al., 2018) and differential association may impact their activity.

TgAP2IX-5 is therefore an essential regulator during the *T. gondii* tachyzoite cell cycle. TgAP2IX-5 controls the activation of the outer core centrosome to induce the budding cycle. It also controls the expression of key proteins for formation of the daughter cell scaffold, ensuring that the proper continuation of the cell cycle is achieved. TgAP2IX-5 is also a master regulator that controls the expression of the TFs that are no longer needed and those that will be further needed for the completion of the budding cycle. It also acts as a limiting factor that ensures that asexual proliferation continues by promoting the inhibition of the differentiation pathway at each round of the cell cycle. TgAP2IX-5 is therefore a master regulator that controls cell cycle and developmental pathways. However, several questions remain to be answered. For example, what are the proteins whose expression are controlled by TgAP2IX-5 and that are responsible of centrosome activation? Moreover, the molecular mechanisms that allow the same TF to act as an activator or a repressor are still unknown and will be the subject of further studies.

2.7 Complementary Experiments

1. TgAP2IX-5 depletion impacts the expression of cell cycle regulated genes at earlier timepoints of auxin treatment

Since the depletion of TgAP2IX-5 was achievable as early as one hour after auxin treatment as demonstrated previously by western blot, we decided to investigate what genes are differentially regulated at earlier time points of auxin treatment. This was carried out in order to identify genes that may be up or downregulated early on after TgAP2IX-5 depletion and could have been masked at the 6 hour

time-point. Therefore, total RNA was extracted from tachyzoites of the iKD TgAP2IX-5 strain grown with or without auxin for 1 hour and 2 hours. Significant changes were identified by analyzing data using Deseq2 with an adjustable p-value cut-off of 0.05 and a minimum fold change of 2 (Figures 8A-B). Depletion of TgAP2IX-5 after 1 hour of auxin treatment led to the downregulation of 117 genes and upregulation of 27 genes. However, the depletion of TgAP2IX-5 after 2 hours of auxin treatment resulted in the downregulation of 603 genes and the upregulation of 20 genes (Figures 8A-B). We then examined the cell cycle expression of the downregulated genes after 1 hour of auxin treatment and 2 hours of auxin treatment and generated heat maps to visualize phases of the cell cycle that demonstrated peaks of expression (Figures 8C-D). We observed that most of the downregulated genes demonstrated a peak of expression during the entire S phase and early M phase. The heat map of downregulated genes generated after 2 hours of auxin treatment also demonstrates a peak of expression of genes during the late cytokinesis and early G1 phase (Figure 8D). Overall, these results demonstrate that TgAP2IX-5 controls genes which peak during the S phase and early M phase based on short durations of auxin treatment (1 hour and 2 hours). When examining the cell cycle expression of the upregulated genes after 1 hour and 2 hours post-auxin treatment. The heat maps generated exhibited heterogeneous peaks of expression along the cell cycle in a similar fashion to the heat map generated after 6 hours of auxin treatment (Figures 9A-B).
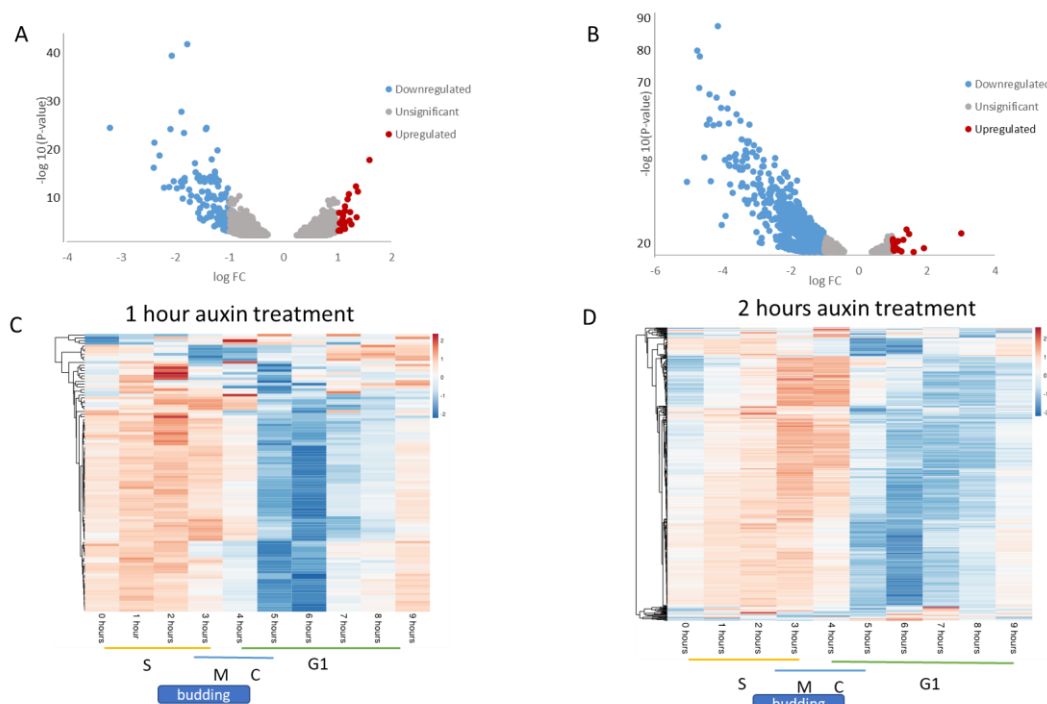
Figure 8- Cell cycle expression of differentially regulated genes after 1hour and 2 hours of auxin treatment. **(A)** Volcano plot of differentially expressed genes

189

analyzed from RNA-sequencing of TgAP2IX-5 iKD parasites treated with auxin for 1 hour. **(B)** Volcano plot of differentially expressed genes analyzed from RNA-sequencing of TgAP2IX-5 iKD parasites treated with auxin for 2 hours. **(C)** Heatmap demonstrating the cell cycle expression of individual transcripts that are downregulated in the iKD TgAP2IX-5 gene in the presence of 1 hour of auxin treatment. The cell cycle phases are represented at the bottom as well as the timing when budding occurs **(D)** Heatmap demonstrating the cell cycle expression of transcripts that are downregulated in the iKD TgAP2IX-5 gene in the presence of 2 hours of auxin treatment.
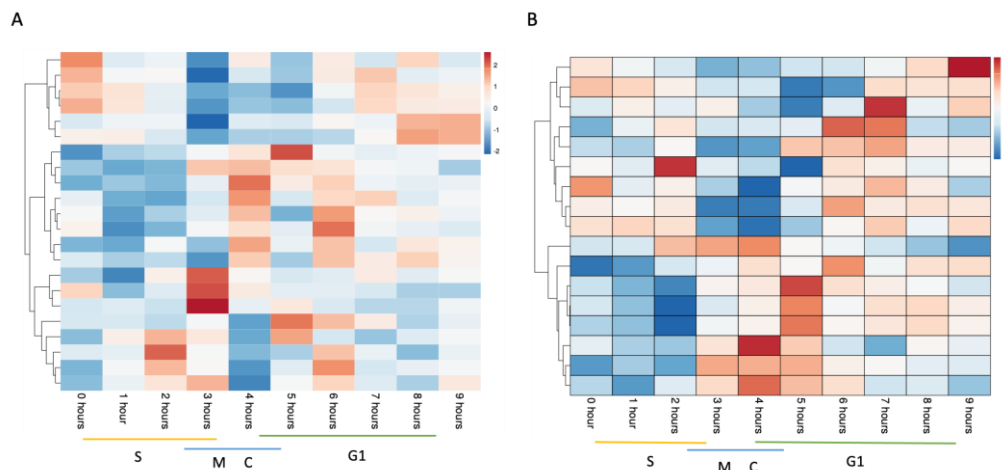
Figure 9: **(A)** Heatmap demonstrating cell cycle expression of upregulated genes in the iKD TgAP2IX-5 parasites after 1 hour of auxin treatment. The cell cycle phases are represented at the bottom. **(B)** Heatmap demonstrating the cell cycle expression of upregulated genes in the iKD TgAP2IX-5 parasites after 2 hours of auxin treatment.

By using RNA-seq, we were able to identify genes that are either directly or indirectly targeted by TgAP2IX-5, based on 1 hour and 2 hours auxin treatment of iKD TgAP2IX-5 parasites. Therefore, in order to determine the genes that are directly targeted by TgAP2IX-5, we over-lapped the ChIP-seq data with the 1 hour and 2 hours lists of downregulated and upregulated genes. After 1 hour auxin treatment, there was an overlap of 47 genes representing a 7% overlap. In the case of 2 hours of auxin treatment, there was a total overlap of 159 genes representing a 23% overlap. When comparing the percentages of overall overlap between the three different durations of auxin treatment (1 hr, 2 hrs, and 6 hrs), it was striking that it was at 2 hours of auxin treatment where most of the overlap occurs between the differentially regulated genes and those directly interacting with TgAP2IX-5 (Figure 10A). These results suggest that it is around 2 hours of auxin treatment where most of the genes which are normally directly activated by TgAP2IX-5 are

downregulated. Heat maps of the downregulated genes which are directly targeted by TgAP2IX-5 based on the 1-hour auxin treatment study demonstrated peaks of expression during the entirety of the S phase and M phase with low peaks of expression during the cytokinesis phase (Figure 10B). A similar trend of peak expression was demonstrated for the 2 hours auxin treatment study (Figure 10C).
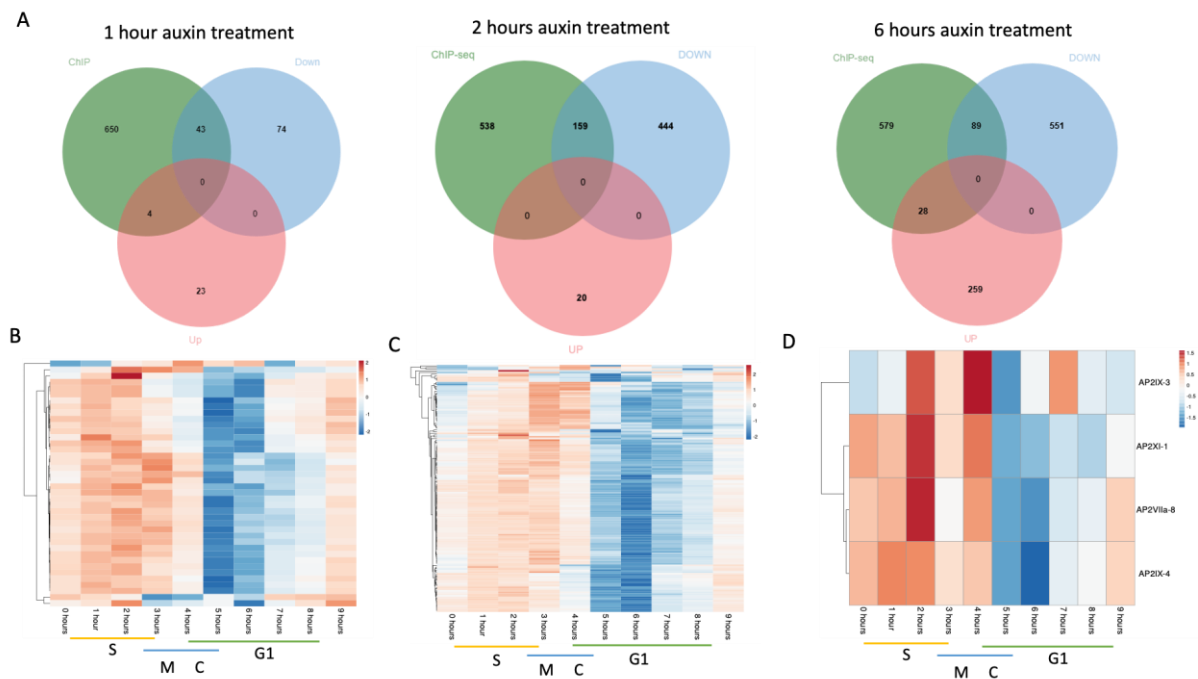
Figure 10: (A)Venn diagrams of overlapping downregulated genes, upregulated genes from RNA-seq after 1 hour of auxin treatment, 2 hours of auxin treatment and 6 hours of auxin treatment and identified promoters of genes directly targeted by TgAP2IX-5. DeSeq2 and MACS2 software were used to analyze RNA-seq and ChIP-seq data, respectively. (B) Heatmap demonstrating cell cycle expression of downregulated genes directly targeted by TgAP2IX-5 after 1 hour of auxin treatment. The cell cycle phases are represented at the bottom. (C) Heatmap demonstrating the cell cycle expression of downregulated genes directly targeted by TgAP2IX-5 after 2 hours of auxin treatment. The cell cycle phases are represented at the bottom. (D) Heatmap of cell cycle expression of ApiAP2 TFs targeted by TgAP2IX-5 from 1 hour and 2 hours auxin treatment of iKD TgAP2IX-5 parasite gene expression study not previously identified from the 6 hours auxin treatment study.

We then searched for potential regulators which are directly regulated by TgAP2IX-5 and therefore might regulate genes which are not directly targeted by TgAP2IX-5. When comparing the ApiAP2 TFs that were targeted by TgAP2IX-5

based on 6 hours of auxin treatment with the ApiAP2 TFs that were targeted by TgAP2IX-5 based on 1 and 2 hours of auxin treatment, we noticed that five ApiAP2 TFs were not identified previously during the 6 hours auxin treatment gene expression study (TgAP2VIIa-8, TgAP2XI-1, TgAP2IX-4, TgAP2VI-1, and TgAP2IV-3). Cell cycle expression profiles of these ApiAP2 TFs demonstrated peaks of expression during the S/M phase with strong peaks of expression during the late S phase (Figure 10D). Additionally to AP2IV-4 which was originally identified after the 6 hours auxin treatment, TgAP2IX-4, which is a known repressor of bradyzoite differentiation (Huang et al., 2017) was also identified to be downregulated in both 1 hour and 2 hours auxin treatment gene expression studies therefore confirming the role of TgAP2IX-5 in regulating life cycle transitions such as bradyzoite differentiation. In conclusion, these results demonstrate that TgAP2IX-5 is responsible for controlling ApiAP2 TFs that are mostly expressed during the S/M phase, among them certain ApiAP2 TFs are most likely responsible for coordinating developmental choices. Strikingly, RNA-sequencing analysis of iKD TgAP2IX-5 parasites treated with auxin for 2 hours revealed a larger number of genes being directly targeted by TgAP2IX-5 and therefore suggests that it is most likely that TgAP2IX-5 depletion has a peak effect on gene expression at around 2 hours after auxin treatment.

2. Domain1 is a novel domain of TgAP2IX-5

Domain 1 is a conserved region of the TgAP2IX-5 protein consisting of 115 amino acids. Domain 1 was first identified by Dr Gissot by carrying out a Basic Local Alignment Search Tool (BLAST) analysis using the TgAP2IX-5 protein sequence as a query against sequences from the *Toxoplasma* genome. This resulted in identifying 4 other proteins possessing a conserved version of domain1. The amino acid sequence of domain1 was demonstrated to be conserved in a number of hypothetical proteins within the *Toxoplasma* genome and which include TGGT1_243460, TGGT1_281960, TGGT1_233380, and TGGT1_297340. These proteins have a sequence identity of 44%, 42%, 39%, and 31%, respectively (Figure 11).

```
TGGT1_289710  VEWHEGFRRPFGTEGRQQLLRHLRQVYNADSAYWGER-LRHANIAFSRIAYATVAELWKIA  1824
TGGT1_281960  VTWTPGFRLPLGAEGRQVLLRRLRRAYHASPPETRDTFLASHGLVFSRMPFATVSELFHLA  318
TGGT1_233380  LQWHEGFTLPLGKDGRGELIKRMRSVHKADREFCRFS-LEGMGIDFKRLAHATVEELWKIA  1001
TGGT1_243460   WVHGFAWPVGADGRRLLLRKLRGVYWSDPDYWQKRLMAEGLYRRDLFTLATVQELFKVT  796


TGGT1_289710  HVMDCFPIALA----FSNRHSATASTG------------VEDGGALTGAPGTGAVG  1864
TGGT1_281960  HLLGVFDFAVQCSEEFGGVSSATAVAGRGNRSGVHSSNASVGAVGASEGASGEGSEG  376
TGGT1_233380  YRWGLFGYAVKLSKKYGKTTTS----------------------------------  1023
TGGT1_243460  HLMG----------------------------------------------------  800


TGGT1_289710  LP-GAAAVGRRA  1875
TGGT1_281960  LRVGASAKRRRA  388
```

Figure 11: Sequence alignment of the *T. gondii* domain1 of the following proteins (TGGT1_ 289710, TGGT1_243460, TGGT1_281960, TGGT1_233380, and TGGT1_297340). Similar amino acids (aa) are highlighted in *gray* while identical aa are highlighted in *black*.

3.   Domain 1 is essential for the function of TgAP2IX-5

In order to elucidate the role of the different regions of the TgAP2IX-5 protein, we studied the role of two different domains within the TgAP2IX-5 TF. The first domain was the well-known AP2 domain which has been identified by many studies previously. The second domain was the novel domain1 (Figure 12A). For this purpose, the complementation plasmid used previously to generate the complemented iKD TgAP2IX-5 strain was used to generate complemented strains in which either the AP2domain or domain1 was deleted from the exogenously tagged TgAP2IX-5 gene (Figures 12B-C). In the case where the mutant strains generated are treated with auxin, there will not be any compensation for the loss of the AP2 domain or domain1.

A

```
   TgAP2IX-5 (TGGT1_289710)

   PLGTPSSLGLFGREAGEGKETPSSRASAENRSHPATGQSKNAKPYPAAGALQAGSQPGAAGPVSPTKAETEGSPSGTKAS  1040
   KSGASGFLAAFEDAAFQQPSEEFIGYCVQKHQARYPTPQNLPGIQMEQQQRRWCASVYYRGCQHKRRFSMGRWGPLGAFY  1120
   AAIEWRQSHYSRLNSLKGIRSPGNSEGAPGSDHKKRRRRSSSGSCSSRSHPALARGSVGPPGPGSLAESAPSEGPEGTET  1200
   ----------------------------------------------------------------------------
   ACAGGTDMRKSTSREKQAGSGPARSRRTKGAASASNGGSLFPVSPYAAPVSPTGPASSFSPPFRPLSNSGSPPLAPANSD  1760
   GAAPVEWHEGFRRPFGTEGRQQLLRHLRQVYNADSAYWGERLRHANIAFSRIAYATVAELWKIAHVMDCFPIALAFSNRH  1840
   SATASTGVEDGGALTGAPGTGAVGLPGAAAVGRRACGAKGEKAKGSRRGNSGNAGATASSKTPQLKQTSALAGGLSSSGA  1920
```

193
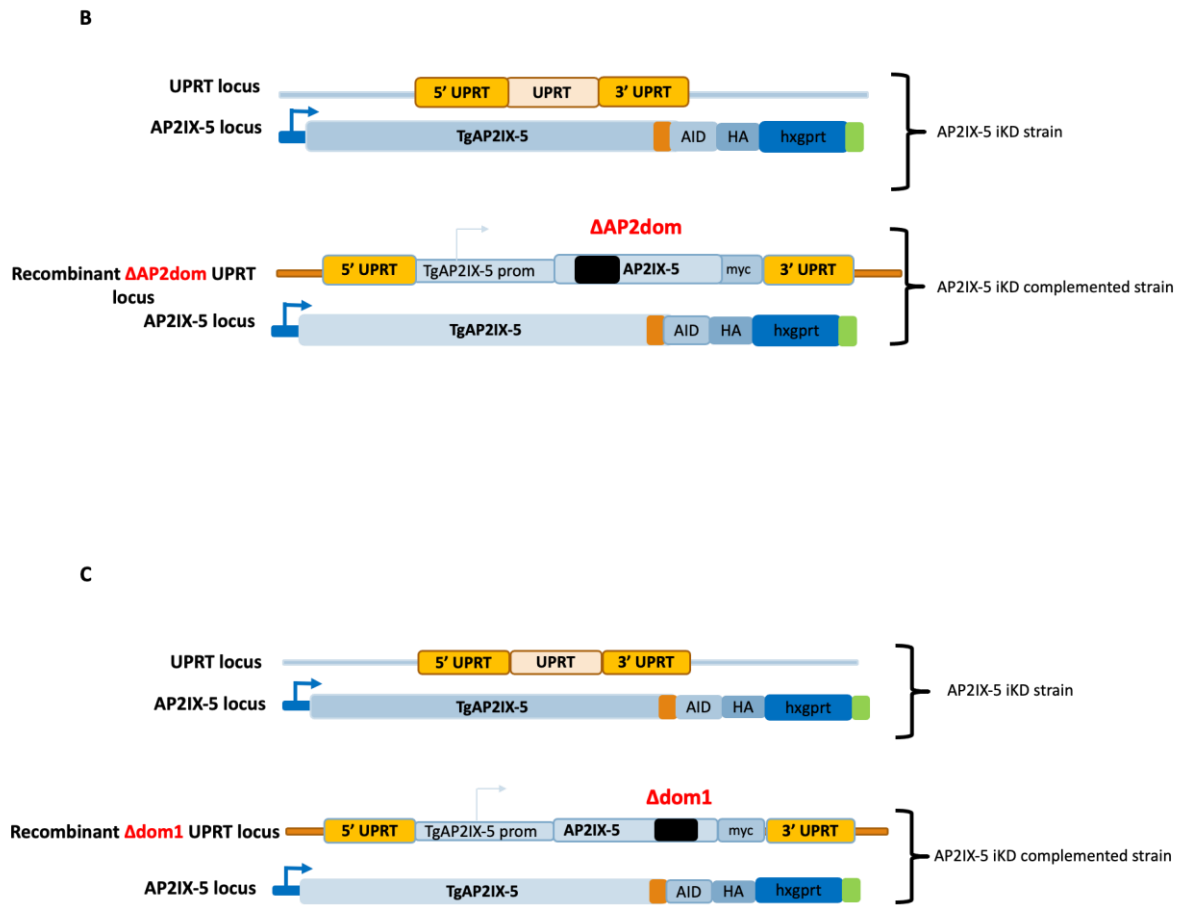
Figure 12: **(A)** Amino acid sequence of TgAP2IX-5 with AP2 domain highlighted in yellow (60 aa) and domain1(115 aa) highlighted in green. Dotted lines represent amino acids between the two domains **(B)** Schematic representation of TgAP2IX-5 complementation construct with deleted AP2domain. **(C)** Schematic representation of TgAP2IX-5 complementation construct with deleted domain1.

The complemented strains were designated as iKDc TgAP2IX-5 ΔAP2 domain and iKDcTgAP2IX-5 Δdomain1 mutants for the sake of simplicity. First, a growth assay was carried out. Surprisingly, the iKDc TgAP2IX-5 Δdomain1 strain presented a severe growth defect in presence of Auxin, while the iKDc TgAP2IX-5 ΔAP2 parasites did not show any growth impairment suggesting that the deletion of AP2 domain did not impact the growth (Figure 13A). In an additional experiment, a plaque assay was carried out where the mutant parasites were left to grow for 1 week in the presence and absence of auxin, Strikingly, the monolayer of HFF cells that was inoculated with iKDc TgAP2IX-5 Δdomain1 parasites in the presence of auxin exhibited no lysis plaques as opposed to the presence of lysis

plaques in wells infected with iKDc TgAP2IX-5 ΔAP2 domain mutant parasites (Figure 13B). In an attempt to study the effect of deleting either the AP2 domain or domain 1 on the most striking phenotype exhibited by the iKD TgAP2IX-5 mutant (multi-nucleation), we carried out nucleus per parasite counts. As expected, there was a significant percentage of iKDc TgAP2IX-5 Δdomain1 parasites with multinucleated parasite in the presence of auxin (Figure 13C).

Overall, these results suggest that domain1 is essential for the function of TgAP2IX-5 whereas the AP2 domain is not.
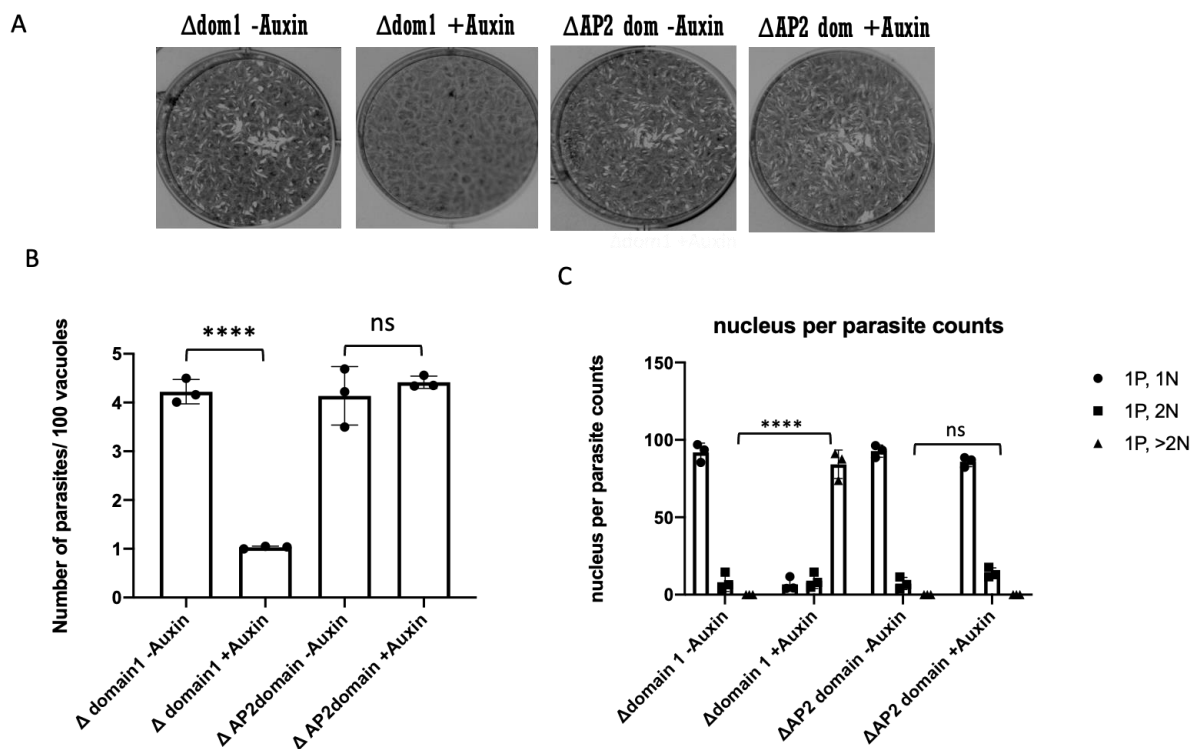
Figure 13: (A) Plaque assay of iKDc TgAP2IX-5 ΔAP2domain mutant parasites and iKDc TgAP2IX-5 Δdomain1 mutant parasites in the presence and absence of auxin. (B) Bar graph representing the growth assay of iKDc TgAP2IX-5 Δdomain1 parasite and iKDc TgAP2IX-5 ΔAP2domain in the presence and absence of auxin. A Student's t-test was carried out, ns p> 0.05, ****P<0.0001; mean ± s.d. (n=3). (C) Bar graph representing nucleus per parasite counts after growth and treatment with auxin for 24 hours. A Student's t-test was performed, ns p>0.05, ****p<0.0001; mean ± s.d. (n=3).

DISCUSSION of the complementary experiments

The striking mutli-nucleated phenotype and total blockage of asexual cell division observed in iKD TgAP2IX-5 mutant parasites laid the foundation for investigating transcriptome changes upon depletion of TgAP2IX-5. In the previous study, depletion of TgAP2IX-5 by treating the mutant parasites with auxin for 6 hours demonstrated a total of 640 genes being differentially regulated (either downregulated or upregulated). Presuming that a larger array of genes is possibly impacted by TgAP2IX-5 depletion, a more thorough investigation with the aim of determining whether auxin treatment for a shorter duration of time would identify genes that were not identified previously from the 6 hour auxin treatment and that were perhaps masked, was carried out. The depletion of TgAP2IX-5 at a shorter timepoint of 2 hours of auxin treatment identified a similar number of genes which were differentially regulated by TgAP2IX-5 (623 genes). Strikingly at 1 hour of auxin treatment, only 117 genes were identified to be differentially regulated, a much smaller pool of genes compared to those identified from 2 hours and 6 hours of auxin treatment. When comparing the nature of genes which were differentially regulated and by focusing mainly on the downregulated genes, we observe that more than half of the downregulated genes identified at 6 hours of auxin treatment are shared with those identified at 2 hours of auxin treatment with the remaining 306 downregulated genes most likely being downregulated as a consequence of a downstream effect of TgAP2IX-5 depletion at 2 hours. When comparing downregulated genes identified at 6 hours auxin treatment to those downregulated at 1 hour auxin treatment, there is a much smaller group of genes that are shared between the two groups consisting of 61 genes. Thus, the downregulation of the genes not shared with those of the 1 hour auxin treatment are downregulated as a consequence of the downstream effect of genes downregulated prior to the 6 hour auxin treatment. Overall, it is most likely that a large proportion of the genes identified to be controlled by TgAP2IX-5 based on the 6 hours auxin treatment are differentially expressed as a downstream effect of the downregulation of genes by TgAP2IX-5 at an earlier timepoint of the cell cycle. When studying the nature of downregulated genes identified at the different time points, we notice that most of the genes identified from all the time points are important for constructing the scaffold of the daughter parasite and consist of genes coding for the inner membrane complex and apical complex. However, it is worthy to note that many of the downregulated genes identified at all time points have yet to be characterized.

When comparing the number of genes that were downregulated and overlapped with the list of genes identified from the ChIP-seq dataset , at 1 hour of auxin treatment, 43 downregulated genes were directly targeted by TgAP2IX-5 whereas

159 and 89 downregulated genes were directly targeted by TgAP2IX-5 after 2 hours and 6 hours of auxin treatment, respectively. Depletion of TgAP2IX-5 after 2 hours of auxin treatment resulted in the largest number of overlapped downregulated genes with the ChIP-seq dataset (159 genes). In addition, when comparing the number of downregulated genes which were directly targeted by TgAP2IX-5 and overlapped between the 1 hour, 2 hours, and 6 hours auxin treatment datasets, we were able to identify only 26 overlapped genes. Thus, it is most likely that the depletion of TgAP2IX-5 after 2 hours of auxin treatment reveals genes directly targeted by TgAP2IX-5 that were masked at the 6 hours-time point of auxin treatment.

TgAP2IX-5 can be mainly described to function mainly as an activator, since 1 hour, 2 hours, and 6 hours of iKD TgAP2IX-5 auxin treatment studies resulted in a very low proportion of upregulated genes when comparing it to the number of downregulated genes (Figure 10A). However, it is at 6 hours of auxin treatment where there is the greatest number of upregulated genes. Furthermore, there is a very small percentage of overlap between the upregulated genes and those directly bound by TgAP2IX-5 in all 3 auxin treatment conditions. Thus, a majority of the genes which are upregulated after 6 hours of auxin treatment and do not overlap with genes identified from the ChIP-seq data are most likely downstream effects of TgAP2IX-5 depletion. In addition, at 1 hour of auxin treatment there were only 4 genes that were upregulated and directly targeted by TgAP2IX-5 and surprisingly at 2 hours of auxin treatment, there were no genes upregulated and directly bound by TgAP2IX-5. Altogether, this further promotes that TgAP2IX-5 most likely functions mainly as an activator of genes.

In the previous study regarding the re-expression of TgAP2IX-5 after its depletion, the parasite was demonstrated to change its mode of division from endodyogeny to endopolygeny once TgAP2IX-5 was re-expressed thus signifying the flexibility of the parasite's mode of cell cycle division. An attempt to study the transcriptomic changes after re-expression of TgAP2IX-5 yielded unsuccessful results. This could be due to the short time frame of TgAP2IX-5 re-expression by washing out auxin for 1 hour after overnight auxin treatment. Although the TgAP2IX-5 protein is re-expressed within 1 hour of auxin treatment as tested by immunofluorescence assays, transcriptome changes were not detected after 1 hour of auxin washout. Perhaps, this time frame of auxin washout was too short and sample collection after allowing for sufficient time for TgAP2IX-5 re-expression should have been carried out instead. Supposing transcriptomic changes had been detected, this would have provided useful insight as to which genes are targeted by TgAP2IX-5 after its-re-expression providing us with genes that might be key in controlling the parasite's switch from one division mode to another.

Two hours of auxin treatment allowed to identify a wider range of proteins directly targeted by TgAP2IX-5. Among these are those which are key in building the daughter parasites scaffold and which were identified previously from the 6 hours auxin treatment study such as IMC4, IMC1, IMC3, ISP1 (Beck et al., 2010), IMC10 (B. R. Anderson-White et al., 2011) and GAPM3 (Harding et al., 2016). In addition to other proteins which are important for maintaining the cytoskeletal structure such as SPM1 (Tran et al., 2012). Furthermore, IMC9 (B. R. Anderson-White et al., 2011) was directly targeted by TgAP2IX-5 based on both the 1 hour and 2 hours of auxin treatment and was not identified in the 6 hours auxin treatment study.

The depletion of TgAP2IX-5 at shorter timepoints at 2 hours of auxin treatment led to the downregulation of the TgAP2IX-4 transcript. However, ChIP-seq does not demonstrate the promoter of the TgAP2IX-4 gene to be bound by TgAP2IX-5. More interestingly, TgAP2IX-4 has been previously demonstrated to be a repressor of the bradyzoite expression program (Huang et al., 2017). This is consistent with the downregulation of TgAP2IV-4, another bradyzoite repressor (J. B. Radke et al., 2018) after 1 hour, 2 hours, and 6 hours of auxin treatment. This advocates that TgAP2IX-5 has an important role in controlling the tachyzoite to bradyzoite developmental switch. Since TgAP2IX-4 peaks during the S/M phase and it has been demonstrated that the developmental transition to the quiescent bradyzoite is executed during S and/or M phase (J. R. Radke et al., 2003), it is most likely that TgAP2IX-5 functions as a molecular checkpoint between cell cycle progression and bradyzoite differentiation. Four additional ApiAP2 TFs of which not much is known (TgAP2VI-1, TgAP2XI-1, TgAP2IX-3, and TgAP2VIIa-8) were downregulated following the depletion of TgAP2IX-5 for 2 hours. The indirect activation of these 4 ApiAP2 TFs could be the downstream effect of the direct activation of 2 other ApiAP2 TFs and which were identified based on the 1-hour auxin treatment study and the 2 hours auxin treatment study, TgAP2XII-9 and TgAP2III-2, respectively. The direct regulation of ApiAP2 TFs by TgAP2IX-5 illustrates the central role of this TF in the continuation of the cell cycle program.

ApiAP2 TFs are characterized by the presence of one or more AP2 DNA-binding domains (Balaji et al., 2005). We identified a novel uncharacterized domain, that we named "domain1". This domain is found to be conserved in several other *T. gondii* proteins (Figure 13A). Most strikingly, the AP2 domain was proven to be non-essential for the function of TgAP2IX-5 whereas domain1 was demonstrated to be essential for TgAP2IX-5 function. However, many questions remain unanswered as to the mechanisms behind the function of domain1. Based on ChIP-seq studies, TgAP2IX-5 was demonstrated to bind to the promoters of several

genes. Whether it is domain1 and/or the AP2 domain that binds to DNA remains unanswered and a topic of further investigation.

Given that domain1 was proven to be essential for the function of TgAP2IX-5 and the AP2 domain not, it is highly likely that it is domain1 that binds DNA. Thus, determination of the DNA motif to which domain1 binds to remains essential to studying domain1-DNA binding. Further analysis is needed to identify such a motif. Thus, a *Toxoplasma*-adapted form of the CUT&RUN method followed by a motif enrichment analysis (Skene & Henikoff, 2017; Waldman et al., 2020) can be carried out. Alternatively, an RSAT analysis can be carried out in order to determine the binding motif of TgAP2IX-5 as was done in the case of TgAP2XI-5 (Walker et al., 2013b). RSAT program analysis can be carried out by analyzing the sequences of promoters to which TgAP2IX-5 binds to according to ChIP-seq analysis. This can be done by utilizing positional bias since we hypothesize that the DNA binding motif would be positioned at the center of the ChIP peak sequences. Determining the DNA motif to which domain1 binds to will allow us to explore many aspects. We can attempt to crystallize domain1 in presence and absence of DNA (apo-form). X-ray crystallography can shed light on the structure of the domain1 protein fold and provide insight on the mechanism of action of domain 1 and can potentially identify the specific residues of the TgAP2IX-5 TF that are actively interacting with the DNA. When taking a closer look at the primary amino acid sequence of domain1, several of the conserved amino acid residues are basic residues (arginine, lysine, and histidine residues) and thus are likely to be directly interacting with DNA either specifically by contacting the DNA base pairs or non-specifically by contacting the DNA's sugar phosphate backbone following a similar mechanism to the ApiAP2 domain of PF14_0633 in *Plasmodium falciparum* where two arginine residues, one asparagine residue, and one serine residue were identified to be in direct contact with DNA base pairs as well as the phosphodiester backbone via histidine (Lindner et al., 2010). However, in order to validate this hypothesis, and in the case where X-ray crystallography might not be feasible as crystallization conditions are quite challenging to obtain in most cases, site-directed mutagenesis of these basic arginine and histidine residues (R1780, R1785, R1788, H1825) to alanine can be carried out. These mutations can be carried out in the exogenous copy of TgAP2IX-5 of the complemented mutant strain to investigate their potential biological relevance. In this case, it is potentially possible to study the effect of mutating these residues on the binding of DNA and thus pinpoint potential residues which are specifically interacting with the DNA motif. Additional experiments consisting of biochemical electrophoresis mobility shift assays (EMSA) in which the domain1 protein consisting of the mutated arginine and histidine residues can be carried out in order to test for the presence of protein-DNA binding. Moreover, biophysical

experiments involving nuclear magnetic resonance assays (NMR) might provide insight into the mechanisms of action of domain1 and thus remain crucial to validate the ability of the novel domain we identify to bind to DNA.

In an alternative experiment, given the presence of identical conserved sequences within domain1 across several proteins (Figure 11), studying the deletion of these conserved regions might pinpoint the essential regions of domain1. When analyzing the conserved sequences of domain1, it is likely that identical segments of residues have an active role in the potential binding of domain1 to DNA. Thus, the deletion of these regions of domain1 will possibly give us more insight into which regions of domain1 are essential for the function of TgAP2IX-5. This can be carried out by generating complementation constructs in which deletions of domain 1 are generated in the copy of the exogenous TgAP2IX-5 complemented parasite strain and studying the essentiality of these domain1 segments for the function of TgAP2IX-5 in a similar manner to what we describe for the initial domain1 characterization experiments.

In this study, the AP2 domain was demonstrated to be non-essential for the function of TgAP2IX-5 thus giving rise to the hypothesis that the AP2 domain is not binding DNA but rather can potentially interact with other AP2 domains of other AP2 TFs. Consistent with the crystallography study carried out on *Plasmodium falciparum* which suggests that two ApiAP2 domains can interact by means of dimerization (Lindner et al., 2010) and also based on previous ApiAP2 cooperation studies (Lesage et al., 2018). This can be the case for TgAP2IX-5, which can potentially interact with other AP2 TFs by means of ApiAP2 domain interaction. However, this remains to be elucidated by further experiments. Potential experiments include the identification of potential AP2 protein partners of TgAP2IX-5 by carrying out co-immunoprecipitation experiments and studying the essentiality of their respective AP2 domains to maintain such interactions.

From another angle, it may be possible that domain1 interacts with the AP2 domain upon DNA binding and triggers a change in the conformation of TgAP2IX-5. Nonetheless, it has been demonstrated in *P. falciparum* that homodimerization of PF14_0633 AP2 domain results in a conformational change driven by a domain-swapping mechanism facilitated by Proline kink-regions to drive dimerization (Lindner et al., 2010). The presence of Pro 1774 in domain1 can potentially contribute to the creation of a kink (hinge-like structure) in the fold of the TgAP2IX-5 protein thus contributing to its dimerization with the AP2 domain. In the case where both domains may potentially interact together, this may increase the binding affinity of the TgAP2IX-5 TF to the promoters of specific genes. However, this possibility is most unlikely given that the loss of the AP2 domain

does not render the TgAP2IX-5 protein unfunctional. Perhaps interaction between domain1 and the AP2 domain enhances binding of TgAP2IX-5 to the promoters of genes but is not essential. This could be further explored by carrying out ChIP-seq experiments on the complemented AP2IX-5 strains with the deleted AP2 domain and domain 1 in the presence of auxin and compare it to that of a control (absence of auxin). This follow-up experiment can identify any changes in the targeting of TgAP2IX-5 to the promoters of genes should they be existent due to the deletion of the AP2 domain.

Alternatively, supposing that the AP2 domain binds DNA, its loss may be compensated for by domain1 and thus it is rendered non-essential for the function of the TgAP2IX-5 TF.

Overall, the most likely hypothesis is that domain 1 binds DNA, which can result in a conformational change of the TgAP2IX-5 protein fold subsequently triggering the AP2 domain to interact with other AP2 domains illustrating plausible ApiAP2 TF cooperation. Thus, studying the protein folds of the different domains present in TgAP2IX-5 TF remains crucial to validate such a hypothesis. In this case, a preliminary study can be carried out by constructing a 3D virtual model based on previously solved crystal structures of ApiAP2 domains by using software such as the Schrodinger software that can give us hints in predicting the fold of this protein and any potential change in structure upon binding to DNA.

In summary, this set of complementary experiments confirms the central role of TgAP2IX-5 as a master regulator of the asexual cell cycle division by controlling the expression of genes crucial for daughter parasite formation. TgAP2IX-5 also promotes the progression of the asexual cell cycle by regulating several ApiAP2 TFs. It also controls bradyzoite-repressing TFs by inhibiting the bradyzoite developmental switch. Furthermore, elucidation of essential regions for the function of TgAP2IX-5 sheds light on possible mechanisms of action of this TF.

V-3- Functional Characterization of protein phosphatase 1 in *Toxoplasma gondii*, TgPP1

For the third part of this PhD study, an iKD mutant of TgPP1 was generated by tagging the N-terminal of the PP1 gene with a T2A-AID-Ty cassette. Before the generation of the iKD *TgPP1* mutant, several attempts to generate an iKD mutant in which the C-terminal of the *TgPP1* gene is tagged yielded unsuccessful results.

However, by the way of N-terminal tagging, we were able to produce the iKD TgPP1 mutant, and a number of experiments were carried out in order to characterize it. The absence of TgPP1 led to a defect in proliferation hence plaque formation was completely hindered when carrying out plaque assays. In addition, studying the Inner Membrane Complex of mutant parasites exhibited that iKD TgPP1 mutant parasites harbored an unstructured IMC. Confocal microscopy allowed us to visualize the collapse of the IMC. Furthermore, phospho-proteomics studies were carried out on the iKD TgPP1 parasite in the presence or absence of 2 hours of auxin treatment. This short duration of auxin treatment led to the hyperphosphorylation of several proteins among them RNA recognition motif proteins and RNB-containing motifs. Yet most strikingly, IMC1 was the most highly phosphorylated protein at Threonine residue 62. Additional phospho-proteomics experiments were carried out for a longer duration for 24 hours of auxin treatment which revealed the differential phosphorylation of several IMC proteins such as IMC17, IMC18, IMC20, and IMC24.

INTRODUCTION

The regulation of crucial functions in the apicomplexan parasite *Toxoplasma gondii* has been shown to involve post-translation modifications. Crucial molecular mechanisms underlying cell division, microneme secretion or exit from the host cell were shown to be regulated via phosphorylation/dephosphorylation of proteins (Yang & Arrizabalaga, 2017). A large repertoire of phosphorylated proteins has been discovered at the tachyzoite stage of this parasite (Treeck et al., 2011). Moreover, protein kinases and phosphatases have been identified in the parasite's genome.

Tachyzoite kinases have been shown to play important roles during the cell cycle division process. TgCDPK7 is an essential kinase for parasite survival which plays an important role in ensuring the proper positioning and duplication of the centrosome is maintained throughout the tachyzoite's cell division (Morlon-Guyot et al., 2014). TgCDPK7 is also responsible for phosphorylating TgRab11a which is essential for the parasite's intracellular division and trafficking of proteins (Bansal et al., 2021). Other protein kinases play important roles in *T. gondii* such as TgArk1 which is involved in regulating the assembly of daughter parasites (Suvorova et al., 2015), TgArk3 kinase which is characterized by its importance in endodyogeny and parasite virulence (Berry et al., 2016), and TgMAPK-L1 which controls proper centrosome replication (Suvorova et al., 2015). In addition, a total of 8 CDK-related kinases designated as TgCrks are cyclically expressed within the *T. gondii* tachyzoite. Five of the TgCrks have been demonstrated to play a major role in regulating cell division by regulating the various cell cycle checkpoints in order to ensure the proper progression of the cell cycle (Alvarez & Suvorova, 2017).

Only few protein phosphatases have been characterized to date in *T. gondii*. Thus far, protein phosphatases belonging to the Mg^{2+}/Mn^{2+} dependent phosphatase (PPM) family have been characterized including TgPPM13 which functions with casein kinase II (CKII) in controlling the binding of Toxofilin to actin thus contributing to the dynamics of actin in the parasite and its overall gliding motility (Delorme et al., 2003; Jan et al., 2007). Additionally, TgPPM5C is implicated in the parasite's lytic cycle (C. Yang et al., 2019) whereas TgPPM3C demonstrated a role in the parasite's virulence *in vivo* (Mayoral et al., 2020).

Among the serine/threonine protein phosphatases, PP1 belonging to the phosphoprotein phosphatase (PPP) family has been extensively studied in other eukaryotes. PP1 has been shown to play a central role in many essential biological processes involving cell division, cellular metabolism, transcription, translation, apoptosis, in addition to several others (Ceulemans & Bollen, 2004).

In *Plasmodium falciparum*, PfPP1 has been shown to be essential during the intraerythrocytic cycle and egress by regulating the activity of a HECT-family ubiquitin E3 ligase in addition to a phospholipid transporter which functions in the rupture of the host cell (Paul et al., 2020).

However, the function of the *T. gondii* PP1 homolog remains to be elucidated. PP1 activity was demonstrated in *T. gondii* by using phosphatase inhibitors (okadaic acid) and which significantly decreased the invasion of the *T. gondii* tachyzoites thus suggesting an important role for TgPP1 in the invasion of the host cell (Delorme et al., 2002). In addition, TgPP1 demonstrated to form a complex with the TgLRR1 protein which negatively regulates TgPP1 activity (Daher et al., 2007). Furthermore, *T. gondii* Inhibitor-2, TgI2 has an inhibitory effect on TgPP1 activity similar as its homolog in *P. falciparum* (Deveuve et al., 2017). However, despite these previous findings regarding PP1 in *T. gondii*, much remains to be explored as many questions remain unanswered regarding the essentiality of TgPP1, the specific proteins targeted by TgPP1, and its main mechanism of action. In this study, we produce an inducible knock-down mutant of TgPP1. We demonstrate that the conditional depletion of TgPP1 results in growth and proliferation defects. Upon the conditional depletion of TgPP1, parasites exhibit a collapsed IMC structure which was further confirmed by electron microscopy. In addition, phospho-proteomics assays of the iKD TgPP1 mutant demonstrate the hyperphosphorylation of several IMC proteins such as IMC1, IMC4, IMC17, IMC18, IMC20, IMC24, and ISP2. Overall, we attempted to functionally characterize TgPP1 and demonstrated its potential effect on the phosphorylation status of several proteins essential for maintaining the tachyzoite's IMC integrity.

3.1 TgPP1 has an important role in parasite proliferation

With the aim of identifying the biological role of TgPP1, an inducible knock-down mutant (iKD TgPP1) was generated using the AID system. For the sake of this study, a transgenic *T. gondii* parasite strain was produced which consists of an HXGPRT-T2A-AID-2Ty insert at the 5' end of the TgPP1 gene using a CRISPR/Cas9 strategy (Figure 1A). The 5'end of the TgPP1 gene of interest was tagged rather than the 3'end after multiple unsuccessful attempts to insert an HXGPRT-AID-HA cassette at the 3'end of the gene of interest.

Verification by Western blot identified a single band which was detected at the expected protein size (~35kDa). The TgPP1 protein was rapidly depleted within just one hour of auxin treatment as was verified by Western blot (Supplementary Figure 1B).
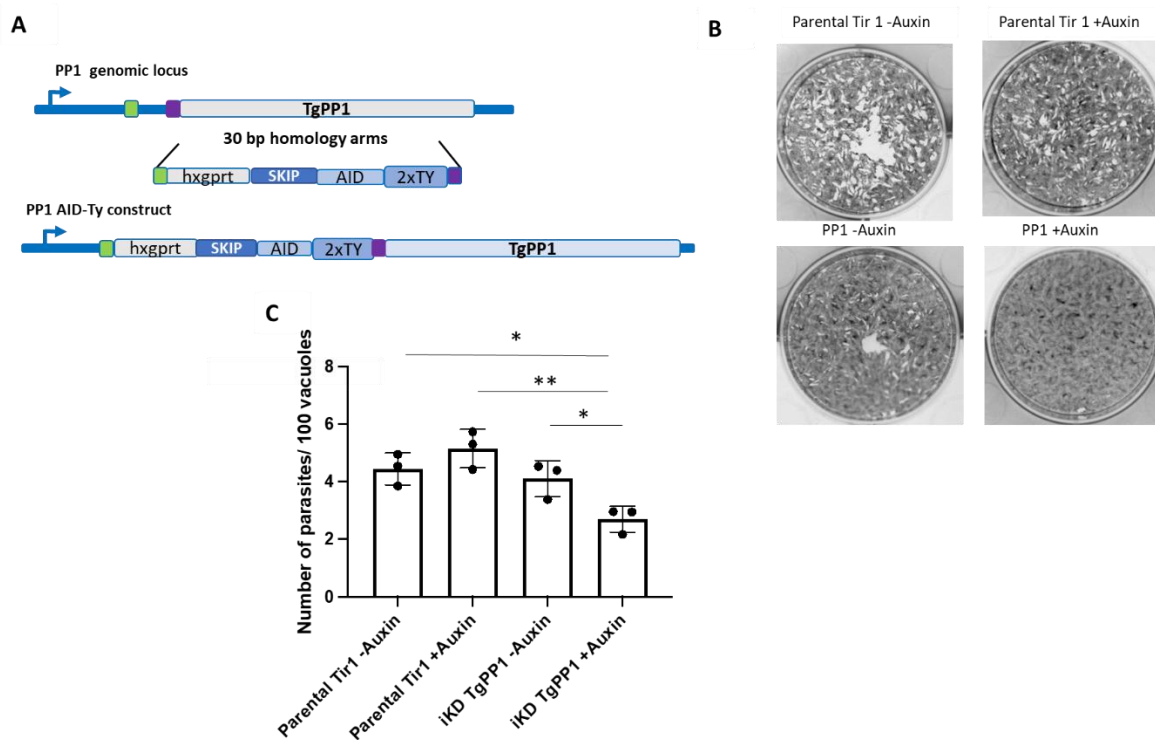
Figure 1: TgPP1 conditional depletion affects the growth and proliferation of the parasite

(A) Schematic representation of iKD TgPP1 construct used to carry out the study which utilizes the AID system in order to deplete TgPP1. **(B)** Plaque assay of the iKD TgPP1 mutant and control parasites in the presence and absence of auxin. **(C)** Bar graph representing a growth assay of the iKD TgPP1 strain after 48h growth. A Student's t-test was performed, *p <0.05, **p<0.01; mean ± s.d. (n=3).
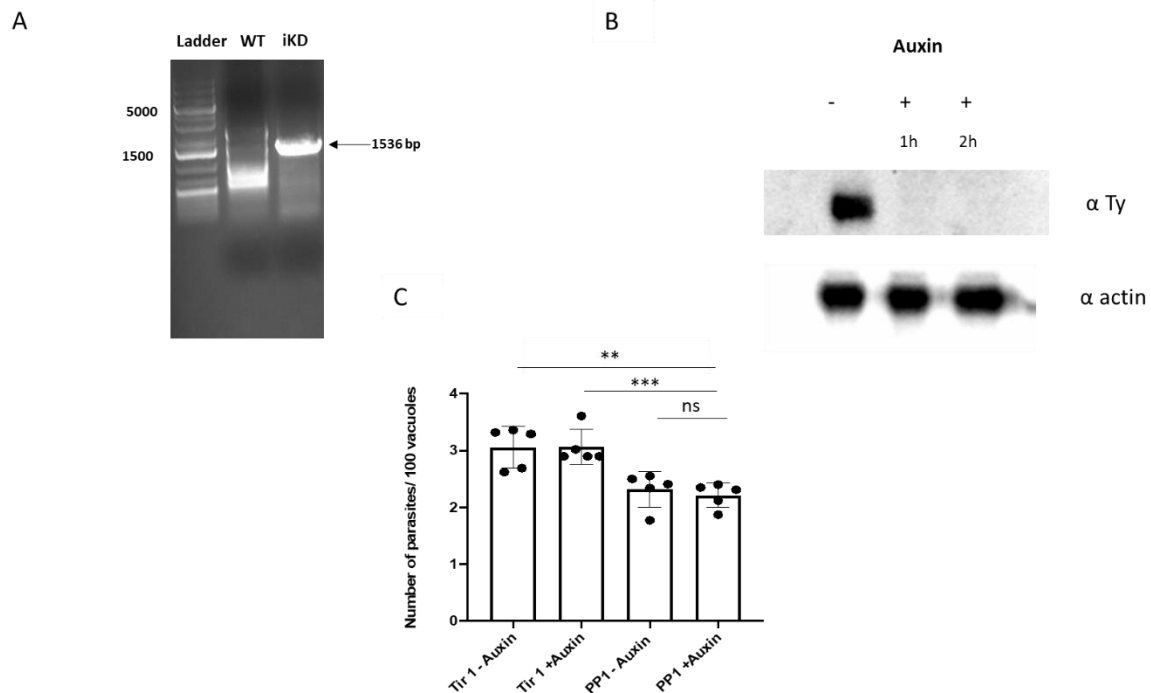
Supplementary Figure 1: iKD TgPP1 mutant validation. (A) PCR confirming the integration of the HXGPRT-2TA-AID-2Ty insert at the correct locus of the iKD TgPP1 mutant's genome. **(B)** Western blot demonstrating the depletion of TgPP1 when adding auxin for different durations of time. **(C)** Growth assay of iKD TgPP1 in the presence and absence of auxin for 24 hours. A Student's t-test was performed, ns >0.05, **$p<0.01$, ***$p<0.001$; mean ± s.d. (n=3).

To characterize the phenotype, a plaque assay was carried out in order to measure the iKD TgPP1 mutant parasites' ability to grow and invade over a time period of 7 days (Figure 1B). The plaque assay demonstrated an absence of plaques in the presence of auxin for the iKD TgPP1 strain. On the contrary, the iKD TgPP1 strain in the absence of auxin exhibited plaques yet these were smaller compared to the parental Tir1 control in the presence and absence of auxin. These results demonstrate that the iKD TgPP1 strain has an initial proliferation defect in the absence of auxin. We then carried out a standard growth assay by leaving the parasite to grow for 24 hours in the presence and absence of auxin only to discover that there was indeed a significantly lower number of parasites per vacuoles when comparing the Parental Tir1 strain to the iKD TgPP1 strain. Strikingly, when comparing the iKD TgPP1 strain in the presence and absence of auxin, the modification of the *TgPP1* locus yielded lower number of parasites per vacuoles counts when compared to the parental strain (Supplementary Figure 1C). In a following experiment, another growth assay was carried out in which the parasite was left to grow for 48 hours. In this case, the iKD TgPP1 mutant parasite

demonstrated a significant growth defect in the presence of auxin (Figure 1C). These results therefore suggest that TgPP1 expression is essential for the proliferation and growth of the parasite.

3.2 Depletion of TgPP1 results in a collapsed Inner Membrane Complex (IMC)

To better assess the phenotype of the iKD TgPP1 mutant, immunofluorescence assays were carried out to label the IMC, a double membrane structure situated right below the plasma membrane of the parasite, was labelled with different markers. Labelling of the IMC with anti-TgIMC1 antibodies allowed us to visualize the effect of TgPP1 depletion on the IMC. After 24 hours of auxin treatment, we were able to clearly observe a collapsed IMC structures in the iKD TgPP1 parasites (Figure 2A, lower panel) compared to the intact IMC structures in the control parasites (Figure 2A, upper and middle panels). The collapsed IMC is apparent as a mesh of intertwined IMC proteins with no clearly formed tachyzoites within the vacuole (Figure 2A).

We observed that ~30% of the parasite population exhibited an unstructured IMC in the case of 24 hours of auxin treatment (Figure 2B), while ~40% of the parasite population harbored an unstructured IMC in the case of 48 hours of auxin treatment (Figure 2C).

Figure 2: (A) Confocal microscopy imaging of the Parental Tir1 and iKD TgPP1 mutant parasites in the presence and absence of auxin labelled with TgEno2 (red) and TgIMC1 (green). DAPI was used to stain the nucleus. The scale bar is indicated in the lower right side of each image. **(B)** Bar graph representing the

percentage of Parental Tir 1 and iKD TgPP1 vacuoles with an unstructured inner membrane complex using anti-TgIMC1 as a marker for IFA assays in the presence or absence of auxin for 24 hours. A Student's t-test was performed, ****p<0.0001; mean ± s.d. (n=3). **(C)** Bar graph representing 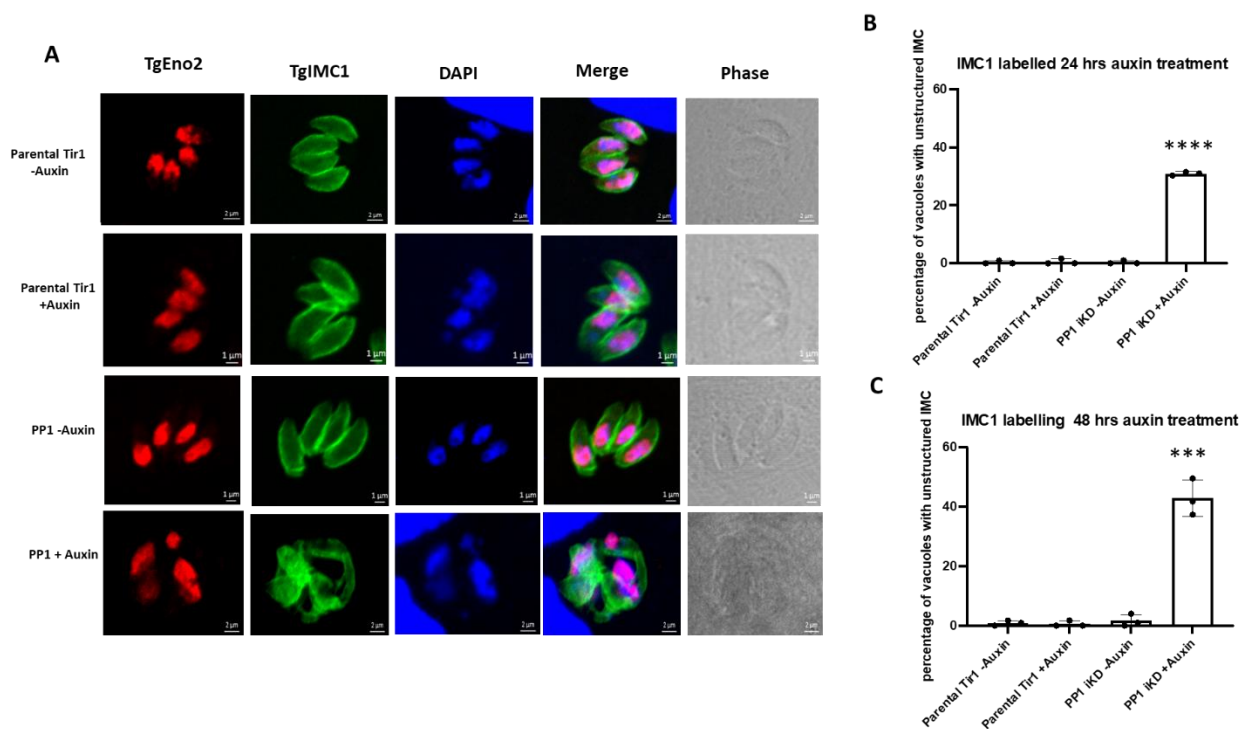the percentage of Parental Tir1 and iKD TgPP1 vacuoles with an unstructured IMC in the presence or absence of auxin for 48 hours. A Student's t-test was performed, ***p<0.001; mean ± s.d. (n=3).

In an attempt to further characterize the unstructured IMC apparent in the iKD TgPP1 strain in the presence of auxin, another component of the IMC was labelled, the IMC Sub-compartment protein 1 (TgISP1). Upon auxin treatment for 24 hours and 48 hours, ISP1 which usually localizes at the very tip of the parasite's apex forming a cap-like structure was instead distributed along the periphery of the iKD TgPP1 mutant parasite (Figure 3A). At 24 hours of auxin treatment ~ 10% of the mutant parasite population exhibited an ISP1 mis-localization phenotype (Figure 3B) whereas ~ 20% of the iKD TgPP1 mutant parasite population exhibited ISP1 mis-localization after 48 hours of auxin treatment (Figure 3C).
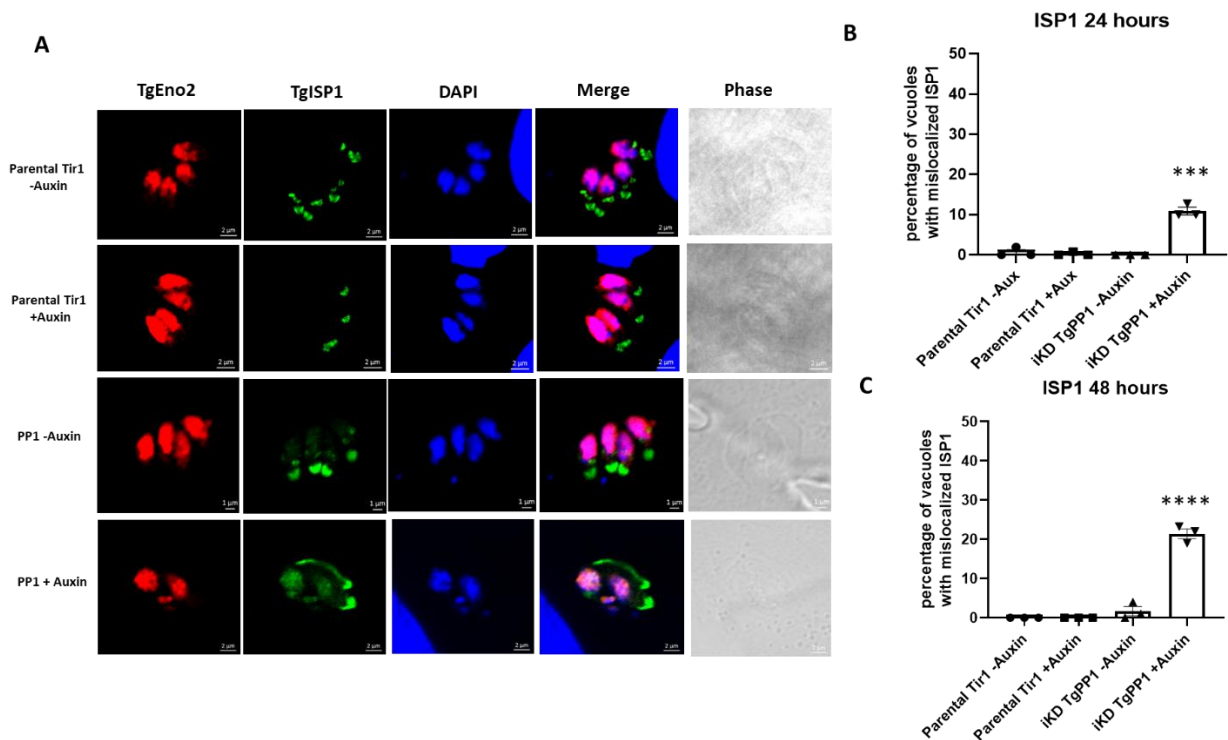
Figure 3: (A) Confocal microscopy imaging of the Parental Tir1 and iKD TgPP1 mutant parasites in the presence and absence of auxin labelled with TgEno2 (red) and TgISP1 (green). DAPI was used to stain the nucleus. The scale bar is indicated in the lower right side of each image. **(B)** Bar graph representing the percentage of Parental Tir 1 and iKD TgPP1 parasite vacuoles with mis-localized TgISP1 using anti-TgISP1 as a marker for IFA assays in the presence or absence of auxin

for 24 hours. A Student's t-test was performed, ***p<0.001; mean ± s.d. (n=3). **(C)** Bar graph representing the percentage of Parental Tir 1 and iKD TgPP1 parasite vacuoles with mis-localized ISP1 by using anti-TgISP1 as a marker for IFA assays in the presence or absence of auxin for 48 hours. A Student's t-test was performed, ****p<0.0001; mean ± s.d. (n=3).

In addition to TgIMC1 and TgISP1, a third marker of the IMC was used for labelling. The acylated gliding associated protein, TgGAP45, is a component of the gildeosome which is targeted to the plasma membrane and is associated with the IMC at its C-terminal region. By using confocal microscopy, we were able to visualize the effect of TgPP1 depletion on TgGAP45 (Figure 4A). In the presence of auxin, TgGAP45 is not properly localized in ~30% of the mutant parasite vacuoles at 24 hours of auxin treatment (Figure 4B) whereas this number is approximately ~40% at 48 hours of auxin treatment (Figure 4C). Altogether, these results confirm that TgPP1 contributes to the structural integrity of the parasite's inner membrane complex.
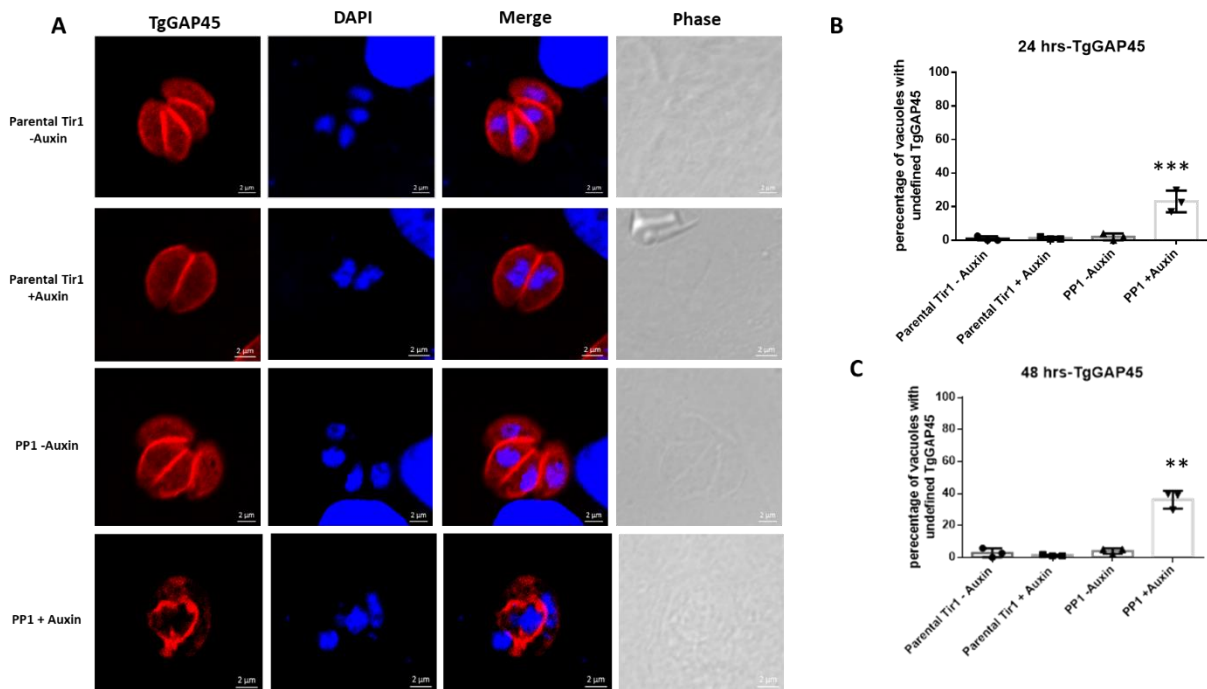
Figure 4: (A) Confocal microscopy imaging of the Parental Tir1 and iKD TgPP1 mutant parasites in the presence and absence of auxin labelled with TgGAP45 (red) DAPI was used to stain the nucleus. The scale bar is indicated in the lower right side of each image. **(B)** Bar graph representing the percentage of parasite vacuoles possessing an undefined TgGAP45 protein after 24 hours of auxin treatment. A Student's t-test was performed, ***p<0.001; mean ± s.d. (n=3). **(C)** Bar graph representing the percentage of parasite vacuoles possessing an

undefined TgGAP45 protein after 48 hours of auxin treatment. A Student's t-test was performed, **p<0.01; mean ± s.d. (n=3).

3.3 TgPP1 depletion results in unsegregated nuclei

A defect in the segregation of nuclear material was observed in the iKD TgPP1 mutant in the presence of auxin. To better assess this phenotype, immunofluorescence assays in which the nucleus was labelled with TgEno2 were carried out (Figure 5A). After 24 hours of auxin treatment, we were clearly able to identify a significant percentage of vacuoles consisting of unsegregated nuclear material. This phenotype of unsegregated nuclear material was also visible at 48 hours of auxin treatment (Figures 5B-C). In addition, the defect of TgPP1 on nuclear segregation is also apparent in the vacuoles presenting IMC defects (Figures 2A,3A,4A).
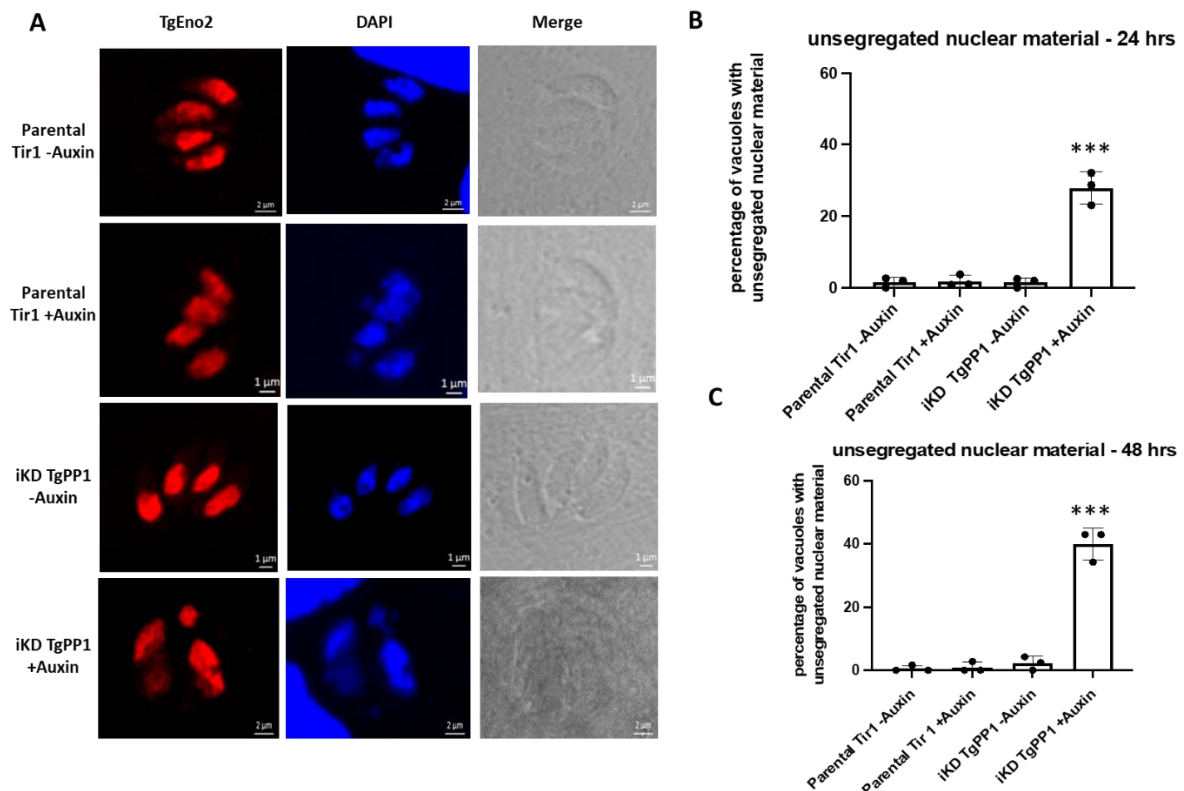
Figure 5: (A) Confocal microscopy imaging of the Parental Tir1 and iKD TgPP1 mutant parasites in the presence and absence of auxin labelled with TgEno2 (red) DAPI was used to stain the nucleus. The scale bar is indicated in the lower right side of each image. (B) Bar graph representing the percentage of parasite vacuoles with unsegregated nucleus after 24 hours of auxin treatment. A Student's t-test was performed, ***p<0.001; mean ± s.d. (n=3). (C) Bar graph representing the

percentage of parasite vacuoles possessing unsegregated nuclei after 48 hours of auxin treatment. A Student's t-test was performed, ***$p<0.001$; mean ± s.d. (n=3).

3.4 TgPP1 depletion disrupts the Inner Membrane Complex (IMC) of the *T. gondii* tachyzoite

By carrying out immunofluorescence assays, we were able to observe the complete collapse of the inner membrane complex in the iKD TgPP1 mutant parasite in the presence of auxin. Therefore, electron microscopy experiments were carried out in order to examine the morphology of the iKD TgPP1 mutant parasites' IMC and plasma membrane in the presence and absence of auxin treatment. Electron microscopy scans demonstrated that the iKD TgPP1 tachyzoites showed an intact plasma membrane and IMC in the absence of auxin (Figure 6A). When treating the iKD TgPP1 parasite with auxin the IMC is no longer present, yet the plasma membrane remains intact (Figure 6B). This is apparent as the IMC is missing and only a single membrane is present (Figure 6B).
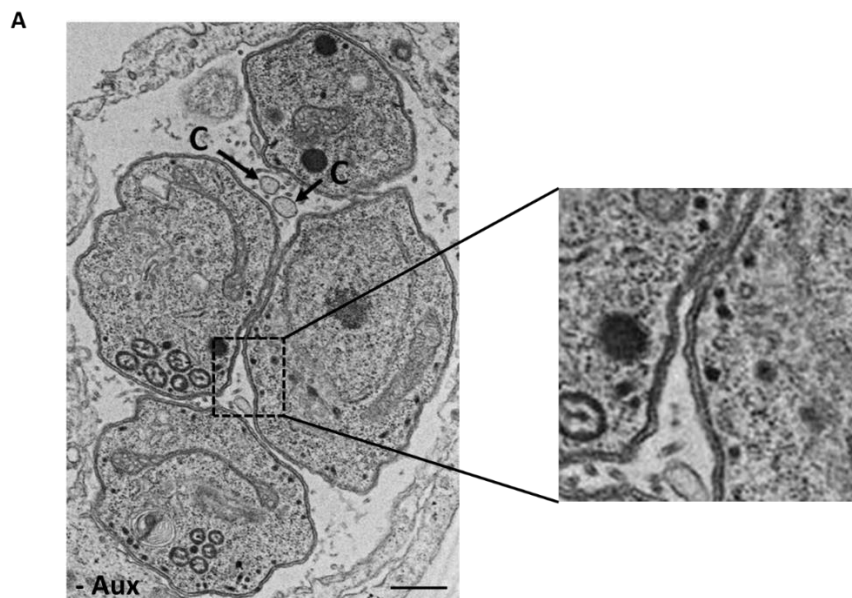
B
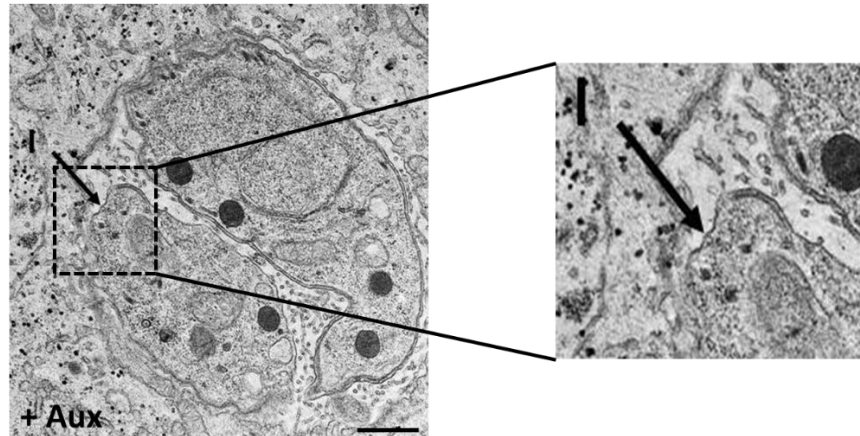
Figure 6: Electron microscopy experiments demonstrate that conditional TgPP1 depletion results in an intact plasma membrane **(A)** Electron microscopy scan demonstrating the structural morphology of the plasma membrane and the inner membrane complex of iKD TgPP1 tachyzoite parasites after 24 hours in the absence of auxin treatment. Both plasma membrane and IMC are intact. **(B)** Electron microscopy scan demonstrating the structural morphology of the plasma membrane and the inner membrane complex of iKD TgPP1 tachyzoite parasites after 48 hours of auxin treatment. I represents missing IMC, C represents cytoplasmic inclusions. Scale bar (5 μm) is indicated at the lower right side in the TEM images. Regions indicated by arrows are zoomed in.

3.5 Absence of TgPP1 has an impact on centrosome, Golgi, and plastid

The *T. gondii* cell cycle exhibits a coordinated timeline in which the parasite's subcellular structures are divided following a chronological order (Nishi et al., 2008). We investigated whether subcellular structures of the iKD TgPP1 mutant were affected in the presence of auxin. To carry out this investigation, the impact of the conditional depletion of TgPP1 on the centrosome, Golgi, and plastid was studied by measuring the ratios of these organelles of interest to the nucleus.

First, the effect of TgPP1 depletion on the division of the outer core of the centrosome was examined. The ratio of the outer centrosome to the nucleus was measured. In both conditions consisting of 24 hours of auxin treatment and 48 hours of auxin treatment, the ratios of the outer core centrosome were recorded after labelling the iKD TgPP1 mutant and Parental Tir1 strain using the anti-TgCentrin1 antibody (Figure 7A). The ratios recorded were around 1 in the presence and absence of auxin at 24 hours and 48 hours of auxin treatment (Figures 7B-C) indicating that TgPP1 does not have an impact on outer core centrosomes division. However, centrosome shape seems to be impacted in the iKD TgPP1 mutant in presence of auxin since the intensity levels of the TgCentrin1 is much dimmer compared to that of the controls (Figure 7A).
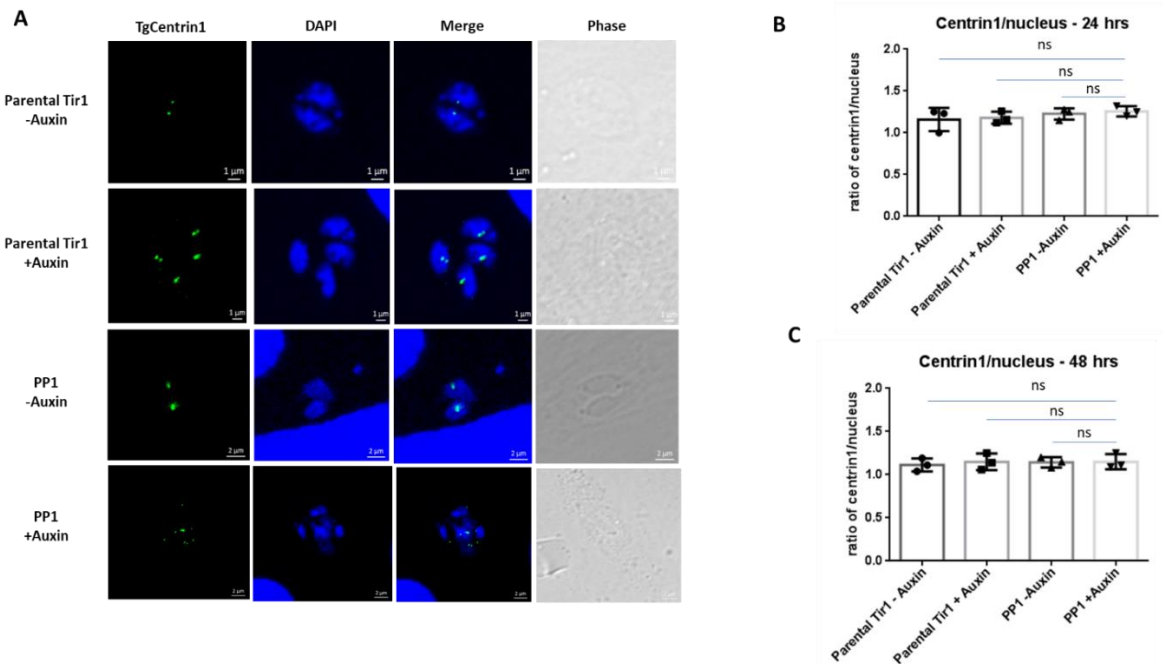
Figure 7: TgPP1 does not have an impact on the division of the outer centrosome core. (A) Confocal microscopy images of the Parental Tir1 (control) and the iKD TgPP1 strain labelled with TgCentrin1 (green) in the presence and absence of Auxin for 48 hours. DAPI was used to stain the nucleus. **(B)** Bar graph representing TgCentrin1: nucleus ratio using the parental and iKD TgPP1 in the absence and presence of auxin treatment for 24 hours. A Student's t-test was performed, ns $p > 0.05$; mean ± s.d. (n=3). **(C)** Bar graph representing the recorded TgCentrin1: nucleus ratios using the parental Tir1 and iKD TgPP1 strain in the absence and presence of auxin for 48 hours. A Student's t-test was performed, ns $p > 0.05$; mean ± s.d. (n=3).

Since there was a qualitative effect of TgPP1 on the division of the centrosome's outer core, we decided to investigate the effect of TgPP1 on the division of the proceeding organelles to divide in the cell cycle. In order to determine the effect of TgPP1 depletion on the division of the Golgi and plastid, the ratios of the Golgi to nucleus and plastid to nucleus were recorded in the parental Tir1 and iKD TgPP1 strain in the presence and absence of auxin. At 24 hours of auxin treatment, there was a significant percentage of parasites (~20%) with abnormal ratios corresponding to Golgi and plastid division (Figure 8B). At 48 hours of auxin treatment, the percentage of parasites with abnormal Golgi and plastid ratios increased to ~27% of the total parasite population (Figure 8C). These results collectively suggest that the depletion of TgPP1 has an impact on the division and segregation of these subcellular structures.
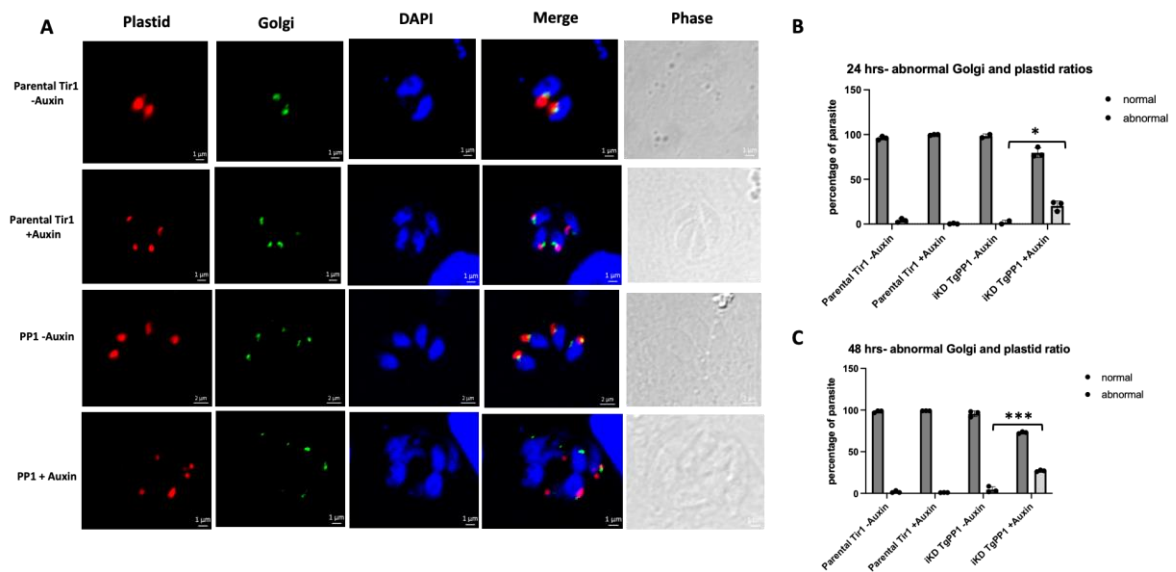
Figure 8: Golgi and plastid are impacted in the absence of TgPP1. (A) Confocal microscopy images of the parental and iKD TgPP1 strain with labelled plastid (red) and Golgi (green) in the presence and absence of 48 hours of auxin treatment. DAPI was used to stain the nucleus. **(B)** Bar graph representing the percentage of parasite with abnormal Golgi and plastid counts using the parental Tir1 and iKD TgPP1 strain in the absence and presence of auxin for 24 hours. A Student's t-test was performed. *p<0.05; mean ± s.d. (n=3). **(C)** Bar graph representing the percentage of parasite with abnormal and normal Golgi and plastid counts using the parental Tir1 and iKD TgPP1 strain in the absence and presence of auxin for 48 hours. ***p<0.001; mean ± s.d. (n=3).

3.6 TgPP1 is responsible for dephosphorylation of the Inner Membrane Complex protein, TgIMC1

The phosphoproteome of the iKD TgPP1 mutant parasites in the presence and absence of auxin for 2 hours was explored.

Overall, there was a total of 7822 different phosphorylation sites identified (Figure 9A, C and supplementary Table 1). However, we were able to identify significant changes for 104 phosphopeptides corresponding to 85 proteins (Figure 9C and supplementary Table 1). Among the 104 phospho-peptides that possessed significant levels of phosphorylation, 40 peptides corresponding to 32 proteins were hyper-phosphorylated whereas 64 peptides corresponding to 58 proteins were hypo-phosphorylated. Significantly phosphorylated peptides were identified by comparing iKD TgPP1 mutant parasites in the absence and presence of auxin for 2 hours. Analysis was carried out for four biological replicates and phosphopeptides with an FDR<0.01 were identified as significantly phosphorylated. We noticed that the protein exhibiting the most hyper-

phosphorylated ratio was IMC1. In addition, the apical cap protein 2 (AC2) was also significantly hyper-phosphorylated. Six IMC proteins, IMC17, ISC1, PMCAA1, and two uncharacterized proteins were hypo-phosphorylated. Furthermore, treatment with auxin for 2 hours resulted in the hypo-phosphorylation of calcium-dependent kinases such as CDPK2A and CDPK6. However, most of the proteins identified to be hyper-phosphorylated or hypo-phosphorylated were of unknown function.

To better assess the effect of TgPP1 depletion, we explored the phospho-proteome of the iKD TgPP1 mutant after 24 hours of auxin treatment when most of the phenotypes are apparent in the population (phospho-proteomics analysis was carried out for three biological triplicates in the case of 24 hours of auxin treatment)

In this case, a total of 7509 different phospho-sites were identified, among them 376 phospho-sites corresponding to 284 proteins exhibited significant changes in phosphorylation levels (Figures 9B, D and Supplementary Table 2). More particularly, 152 peptides were found to be hyper-phosphorylated corresponding to 114 proteins whereas 224 peptides were discovered to be hypo-phosphorylated corresponding to 178 proteins. Inner Membrane Complex proteins, IMC4, IMC18, and IMC20 were found to be hyper-phosphorylated while ISP2, IMC5 and IMC24 were found to be hypo-phosphorylated. Interestingly, IMC17 was found to be hyperphosphorylated at certain sites and hypo-phosphorylated at others. Two apical cap proteins were demonstrated to be hypo-phosphorylated (AC4 and AC10) whereas one apical cap protein (AC2) was identified as hyper-phosphorylated. Furthermore, microtubule associated protein SPM2 was found to be hyperphosphorylated. Four ApiAP2 TFs associated with transcriptional control were hyperphosphorylated (AP2XI-2, AP2XII-5, AP2XII-8, and AP2VIIa-4) whereas 4 other proteins responsible for gene regulation were hypo-phosphorylated and included 3 ApiAP2 TFs (AP2IX-7, AP2XII-1, AP2VIIa-3) and a single Myb-family DNA-binding protein.

Additionally, two CDPKs were also found to be significantly hypo-phosphorylated and this included CDPK7, an essential protein for parasite survival (Morlon-Guyot et al., 2014) and CDPK2A. In addition, we identified the hypo-phosphorylation of GPAT, a suggested target of CDPK7 (Bansal et al., 2021).

When overlapping the proteins that were either significantly hyper-phosphorylated or hypo-phosphorylated after 2 hours and 24 hours of auxin treatment, we observe only 9 hypo-phosphorylated overlapped proteins whereas only 2 hyperphosphorylated proteins were overlapped (Figure 9E-F). The overlapped hypo-phosphorylated proteins included IMC protein, IMC17 (TGGT1_286580) and a major facilitator family transporter protein (TGGT1_253700). The other hypo-phosphorylated overlapped proteins are not yet characterized whereas the two overlapped hyper-phosphorylated proteins

consisted of apical cap protein 2 (AC2) and a trehalose phosphatase which has an implication in the isoprenoid metabolic pathway (Imlay & Odom, 2014).
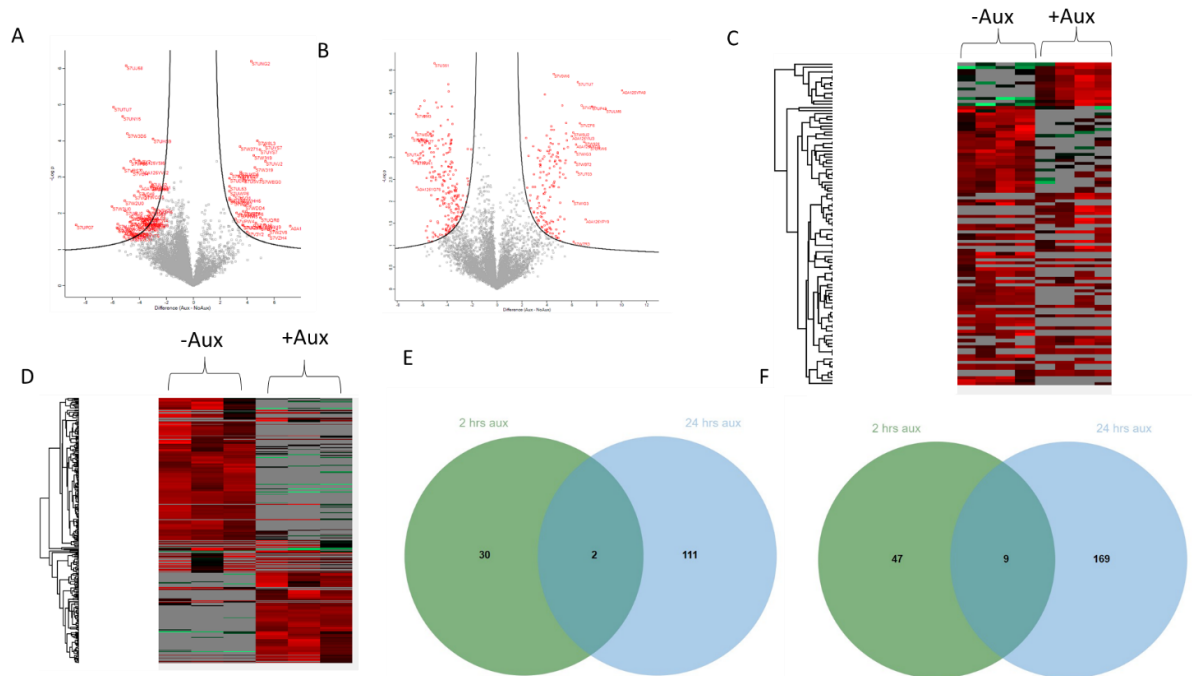
Figure 9: Phosphoproteome of iKD TgPP1 mutant parasites after 2 hours and 24 hours of auxin treatment. (A) Volcano plot of the total phosphosites detected from the phosphoproteomics analysis in the iKD TgPP1 mutant parasites in the presence of 2 hours of auxin treatment (n=7822) **(B)** Volcano plot of the total phosphosites detected from the phosphoproteomics analysis in the iKD TgPP1 strain after 24 hours of auxin treatment (n= 7509) **(C)** Heat map demonstrating the hierarchical clustering of phosphosites with significant differentiation between iKD TgPP1 mutant parasites not treated with auxin and those treated with auxin for 2 hours. **(D)** Heat map demonstrating the hierarchical clustering of phosphosites with a significant difference between the iKD TgPP1 mutant parasites not treated with auxin and those treated with auxin for 24 hours. **(E)** Venn Diagram representing the overlap of hyper-phosphorylated proteins 2 hours after auxin treatment and 24 hours after auxin treatment **(F)** Venn Diagram representing the overlap of hypo-phosphorylated proteins 2 hours after auxin treatment and 24 hours after auxin treatment.

Gene ID	Protein description	Phosphorylation score	Amino acid
TGGT1_286580	IMC17	-8.67752	Threonine 615
TGGT1_312100	PMCAA1	-5.90201	Threonine 491
TGGT1_235340	ISC1	-5.02973	Serine 98
TGGT1_217510	Uncharacterized IMC protein	-4.6033	Serine 2
TGGT1_306190	Uncharacterized IMC protein	-4.36629	Threonine 101
TGGT1_231640	IMC1	7.1984	Threonine 62

Supplementary Table 1: IMC proteins significantly hyper- (positive phosphorylation score) and/or hypo-phosphorylated (negative phosphorylation score) after 2 hours of auxin treatment.

Gene ID	Protein description	Phosphorylation score	Amino acid
TGGT1_237820	ISP2	-5.47349	Serine 30
TGGT1_311480	Uncharacterized IMC protein	-4.90895	Serine 231
TGGT1_306190	Uncharacterized IMC protein	-4.73855	Serine 297
TGGT1_311480	Uncharacterized IMC protein	-4.69999	Serine 228
TGGT1_286580	IMC17	-4.33155	Threonine 872
TGGT1_258470	IMC24	-4.1009	Serine 28
TGGT1_231630	IMC4	3.28531	Serine 32
TGGT1_271930	IMC20	4.05312	Threonine 127
TGGT1_295360	IMC18	4.76741	Threonine 209
TGGT1_222400	Uncharacterized IMC protein	4.9533	Serine 498
TGGT1_312100	PMCAA1	6.47824	Serine 533
TGGT1_286580	IMC17	5.45417	Serine 666
TGGT1_286580	IMC17	5.54993	Threonine 669
TGGT1_286580	IMC17	5.70877	Serine 660
TGGT1_231630	IMC4	7.11649	Serine 398

Supplementary Table 2: IMC proteins significantly hyper- (positive phosphorylation score) and/or hypo-phosphorylated (negative phosphorylation score) after 24 hours of auxin treatment.

3.7 Discussion and future perspectives

1 Phenotypic characterization of iKD TgPP1

TgPP1 depletion was demonstrated to hinder the normal growth of the parasite. However, a standard growth assay at 24 hours of growth did not yield any significant difference in growth. In contrast, 48 hours auxin treatment was sufficient to induce a significant growth defect. This suggests that the iKD TgPP1 parasite replication is significantly impacted (Figure 1C, supplementary Figure 1C). Analysis of the parasites at 24 hours post-auxin treatment, showed that the replication of the parasite is impacted. However, the TgPP1 iKD without auxin also showed slower growth (Supplementary Figure 1C). It is most likely that the longer duration of auxin treatment (48 hours) is required for the TgPP1 depletion

to have a subsequent impact on the replication of the parasite. The growth defect we observe is most likely a consequence of accumulation of tachyzoites with collapsed IMC structures and unsegregated nuclear material. This was further confirmed by the plaque assays, showing that after 7 days, no lysis plaques are apparent in presence of auxin.

The *T. gondii* tachyzoite's asexual cell cycle is characterized by independent nuclear and budding cycles (Suvorova et al., 2015). In this study, the impact of TgPP1 depletion on the two independent cycles (nuclear and budding cycle) is clearly apparent. Upon depletion of TgPP1, the budding of the daughter parasites is affected qualitatively based solely on visual inspection. However, no quantification was carried out to measure the effect of TgPP1 depletion on the parasite's ability to form daughter cells (budding capability) as this proves to be quite challenging given the collapsed IMC phenotype that occurs in the presence of auxin rendering the tachyzoite peripheries with unclear IMC boundaries at the peripheries of the daughter parasites.

2 The link between differentially phosphorylated proteins and collapsed IMC upon TgPP1 depletion

The most noticeable phenotype following TgPP1 depletion was the collapse of the IMC structure, which is situated right below the plasma membrane. This IMC defect was first detected by labelling the IMC in immunofluorescence assays and was later confirmed by electron microscopy where tachyzoites of the iKD TgPP1 mutant parasite exhibited absent IMC. Based on the EM scans of the iKD TgPP1 parasite, in the presence of auxin, the plasma membrane of the parasite remains intact. This is most likely due to the significant differential phosphorylation of several IMC proteins such as IMC1, IMC4, IMC5, IMC17, IMC18, IMC20, IMC24, ISP2, ISC1. Upon depletion of TgPP1, hypo-phosphorylation or hyper-phosphorylation of these IMC proteins most likely leads to an accumulation of disrupted IMC proteins which contributes to the overall collapsed IMC structure that is observed via EM microscopy (Figures 6A-B). Interestingly, it is at longer durations of auxin treatment (24 hours) where a larger number of IMC proteins' phosphorylation is targeted.

The depletion of TgPP1 affected other IMC components such as ISP1, which normally localizes to the apical cap of the parasite and is associated with the IMC (Beck et al., 2010). In the presence of auxin, ISP1 localizes to the periphery of the tachyzoite rather than at the apical cap (Figure 3A) giving rise to a mis-localization of this protein. However, no known phosphorylation sites have been reported thus far for TgISP1 (Treeck et al., 2011). TgISP proteins have the

capability of multimerizing into a Pleckstrin homology (PH) fold which is rich in high affinity binding sites for inositol phosphates which are membrane associated (Tonkin et al., 2014). This correlated with the presence of phosphatidyl-inositol 3 and 4- kinase (TGGT1_215700) as a significantly hyper-phosphorylated protein (~5-fold) in the iKD TgPP1 mutant when treated with auxin. However, whether phosphatidyl-inositol 3-4 kinase has a role in TgISPs anchoring remains to be explored. Crystallography structure studies carried out on TgISP1 and TgISP3 suggested that the multimerization and phosphorylation of serine residues of ISP proteins are responsible for the regulation of the biological function of ISP proteins (Tonkin et al., 2014). Moreover, the phosphorylation of three serine residues on TgISP2 has been identified in *T. gondii* (Treeck et al., 2011). This coincides with the hypo-phosphorylation of serine residues of TgISP2 upon TgPP1 depletion. It would be of interest to study the localization of TgISP2 in the iKD TgPP1 mutant in order to verify whether the localization is affected as was the case with TgISP1. In order to explore this, a knock-in mutant in the iKD TgPP1 strain consisting of ectopically tagged *ISP2* gene can be produced and used to verify the localization of the ISP2 protein in the presence of auxin.

TgGAP45 is major component of the glideosome which is responsible for facilitating gliding motility in *T. gondii* and possesses a crucial function in the invasion of host cells and egress (Frenal et al., 2014). The glideosome complex proteins are highly modified by phosphorylation (Gilk et al., 2009). GAP45 is anchored to the IMC from its C-terminal region and embedded within the plasma membrane from its N-terminal part. TgPP1 depletion impacted the IMC formation and therefore may also impact GAP45 localization. It is most likely that the invasion of iKD TgPP1 mutant parasites is impacted due to the partial absence of IMC. This may be linked to a previous study where the PP1 phosphatase activity was inhibited by okadaic acid (OA). In this study, the invasiveness of tachyzoite parasites was significantly impaired by around 50% (Delorme et al., 2002).

As observed by EM, IMC disruption leads to a defect in the structural morphology of the mutant parasite in the presence of auxin. The normal arc-shape of the tachyzoite is no longer apparent and oddly shaped-tachyzoites are present instead. Additionally, odd curvatures and abnormal invaginations were present on the outer surface of the plasma membrane of the iKD TgPP1 mutant parasite in the presence of auxin (Figure 6B) which might possibly be due to the loss of the IMC. The parasite tachyzoite form is maintained by means of several IMC proteins which provide the pellicle with tensile strength. These proteins consist of an IMC-associated network of alveolins and include IMC1, IMC4, and IMC5 (Anderson-White et al., 2011; Mann, 2001). In addition, IMC7, IMC12, and IMC14 were demonstrated to be associated with the tachyzoite cytoskeleton and function in maintaining the structural integrity of the extracellular tachyzoite (Dubey et al.,

2017). In our study, hypo-phosphorylation of IMC4 and IMC5 was identified. Differential phosphorylation of these proteins may contribute to the morphological defects of the IMC after depletion of TgPP1.

Furthermore, IMC suture component proteins (ISCs) were demonstrated to have a role in maintaining the structural morphology of the tachyzoite (Chen et al., 2017). Other differentially phosphorylated proteins included IMC suture protein, ISC1 which was demonstrated to be hypo-phosphorylated upon TgPP1 depletion. ISC proteins play an important role in suturing the IMC plates together (Chen et al., 2015). The hypo-phosphorylation of ISC1 could potentially contribute to a collapsed IMC structure. In addition, the phosphorylation status of ISC1 upon depletion of PP1 may affect its anchoring into the underlying IMC cytoskeleton network and may contribute to the phenotype of the TgPP1 mutants.

It has also come to our thought that the tubulin-based cytoskeleton of the mutant parasites might be affected since the cytoskeleton is known to contribute to maintaining the tachyzoite's structural integrity (Morrissette & Gubbels, 2020). Microtubule associated proteins (MAPs) promote the stability of subpellicular microtubules. SPM2 is a MAP protein which has been identified as significantly hyper-phosphorylated. However, the impact of TgPP1 depletion on the parasite's cytoskeleton microtubules remains unexplored and can be explored by visualization of the cytoskeleton after ectopically expressing α/ß tubulin followed by using ultrastructural expansion microscopy (U-ExM).

Consistent with the unstructured IMC phenotype observed by IFA and EM, phospho-proteomics analysis of the iKD TgPP1 mutant after 2 hours of auxin treatment exhibited IMC1 as the most hyper-phosphorylated protein particularly at Threonine residue 62. However, further experiments are needed in order to validate whether it is specifically the hyper-phosphorylation of Threonine residue 62 that is causing the collapsed IMC phenotype. This can be carried out by generating an iKD mutant of IMC1 and complementing with a copy of the IMC1 gene at an exogenous locus in which IMC1 consists of an Alanine residue at position 62 rather than a Threonine residue. Several attempts to produce an iKD TgIMC1 mutant were carried out but to no avail. However, this could be due to technical issues and the generation of such a mutant could be possible. On the other hand, the essentiality of IMC1 suggested by the Genome-wide CRISPR screen (Sidik et al., 2016) could hinder the production of an inducible knocked-down mutant of IMC1.

3 The link between differentially phosphorylated proteins and cell cycle defects upon TgPP1 depletion

Calcium-dependent kinases such as CDPK6, CDPK7, and CDPK2A were differentially phosphorylated upon TgPP1 depletion. Little is known about the function of CDPK2A. CDPK7 has an essential role in regulating the tachyzoite's cell cycle division. It has been previously exhibited that CDPK7 plays a major role in maintaining the integrity of the centrosome (Morlon-Guyot et al., 2014). Given that the centrosome shape is impacted in the iKD TgPP1 mutant and that CDPK7 is highly hypo-phosphorylated, modulating the normal phosphorylation status of CDPK7 may be linked to the abnormal centrosome shape that we observe. However, the disruption of CDPK7 altered the number of centrosomes during division which we do not observe in the iKD TgPP1 mutant parasite (Figures 7B-C).

In addition, Cep250 was identified as hyper-phosphorylated upon TgPP1 depletion. Consistent with a recent study carried out on Cep250. It has been demonstrated that Cep250 does not play a role in the splitting of the centrosome but rather functions in maintaining the overall centrosome integrity by connecting the inner and outer core centrosomes (C.-T. Chen & Gubbels, 2019). It may be likely that the hyper-phosphorylation of Cep250 contributes to the defect in centrosomal integrity that we observe in the iKD TgPP1 mutant.

Myosin F was identified as significantly hypo-phosphorylated following the depletion of TgPP1. MyoF has been demonstrated to being crucial for the proper orientation of the centrosomes. The disruption of MyoF function results in an impairment in the inheritance of apicoplast. Mutant parasites depleted of TgMyoF exhibit a delayed death phenotype (Heaslip et al., 2016; Jacot et al., 2013). The modified phosphorylation level of MyosinF can be possibly implicated in the abnormal apicoplast ratios we observe in the iKD TgPP1 mutant parasite in the presence of auxin.

4 Apical complex phosphorylation and TgPP1

Moreover, we observed the altered phosphorylation of apical cap protein, AC10. In a previous study it has been shown that the depletion of AC10 severely impacted the tachyzoite leading to a drastic defect in microneme secretion and subsequent tachyzoite invasion and egress (Tosetti et al., 2020). In addition, the conditional depletion of AC10 resulted in severe defects of the apical complex in mature mother parasites such that the apical polar ring and conoid proteins are lost during the final steps of daughter parasite formation (Tosetti et al., 2020).

Therefore, modulation of the phosphorylation level of AC10 may trigger a conoid defect. This can be investigated by carrying out Expansion Microscopy or Focus Ion Beam Scanning Electron Microscopy (FIB-SEM) in order to visualize conoid morphology. Interestingly enough, a MAP kinase, ERK7 (TGGT1_233010) was identified as significantly hyper-phosphorylated in the iKD PP1 mutant in the presence of auxin, and this coincides quite nicely with the possible conoid defect as a previous study in which the role of ERK7 was studied indicates that it is essential for proper apical complex biogenesis (O'Shaughnessy et al., 2020). ERK7 is characterized by autophosphorylation activity which is inhibited by AC9 (Back et al., 2020).

5 Bradyzoite differentiation and TgPP1

Bradyzoite-associated marker MAG1 which is found in the bradyzoite's cyst matrix (Parmley et al., 1994) was extremely hyper-phosphorylated (>5-fold) suggesting a possible dysregulation in the expression of tachyzoite and bradyzoite associated genes. AP2 transcription factor AP2XI-2 has been identified as a bradyzoite repressor (unpublished data) and is also present within the list of significantly hyper-phosphorylated proteins. Thus, suggesting it might be likely that the depletion of TgPP1 has an effect on genes controlling developmental transitions. Another AP2 TF, AP2IX-7 was identified as significantly hypo-phosphorylated and is implicated in gene regulation by associating with histone modifying enzyme GCN5b (Harris et al., 2019) suggesting an alteration in the expression of stage-specific genes might be possible. The expression of bradyzoite-specific genes can be explored by studying the gene expression of the iKD TgPP1 mutant parasites by using RNA-sequencing. From another perspective, it would be of interest to study the effect of PP1 depletion during the bradyzoite stage by creating a mutant parasite in which PP1 is depleted in a Type II bradyzoite-forming cyst strain.

It is highly likely that TgPP1 is responsible for triggering several phosphorylation cascades, due to the larger number of proteins being differentially phosphorylated in the phospho-proteomics study with a longer duration of auxin treatment (24 hours). Since there was very little overlap between the proteins that were hyper-phosphorylated and hypo-phosphorylated at 2 hours and 24 hours, it is most likely that TgPP1 functions in dephosphorylating several proteins at an early time-point of the cell cycle among them kinases which then trigger the phosphorylation of a large number of proteins and could potentially lead to triggering an IMC phosphorylation cascade.

This study allowed to shed light on the biological function of PP1 in *T. gondii*. TgPP1 is demonstrated as essential for parasite tachyzoite growth and

proliferation. The disruption of the IMC is identified as a hallmark of the phenotype of the iKD TgPP1 mutant. In addition, phospho-proteomics analysis suggests the central role of PP1 in several biological processes. However, future studies are still needed to validate the contribution of TgPP1 to various parasite pathways and the mechanisms followed by TgPP1 to carry out its biological functions.

General Conclusions and Discussions

Chapter VI- General Conclusions and Discussions

This PhD project combined a study of transcriptional and post-transcriptional regulation of the *T. gondii* tachyzoite's asexual cell cycle by portraying the importance of ApiAP2 TFs during transcriptional regulation as well as the implication of a protein phosphatase, TgPP1 in post-transcriptional regulation of the tachyzoite's cell cycle.

The importance of ApiAP2 TFs lies in their role of striking a correct balance between the rapidly replicating tachyzoite and the establishment of the chronic tissue cyst in order to ensure transmission of the parasite. This balance remains crucial for the overall successful survival of the parasite. In this PhD study, the roles of three different ApiAP2 TFs were studied; TgAP2X-10, TgAP2III-1, and TgAP2IX-5. Cooperativity between ApiAP2 TFs has been identified as a distinct characteristic of these specific TFs in *T. gondii*. Such cooperativity between ApiAP2 TFs has been previously exhibited between two ApiAP2 TFs, TgAP2XI-5 and TgAP2X-5, which are involved in regulating the expression of virulence factor genes (Lesage et al., 2018). Despite the limited insight that was achieved from gene expression studies of HFF cells infected with the direct knock-out mutants of TgAP2X-10 and TgAP2III-1, it is very likely that the effect observed of these two ApiAP2 TFs on bradyzoite differentiation might be the downstream effect of a potential cooperation between either or both of TgAP2X-10, TgAP2III-1, and other ApiAP2 TFs shown to have a role in bradyzoite differentiation. In fact, multiple TFs were shown to date to contribute to the establishment of the bradyzoite expression program. This includes a Myb-like TF, BFD1, which was shown to be required for the initial induction of the bradyzoite expression program (Waldman et al., 2020). Other factors, such as AP2XI-4 and AP2IV-3 were shown to be important for supporting the maintenance of the activation program (Hong et al., 2017; Walker et al., 2013). In contrast, AP2IX-9 and AP2IV-4 were shown to ensure the repression of the bradyzoite expression program in tachyzoites (Radke et al., 2013, 2018). This highlights the complexity of transcriptional regulation of the differentiation in *T. gondii*. The establishment of the bradyzoite specific expression program relies on multiple regulators and their regulation is probably inter-dependent. Producing mutant strains for each of the individual ApiAP2 TFs will probably yield more insights on their respective role during differentiation. Stingingly, the integration of the role of these regulators with chromatin remodeling and modifying complexes, such as the MORC-HDAC3 complex (Farhat et al., 2020) is still missing. However, there is no doubt that both mechanisms act in concert to achieve the transcriptional control of gene expression during the crucial events leading to differentiation.

Another layer of regulation is also achieved during the cell-cycle of the tachyzoite. As highlighted before, the interconnection between cell cycle and differentiation has been shown for years (J.R. Radke et al., 2003). However, how these two complex mechanisms were connected at the molecular level was not understood. It was already shown that certain cell-cycle regulated ApiAP2 TFs were involved in differentiation, namely AP2XI-4, AP2IV-3, AP2IV-4, and AP2IX-4 indicating that these TFs should be expressed at a certain point of the cell-cycle to carry out their role. By studying the role of TgAP2IX-5, we showed for the first time a direct link between the continuation of the cell-cycle and the inhibition of the bradyzoite differentiation pathway. Indeed, TgAP2IX-5 was shown to have a role in bradyzoite differentiation by directly controlling the expression of the known bradyzoite repressor, TgAP2IV-4. A cell-cycle arrest at a timepoint where TgAP2IX-5 is not expressed, for example G_0 as described before (J.R. Radke et al., 2003), may block the expression of TgAP2IV-4 and therefore pave the way for the initiation of the bradyzoite expression program. Conversely, when TgAP2IX-5 is expressed and daughter cell formation initiated, the tachyzoite cell cycle continues and the differentiation is prevented through the expression of TgAP2IV-4. It would be of interest to dissect the other potential TFs that are directly regulated by TgAP2IX-5 to clarify their role during differentiation. They may work in concert or cooperatively to repress the initiation of the bradyzoite expression program. The intertwined regulation network of regulators of cell-cycle and differentiation point toward a clear molecular mechanism controlling both events. However, many other actors may be implicated in the control of these mechanisms. It would be of interest for example, to identify the TFs that are responsible for the expression of BFD1. It would be therefore not surprising that some of these would show a cell-cycle dependent expression.

Since the first studies highlighting the highly ordered profiles of gene expression during *P. falciparum* asexual division in the erythrocyte (Bozdech et al., 2003; Le Roch et al., 2003) or the cell-cycle dependent expression profiles of the *T. gondii* tachyzoite (Behnke et al., 2010), it has been suggested that a cascade of interdependent transcriptional regulators are at play during these two events. In *P. berghei*, the production of knock-out mutants of ApiAP2 genes have shown their inter-dependence, the co-regulation of multiple gene clusters and the partial overlap of their function (Modrzynska et al., 2017). However, such a systematic characterization is missing for *T. gondii*. Nevertheless, the study of the TgAP2IX-5 mutant demonstrated that this TF directly controls other TFs such as AP2XII-9, AP2III-2 and AP2XII-2 that may in turn control expression during the subsequent steps of the cell cycle. This has been confirmed partially by a study of TgAP2XII-2, the only other ApiAP2 TF characterized thus far to have an important role in the tachyzoite's asexual cell cycle. A mutant targeting this gene leads to a delayed S phase thus demonstrating its central role in the smooth progression of the subsequent steps of the cell cycle (Srivastava et al., 2020). This illustrates that during the tachyzoite cell cycle, the transcript expression cascade is controlled at least partially by a cascade of expression of ApiAP2 TFs. The fact that the previously expressed ApiAP2 TF controls the ones that are necessary for the subsequent steps provide the molecular mechanism underlying the waves of expression identified during the tachyzoite cell cycle. The apparent absence of

classical cell cycle checkpoints may be compensated by the hierarchical organization of the ApiAP2 TF expression.

Both TgAP2IX-5 and TgPP1 proteins have a regulatory effect on the formation of the inner membrane complex (IMC). However, a closer comparison between the effect of each protein on the IMC demonstrates that TgAP2IX-5 affects only the daughter parasite IMC formation as opposed to TgPP1 which may affect the IMC of both mother and developing daughter parasites.

The role of TgPP1 in maintaining the balance of phosphorylation of IMC proteins which are essential for the formation of daughter parasite IMC might also be linked to the mutant parasite's affected budding ability. However, the nature of the collapsed IMC phenotype renders this challenging to study given the meshed IMC protein network present upon TgPP1 depletion. It might be likely that exclusively labelling nascent parasite IMC proteins might relieve the appearance of a meshed network and facilitate studying the ability of the parasite to produce daughter parasites and thus allow us to link the transcriptional effect of TgAP2IX-5 on parasite budding to the post-transcriptional role of TgPP1.

What was most striking was that several key IMC proteins determined to be directly controlled by TgAP2IX-5 were also identified as differentially phosphorylated by TgPP1. For example, TgIMC1 and TgIMC4 overlap between RNA-seq, ChIP-seq datasets of the iKD TgAP2IX-5 mutant and phospho-proteomics datasets of the iKD TgPP1 mutant thus demonstrating that indeed both TgAP2IX-5 and TgPP1 have important roles in the formation of IMC. This is also true for AC2 and AC7. However, the timing at which each of TgAP2IX-5 and TgPP1 are crucial for the parasite to maintain its IMC is what distinguishes each of these proteins apart with TgAP2IX-5 having an impact on IMC genes at a transcriptional level while TgPP1 has an effect on IMC proteins post-transcriptionally by modulating their phosphorylation state. This indicates that the control of IMC formation requires a combination of both transcriptional and post-transcriptional regulation.

The conditional depletion of TgPP1 has pleiotropic effects on the parasite's cell cycle. Both nuclear and budding cycle seemed to be affected. This demonstrates that TgPP1 has an effect on a wider number of organelles at moderate levels compared to TgAP2IX-5 where a complete blockage in the budding cycle is observed specifically at the time of plastid elongation during division. Some of these pleiotropic effects may be explained by the differential phosphorylation of centrosome proteins such as TgCep250 and TgCDPK7. Indeed, TgCep250 localized at both outer and inner core centrosome and is important for the structural integrity of the centrosome (Chen & Gubbels, 2019). In the TgAP2IX-5 iKD, the centrosome division and integrity were unaffected underlining the fundamental difference in the two proteins' function.

The potential role of TgPP1 in transcriptional regulation remains to be explored. Its original localization in the nucleus and the cytoplasm (Daher et al., 2007), may indicate a potential role in regulating transcriptional mechanisms. It may also be

involved in other mechanisms such as splicing and DNA replication. PfPP1 localization is similar but the protein function was mainly demonstrated in nuclear division (Kumar et al., 2002; Paul et al., 2020) rather than in transcription regulation.

Overall, this PhD study shed light on the regulation of the tachyzoite's asexual cell cycle and demonstrated the key role of an ApiAP2 TF, TgAP2IX-5, and a phosphoprotein phosphatase, TgPP1 in regulating the asexual cell cycle. In addition to studying the role of TgAP2X-10 and TgAP2III-1 in developmental life cycle transitions. Despite the many findings of this study, several questions remain unanswered, the most prominent one being the functional link between the transcriptional and post-transcriptional regulation of the asexual cell cycle of the tachyzoite. Further studies are needed in order to shed light on this topic.

Bibliography

Adomako-Ankomah, Y., Wier, G. M., Borges, A. L., Wand, H. E., & Boyle, J. P. (2014). Differential Locus Expansion Distinguishes Toxoplasmatinae Species and Closely Related Strains of Toxoplasma gondii. *MBio*, *5*(1), e01003-13. https://doi.org/10.1128/mBio.01003-13

Agop-Nersesian, C., Egarter, S., Langsley, G., Foth, B. J., Ferguson, D. J. P., & Meissner, M. (2010). Biogenesis of the Inner Membrane Complex Is Dependent on Vesicular Transport by the Alveolate Specific GTPase Rab11B. *PLoS Pathogens*, *6*(7). https://doi.org/10.1371/journal.ppat.1001029

Aguirre, A. A., Longcore, T., Barbieri, M., Dabritz, H., Hill, D., Klein, P. N., Lepczyk, C., Lilly, E. L., McLeod, R., Milcarsky, J., Murphy, C. E., Su, C., VanWormer, E., Yolken, R., & Sizemore, G. C. (2019). The One Health Approach to Toxoplasmosis: Epidemiology, Control, and Prevention Strategies. *EcoHealth*, *16*(2), 378–390. https://doi.org/10.1007/s10393-019-01405-7

Ajioka, J. W., Fitzpatrick, J. M., & Reitter, C. P. (2001). Toxoplasma gondii genomics: Shedding light on pathogenesis and chemotherapy. *Expert Reviews in Molecular Medicine*, *3*(01). https://doi.org/10.1017/S1462399401002204

Alaganan, A., Fentress, S. J., Tang, K., Wang, Q., & Sibley, L. D. (2014). Toxoplasma GRA7 effector increases turnover of immunity-related GTPases and contributes to acute virulence in the mouse. *Proceedings of the National Academy of Sciences*, *111*(3), 1126–1131. https://doi.org/10.1073/pnas.1313501111

Albert, I., Mavrich, T. N., Tomsho, L. P., Qi, J., Zanton, S. J., Schuster, S. C., & Pugh, B. F. (2007). Translational and rotational settings of H2A.Z nucleosomes across the Saccharomyces cerevisiae genome. *Nature*, *446*(7135), 572–576. https://doi.org/10.1038/nature05632

Alexander, D. L., Mital, J., Ward, G. E., Bradley, P., & Boothroyd, J. C. (2005). Identification of the Moving Junction Complex of Toxoplasma gondii: A Collaboration between Distinct Secretory Organelles. *PLoS Pathogens*, *1*(2), e17. https://doi.org/10.1371/journal.ppat.0010017

Allen, M. D., Yamasaki, K., Ohme-Takagi, M., Tateno, M., & Suzuki, M. (1998). A novel mode of DNA recognition by a β-sheet revealed by the solution structure of the GCC-box binding domain in complex with DNA. *The EMBO Journal*, *17*(18), 5484–5496. https://doi.org/10.1093/emboj/17.18.5484

Allis, C. D., Berger, S. L., Cote, J., Dent, S., Jenuwien, T., Kouzarides, T., Pillus, L., Reinberg, D., Shi, Y., Shiekhattar, R., Shilatifard, A., Workman, J., & Zhang, Y. (2007). New Nomenclature for Chromatin-Modifying Enzymes. *Cell*, *131*(4), 633–636. https://doi.org/10.1016/j.cell.2007.10.039

Altschul, S. F., Gish, W., Miller, W., Myers, E. W., & Lipman, D. J. (1990). *Basic Local Alignment Search Tool*. 8.

Alvarez, C. A., & Suvorova, E. S. (2017). Checkpoints of apicomplexan cell division identified in Toxoplasma gondii. *PLoS Pathogens*, *13*(7). https://doi.org/10.1371/journal.ppat.1006483

Amberg-Johnson, K., Hari, S. B., Ganesan, S. M., Lorenzi, H. A., Sauer, R. T., Niles, J. C., & Yeh, E. (2017). Small molecule inhibition of apicomplexan FtsH1 disrupts plastid biogenesis in human pathogens. *ELife*, *6*. https://doi.org/10.7554/eLife.29865

Amberg-Johnson, K., & Yeh, E. (2019). Host Cell Metabolism Contributes to Delayed-Death Kinetics of Apicoplast Inhibitors in Toxoplasma gondii. *Antimicrobial Agents and Chemotherapy*, *63*(2). https://doi.org/10.1128/AAC.01646-18

Andenmatten, N., Egarter, S., Jackson, A. J., Jullien, N., Herman, J.-P., & Meissner, M. (2013). Conditional genome engineering in Toxoplasma gondii uncovers alternative invasion mechanisms. *Nature Methods*, *10*(2), 125–127. https://doi.org/10.1038/nmeth.2301

Anderson-White, B., Beck, J. R., Chen, C.-T., Meissner, M., Bradley, P. J., & Gubbels, M.-J. (2012). Cytoskeleton Assembly in Toxoplasma gondii Cell Division. In *International Review of Cell and Molecular Biology* (Vol. 298, pp. 1–31). Elsevier. https://doi.org/10.1016/B978-0-12-394309-5.00001-8

Anderson-White, B. R., Ivey, F. D., Cheng, K., Szatanek, T., Lorestani, A., Beckers, C. J., Ferguson, D. J. P., Sahoo, N., & Gubbels, M.-J. (2011). A family of intermediate filament-like proteins is sequentially assembled into the cytoskeleton of Toxoplasma gondii. *Cellular Microbiology*, *13*(1), 18. https://doi.org/10.1111/j.1462-5822.2010.01514.x

Aravind, L. (1998). AT-hook motifs identified in a wide variety of DNA-binding proteins. *Nucleic Acids Research*, *26*(19), 4413–4421. https://doi.org/10.1093/nar/26.19.4413

Aravind, L., Anantharaman, V., Balaji, S., Babu, M., & Iyer, L. (2005). The many faces of the helix-turn-helix domain: Transcription regulation and beyond. *FEMS Microbiology Reviews*, *29*(2), 231–262. https://doi.org/10.1016/j.femsre.2004.12.008

Aravind, L., Iyer, L. M., Wellems, T. E., & Miller, L. H. (2003). Plasmodium Biology. *Cell*, *115*(7), 771–785. https://doi.org/10.1016/S0092-8674(03)01023-7

Attias, M., Miranda, K., & De Souza, W. (2019). Development and fate of the residual body of Toxoplasma gondii. *Experimental Parasitology*, *196*, 1–11. https://doi.org/10.1016/j.exppara.2018.11.004

Aubert, D., Ajzenberg, D., Richomme, C., Gilot-Fromont, E., Terrier, M. E., de Gevigney, C., Game, Y., Maillard, D., Gibert, P., Dardé, M. L., & Villena, I. (2010). Molecular and biological characteristics of Toxoplasma gondii isolates from wildlife in France. *Veterinary Parasitology*, *171*(3–4), 346–349. https://doi.org/10.1016/j.vetpar.2010.03.033

Back, P. S., O'Shaughnessy, W. J., Moon, A. S., Dewangan, P. S., Hu, X., Sha, J., Wohlschlegel, J. A., Bradley, P. J., & Reese, M. L. (2020). Ancient MAPK ERK7 is regulated by an unusual inhibitory scaffold required for Toxoplasma apical complex biogenesis. *Proceedings of the National Academy of Sciences of the United States of America*, *117*(22), 12164. https://doi.org/10.1073/pnas.1921245117

Balaji, S., Babu, M. M., Iyer, L. M., & Aravind, L. (2005). Discovery of the principal specific transcription factors of Apicomplexa and their implication for the evolution of the AP2-integrase DNA binding domains. *Nucleic Acids Research*, *33*(13), 3994. https://doi.org/10.1093/nar/gki709

Bansal, P., Antil, N., Kumar, M., Yamaryo-Botté, Y., Rawat, R. S., Pinto, S., Datta, K. K., Katris, N. J., Botté, C. Y., Prasad, T. S. K., & Sharma, P. (2021). Protein kinase TgCDPK7 regulates vesicular trafficking and phospholipid synthesis in Toxoplasma gondii. *PLOS Pathogens*, *17*(2), e1009325. https://doi.org/10.1371/journal.ppat.1009325

Baptista, C. G., Lis, A., Deng, B., Gas-Pascual, E., Dittmar, A., Sigurdson, W., West, C. M., & Blader, I. J. (2019). Toxoplasma F-box protein 1 is required for daughter cell scaffold function during parasite replication. *PLOS Pathogens*, *15*(7), e1007946. https://doi.org/10.1371/journal.ppat.1007946

Bargieri, D. Y., Andenmatten, N., Lagal, V., Thiberge, S., Whitelaw, J. A., Tardieux, I., https://fichier.pasteur-lille.fr/f/69969 https://fichier.pasteur-lille.fr/f/69969, M., & Ménard, R. (2013). Apical membrane antigen 1 mediates apicomplexan parasite attachment but is dispensable for host cell invasion. *Nature Communications*, *4*(1), 2552. https://doi.org/10.1038/ncomms3552

Barkhuff, W. D., Gilk, S. D., Whitmarsh, R., Tilley, L. D., Hunter, C., & Ward, G. E. (2011). Targeted Disruption of TgPhIL1 in Toxoplasma gondii Results in Altered Parasite Morphology and Fitness. *PLoS ONE*, *6*(8). https://doi.org/10.1371/journal.pone.0023977

Barylyuk, K., Koreny, L., Ke, H., Butterworth, S., Crook, O. M., Lassadi, I., Gupta, V., Tromer, E., Mourier, T., Stevens, T. J., Breckels, L. M., Pain, A., Lilley, K. S., & Waller, R. F. (2020). A Comprehensive Subcellular Atlas of the Toxoplasma Proteome via hyperLOPIT Provides Spatial Context for Protein Functions. *Cell Host & Microbe*, *28*(5), 752. https://doi.org/10.1016/j.chom.2020.09.011

Beck, J. R., Rodriguez-Fernandez, I. A., Leon, J. C. de, Huynh, M.-H., Carruthers, V. B., Morrissette, N. S., & Bradley, P. J. (2010). A Novel Family of Toxoplasma IMC Proteins Displays a Hierarchical Organization and Functions in Coordinating Parasite Division. *PLoS Pathogens*, *6*(9). https://doi.org/10.1371/journal.ppat.1001094

Behnke, M. S., Khan, A., Wootton, J. C., Dubey, J. P., Tang, K., & Sibley, L. D. (2011). Virulence differences in Toxoplasma mediated by amplification of a family of polymorphic pseudokinases. *Proceedings of the National Academy of Sciences*, *108*(23), 9631–9636. https://doi.org/10.1073/pnas.1015338108

Behnke, M. S., Radke, J. B., Smith, A. T., Sullivan, W. J., Jr, & White, M. W. (2008). The transcription of bradyzoite genes in Toxoplasma gondii is controlled by autonomous promoter elements. *Molecular Microbiology*, *68*(6), 1502. https://doi.org/10.1111/j.1365-2958.2008.06249.x

Behnke, M. S., Wootton, J. C., Lehmann, M. M., Radke, J. B., Lucas, O., Nawas, J., Sibley, L. D., & White, M. W. (2010). Coordinated progression through two subtranscriptomes underlies the tachyzoite cycle of Toxoplasma gondii. *PloS One*, *5*(8), e12354. https://doi.org/10.1371/journal.pone.0012354

Behnke, M. S., Zhang, T. P., Dubey, J. P., & Sibley, L. D. (2014). Toxoplasma gondii merozoite gene expression analysis with comparison to the life cycle discloses a unique expression state during enteric development. *BMC Genomics*, *15*(1). https://doi.org/10.1186/1471-2164-15-350

Berndt, N., Campbell, D. G., Caudwell, F. B., Cohen, P., Silva, E. F. da C. e, Silva, O. B. da C. e, & Cohen, P. T. W. (1987). Isolation and sequence analysis of a cDNA clone encoding a type-1 protein phosphatase catalytic subunit: Homology with protein phosphatase 2A. *FEBS Letters*, *223*(2), 340–346. https://doi.org/10.1016/0014-5793(87)80316-2

Berry, L., Chen, C.-T., Francia, M. E., Guerin, A., Graindorge, A., Saliou, J.-M., Grandmougin, M., Wein, S., Bechara, C., Morlon-Guyot, J., Bordat, Y., Gubbels, M.-J., Lebrun, M., Dubremetz, J.-F., & Daher, W. (2018). Toxoplasma gondii chromosomal passenger complex is essential for the organization of a functional mitotic spindle: A prerequisite for productive endodyogeny. *Cellular and Molecular Life Sciences*, *75*(23), 4417–4443. https://doi.org/10.1007/s00018-018-2889-6

Berry, L., Chen, C.-T., Reininger, L., Carvalho, T. G., El Hajj, H., Morlon-Guyot, J., Bordat, Y., Lebrun, M., Gubbels, M.-J., Doerig, C., & Daher, W. (2016). The conserved apicomplexan Aurora kinase TgArk3 is involved in endodyogeny, duplication rate

and parasite virulence: Apicomplexan Aurora kinases. *Cellular Microbiology*, *18*(8), 1106–1120. https://doi.org/10.1111/cmi.12571

Besteiro, S., Dubremetz, J.-F., & Lebrun, M. (2011). The moving junction of apicomplexan parasites: A key structure for invasion: The moving junction of apicomplexan parasites. *Cellular Microbiology*, *13*(6), 797–805. https://doi.org/10.1111/j.1462-5822.2011.01597.x

Besteiro, S., Michelin, A., Poncet, J., Dubremetz, J.-F., & Lebrun, M. (2009). Export of a Toxoplasma gondii Rhoptry Neck Protein Complex at the Host Cell Membrane to Form the Moving Junction during Invasion. *PLoS Pathogens*, *5*(2), e1000309. https://doi.org/10.1371/journal.ppat.1000309

Bhatti, M. M., Livingston, M., Mullapudi, N., Sullivan, W. J., & Jr. (2006). Pair of Unusual GCN5 Histone Acetyltransferases and ADA2 Homologues in the Protozoan Parasite Toxoplasma gondii. *Eukaryotic Cell*, *5*(1), 62. https://doi.org/10.1128/EC.5.1.62-76.2006

Bierly, A. L., Shufesky, W. J., Sukhumavasi, W., Morelli, A. E., & Denkers, E. Y. (2008). Dendritic Cells Expressing Plasmacytoid Marker PDCA-1 Are Trojan Horses during *Toxoplasma gondii* Infection. *The Journal of Immunology*, *181*(12), 8485–8491. https://doi.org/10.4049/jimmunol.181.12.8485

Billker, O., Lourido, S., & Sibley, L. D. (2009). Calcium-Dependent Signaling and Kinases in Apicomplexan Parasites. *Cell Host & Microbe*, *5*(6), 612–622. https://doi.org/10.1016/j.chom.2009.05.017

Bisio, H., Lunghi, M., Brochet, M., & Soldati-Favre, D. (2019). Phosphatidic acid governs natural egress in Toxoplasma gondii via a guanylate cyclase receptor platform. *Nature Microbiology*, *4*(3), 420–428. https://doi.org/10.1038/s41564-018-0339-8

Bissig, C., & Gruenberg, J. (2014). ALIX and the multivesicular endosome: ALIX in Wonderland. *Trends in Cell Biology*, *24*(1), 19–25. https://doi.org/10.1016/j.tcb.2013.10.009

Black, M. W., & Boothroyd, J. C. (2000). Lytic Cycle of Toxoplasma gondii. *Microbiology and Molecular Biology Reviews*, *64*(3), 607–623. https://doi.org/10.1128/MMBR.64.3.607-623.2000

Blader, I., Coleman, B., Chen, C.-T., & Gubbels, M.-J. (2015). The lytic cycle of Toxoplasma gondii: 15 years later. *Annual Review of Microbiology*, *69*, 463. https://doi.org/10.1146/annurev-micro-091014-104100

Blanchard, J. L., & Hicks, J. S. (1999). The Non-Photosynthetic Plastid in Malarial Parasites and Other Apicomplexans is Derived from Outside the Green Plastid Lineage. *The Journal of Eukaryotic Microbiology*, *46*(4), 367–375. https://doi.org/10.1111/j.1550-7408.1999.tb04615.x

Blank, M. L., & Boyle, J. P. (2018). Effector variation at tandem gene arrays in tissue-dwelling coccidia: Who needs antigenic variation anyway? *Current Opinion in Microbiology*, *46*, 86–92. https://doi.org/10.1016/j.mib.2018.09.001

Blazek, E., Mittler, G., & Meisterernst, M. (2005). The Mediator of RNA polymerase II. *Chromosoma*, *113*(8), 399–408. https://doi.org/10.1007/s00412-005-0329-5

Bohm, S., Frishman, D., & Mewes, H. W. (1997). Variations of the C2H2 zinc finger motif in the yeast genome and classification of yeast zinc finger proteins. *Nucleic Acids Research*, *25*(12), 2464–2469. https://doi.org/10.1093/nar/25.12.2464

Bohne, W., Wirsing, A., & Gross, U. (1997). Bradyzoite-specific gene expression in Toxoplasma gondii requires minimal genomic elements. *Molecular and Biochemical Parasitology*, 10.

Bookwalter, C. S., Kelsen, A., Leung, J. M., Ward, G. E., & Trybus, K. M. (2014). A *Toxoplasma gondii* Class XIV Myosin, Expressed in *Sf* 9 Cells with a Parasite Co-

chaperone, Requires Two Light Chains for Fast Motility. *Journal of Biological Chemistry*, *289*(44), 30832–30841. https://doi.org/10.1074/jbc.M114.572453

Boothroyd, J.C., Black, M., Bonnefoy, S., Hehl, A., Knoll, L.J. (1997). Genetic and biochemical analysis of development in Toxoplasma gondii. *Philosophical transactions of the Royal Society of London Series B, Biological sciences*, 352, 1347-1354.

Boothroyd, J. C., & Dubremetz, J.-F. (2008). Kiss and spit: The dual roles of Toxoplasma rhoptries. *Nature Reviews Microbiology*, *6*(1), 79–88. https://doi.org/10.1038/nrmicro1800

Boothroyd, J. C., & Grigg, M. E. (2002). Population biology of Toxoplasma gondii and its relevance to human infection: Do different strains cause different disease? *Current Opinion in Microbiology*, *5*(4), 438–442. https://doi.org/10.1016/S1369-5274(02)00349-1

Boucher, L. E., & Bosch, J. (2015). The apicomplexan glideosome and adhesins – Structures and function. *Journal of Structural Biology*, *190*(2), 93–114. https://doi.org/10.1016/j.jsb.2015.02.008

Bougdour, A., Durandau, E., Brenier-Pinchart, M.-P., Ortet, P., Barakat, M., Kieffer, S., Curt-Varesano, A., Curt-Bertini, R.-L., Bastien, O., Coute, Y., Pelloux, H., & Hakimi, M.-A. (2013). Host Cell Subversion by Toxoplasma GRA16, an Exported Dense Granule Protein that Targets the Host Cell Nucleus and Alters Gene Expression. *Cell Host & Microbe*, *13*(4), 489–500. https://doi.org/10.1016/j.chom.2013.03.002

Bougdour, A., Maubon, D., Baldacci, P., Ortet, P., Bastien, O., Bouillon, A., Barale, J.-C., Pelloux, H., Ménard, R., & Hakimi, M.-A. (2009). Drug inhibition of HDAC3 and epigenetic control of differentiation in Apicomplexa parasites. *Journal of Experimental Medicine*, *206*(4), 953–966. https://doi.org/10.1084/jem.20082826

Bougdour, A., Tardieux, I., & Hakimi, M.-A. (2014). Toxoplasma exports dense granule proteins beyond the vacuole to the host cell nucleus and rewires the host genome expression. *Cellular Microbiology*, *16*(3), 334–343. https://doi.org/10.1111/cmi.12255

Bozdech, Z., Llinás, M., Pulliam, B. L., Wong, E. D., Zhu, J., & DeRisi, J. L. (2003). The Transcriptome of the Intraerythrocytic Developmental Cycle of Plasmodium falciparum. *PLOS Biology*, *1*(1), e5. https://doi.org/10.1371/journal.pbio.0000005

Bradley, P. J., & Sibley, L. D. (2007). Rhoptries: An arsenal of secreted virulence factors. *Current Opinion in Microbiology*, *10*(6), 582–587. https://doi.org/10.1016/j.mib.2007.09.013

Braun, L., Brenier-Pinchart, M.-P., Yogavel, M., Curt-Varesano, A., Curt-Bertini, R.-L., Hussain, T., Kieffer-Jaquinod, S., Coute, Y., Pelloux, H., Tardieux, I., Sharma, A., Belrhali, H., Bougdour, A., & Hakimi, M.-A. (2013). A Toxoplasma dense granule protein, GRA24, modulates the early immune response to infection by promoting a direct and sustained host p38 MAPK activation. *Journal of Experimental Medicine*, *210*(10), 2071–2086. https://doi.org/10.1084/jem.20130103

Braun, L., Cannella, D., Pinheiro, A. M., Kieffer, S., Belrhali, H., Garin, J., & Hakimi, M.-A. (2009). The small ubiquitin-like modifier (SUMO)-conjugating system of Toxoplasma gondii. *International Journal for Parasitology*, *39*(1), 81–90. https://doi.org/10.1016/j.ijpara.2008.07.009

Braun, L., Brenier-Pinchart, M.P, Hammoudi, P.M., Cannella, D., Kieffer-Jaquinod, S., Vollaire, J., Josserand, V., Touquet, B., Coute, Y., Tardieux, I., Bougdour, A., & Hakimi, M.-A. (2019). The Toxoplasma effector TEEGR promotes parasite persistence by modulating NF-kB signalling via EZH2. *Nature Microbiology*, 4, 1028-1220. https://doi.org/10.1038/s41564-019-0431-8

Brautigan, D. L. (2013). Protein Ser/ Thr phosphatases – the ugly ducklings of cell signalling. *The FEBS Journal*, *280*(2), 324–325. https://doi.org/10.1111/j.1742-4658.2012.08609.x

Brautigan, D. L., & Shenolikar, S. (2018). Protein Serine/Threonine Phosphatases: Keys to Unlocking Regulators and Substrates. *Annual Review of Biochemistry*. https://doi.org/10.1146/annurev-biochem-062917-012332

Bromley, E., Leeds, N., Clark, J., McGregor, E., Ward, M., Dunn, M. J., & Tomley, F. (2003). Defining the protein repertoire of microneme secretory organelles in the apicomplexan parasiteEimeria tenella. *PROTEOMICS*, *3*(8), 1553–1561. https://doi.org/10.1002/pmic.200300479

Brooks, C. F., Francia, M. E., Gissot, M., Croken, M. M., Kim, K., & Striepen, B. (2011). *Toxoplasma gondii* sequesters centromeres to a specific nuclear region throughout the cell cycle. *Proceedings of the National Academy of Sciences*, *108*(9), 3767–3772. https://doi.org/10.1073/pnas.1006741108

Brown, K. M., Long, S., & Sibley, L. D. (2017). *Plasma Membrane Association by N-Acylation Governs PKG Function in*. *8*(3), 14.

Brown, K. M., Long, S., & Sibley, L. D. (2018). Conditional Knockdown of Proteins Using Auxin-inducible Degron (AID) Fusions in Toxoplasma gondii. *Bio-Protocol*, *8*(4). https://doi.org/10.21769/BioProtoc.2728

Brown, K. M., & Sibley, L. D. (2018). Essential cGMP Signaling in Toxoplasma Is Initiated by a Hybrid P-Type ATPase-Guanylate Cyclase. *Cell Host & Microbe*, *24*(6), 804-816.e6. https://doi.org/10.1016/j.chom.2018.10.015

Buchholz, K. R., Fritz, H. M., Chen, X., Durbin-Johnson, B., Rocke, D. M., Ferguson, D. J., Conrad, P. A., & Boothroyd, J. C. (2011). Identification of Tissue Cyst Wall Components by Transcriptome Analysis of *In Vivo* and In Vitro Toxoplasma gondii Bradyzoites. *Eukaryotic Cell*, *10*(12), 1637–1647. https://doi.org/10.1128/EC.05182-11

Bullen, H. E., Jia, Y., Yamaryo-Botté, Y., Bisio, H., Zhang, O., Jemelin, N. K., Marq, J.-B., Carruthers, V., Botté, C. Y., & Soldati-Favre, D. (2016). Phosphatidic Acid-Mediated Signaling Regulates Microneme Secretion in Toxoplasma. *Cell Host & Microbe*, *19*(3), 349–360. https://doi.org/10.1016/j.chom.2016.02.006

Bullen, H. E., Tonkin, C. J., O'Donnell, R. A., Tham, W.-H., Papenfuss, A. T., Gould, S., Cowman, A. F., Crabb, B. S., & Gilson, P. R. (2009). A Novel Family of Apicomplexan Glideosome-associated Proteins with an Inner Membrane-anchoring Role. *The Journal of Biological Chemistry*, *284*(37), 25353. https://doi.org/10.1074/jbc.M109.036772

Bunnik, E. M., Venkat, A., Shao, J., McGovern, K. E., Batugedara, G., Worth, D., Prudhomme, J., Lapp, S. A., Andolina, C., Ross, L. S., Lawres, L., Brady, D., Sinnis, P., Nosten, F., Fidock, D. A., Wilson, E. H., Tewari, R., Galinski, M. R., Ben Mamoun, C., … Le Roch, K. G. (2019). Comparative 3D genome organization in apicomplexan parasites. *Proceedings of the National Academy of Sciences*, *116*(8), 3183–3192. https://doi.org/10.1073/pnas.1810815116

Butcher, B. A., Fox, B. A., Rommereim, L. M., Kim, S. G., Maurer, K. J., Yarovinsky, F., Herbert, D. R., Bzik, D. J., & Denkers, E. Y. (2011). Toxoplasma gondii Rhoptry Kinase ROP16 Activates STAT3 and STAT6 Resulting in Cytokine Inhibition and Arginase-1-Dependent Growth Control. *PLoS Pathogens*, *7*(9), e1002236. https://doi.org/10.1371/journal.ppat.1002236

Butler, C. L., Lucas, O., Wuchty, S., Xue, B., Uversky, V. N., & White, M. (2014). Identifying Novel Cell Cycle Proteins in Apicomplexa Parasites through Co-

Expression Decision Analysis. *PLoS ONE*, *9*(5), e97625. https://doi.org/10.1371/journal.pone.0097625

Buxton, D. (1993). Toxoplasmosis: The first commercial vaccine. *Parasitology Today*, *9*(9), 335–337. https://doi.org/10.1016/0169-4758(93)90236-9

Caffaro, C. E., & Boothroyd, J. C. (2011). Evidence for Host Cells as the Major Contributor of Lipids in the Intravacuolar Network of Toxoplasma-Infected Cells. *Eukaryotic Cell*, *10*(8), 1095–1099. https://doi.org/10.1128/EC.00002-11

Caldas, L. A., & de Souza, W. (2010). Microscopic analysis of calcium ionophore activated egress of Toxoplasma gondii from the host cell. *Veterinary Parasitology*, 11.

Caldas, L., & De Souza, W. (2018). A Window to Toxoplasma gondii Egress. *Pathogens*, *7*(3), 69. https://doi.org/10.3390/pathogens7030069

Campbell, T. L., De Silva, E. K., Olszewski, K. L., Elemento, O., & Llinás, M. (2010). Identification and Genome-Wide Prediction of DNA Binding Specificities for the ApiAP2 Family of Regulators from the Malaria Parasite. *PLoS Pathogens*, *6*(10), e1001165. https://doi.org/10.1371/journal.ppat.1001165

Camps, M., Arrizabalaga, G., & Boothroyd, J. (2002). An rRNA mutation identifies the apicoplast as the target for clindamycin in Toxoplasma gondii: Apicoplast is a target of clindamycin. *Molecular Microbiology*, *43*(5), 1309–1318. https://doi.org/10.1046/j.1365-2958.2002.02825.x

Carruthers, V.B., Sibley, L.D. (1997). Sequential protein secretion from three distinct organelles of Toxoplasma gondii accompanies invasion of human fibroblasts. Eur.J. Cell Biol.73, 114-123. http://pubmed.ncbi.nlm.nih.gov/9208224/

Carruthers, V. B., Giddings, O. K., & Sibley, L. D. (1999). Secretion of micronemal proteins is associated with toxoplasma invasion of host cells. *Cellular Microbiology*, *1*(3), 225–235. https://doi.org/10.1046/j.1462-5822.1999.00023.x

Carruthers, V. B., & Tomley, F. M. (2008). Receptor-ligand interaction and invasion: Microneme proteins in apicomplexans. *Sub-Cellular Biochemistry*, *47*, 33.

Carruthers, V., & Boothroyd, J. C. (2007). Pulling together: An integrated model of Toxoplasma cell invasion. *Current Opinion in Microbiology*, *10*(1), 83–89. https://doi.org/10.1016/j.mib.2006.06.017

Cérède, O., Dubremetz, J. F., Soête, M., Deslée, D., Vial, H., Bout, D., & Lebrun, M. (2005). Synergistic role of micronemal proteins in Toxoplasma gondii virulence. *Journal of Experimental Medicine*, *201*(3), 453–463. https://doi.org/10.1084/jem.20041672

Cerutti, A., Blanchard, N., & Besteiro, S. (2020). The Bradyzoite: A Key Developmental Stage for the Persistence and Pathogenesis of Toxoplasmosis. *Pathogens*, *9*(3). https://doi.org/10.3390/pathogens9030234

Ceulemans, H., & Bollen, M. (2004). Functional diversity of protein phosphatase-1, a cellular economizer and reset button. *Physiological Reviews*, *84*(1). https://doi.org/10.1152/physrev.00013.2003

Chandramohanadas, R., Davis, P. H., Beiting, D. P., Harbut, M. B., Darling, C., Velmourougane, G., Lee, M. Y., Greer, P. A., Roos, D. S., & Greenbaum, D. C. (2009). Apicomplexan Parasites Co-Opt Host Calpains to Facilitate Their Escape from Infected Cells. *Science*, *324*(5928), 794–797. https://doi.org/10.1126/science.1171085

Chang, B., Chen, Y., Zhao, Y., & Bruick, R. K. (2007). JMJD6 Is a Histone Arginine Demethylase. *Science*, *318*(5849), 444–447. https://doi.org/10.1126/science.1145801

Charron, A. J., & Sibley, L. D. (2004). Molecular Partitioning during Host Cell Penetration by Toxoplasma gondii: Membrane Dynamics at the Moving Junction. *Traffic*, *5*(11), 855–867. https://doi.org/10.1111/j.1600-0854.2004.00228.x

Chen, A. L., Kim, E. W., Toh, J. Y., Vashisht, A. A., Rashoff, A. Q., Van, C., Huang, A. S., Moon, A. S., Bell, H. N., Bentolila, L. A., Wohlschlegel, J. A., & Bradley, P. J. (2015). Novel Components of the Toxoplasma Inner Membrane Complex Revealed by BioID. *MBio*, *6*(1). https://doi.org/10.1128/mBio.02357-14

Chen, A. L., Moon, A. S., Bell, H. N., Huang, A. S., Vashisht, A. A., Toh, J. Y., Lin, A. H., Nadipuram, S. M., Kim, E. W., Choi, C. P., Wohlschlegel, J. A., & Bradley, P. J. (2017). Novel insights into the composition and function of the Toxoplasma IMC sutures. *Cellular Microbiology*, *19*(4). https://doi.org/10.1111/cmi.12678

Chen, C.-T., & Gubbels, M.-J. (2013). The Toxoplasma gondii centrosome is the platform for internal daughter budding as revealed by a Nek1 kinase mutant. *Journal of Cell Science*, *126*(Pt 15), 3344–3355. https://doi.org/10.1242/jcs.123364

Chen, C.-T., & Gubbels, M.-J. (2015). Apicomplexan cell cycle flexibility: Centrosome controls the clutch. *Trends in Parasitology*, *31*(6), 229–230. https://doi.org/10.1016/j.pt.2015.04.003

Chen, C.-T., & Gubbels, M.-J. (2019). TgCep250 is dynamically processed through the division cycle and is essential for structural integrity of the *Toxoplasma* centrosome. *Molecular Biology of the Cell*, *30*(10), 1160–1169. https://doi.org/10.1091/mbc.E18-10-0608

Chen, M. J., Dixon, J. E., & Manning, G. (2017). Genomics and evolution of protein phosphatases. *Science Signaling*, *10*(474), eaag1796. https://doi.org/10.1126/scisignal.aag1796

Chevalier, B. S. (2001). Homing endonucleases: Structural and functional insight into the catalysts of intron/intein mobility. *Nucleic Acids Research*, *29*(18), 3757–3774. https://doi.org/10.1093/nar/29.18.3757

Choi, S.-W., Keyes, M. K., & Horrocks, P. (2006). LC/ESI-MS demonstrates the absence of 5-methyl-2′-deoxycytosine in Plasmodium falciparum genomic DNA. *Molecular and Biochemical Parasitology*, *150*(2), 350–352. https://doi.org/10.1016/j.molbiopara.2006.07.003

Chung, H., Schäfer, U., Jäckle, H., & Böhm, S. (2002). Genomic expansion and clustering of ZAD-containing C2H2 zinc-finger genes in *Drosophila*. *EMBO Reports*, *3*(12), 1158–1162. https://doi.org/10.1093/embo-reports/kvf243

Cinar, H. N., Qvarnstrom, Y., Wei-Pridgeon, Y., Li, W., Nascimento, F. S., Arrowood, M. J., Murphy, H. R., Jang, A., Kim, E., Kim, R., Silva, A. da, & Gopinath, G. R. (2016). Comparative sequence analysis of Cyclospora cayetanensis apicoplast genomes originating from diverse geographical regions. *Parasites & Vectors*, *9*. https://doi.org/10.1186/s13071-016-1896-4

Cleary, M. D., Singh, U., Blader, I. J., Brewer, J. L., & Boothroyd, J. C. (2002). Toxoplasma gondii Asexual Development: Identification of Developmentally Regulated Genes and Distinct Patterns of Gene Expression. *Eukaryotic Cell*, *1*(3), 329–340. https://doi.org/10.1128/EC.1.3.329-340.2002

Clough, B., & Frickel, E.-M. (2017). The Toxoplasma Parasitophorous Vacuole: An Evolving Host–Parasite Frontier. *Trends in Parasitology*, *33*(6), 473–488. https://doi.org/10.1016/j.pt.2017.02.007

Coombes, J. L., Charsar, B. A., Han, S.-J., Halkias, J., Chan, S. W., Koshy, A. A., Striepen, B., & Robey, E. A. (2013). Motile invaded neutrophils in the small intestine of Toxoplasma gondii-infected mice reveal a potential mechanism for parasite spread. *Proceedings of the National Academy of Sciences*, *110*(21), E1913–E1922. https://doi.org/10.1073/pnas.1220272110

Coppens, I., Dunn, J. D., Romano, J. D., Pypaert, M., Zhang, H., Boothroyd, J. C., & Joiner, K. A. (2006). Toxoplasma gondii Sequesters Lysosomes from Mammalian Hosts in the Vacuolar Space. *Cell*, *125*(2), 261–274. https://doi.org/10.1016/j.cell.2006.01.056

Coppens, I., & Joiner, K. A. (2003). Host but Not Parasite Cholesterol Controls Toxoplasma Cell Entry by Modulating Organelle Discharge. *Molecular Biology of the Cell*, *14*(9), 3804. https://doi.org/10.1091/mbc.E02-12-0830

Coppens, I., & Vielemeyer, O. (2005). Insights into unique physiological features of neutral lipids in Apicomplexa: From storage to potential mediation in parasite metabolic activities. *International Journal for Parasitology*, *35*(6), 597–615. https://doi.org/10.1016/j.ijpara.2005.01.009

Corden, J. L. (2013). The RNA Polymerase II C-terminal Domain: Tethering Transcription to Transcript and Template. *Chemical Reviews*, *113*(11), 8423. https://doi.org/10.1021/cr400158h

Cori, G. T., & Cori, C. F. (1945). THE ENZYMATIC CONVERSION OF PHOSPHORYLASE a TO b. *Journal of Biological Chemistry*, *158*(2), 321–332. https://doi.org/10.1016/S0021-9258(18)43139-0

Coulson, R. M. R. (2003). The phylogenetic diversity of eukaryotic transcription. *Nucleic Acids Research*, *31*(2), 653–660. https://doi.org/10.1093/nar/gkg156

Courjol, F., & Gissot, M. (2018). A coiled-coil protein is required for coordination of karyokinesis and cytokinesis in *Toxoplasma gondii*. *Cellular Microbiology*, *20*(6), e12832. https://doi.org/10.1111/cmi.12832

Courret, N., Darche, S., Sonigo, P., Milon, G., Buzoni-Gâtel, D., & Tardieux, I. (2006). CD11c- and CD11b-expressing mouse leukocytes transport single Toxoplasma gondii tachyzoites to the brain. *Blood*, *107*(1), 309–316. https://doi.org/10.1182/blood-2005-02-0666

Couvreur, G., Sadak, A., Fortier, B., & Dubremetz, J. F. (1988). Surface antigens of *Toxoplasma gondii*. *Parasitology*, *97*(1), 1–10. https://doi.org/10.1017/S0031182000066695

Couvreur, J. (1974). TOXOPLASMOSIS IN PREGNANCY AND ITS TRANSMISSION TO THE FETUS* GEORGES DESMONTS, M.D. *Bull. N. Y. Acad. Med.*, *50*(2), 14.

Craver, M. P. J., Rooney, P. J., & Knoll, L. J. (2010). Isolation of Toxoplasma gondii development mutants identifies a potential proteophosphogylcan that enhances cyst wall formation. *Molecular and Biochemical Parasitology*, *169*(2), 120–123. https://doi.org/10.1016/j.molbiopara.2009.10.006

Daher, W., Oria, G., Fauquenoy, S., Cailliau, K., Browaeys, E., Tomavo, S., & Khalife, J. (2007). A Toxoplasma gondii Leucine-Rich Repeat Protein Binds Phosphatase Type 1 Protein and Negatively Regulates Its Activity. *Eukaryotic Cell*, *6*(9), 1606–1617. https://doi.org/10.1128/EC.00260-07

Dalmasso, M. C., Echeverria, P. C., Zappia, M. P., Hellman, U., Dubremetz, J. F., & Angel, S. O. (2006). Toxoplasma gondii has two lineages of histones 2b (H2B) with different expression profiles. *Molecular and Biochemical Parasitology*, *148*(1), 103–107. https://doi.org/10.1016/j.molbiopara.2006.03.005

Dalmasso, M. C., Onyango, D. O., Naguleswaran, A., Sullivan, W. J., & Angel, S. O. (2009). Toxoplasma H2A Variants Reveal Novel Insights into Nucleosome Composition and Functions for this Histone Family. *Journal of Molecular Biology*, *392*(1), 33–47. https://doi.org/10.1016/j.jmb.2009.07.017

Dautu, G., Ueno, A., Munyaka, B., Carmen, G., Makino, S., Kobayashi, Y., & Igarashi, M. (2008). Molecular and biochemical characterization of Toxoplasma gondii β-hydroxyacyl-acyl carrier protein dehydratase (FABZ). *Parasitology Research*, *102*(6), 1301–1309. https://doi.org/10.1007/s00436-008-0909-4

de Koning-Ward, T. F., Gilson, P. R., Boddey, J. A., Rug, M., Smith, B. J., Papenfuss, A. T., Sanders, P. R., Lundie, R. J., Maier, A. G., Cowman, A. F., & Crabb, B. S. (2009). A newly discovered protein export machine in malaria parasites. *Nature*, *459*(7249), 945–949. https://doi.org/10.1038/nature08104

de Souza, W., & Attias, M. (2015). New views of the Toxoplasma gondii parasitophorous vacuole as revealed by Helium Ion Microscopy (HIM). *Journal of Structural Biology*, *191*(1), 76–85. https://doi.org/10.1016/j.jsb.2015.05.003

Del Carmen, M. G., Mondragón, M., González, S., & Mondragón, R. (2009). Induction and regulation of conoid extrusion in *Toxoplasma gondii*. *Cellular Microbiology*, *11*(6), 967–982. https://doi.org/10.1111/j.1462-5822.2009.01304.x

Delbac, F., Sänger, A., Neuhaus, E. M., Stratmann, R., Ajioka, J. W., Toursel, C., Herm-Götz, A., Tomavo, S., Soldati, T., & Soldati, D. (2001). Toxoplasma gondii myosins B/C: One gene, two tails, two localizations, and a role in parasite division. *The Journal of Cell Biology*, *155*(4), 613. https://doi.org/10.1083/jcb.200012116

Delorme, V., Cayla, X., Faure, G., Garcia, A., & Tardieux, I. (2003). Actin Dynamics Is Controlled by a Casein Kinase II and Phosphatase 2C Interplay on Toxoplasma gondii Toxofilin. *Molecular Biology of the Cell*, *14*(5), 1900. https://doi.org/10.1091/mbc.E02-08-0462

Delorme, V., Garcia, A., Cayla, X., & Tardieux, I. (2002). A role for Toxoplasma gondii type 1 ser/thr protein phosphatase in host cell invasion. *Microbes and Infection*, *4*(3), 271–278. https://doi.org/10.1016/S1286-4579(02)01538-1

Demar, M., Hommel, D., Djossou, F., Peneau, C., Boukhari, R., Louvel, D., Bourbigot, A.-M., Nasser, V., Ajzenberg, D., Darde, M.-L., & Carme, B. (2012). Acute toxoplasmoses in immunocompetent patients hospitalized in an intensive care unit in French Guiana. *Clinical Microbiology and Infection*, *18*(7), E221–E231. https://doi.org/10.1111/j.1469-0691.2011.03648.x

Deshmukh, A. S., Mitra, P., Kolagani, A., & Gurupwar, R. (2018). Cdk-related kinase 9 regulates RNA polymerase II mediated transcription in Toxoplasma gondii. *Biochimica et Biophysica Acta (BBA) - Gene Regulatory Mechanisms*, *1861*(6), 572–585. https://doi.org/10.1016/j.bbagrm.2018.02.004

Deshmukh, A. S., Mitra, P., & Maruthi, M. (2016). Cdk7 mediates RPB1-driven mRNA synthesis in Toxoplasma gondii. *Scientific Reports*, *6*(1), 35288. https://doi.org/10.1038/srep35288

Deveuve, Q., Lesage, K., Mouveaux, T., & Gissot, M. (2017). The Toxoplasma gondii inhibitor-2 regulates protein phosphatase 1 activity through multiple motifs. *Parasitology Research*, *116*(9), 2417–2426. https://doi.org/10.1007/s00436-017-5543-6

Dikic, I. (2002). CIN85/CMS family of adaptor molecules. *FEBS Letters*, *529*(1), 110–115. https://doi.org/10.1016/S0014-5793(02)03188-5

Dixon, S. E., Stilger, K. L., Elias, E. V., Naguleswaran, A., & Sullivan, W. J. (2010). A decade of epigenetic research in Toxoplasma gondii. *Molecular and Biochemical Parasitology*, *173*(1), 1–9. https://doi.org/10.1016/j.molbiopara.2010.05.001

Donahue, C. G., Carruthers, V. B., Gilk, S. D., & Ward, G. E. (2000). The Toxoplasma homolog of Plasmodium apical membrane antigen-1 (AMA-1) is a microneme protein secreted in response to elevated intracellular calcium levels. *Molecular and Biochemical Parasitology*, *111*(1), 15–30. https://doi.org/10.1016/S0166-6851(00)00289-9

Dos Santos Pacheco, N., Tosetti, N., Koreny, L., Waller, R. F., & Soldati-Favre, D. (2020). Evolution, Composition, Assembly, and Function of the Conoid in Apicomplexa. *Trends in Parasitology*, *36*(8), 688–704. https://doi.org/10.1016/j.pt.2020.05.001

Dubey, J. P. (1997a). Tissue cyst tropism in Toxoplasma gondii: A comparison of tissue cyst formation in organs of cats, and rodents fed oocysts. *Parasitology*, *115*(1), 15–20. https://doi.org/10.1017/S0031182097008949

Dubey, J. P. (1997b). Distribution of Tissue Cysts in Organs of Rats Fed Toxoplasma gondii Oocysts. *The Journal of Parasitology*, *83*(4), 755. https://doi.org/10.2307/3284258

Dubey, J. P. (1998). Advances in the life cycle of Toxoplasma gondii. *International Journal for Parasitology*, *28*(7), 1019–1024. https://doi.org/10.1016/S0020-7519(98)00023-X

Dubey, J. P. (2002). A review of toxoplasmosis in wild birds. *Veterinary Parasitology*, 33.

Dubey, J. P. (2006). Comparative infectivity of oocysts and bradyzoites of Toxoplasma gondii for intermediate (mice) and definitive (cats) hosts. *Veterinary Parasitology*, *140*(1–2), 69–75. https://doi.org/10.1016/j.vetpar.2006.03.018

Dubey, J. P. (2008). The History of *Toxoplasma gondii*—The First 100 Years. *Journal of Eukaryotic Microbiology*, *55*(6), 467–475. https://doi.org/10.1111/j.1550-7408.2008.00345.x

Dubey, J. P., Darrington, C., Tiao, N., Ferreira, L. R., Choudhary, S., Molla, B., Saville, W. J. A., Tilahun, G., Kwok, O. C. H., & Gebreyes, W. A. (2013). Isolation of Viable *Toxoplasma gondii* from Tissues and Feces of Cats from Addis Ababa, Ethiopia. *Journal of Parasitology*, *99*(1), 56–58. https://doi.org/10.1645/GE-3229.1

Dubey, J. P., & Frenkel, J. K. (1972). Cyst-Induced Toxoplasmosis in Cats*. *The Journal of Protozoology*, *19*(1), 155–177. https://doi.org/10.1111/j.1550-7408.1972.tb03431.x

Dubey, J. P., Lindsay, D. S., & Speer, C. A. (1998). Structures of Toxoplasma gondii Tachyzoites, Bradyzoites, and Sporozoites and Biology and Development of Tissue Cysts. *Clinical Microbiology Reviews*, *11*(2), 267–299. https://doi.org/10.1128/CMR.11.2.267

Dubey, R., Harrison, B., Dangoudoubiyam, S., Bandini, G., Cheng, K., Kosber, A., Agop-Nersesian, C., Howe, D. K., Samuelson, J., Ferguson, D. J. P., & Gubbels, M.-J. (2017). Differential Roles for Inner Membrane Complex Proteins across Toxoplasma gondii and Sarcocystis neurona Development. *MSphere*, *2*(5). https://doi.org/10.1128/mSphere.00409-17

Dubois, D. J., & Soldati-Favre, D. (2019). Biogenesis and secretion of micronemes in Toxoplasma gondii. *Cellular Microbiology*, *21*(5). https://doi.org/10.1111/cmi.13018

Dubremetz, J. F. (2007). Rhoptries are major players in Toxoplasma gondii invasion and host cell interaction. *Cellular Microbiology*, *9*(4), 841–848. https://doi.org/10.1111/j.1462-5822.2007.00909.x

Dubremetz, J. F., Achbarou, A., Bermudes, D., & Joiner, K. A. (1993). Kinetics and pattern of organelle exocytosis duringToxoplasma gondii/host-cell interaction. *Parasitology Research*, *79*(5), 402–408. https://doi.org/10.1007/BF00931830

Dustin, M. L., Olszowy, M. W., Holdorf, A. D., Li, J., Bromley, S., Desai, N., Widder, P., Rosenberger, F., van der Merwe, P. A., Allen, P. M., & Shaw, A. S. (1998). A Novel Adaptor Protein Orchestrates Receptor Patterning and Cytoskeletal Polarity in T-Cell Contacts. *Cell*, *94*(5), 667–677. https://doi.org/10.1016/S0092-8674(00)81608-6

Dzierszinski, F., Mortuaire, M., Dendouga, N., Popescu, O., & Tomavo, S. (2001). Differential expression of two plant-like enolases with distinct enzymatic and antigenic properties during stage conversion of the protozoan parasite Toxoplasma gondii. *Journal of Molecular Biology*, *309*(5), 1017–1027. https://doi.org/10.1006/jmbi.2001.4730

Egloff, M. P., Johnson, D. F., Moorhead, G., Cohen, P. T., Cohen, P., & Barford, D. (1997). Structural basis for the recognition of regulatory subunits by the catalytic subunit of protein phosphatase 1. *The EMBO Journal*, *16*(8), 1876. https://doi.org/10.1093/emboj/16.8.1876

Egloff, M.-P., Cohen, P. T. W., Reinemer, P., & Barford, D. (1995). Crystal Structure of the Catalytic Subunit of Human Protein Phosphatase 1 and its Complex with Tungstate. *Journal of Molecular Biology*, *254*(5), 942–959. https://doi.org/10.1006/jmbi.1995.0667

Ehrenhofer-Murray, A. E. (2004). Chromatin dynamics at DNA replication, transcription and repair. *European Journal of Biochemistry*, *271*(12), 2335–2349. https://doi.org/10.1111/j.1432-1033.2004.04162.x

El Bissati, K., Suvorova, E. S., Xiao, H., Lucas, O., Upadhya, R., Ma, Y., Hogue Angeletti, R., White, M. W., Weiss, L. M., & Kim, K. (2016). *Toxoplasma gondii* Arginine Methyltransferase 1 (PRMT1) Is Necessary for Centrosome Dynamics during Tachyzoite Cell Division. *MBio*, *7*(1), e02094-15, /mbio/7/1/e02094-15.atom. https://doi.org/10.1128/mBio.02094-15

Engelberg, K., Chen, C.-T., Bechtel, T., Guzmán, V. S., Drozda, A. A., Chavan, S., Weerapana, E., & Gubbels, M.-J. (2020). The apical annuli of Toxoplasma gondii are composed of coiled-coil and signalling proteins embedded in the inner membrane complex sutures. *Cellular Microbiology*, *22*(1), e13112. https://doi.org/10.1111/cmi.13112

Engelberg, K., Ivey, F. D., Lin, A., Kono, M., Lorestani, A., Faugno-Fusci, D., Gilberger, T.-W., White, M., & Gubbels, M.-J. (2016). A MORN1-associated HAD phosphatase in the basal complex is essential for Toxoplasma gondii daughter budding. *Cellular Microbiology*, *18*(8), 1153. https://doi.org/10.1111/cmi.12574

Englbrecht, C. C., Schoof, H., & Böhm, S. (2004). Conservation, diversification and expansion of C2H2 zinc finger proteins in the Arabidopsis thaliana genome. *BMC Genomics*, *5*(1), 39. https://doi.org/10.1186/1471-2164-5-39

Escalante, A. A., & Ayala, F. J. (1995). Evolutionary origin of Plasmodium and other Apicomplexa based on rRNA genes. *Proceedings of the National Academy of Sciences of the United States of America*, *92*(13), 5793–5797.

Etheridge, R. D., Alaganan, A., Tang, K., Lou, H. J., Turk, B. E., & Sibley, L. D. (2014). The Toxoplasma Pseudokinase ROP5 Forms Complexes with ROP18 and ROP17 Kinases that Synergize to Control Acute Virulence in Mice. *Cell Host & Microbe*, *15*(5), 537–550. https://doi.org/10.1016/j.chom.2014.04.002

Farhat, D. C., Swale, C., Dard, C., Cannella, D., Ortet, P., Barakat, M., Sindikubwabo, F., Belmudes, L., Bock, P.-J. D., Couté, Y., Bougdour, A., & Hakimi, M.-A. (2020). A MORC-driven transcriptional switch controls Toxoplasma developmental trajectories and sexual commitment. *Nature Microbiology*, *5*(4), 570. https://doi.org/10.1038/s41564-020-0674-4

Featherstone, M. (2002). Coactivators in transcription initiation: Here are your orders. *Current Opinion in Genetics & Development*, *12*(2), 149–155. https://doi.org/10.1016/S0959-437X(02)00280-0

Felgueiras, J., Jerónimo, C., & Fardilha, M. (2020). Protein phosphatase 1 in tumorigenesis: Is it worth a closer look? *Biochimica et Biophysica Acta (BBA) - Reviews on Cancer*, *1874*(2), 188433. https://doi.org/10.1016/j.bbcan.2020.188433

Fellows, J. D., Cipriano, M. J., Agrawal, S., & Striepen, B. (2017). A Plastid Protein That Evolved from Ubiquitin and Is Required for Apicoplast Protein Import in Toxoplasma gondii. *MBio*, *8*(3). https://doi.org/10.1128/mBio.00950-17

Ferguson, D. J. P. (2002). Toxoplasma gondii and sex: Essential or optional extra? *Trends in Parasitology*, *18*(8), 351–355. https://doi.org/10.1016/S1471-4922(02)02330-9

Ferguson, D. J. P., Campbell, S. A., Henriquez, F. L., Phan, L., Mui, E., Richards, T. A., Muench, S. P., Allary, M., Lu, J. Z., Prigge, S. T., Tomley, F., Shirley, M. W., Rice, D. W., McLeod, R., & Roberts, C. W. (2007). Enzymes of type II fatty acid synthesis

and apicoplast differentiation and division in Eimeria tenella. *International Journal for Parasitology*, *37*(1), 33–51. https://doi.org/10.1016/j.ijpara.2006.10.003

Ferguson, D. J. P., & Hutchison, W. M. (1987a). An ultrastructural study of the early development and tissue cyst formation of Toxoplasma gondii in the brains of mice. *Parasitology Research*, *73*(6), 483–491. https://doi.org/10.1007/BF00535321

Ferguson, D. J. P., & Hutchison, W. M. (1987b). The host-parasite relationship ofToxoplasma gondii in the brains of chronically infected mice. *Virchows Archiv A Pathological Anatomy and Histopathology*, *411*(1), 39–43. https://doi.org/10.1007/BF00734512

Ferguson, D. J. P., Sahoo, N., Pinches, R. A., Bumstead, J. M., Tomley, F. M., & Gubbels, M.-J. (2008). MORN1 Has a Conserved Role in Asexual and Sexual Development across the Apicomplexa. *Eukaryotic Cell*, *7*(4), 698–711. https://doi.org/10.1128/EC.00021-08

Ferreira, M., Beullens, M., Bollen, M., & Aleyde, V. E. (2019). Functions and therapeutic potential of protein phosphatase 1: Insights from mouse genetics. *Biochimica et Biophysica Acta. Molecular Cell Research*, *1866*(1). https://doi.org/10.1016/j.bbamcr.2018.07.019

Fichera, M. E., Bhopale, M. K., & Roos, D. S. (1995). In vitro assays elucidate peculiar kinetics of clindamycin action against Toxoplasma gondii. *Antimicrobial Agents and Chemotherapy*, *39*(7), 1530. https://doi.org/10.1128/aac.39.7.1530

Fichera, M. E., & Roos, D. S. (1997). A plastid organelle as a drug target in apicomplexan parasites. *Nature*, *390*(6658), 407–409. https://doi.org/10.1038/37132

Flament-Durand, J., CoËrs, C., Waelbroeck, C., Van Geertruyden, J., & Toussaint, Ch. (1967). Encephalite Et Myosite A Toxoplasmes Au Cours D'Un Traitement Immuno-Depresseur (*) [1]. *Acta Clinica Belgica*, *22*(1), 44–54. https://doi.org/10.1080/17843286.1967.11716632

Fleckenstein, M. C., Reese, M. L., Könen-Waisman, S., Boothroyd, J. C., Howard, J. C., & Steinfeldt, T. (2012). A Toxoplasma gondii Pseudokinase Inhibits Host IRG Resistance Proteins. *PLoS Biology*, *10*(7), e1001358. https://doi.org/10.1371/journal.pbio.1001358

Foussard, F., Leriche, M. A., & Dubremetz, J. F. (1991). Characterization of the lipid content of *Toxoplasma gondii* rhoptries. *Parasitology*, *102*(3), 367–370. https://doi.org/10.1017/S0031182000064313

Fox, B. A., Falla, A., Rommereim, L. M., Tomita, T., Gigley, J. P., Mercier, C., Cesbron-Delauw, M.-F., Weiss, L. M., & Bzik, D. J. (2011). Type II Toxoplasma gondii *KU80* Knockout Strains Enable Functional Analysis of Genes Required for Cyst Development and Latent Infection. *Eukaryotic Cell*, *10*(9), 1193–1206. https://doi.org/10.1128/EC.00297-10

Fox, B. A., Guevara, R. B., Rommereim, L. M., Falla, A., Bellini, V., Pètre, G., Rak, C., Cantillana, V., Dubremetz, J.-F., Cesbron-Delauw, M.-F., Taylor, G. A., Mercier, C., & Bzik, D. J. (2019). Toxoplasma gondii Parasitophorous Vacuole Membrane-Associated Dense Granule Proteins Orchestrate Chronic Infection and GRA12 Underpins Resistance to Host Gamma Interferon. *MBio*, *10*(4). https://doi.org/10.1128/mBio.00589-19

Fox, B. A., Rommereim, L. M., Guevara, R. B., Falla, A., Hortua Triana, M. A., Sun, Y., & Bzik, D. J. (2016). The Toxoplasma gondii Rhoptry Kinome Is Essential for Chronic Infection. *MBio*, *7*(3). https://doi.org/10.1128/mBio.00193-16

Francia, M. E., Jordan, C. N., Patel, J. D., Sheiner, L., Demerly, J. L., Fellows, J. D., de Leon, J. C., Morrissette, N. S., Dubremetz, J.-F., & Striepen, B. (2012). Cell Division in Apicomplexan Parasites Is Organized by a Homolog of the Striated Rootlet Fiber

of Algal Flagella. *PLoS Biology*, *10*(12), e1001444. https://doi.org/10.1371/journal.pbio.1001444

Francia, M. E., & Striepen, B. (2014). Cell division in apicomplexan parasites. *Nature Reviews Microbiology*, *12*(2), 125–136. https://doi.org/10.1038/nrmicro3184

Frénal, K., Dubremetz, J.-F., Lebrun, M., & Soldati-Favre, D. (2017). Gliding motility powers invasion and egress in Apicomplexa. *Nature Reviews Microbiology*, *15*(11), 645–660. https://doi.org/10.1038/nrmicro.2017.86

Frénal, K., Jacot, D., Hammoudi, P.-M., Graindorge, A., Maco, B., & Soldati-Favre, D. (2017). Myosin-dependent cell-cell communication controls synchronicity of division in acute and chronic stages of Toxoplasma gondii. *Nature Communications*, *8*(1), 15710. https://doi.org/10.1038/ncomms15710

Frénal, K., Marq, J.-B., Jacot, D., Polonais, V., & Soldati-Favre, D. (2014). Plasticity between MyoC- and MyoA-Glideosomes: An Example of Functional Compensation in Toxoplasma gondii Invasion. *PLoS Pathogens*, *10*(11), e1004504. https://doi.org/10.1371/journal.ppat.1004504

Frénal, K., Polonais, V., Marq, J.-B., Stratmann, R., Limenitakis, J., & Soldati-Favre, D. (2010). Functional Dissection of the Apicomplexan Glideosome Molecular Architecture. *Cell Host & Microbe*, *8*(4), 343–357. https://doi.org/10.1016/j.chom.2010.09.002

Fry, C. J. (2002). TRANSCRIPTION: Unlocking the Gates to Gene Expression. *Science*, *295*(5561), 1847–1848. https://doi.org/10.1126/science.1070260

Fung, C., Beck, J. R., Robertson, S. D., Gubbels, M.-J., & Bradley, P. J. (2012). Toxoplasma ISP4 is a central IMC Sub-compartment Protein whose localization depends on palmitoylation but not myristoylation. *Molecular and Biochemical Parasitology*, *184*(2), 99–108. https://doi.org/10.1016/j.molbiopara.2012.05.002

Gaji, R. Y., Sharp, A. K., & Brown, A. M. (2021). Protein kinases in Toxoplasma gondii. *International Journal for Parasitology*, *51*(6), 415–429. https://doi.org/10.1016/j.ijpara.2020.11.006

Garnham, P. C. C., Baker, J. R., & Bird, R. G. (1962). Fine Structure of Cystic Form of Toxoplasma gondii. *BMJ*, *1*(5271), 83–82. https://doi.org/10.1136/bmj.1.5271.83

Garrison, E., Treeck, M., Ehret, E., Butz, H., Garbuz, T., Oswald, B. P., Settles, M., Boothroyd, J., & Arrizabalaga, G. (2012). A Forward Genetic Screen Reveals that Calcium-dependent Protein Kinase 3 Regulates Egress in Toxoplasma. *PLoS Pathogens*, *8*(11). https://doi.org/10.1371/journal.ppat.1003049

Gaskins, E., Gilk, S., DeVore, N., Mann, T., Ward, G., & Beckers, C. (2004). Identification of the membrane receptor of a class XIV myosin in Toxoplasma gondii. *The Journal of Cell Biology*, *165*(3), 383. https://doi.org/10.1083/jcb.200311137

Gay, G., Braun, L., Brenier-Pinchart, M.-P., Vollaire, J., Josserand, V., Bertini, R.-L., Varesano, A., Touquet, B., De Bock, P.-J., Coute, Y., Tardieux, I., Bougdour, A., & Hakimi, M.-A. (2016). Toxoplasma gondii TgIST co-opts host chromatin repressors dampening STAT1-dependent gene regulation and IFN-γ–mediated host defenses. *Journal of Experimental Medicine*, *213*(9), 1779–1798. https://doi.org/10.1084/jem.20160340

Gilbert, L. A., Ravindran, S., Turetzky, J. M., Boothroyd, J. C., & Bradley, P. J. (2007). Toxoplasma gondii Targets a Protein Phosphatase 2C to the Nuclei of Infected Host Cells. *Eukaryotic Cell*, *6*(1), 73. https://doi.org/10.1128/EC.00309-06

Gilk, S. D., Raviv, Y., Hu, K., Murray, J. M., Beckers, C. J. M., & Ward, G. E. (2006). Identification of PhIL1, a Novel Cytoskeletal Protein of the Toxoplasma gondii Pellicle, through Photosensitized Labeling with 5-[125I]Iodonaphthalene-1-Azide. *Eukaryotic Cell*, *5*(10), 1622. https://doi.org/10.1128/EC.00114-06

Gissot, M., Briquet, S., Refour, P., Boschet, C., & Vaquero, C. (2005). PfMyb1, a Plasmodium falciparum Transcription Factor, is Required for Intra-erythrocytic Growth and Controls Key Genes for Cell Cycle Regulation. *Journal of Molecular Biology*, *346*(1), 29–42. https://doi.org/10.1016/j.jmb.2004.11.045

Gissot, M., Choi, S.-W., Thompson, R. F., Greally, J. M., & Kim, K. (2008). Toxoplasma gondii and Cryptosporidium parvum Lack Detectable DNA Cytosine Methylation. *Eukaryotic Cell*, *7*(3), 537–540. https://doi.org/10.1128/EC.00448-07

Gissot, M., Hovasse, A., Chaloin, L., Schaeffer-Reiss, C., Van Dorsselaer, A., & Tomavo, S. (2017). An evolutionary conserved zinc finger protein is involved in *Toxoplasma gondii* mRNA nuclear export: A zinc finger protein is involved in mRNA nuclear export. *Cellular Microbiology*, *19*(2), e12644. https://doi.org/10.1111/cmi.12644

Gissot, M., Kelly, K. A., Ajioka, J. W., Greally, J. M., & Kim, K. (2007). Epigenomic Modifications Predict Active Promoters and Gene Structure in Toxoplasma gondii. *PLOS Pathogens*, *3*(6), e77. https://doi.org/10.1371/journal.ppat.0030077

Gissot, M., Walker, R., Delhaye, S., Huot, L., Hot, D., & Tomavo, S. (2012). Toxoplasma gondii Chromodomain Protein 1 Binds to Heterochromatin and Colocalises with Centromeres and Telomeres at the Nuclear Periphery. *PLoS ONE*, *7*(3), e32671. https://doi.org/10.1371/journal.pone.0032671

Gold, D. A., Kaplan, A. D., Lis, A., Bett, G. C. L., Rosowski, E. E., Cirelli, K. M., Bougdour, A., Sidik, S. M., Beck, J. R., Lourido, S., Egea, P. F., Bradley, P. J., Hakimi, M.-A., Rasmusson, R. L., & Saeij, J. P. J. (2015). The Toxoplasma Dense Granule Proteins GRA17 and GRA23 Mediate the Movement of Small Molecules between the Host and the Parasitophorous Vacuole. *Cell Host & Microbe*, *17*(5), 642–652. https://doi.org/10.1016/j.chom.2015.04.003

Goldberg, J., Huang, H., Kwon, Y., Greengard, P., Nairn, A. C., & Kuriyan, J. (1995). Three-dimensional structure of the catalytic subunit of protein serine/threonine phosphatase-1. *Nature*, *376*(6543), 745–753. https://doi.org/10.1038/376745a0

Gould, S. B., Tham, W.-H., Cowman, A. F., McFadden, G. I., & Waller, R. F. (2008). Alveolins, a New Family of Cortical Proteins that Define the Protist Infrakingdom Alveolata. *Molecular Biology and Evolution*, *25*(6), 1219–1230. https://doi.org/10.1093/molbev/msn070

Graindorge, A., Frénal, K., Jacot, D., Salamun, J., Marq, J. B., & Soldati-Favre, D. (2016). The Conoid Associated Motor MyoH Is Indispensable for Toxoplasma gondii Entry and Exit from Host Cells. *PLOS Pathogens*, *12*(1), e1005388. https://doi.org/10.1371/journal.ppat.1005388

Gubbels, M.-J. (2006). A MORN-repeat protein is a dynamic component of the Toxoplasma gondii cell division apparatus. *Journal of Cell Science*, *119*(11), 2236–2245. https://doi.org/10.1242/jcs.02949

Gubbels, M.-J., Coppens, I., Zarringhalam, K., Duraisingh, M. T., & Engelberg, K. (2021). The Modular Circuitry of Apicomplexan Cell Division Plasticity. *Frontiers in Cellular and Infection Microbiology*, *11*. https://doi.org/10.3389/fcimb.2021.670049

Gubbels, M.-J., Keroack, C. D., Dangoudoubiyam, S., Worliczek, H. L., Paul, A. S., Bauwens, C., Elsworth, B., Engelberg, K., Howe, D. K., Coppens, I., & Duraisingh, M. T. (2020). Fussing About Fission: Defining Variety Among Mainstream and Exotic Apicomplexan Cell Division Modes. *Frontiers in Cellular and Infection Microbiology*, *10*. https://doi.org/10.3389/fcimb.2020.00269

Gubbels, M.-J., Lehmann, M., Muthalagi, M., Jerome, M. E., Brooks, C. F., Szatanek, T., Flynn, J., Parrot, B., Radke, J., Striepen, B., & White, M. W. (2008). Forward Genetic Analysis of the Apicomplexan Cell Division Cycle in Toxoplasma gondii. *PLoS Pathogens*, *4*(2), e36. https://doi.org/10.1371/journal.ppat.0040036

Gubbels, M.-J., White, M., & Szatanek, T. (2008). The cell cycle and Toxoplasma gondii cell division: Tightly knit or loosely stitched? *International Journal for Parasitology*, *38*(12), 1343–1358. https://doi.org/10.1016/j.ijpara.2008.06.004

Guérin, A., Corrales, R. M., Parker, M. L., Lamarque, M. H., Jacot, D., El Hajj, H., Soldati-Favre, D., Boulanger, M. J., & Lebrun, M. (2017). Efficient invasion by Toxoplasma depends on the subversion of host protein networks. *Nature Microbiology*, *2*(10), 1358–1366. https://doi.org/10.1038/s41564-017-0018-1

Guevara, R. B., Fox, B. A., & Bzik, D. J. (2020). Toxoplasma gondii Parasitophorous Vacuole Membrane-Associated Dense Granule Proteins Regulate Maturation of the Cyst Wall. *MSphere*, *5*(1). https://doi.org/10.1128/mSphere.00851-19

Guevara, R. B., Fox, B. A., & Bzik, D. J. (2021). A Family of Toxoplasma gondii Genes Related to GRA12 Regulate Cyst Burdens and Cyst Reactivation. *MSphere*, *6*(2). https://doi.org/10.1128/mSphere.00182-21

Guevara, R. B., Fox, B. A., Falla, A., & Bzik, D. J. (2019). *Toxoplasma gondii* Intravacuolar-Network-Associated Dense Granule Proteins Regulate Maturation of the Cyst Matrix and Cyst Wall. *MSphere*, *4*(5), e00487-19, /msphere/4/5/mSphere487-19.atom. https://doi.org/10.1128/mSphere.00487-19

Guttery, D. S., Poulin, B., Ramaprasad, A., Wall, R. J., Ferguson, D. J. P., Brady, D., Patzewitz, E.-M., Whipple, S., Straschil, U., Wright, M. H., Mohamed, A. M. A. H., Radhakrishnan, A., Arold, S. T., Tate, E. W., Holder, A. A., Wickstead, B., Pain, A., & Tewari, R. (2014). Genome-wide Functional Analysis of Plasmodium Protein Phosphatases Reveals Key Regulators of Parasite Development and Differentiation. *Cell Host & Microbe*, *16*(1), 128–140. https://doi.org/10.1016/j.chom.2014.05.020

Hadariová, L., Vesteg, M., Hampl, V., & Krajčovič, J. (2018). Reductive evolution of chloroplasts in non-photosynthetic plants, algae and protists. *Current Genetics*, *64*(2), 365–387. https://doi.org/10.1007/s00294-017-0761-0

Håkansson, S., Charron, A. J., & Sibley, L. D. (2001). Toxoplasma evacuoles: A two-step process of secretion and fusion forms the parasitophorous vacuole. *The EMBO Journal*, *20*(12), 3132. https://doi.org/10.1093/emboj/20.12.3132

Håkansson, S., Morisaki, H., Heuser, J., & Sibley, L. D. (1999). Time-Lapse Video Microscopy of Gliding Motility in *Toxoplasma gondii* Reveals a Novel, Biphasic Mechanism of Cell Locomotion. *Molecular Biology of the Cell*, *10*(11), 3539–3547. https://doi.org/10.1091/mbc.10.11.3539

Hakimi, M.-A., Olias, P., & Sibley, L. D. (2017). Toxoplasma Effectors Targeting Host Signaling and Transcription. *Clinical Microbiology Reviews*, *30*(3), 615. https://doi.org/10.1128/CMR.00005-17

Halonen, S. K., Lyman, W. D., & Chiu, F. C. (1996). Growth and Development of *Toxoplasma Gondii* in Human Neurons and Astrocytes. *Journal of Neuropathology & Experimental Neurology*, *55*(11), 1150–1156. https://doi.org/10.1097/00005072-199611000-00006

Hammarton, T.C. (2019). Who Needs a Contractile Actomyosin Ring? The Plethora of Alternative Ways to Divide a Protozoan Parasite. Front. Cell. Infect. Microbiol, 9,397. https://doi.org/10.3389/fcimb.2019.00397

Harding, C. R., Egarter, S., Gow, M., Jiménez-Ruiz, E., Ferguson, D. J. P., & Meissner, M. (2016). Gliding Associated Proteins Play Essential Roles during the Formation of the Inner Membrane Complex of Toxoplasma gondii. *PLOS Pathogens*, *12*(2), e1005403. https://doi.org/10.1371/journal.ppat.1005403

Harding, C. R., & Frischknecht, F. (2020). The Riveting Cellular Structures of Apicomplexan Parasites. *Trends in Parasitology*, *36*(12), 979–991. https://doi.org/10.1016/j.pt.2020.09.001

Harding, C. R., Gow, M., Kang, J. H., Shortt, E., Manalis, S. R., Meissner, M., & Lourido, S. (2019). Alveolar proteins stabilize cortical microtubules in Toxoplasma gondii. *Nature Communications*, *10*. https://doi.org/10.1038/s41467-019-08318-7

Harris, M. T., Jeffers, V., Martynowicz, J., True, J. D., Mosley, A. L., & Sullivan, W. J. (2019). A novel GCN5b lysine acetyltransferase complex associates with distinct transcription factors in the protozoan parasite Toxoplasma gondii. *Molecular and Biochemical Parasitology*, *232*, 111203. https://doi.org/10.1016/j.molbiopara.2019.111203

Harrison, S. C., & Aggarwal, A. K. (1990). DNA Recognition by Proteins with the Helix-Turn-Helix Motif. *Annual Review of Biochemistry*, *59*(1), 933–969. https://doi.org/10.1146/annurev.bi.59.070190.004441

Hartmann, J., Hu, K., He, C. Y., Pelletier, L., Roos, D. S., & Warren, G. (2006). Golgi and centrosome cycles in Toxoplasma gondii. *Molecular and Biochemical Parasitology*, *145*(1), 125–127. https://doi.org/10.1016/j.molbiopara.2005.09.015

He, H., Brenier-Pinchart, M.-P., Braun, L., Kraut, A., Touquet, B., Couté, Y., Tardieux, I., Hakimi, M.-A., & Bougdour, A. (2018). Characterization of a Toxoplasma effector uncovers an alternative GSK3/β-catenin-regulatory pathway of inflammation. *ELife*, *7*, e39887. https://doi.org/10.7554/eLife.39887

He, X., Grigg, M. E., Boothroyd, J. C., & Garcia, K. C. (2002). Structure of the immunodominant surface antigen from the Toxoplasma gondii SRS superfamily. *Nature Structural Biology*. https://doi.org/10.1038/nsb819

Heaslip, A. T., Dzierszinski, F., Stein, B., & Hu, K. (2010). TgMORN1 Is a Key Organizer for the Basal Complex of Toxoplasma gondii. *PLoS Pathogens*, *6*(2). https://doi.org/10.1371/journal.ppat.1000754

Heaslip, A. T., Nelson, S. R., & Warshaw, D. M. (2016). Dense granule trafficking in *Toxoplasma gondii* requires a unique class 27 myosin and actin filaments. *Molecular Biology of the Cell*, *27*(13), 2080–2089. https://doi.org/10.1091/mbc.E15-12-0824

Hehl, A. B., Basso, W. U., Lippuner, C., Ramakrishnan, C., Okoniewski, M., Walker, R. A., Grigg, M. E., Smith, N. C., & Deplazes, P. (2015). Asexual expansion of Toxoplasma gondii merozoites is distinct from tachyzoites and entails expression of non-overlapping gene families to attach, invade, and replicate within feline enterocytes. *BMC Genomics*, *16*(1). https://doi.org/10.1186/s12864-015-1225-x

Hehl, A. B., Lekutis, C., Grigg, M. E., Bradley, P. J., Dubremetz, J.-F., Ortega-Barria, E., & Boothroyd, J. C. (2000). Toxoplasma gondii Homologue ofPlasmodium Apical Membrane Antigen 1 Is Involved in Invasion of Host Cells. *Infection and Immunity*, *68*(12), 7078–7086. https://doi.org/10.1128/IAI.68.12.7078-7086.2000

Hermanns, T., Müller, U. B., Könen-Waisman, S., Howard, J. C., & Steinfeldt, T. (2016). The *Toxoplasma gondii* rhoptry protein ROP18 is an Irga6-specific kinase and regulated by the dense granule protein GRA7. *Cellular Microbiology*, *18*(2), 244–259. https://doi.org/10.1111/cmi.12499

Herm-Gotz, A. (2002). Toxoplasma gondii myosin A and its light chain: A fast, single-headed, plus-end-directed motor. *The EMBO Journal*, *21*(9), 2149–2158. https://doi.org/10.1093/emboj/21.9.2149

Heroes, E., Lesage, B., Görnemann, J., Beullens, M., Meervelt, L. V., & Bollen, M. (2013). The PP1 binding code: A molecular-lego strategy that governs specificity. *The FEBS Journal*, *280*(2), 584–595. https://doi.org/10.1111/j.1742-4658.2012.08547.x

Hong, D.-P., Radke, J. B., & White, M. W. (2017). Opposing Transcriptional Mechanisms Regulate Toxoplasma Development. *MSphere*, *2*(1). https://doi.org/10.1128/mSphere.00347-16

Howe, D. K., & Sibley, L. D. (1995). Toxoplasma gondii Comprises Three Clonal Lineages: Correlation of Parasite Genotype with Human Disease. *Journal of Infectious Diseases*, *172*(6), 1561–1566. https://doi.org/10.1093/infdis/172.6.1561

Hu, K. (2008). Organizational Changes of the Daughter Basal Complex during the Parasite Replication of Toxoplasma gondii. *PLoS Pathogens*, *4*(1), e10. https://doi.org/10.1371/journal.ppat.0040010

Hu, K., Johnson, J., Florens, L., Fraunholz, M., Suravajjala, S., DiLullo, C., Yates, J., Roos, D. S., & Murray, J. M. (2006). Cytoskeletal Components of an Invasion Machine— The Apical Complex of Toxoplasma gondii. *PLoS Pathogens*, *2*(2), e13. https://doi.org/10.1371/journal.ppat.0020013

Hu, K., Roos, D. S., & Murray, J. M. (2002). A novel polymer of tubulin forms the conoid of Toxoplasma gondii. *Journal of Cell Biology*, *156*(6), 1039–1050. https://doi.org/10.1083/jcb.200112086

Huang, S., Holmes, M. J., Radke, J. B., Hong, D.-P., Liu, T.-K., White, M. W., & Sullivan, W. J. (2017). *Toxoplasma gondii AP2IX-4 Regulates Gene Expression during Bradyzoite Development*. *2*(2), 16.

Hunter, C. A., Roberts, C. W., & Alexander, J. (1992). Kinetics of cytokine mRNA production in the brains of mice with progressive toxoplasmic encephalitis. *European Journal of Immunology*, *22*(9), 2317–2322. https://doi.org/10.1002/eji.1830220921

Hunter, C. A., & Sibley, L. D. (2012). Modulation of innate immunity by Toxoplasma gondii virulence effectors. *Nature Reviews Microbiology*, *10*(11), 766–778. https://doi.org/10.1038/nrmicro2858

Huynh, M.-H., & Carruthers, V. B. (2006). Toxoplasma MIC2 Is a Major Determinant of Invasion and Virulence. *PLoS Pathogens*, *2*(8). https://doi.org/10.1371/journal.ppat.0020084

Huynh, M.-H., & Carruthers, V. B. (2009). Tagging of Endogenous Genes in a Toxoplasma gondii Strain Lacking Ku80. *Eukaryotic Cell*, *8*(4), 530–539. https://doi.org/10.1128/EC.00358-08

Huynh, M.-H., Rabenau, K. E., Harper, J. M., Beatty, W. L., Sibley, L. D., & Carruthers, V. B. (2003). Rapid invasion of host cells by Toxoplasma requires secretion of the MIC2–M2AP adhesive protein complex. *The EMBO Journal*, *22*(9), 2082. https://doi.org/10.1093/emboj/cdg217

Imlay, L., & Odom, A. R. (2014). Isoprenoid Metabolism in Apicomplexan Parasites. *Current Clinical Microbiology Reports*, *1*(3–4), 37–50. https://doi.org/10.1007/s40588-014-0006-7

Iuchi, S. (2001). Three classes of C2H2 zinc finger proteins: *Cellular and Molecular Life Sciences*, *58*(4), 625–635. https://doi.org/10.1007/PL00000885

Jacot, D., Daher, W., & Soldati-Favre, D. (2013). Toxoplasma gondii myosin F, an essential motor for centrosomes positioning and apicoplast inheritance. *The EMBO Journal*, *32*(12), 1702. https://doi.org/10.1038/emboj.2013.113

Jacot, D., Tosetti, N., Pires, I., Stock, J., Graindorge, A., Hung, Y.-F., Han, H., Tewari, R., Kursula, I., & Soldati-Favre, D. (2016). An Apicomplexan Actin-Binding Protein Serves as a Connector and Lipid Sensor to Coordinate Motility and Invasion. *Cell Host & Microbe*, *20*(6), 731–743. https://doi.org/10.1016/j.chom.2016.10.020

Jan, G., Delorme, V., David, V., Revenu, C., Rebollo, A., Cayla, X., & Tardieux, I. (2007). The toxofilin–actin–PP2C complex of Toxoplasma: Identification of interacting domains. *Biochemical Journal*, *401*(Pt 3), 711. https://doi.org/10.1042/BJ20061324

Janouskovec, J., Horak, A., Obornik, M., Lukes, J., & Keeling, P. J. (2010). A common red algal origin of the apicomplexan, dinoflagellate, and heterokont plastids. *Proceedings*

of the National Academy of Sciences, *107*(24), 10949–10954. https://doi.org/10.1073/pnas.1003335107

Jayabalasingham, B., Bano, N., & Coppens, I. (2010). Metamorphosis of the malaria parasite in the liver is associated with organelle clearance. *Cell Research*, *20*(9), 1043–1059. https://doi.org/10.1038/cr.2010.88

Jeffers, V., Gao, H., Checkley, L. A., Liu, Y., Ferdig, M. T., Sullivan, W. J., & Jr. (2016). Garcinol Inhibits GCN5-Mediated Lysine Acetyltransferase Activity and Prevents Replication of the Parasite Toxoplasma gondii. *Antimicrobial Agents and Chemotherapy*, *60*(4), 2164. https://doi.org/10.1128/AAC.03059-15

Jeffers, V., & Sullivan, W. J. (2012). Lysine Acetylation Is Widespread on Proteins of Diverse Function and Localization in the Protozoan Parasite Toxoplasma gondii. *Eukaryotic Cell*, *11*(6), 735–742. https://doi.org/10.1128/EC.00088-12

Jeffers, V., Yang, C., Huang, S., Sullivan, W. J., & Jr. (2017). Bromodomains in Protozoan Parasites: Evolution, Function, and Opportunities for Drug Development. *Microbiology and Molecular Biology Reviews : MMBR*, *81*(1). https://doi.org/10.1128/MMBR.00047-16

Jenuwein, T. (2001). Translating the Histone Code. *Science*, *293*(5532), 1074–1080. https://doi.org/10.1126/science.1063127

Jewett, T. J., & Sibley, L. D. (2003). Aldolase Forms a Bridge between Cell Surface Adhesins and the Actin Cytoskeleton in Apicomplexan Parasites. *Molecular Cell*, *11*(4), 885–894. https://doi.org/10.1016/S1097-2765(03)00113-8

Ji, D.-D., & Arnot, D. E. (1997). A Plasmodium falciparum homologue of the ATPase subunit of a multi-protein complex involved in chromatin remodelling for transcription. *Molecular and Biochemical Parasitology*, 12.

Jiang, Y. (2006). Regulation of the Cell Cycle by Protein Phosphatase 2A in Saccharomyces cerevisiae. *Microbiology and Molecular Biology Reviews*, *70*(2), 440–449. https://doi.org/10.1128/MMBR.00049-05

Jofuku, K. D., & Laboratories, S. (1994). *Control of Arabidopsis Flower and Seed Development by the Homeotic Gene APETALA2*. 16.

Johnson, T. M., Rajfur, Z., Jacobson, K., & Beckers, C. J. (2007). Immobilization of the Type XIV Myosin Complex in Toxoplasma gondii. *Molecular Biology of the Cell*, *18*(8), 3039. https://doi.org/10.1091/mbc.E07-01-0040

Jomaa, H., Wiesner, J., Sanderbrand, S., Altincicek, B., Weidemeyer, C., Hintz, M., Türbachova, I., Eberl, M., Zeidler, J., Lichtenthaler, H. K., Soldati, D., & Beck, E. (1999). Inhibitors of the Nonmevalonate Pathway of Isoprenoid Biosynthesis as Antimalarial Drugs. *Science*, *285*(5433), 1573–1576. https://doi.org/10.1126/science.285.5433.1573

Jones, N. G., Wang, Q., & Sibley, L. D. (2017). Secreted protein kinases regulate cyst burden during chronic toxoplasmosis: Secreted kinases in chronic toxoplasmosis. *Cellular Microbiology*, *19*(2), e12651. https://doi.org/10.1111/cmi.12651

Kafsack, B. F. C., & Carruthers, V. B. (2010). Apicomplexan perforin-like proteins. *Communicative & Integrative Biology*, *3*(1), 18–23. https://doi.org/10.4161/cib.3.1.9794

Kafsack, B. F. C., Pena, J. D. O., Coppens, I., Ravindran, S., Boothroyd, J. C., & Carruthers, V. B. (2009). Rapid Membrane Disruption by a Perforin-Like Protein Facilitates Parasite Exit from Host Cells. *Science*, *323*(5913), 530–533. https://doi.org/10.1126/science.1165740

Kagaya, Y., Ohmiya, K., & Hattori, T. (1999). RAV1, a novel DNA-binding protein, binds to bipartite recognition sequence through two distinct DNA-binding domains uniquely

found in higher plants. *Nucleic Acids Research*, *27*(2), 470–478. https://doi.org/10.1093/nar/27.2.470

Kamada, R., Kudoh, F., Ito, S., Tani, I., Janairo, J. I. B., Omichinski, J. G., & Sakaguchi, K. (2020). Metal-dependent Ser/Thr protein phosphatase PPM family: Evolution, structures, diseases and inhibitors. *Pharmacology & Therapeutics*, *215*, 107622. https://doi.org/10.1016/j.pharmthera.2020.107622

Kanei-Ishii, C., Nomura, T., Ogata, K., Sarai, A., Yasukawa, T., Tashiro, S., Takahashi, T., Tanaka, Y., & Ishii, S. (1996). Structure and Function of the Proteins Encoded by the myb Gene Family. In L. Wolff & A. S. Perkins (Eds.), *Molecular Aspects of Myeloid Stem Cell Development* (Vol. 211, pp. 89–98). Springer Berlin Heidelberg. https://doi.org/10.1007/978-3-642-85232-9_9

Kappe, S., Bruderer, T., Gantt, S., Fujioka, H., Nussenzweig, V., & Ménard, R. (1999). Conservation of a Gliding Motility and Cell Invasion Machinery in Apicomplexan Parasites. *Journal of Cell Biology*, *147*(5), 937–944. https://doi.org/10.1083/jcb.147.5.937

Katris, N. J., Dooren, G. G. van, McMillan, P. J., Hanssen, E., Tilley, L., & Waller, R. F. (2014). The Apical Complex Provides a Regulated Gateway for Secretion of Invasion Factors in Toxoplasma. *PLOS Pathogens*, *10*(4), e1004074. https://doi.org/10.1371/journal.ppat.1004074

Katzer, F., Burrells, A., & Opsteegh, M. (2014). Toxoplasma gondii. In *Microbiology of Waterborne Diseases* (pp. 417–440). Elsevier. https://doi.org/10.1016/B978-0-12-415846-7.00021-4

Kaya, G. (2001). An Overview of Classification of the Phylum Apicomplxa. *Kafkas Univ Vet Fak Derg,* 7(2), 223-228.

Keeling, P. J., Burger, G., Durnford, D. G., Lang, B. F., Lee, R. W., Pearlman, R. E., Roger, A. J., & Gray, M. W. (2005). The tree of eukaryotes. *Trends in Ecology & Evolution*, *20*(12), 670–676. https://doi.org/10.1016/j.tree.2005.09.005

Kessler, H., Herm-Götz, A., Hegge, S., Rauch, M., Soldati-Favre, D., Frischknecht, F., & Meissner, M. (2008). Microneme protein 8 – a new essential invasion factor in *Toxoplasma gondii*. *Journal of Cell Science*, *121*(7), 947–956. https://doi.org/10.1242/jcs.022350

Khan, A., Fux, B., Su, C., Dubey, J. P., Darde, M. L., Ajioka, J. W., Rosenthal, B. M., & Sibley, L. D. (2007). Recent transcontinental sweep of Toxoplasma gondii driven by a single monomorphic chromosome. *Proceedings of the National Academy of Sciences*, *104*(37), 14872–14877. https://doi.org/10.1073/pnas.0702356104

Khelifa, A. S., Guillen Sanchez, C., Lesage, K. M., Huot, L., Mouveaux, T., Pericard, P., Barois, N., Touzet, H., Marot, G., Roger, E., & Gissot, M. (2021). TgAP2IX-5 is a key transcriptional regulator of the asexual cell cycle division in Toxoplasma gondii. *Nature Communications*, *12*(1), 116. https://doi.org/10.1038/s41467-020-20216-x

Kim, K. (2018). The Epigenome, Cell Cycle, and Development in Toxoplasma. *Annual Review of Microbiology*. https://doi.org/10.1146/annurev-micro-090817-062741

Kim, K., Jeffers, V., & Sullivan, W. J. (2020). Regulation of gene expression in Toxoplasma gondii. In *Toxoplasma gondii* (pp. 941–982). Elsevier. https://doi.org/10.1016/B978-0-12-815041-2.00021-9

Kohler, S. (1997). A Plastid of Probable Green Algal Origin in Apicomplexan Parasites. *Science*, *275*(5305), 1485–1489. https://doi.org/10.1126/science.275.5305.1485

Kono, M., Heincke, D., Wilcke, L., Wong, T., Bruns, C., Herrmann, S., Spielmann, T., & Gilberger, T. W. (2016). Pellicle formation in the malaria parasite. *Journal of Cell Science*, jcs.181230. https://doi.org/10.1242/jcs.181230

Konstantinovic, N., Guegan, H., Stäjner, T., Belaz, S., & Robert-Gangneux, F. (2019). Treatment of toxoplasmosis: Current options and future perspectives. *Food and Waterborne Parasitology*, *15*, e00036. https://doi.org/10.1016/j.fawpar.2019.e00036

Koreny, L., Zeeshan, M., Barylyuk, K., Tromer, E. C., van Hooff, J. J. E., Brady, D., Ke, H., Chelaghma, S., Ferguson, D. J. P., Eme, L., Tewari, R., & Waller, R. F. (2021). Molecular characterization of the conoid complex in Toxoplasma reveals its conservation in all apicomplexans, including Plasmodium species. *PLOS Biology*, *19*(3), e3001081. https://doi.org/10.1371/journal.pbio.3001081

Kremer, K., Kamin, D., Rittweger, E., Wilkes, J., Flammer, H., Mahler, S., Heng, J., Tonkin, C. J., Langsley, G., Hell, S. W., Carruthers, V. B., Ferguson, D. J. P., & Meissner, M. (2013). An Overexpression Screen of Toxoplasma gondii Rab-GTPases Reveals Distinct Transport Routes to the Micronemes. *PLoS Pathogens*, *9*(3). https://doi.org/10.1371/journal.ppat.1003213

Krizek, B. A. (2003). AINTEGUMENTA utilizes a mode of DNA recognition distinct from that used by proteins containing a single AP2 domain. *Nucleic Acids Research*, *31*(7), 1859–1868. https://doi.org/10.1093/nar/gkg292

Kumar, R., Adams, B., Oldenburg, A., Musiyenko, A., & Barik, S. (2002). Characterisation and expression of a PP1 serine/threonine protein phosphatase (PfPP1) from the malaria parasite, Plasmodium falciparum: demonstration of its essential role using RNA interference. Malaria journal, 1, 5. https://doi.org/10.1186/1475-2875-1-5

Kutuzov, M. A., & Andreeva, A. V. (2008). Protein Ser/Thr phosphatases of parasitic protozoa. *Molecular and Biochemical Parasitology*, *161*(2), 81–90. https://doi.org/10.1016/j.molbiopara.2008.06.008

Labesse, G., Gelin, M., Bessin, Y., Lebrun, M., Papoin, J., Cerdan, R., Arold, S. T., & Dubremetz, J.-F. (2009). ROP2 from Toxoplasma gondii: A Virulence Factor with a Protein-Kinase Fold and No Enzymatic Activity. *Structure*, *17*(1), 139–146. https://doi.org/10.1016/j.str.2008.11.005

Lainson, R. (1958). Observations on the development and nature of pseudocysts and cysts of Toxoplasma gondii. *Transactions of the Royal Society of Tropical Medicine and Hygiene*, *52*(5), 396–407. https://doi.org/10.1016/0035-9203(58)90123-8

Lamarque, M. H., Roques, M., Kong-Hap, M., Tonkin, M. L., Rugarabamu, G., Marq, J.-B., Penarete-Vargas, D. M., Boulanger, M. J., Soldati-Favre, D., & Lebrun, M. (2014). Plasticity and redundancy among AMA–RON pairs ensure host cell entry of Toxoplasma parasites. *Nature Communications*, *5*(1), 1–13. https://doi.org/10.1038/ncomms5098

Landschulz, W. H., Johnson, P. F., & McKnight, S. L. (1988). The leucine zipper: A hypothetical structure common to a new class of DNA binding proteins. *Science*, *240*(4860), 1759–1764. https://doi.org/10.1126/science.3289117

Leander, B. S., & Keeling, P. J. (2003). Morphostasis in alveolate evolution. *Trends in Ecology & Evolution*, *18*(8), 395–402. https://doi.org/10.1016/S0169-5347(03)00152-6

Lebrun, A., & Lavery, R. (1999). Modeling DNA deformations induced by minor groove binding proteins. *Biopolymers*, *49*, 341.

Lebrun, M., Carruthers, V. B., & Cesbron-Delauw, M.-F. (2020). Toxoplasma secretory proteins and their roles in parasite cell cycle and infection. In *Toxoplasma gondii* (pp. 607–704). Elsevier. https://doi.org/10.1016/B978-0-12-815041-2.00014-1

Lebrun, M., Michelin, A., El Hajj, H., Poncet, J., Bradley, P. J., Vial, H., & Dubremetz, J. F. (2005). The rhoptry neck protein RON4 relocalizes at the moving junction during Toxoplasma gondii invasion. *Cellular Microbiology*, *7*(12), 1823–1833. https://doi.org/10.1111/j.1462-5822.2005.00646.x

Lee, J.-O., Rieu, P., Arnaout, M. A., & Liddington, R. (1995). Crystal structure of the A domain from the a subunit of integrin CR3 (CD11 b/CD18). *Cell*, *80*(4), 631–638. https://doi.org/10.1016/0092-8674(95)90517-0

Lee, M., Gippert, G., Soman, K., Case, D., & Wright, P. (1989). Three-dimensional solution structure of a single zinc finger DNA-binding domain. *Science*, *245*(4918), 635–637. https://doi.org/10.1126/science.2503871

Lee, S.-B., & Lee, T.-G. (2017). Toxoplasmic Encephalitis in Patient with Acquired Immunodeficiency Syndrome. *Brain Tumor Research and Treatment*, *5*(1), 34. https://doi.org/10.14791/btrt.2017.5.1.34

Lekutis, C., Ferguson, D. J. P., Grigg, M. E., Camps, M., & Boothroyd, J. C. (2001). Surface antigens of Toxoplasma gondii: Variations on a theme. *International Journal for Parasitology*, *31*(12), 1285–1292. https://doi.org/10.1016/S0020-7519(01)00261-2

Lemgruber, L., Lupetti, P., Souza, W. D., & Vommaro, R. C. (2011). New details on the fine structure of the rhoptry of Toxoplasma gondii. *Microscopy Research and Technique*, *74*(9), 812–818. https://doi.org/10.1002/jemt.20960

Lemon, B. (2000). Orchestrated response: A symphony of transcription factors for gene control. *Genes & Development*, *14*(20), 2551–2569. https://doi.org/10.1101/gad.831000

Lentini, G., Dubois, D. J., Maco, B., Soldati-Favre, D., & Frénal, K. (2019). The roles of Centrin 2 and Dynein Light Chain 8a in apical secretory organelles discharge of Toxoplasma gondii. *Traffic*, *20*(8), 583–600. https://doi.org/10.1111/tra.12673

Lentini, G., Kong-Hap, M., Hajj, H. E., Francia, M., Claudet, C., Striepen, B., Dubremetz, J.-F., & Lebrun, M. (2015). Identification and characterization of Toxoplasma SIP, a conserved apicomplexan cytoskeleton protein involved in maintaining the shape, motility and virulence of the parasite. *Cellular Microbiology*, *17*(1), 62. https://doi.org/10.1111/cmi.12337

Leon, J. C. de, Scheumann, N., Beatty, W., Beck, J. R., Tran, J. Q., Yau, C., Bradley, P. J., Gull, K., Wickstead, B., & Morrissette, N. S. (2013). A SAS-6-Like Protein Suggests that the Toxoplasma Conoid Complex Evolved from Flagellar Components. *Eukaryotic Cell*, *12*(7), 1009. https://doi.org/10.1128/EC.00096-13

Le Roch, K. G., Zhou, Y., Blair, P. L., Grainger, M., Moch, J. K., Haynes, J. D., De la Vega, P., Holder, A. A., Batalov, S., Carucci, D. J., & Winzeler, E. A. (2003). Discovery of Gene Function by Expression Profiling of the Malaria Parasite Life Cycle. *Science*, *301*(5639), 1503–1508. https://doi.org/10.1126/science.1087025

Leroux, L.-P., Dasanayake, D., Rommereim, L. M., Fox, B. A., Bzik, D. J., Jardim, A., & Dzierszinski, F. S. (2015). Secreted Toxoplasma gondii molecules interfere with expression of MHC-II in interferon gamma-activated macrophages. *International Journal for Parasitology*, *45*(5), 319–332. https://doi.org/10.1016/j.ijpara.2015.01.003

Lesage, K. M., Huot, L., Mouveaux, T., Courjol, F., Saliou, J.-M., & Gissot, M. (2018). Cooperative binding of ApiAP2 transcription factors is crucial for the expression of virulence genes in Toxoplasma gondii. *Nucleic Acids Research*, *46*(12), 6057–6068. https://doi.org/10.1093/nar/gky373

Leung, J. M., Liu, J., Wetzel, L. A., & Hu, K. (2019). Centrin2 from the human parasite Toxoplasma gondii is required for its invasion and intracellular replication. *Journal of Cell Science*, *132*(13). https://doi.org/10.1242/jcs.228791

Leung, J. M., Nagayasu, E., Hwang, Y.-C., Liu, J., Pierce, P. G., Phan, I. Q., Prentice, R. A., Murray, J. M., & Hu, K. (2020). A doublecortin-domain protein of Toxoplasma and its orthologues bind to and modify the structure and organization of tubulin polymers. *BMC Molecular and Cell Biology*, *21*. https://doi.org/10.1186/s12860-020-0249-5

Leung, J. M., Rould, M. A., Konradt, C., Hunter, C. A., & Ward, G. E. (2014). Disruption of TgPHIL1 Alters Specific Parameters of Toxoplasma gondii Motility Measured in a Quantitative, Three-Dimensional Live Motility Assay. *PLoS ONE*, *9*(1), e85763. https://doi.org/10.1371/journal.pone.0085763

Li, B., Carey, M., & Workman, J. L. (2007). The Role of Chromatin during Transcription. *Cell*, *128*(4), 707–719. https://doi.org/10.1016/j.cell.2007.01.015

Li, J.-X., He, J.-J., Elsheikha, H. M., Chen, D., Zhai, B.-T., Zhu, X.-Q., & Yan, H.-K. (2019). Toxoplasma gondii ROP17 inhibits the innate immune response of HEK293T cells to promote its survival. *Parasitology Research*, *118*(3), 783–792. https://doi.org/10.1007/s00436-019-06215-y

Lindner, S. E., De Silva, E. K., Keck, J. L., & Llinás, M. (2010). Structural Determinants of DNA Binding by a P. falciparum ApiAP2 Transcriptional Regulator. *Journal of Molecular Biology*, *395*(3), 558–567. https://doi.org/10.1016/j.jmb.2009.11.004

Lippuner, C., Ramakrishnan, C., Basso, W. U., Schmid, M. W., Okoniewski, M., Smith, N. C., Hässig, M., Deplazes, P., & Hehl, A. B. (2018). RNA-Seq analysis during the life cycle of Cryptosporidium parvum reveals significant differential gene expression between proliferating stages in the intestine and infectious sporozoites. *International Journal for Parasitology*, *48*(6), 413–422. https://doi.org/10.1016/j.ijpara.2017.10.007

Lipsick J.S. (1996). One billion years of Myb. *Oncogene*, *13*(2). http://pubmed.ncbi.nlm.nih.gov/8710361/

Liu, L., Michowski, W., Kolodziejczyk, A., & Sicinski, P. (2019). The cell cycle in stem cell proliferation, pluripotency and differentiation. *Nature Cell Biology*, *21*(9), 1060–1067. https://doi.org/10.1038/s41556-019-0384-4

Liu, Q., Wang, Z.-D., Huang, S.-Y., & Zhu, X.-Q. (2015). Diagnosis of toxoplasmosis and typing of Toxoplasma gondii. *Parasites & Vectors*, *8*(1), 292. https://doi.org/10.1186/s13071-015-0902-6

Llinás, M., & DeRisi, J. L. (2004). Pernicious plans revealed: Plasmodium falciparum genome wide expression analysis. *Current Opinion in Microbiology*, *7*(4), 382–387. https://doi.org/10.1016/j.mib.2004.06.014

Long, S., Brown, K. M., Drewry, L. L., Anthony, B., Phan, I. Q. H., & Sibley, L. D. (2017). Calmodulin-like proteins localized to the conoid regulate motility and cell invasion by Toxoplasma gondii. *PLoS Pathogens*, *13*(5). https://doi.org/10.1371/journal.ppat.1006379

Lorenzi, H., Khan, A., Behnke, M. S., Namasivayam, S., Swapna, L. S., Hadjithomas, M., Karamycheva, S., Pinney, D., Brunk, B. P., Ajioka, J. W., Ajzenberg, D., Boothroyd, J. C., Boyle, J. P., Dardé, M. L., Diaz-Miranda, M. A., Dubey, J. P., Fritz, H. M., Gennari, S. M., Gregory, B. D., … Sibley, L. D. (2016). Local admixture of amplified and diversified secreted pathogenesis determinants shapes mosaic Toxoplasma gondii genomes. *Nature Communications*, *7*(1), 10147. https://doi.org/10.1038/ncomms10147

Lorestani, A., Ivey, F. D., Thirugnanam, S., Busby, M. A., Marth, G. T., Cheeseman, I. M., & Gubbels, M.-J. (2012). Targeted proteomic dissection of Toxoplasma cytoskeleton sub-compartments using MORN1. *Cytoskeleton (Hoboken, N.J.)*, *69*(12), 1069. https://doi.org/10.1002/cm.21077

Lorestani, A., Sheiner, L., Yang, K., Robertson, S. D., Sahoo, N., Brooks, C. F., Ferguson, D. J. P., Striepen, B., & Gubbels, M.-J. (2010). A Toxoplasma MORN1 Null Mutant Undergoes Repeated Divisions but Is Defective in Basal Assembly, Apicoplast Division and Cytokinesis. *PLoS ONE*, *5*(8). https://doi.org/10.1371/journal.pone.0012302

Lourido, S., & Moreno, S. N. J. (2015). The calcium signaling toolkit of the Apicomplexan parasites Toxoplasma gondii and Plasmodium spp. *Cell Calcium*, *57*(3), 186–193. https://doi.org/10.1016/j.ceca.2014.12.010

Lourido, S., Tang, K., & Sibley, L. D. (2012). Distinct signalling pathways control *Toxoplasma* egress and host-cell invasion: Distinct signalling pathways control *Toxoplasma* egress and invasion. *The EMBO Journal*, *31*(24), 4524–4534. https://doi.org/10.1038/emboj.2012.299

Lourido, S., Shuman, J., Zhang, C., Shokat, K.M., Hui, R., &Sibley, L. D. (2010, May 20). *Calcium-dependent protein kinase 1 is an essential regulator of exocytosis in Toxoplasma*. Nature; Nature. https://doi.org/10.1038/nature09022

Luft, B. J., Hafner, R., Korzun, A. H., Leport, C., Antoniskis, D., Bosler, E. M., Bourland, D. D., Uttamchandani, R., Fuhrer, J., Jacobson, J., Morlat, P., Vilde, J.-L., Remington, J. S., & Team, the A. 077p/ANRS 009 S. (2010, January 15). *Toxoplasmic Encephalitis in Patients with the Acquired Immunodeficiency Syndrome* (world) [Research-article]. Http://Dx.Doi.Org.Proxy.Insermbiblio.Inist.Fr/10.1056/NEJM199309303291403; Massachusetts Medical Society. https://doi.org/10.1056/NEJM199309303291403

Lusser, A., & Kadonaga, J. T. (2003). Chromatin remodeling by ATP-dependent molecular machines. *BioEssays*, *25*(12), 1192–1200. https://doi.org/10.1002/bies.10359

Magnani, E., Sjölander, K., & Hake, S. (2004). From Endonucleases to Transcription Factors: Evolution of the AP2 DNA Binding Domain in Plants[W]. *The Plant Cell*, *16*(9), 2265–2277. https://doi.org/10.1105/tpc.104.023135

Magno, R. C., Lemgruber, L., Vommaro, R. C., De Souza, W., & Attias, M. (2005). Intravacuolar network may act as a mechanical support forToxoplasma gondii inside the parasitophorous vacuole. *Microscopy Research and Technique*, *67*(1), 45–52. https://doi.org/10.1002/jemt.20182

Magno, R. C., Straker, L. C., de Souza, W., & Attias, M. (2005). Interrelations between the Parasitophorous Vacuole of *Toxoplasma gondii* and Host Cell Organelles. *Microscopy and Microanalysis*, *11*(2), 166–174. https://doi.org/10.1017/S1431927605050129

Maldonado, Y. A., Read, J. S., & COMMITTEE ON INFECTIOUS DISEASES. (2017). Diagnosis, Treatment, and Prevention of Congenital Toxoplasmosis in the United States. *Pediatrics*, *139*(2), e20163860. https://doi.org/10.1542/peds.2016-3860

Mallo, N., Fellows, J., Johnson, C., & Sheiner, L. (2018). Protein Import into the Endosymbiotic Organelles of Apicomplexan Parasites. *Genes*, *9*(8), 412. https://doi.org/10.3390/genes9080412

Mamoun, C. B., & Goldberg, D. E. (2001). Plasmodium protein phosphatase 2C dephosphorylates translation elongation factor 1β and inhibits its PKC-mediated nucleotide exchange activity in vitro. *Molecular Microbiology*, *39*(4), 973–981. https://doi.org/10.1046/j.1365-2958.2001.02289.x

Mamoun, C. B., Sullivan, D. J., Banerjee, R., & Goldberg, D. E. (1998). Identification and Characterization of an Unusual Double Serine/Threonine Protein Phosphatase 2C in the Malaria ParasitePlasmodium falciparum. *Journal of Biological Chemistry*, *273*(18), 11241–11247. https://doi.org/10.1074/jbc.273.18.11241

Manger, I. D., Hehl, A. B., & Boothroyd, J. C. (1998). The Surface of Toxoplasma Tachyzoites Is Dominated by a Family of Glycosylphosphatidylinositol-Anchored Antigens Related to SAG1. *Infection and Immunity*, *66*(5), 2237.

Mann, T. (2001). Characterization of the subpellicular network, a filamentous membrane skeletal component in the parasite Toxoplasma gondii. *Molecular and Biochemical Parasitology*, *115*(2), 257–268. https://doi.org/10.1016/S0166-6851(01)00289-4

Manning, G. (2002). The Protein Kinase Complement of the Human Genome. *Science*, *298*(5600), 1912–1934. https://doi.org/10.1126/science.1075762

Markus, B. M., Waldman, B. S., Lorenzi, H. A., & Lourido, S. (2020). High-Resolution Mapping of Transcription Initiation in the Asexual Stages of Toxoplasma gondii. *Frontiers in Cellular and Infection Microbiology*, *10*. https://doi.org/10.3389/fcimb.2020.617998

Matrajt, M., Platt, C. D., Sagar, A. D., Lindsay, A., Moulton, C., & Roos, D. S. (2004). Transcript initiation, polyadenylation, and functional promoter mapping for the dihydrofolate reductase-thymidylate synthase gene of Toxoplasma gondii. *Molecular and Biochemical Parasitology*, *137*(2), 229–238. https://doi.org/10.1016/j.molbiopara.2003.12.015

Matsuzaki, M., Kikuchi, T., Kita, K., Kojima, S., & Kuroiwa, T. (2001). Large amounts of apicoplast nucleoid DNA and its segregation inToxoplasma gondii. *Protoplasma*, *218*(3–4), 180–191. https://doi.org/10.1007/BF01306607

Matthiesen, S. H., Shenoy, S. M., Kim, K., Singer, R. H., & Satir, B. H. (2001). A parafusin-related Toxoplasma protein in Ca2+-regulated secretory organelles. *European Journal of Cell Biology*, *80*(12), 775–783. https://doi.org/10.1078/0171-9335-00214

Matthiesen, S. H., Shenoy, S. M., Kim, K., Singer, R. H., & Satir, B. H. (2003). Role of the parafusin orthologue, PRP1, in microneme exocytosis and cell invasion in *Toxoplasma gondii*. *Cellular Microbiology*, *5*(9), 613–624. https://doi.org/10.1046/j.1462-5822.2003.00305.x

Mayoral, J., Tomita, T., Tu, V., Aguilan, J. T., Sidoli, S., & Weiss, L. M. (2020). Toxoplasma gondii PPM3C, a secreted protein phosphatase, affects parasitophorous vacuole effector export. *PLoS Pathogens*, *16*(12). https://doi.org/10.1371/journal.ppat.1008771

Mazumdar, J., H. Wilson, E., Masek, K., A. Hunter, C., & Striepen, B. (2006). Apicoplast fatty acid synthesis is essential for organelle biogenesis and parasite survival in Toxoplasma gondii. *Proceedings of the National Academy of Sciences*, *103*(35), 13192–13197. https://doi.org/10.1073/pnas.0603391103

McAuley, J. B. (2014). Congenital Toxoplasmosis. *Journal of the Pediatric Infectious Diseases Society*, *3*(Suppl 1), S30. https://doi.org/10.1093/jpids/piu077

McCabe, R. E., Brooks, R. G., Dorfman, R. F., & Remington, J. S. (1987). Clinical Spectrum in 107 Cases of Toxoplasmic Lymphadenopathy. *Clinical Infectious Diseases*, *9*(4), 754–774. https://doi.org/10.1093/clinids/9.4.754

McCoy, J. M., Whitehead, L., Dooren, G. G. van, & Tonkin, C. J. (2012). TgCDPK3 Regulates Calcium-Dependent Egress of Toxoplasma gondii from Host Cells. *PLoS Pathogens*, *8*(12). https://doi.org/10.1371/journal.ppat.1003066

McFadden, G. I., Reith, M. E., Munholland, J., & Lang-Unnasch, N. (1996). Plastid in human parasites. *Nature*, *381*(6582), 482–482. https://doi.org/10.1038/381482a0

Meissner, M., Reiss, M., Viebig, N., Carruthers, V. B., Toursel, C., Tomavo, S., Ajioka, J. W., & Soldati, D. (2002). A family of transmembrane microneme proteins of Toxoplasma gondii contain EGF-like domains and function as escorters. *Journal of Cell Science*, *115*(3), 563–574. https://doi.org/10.1242/jcs.115.3.563

Meissner, M., & Soldati, D. (2005). The transcription machinery and the molecular toolbox to control gene expression in Toxoplasma gondii and other protozoan parasites. *Microbes and Infection*, *7*(13), 1376–1384. https://doi.org/10.1016/j.micinf.2005.04.019

Mercier, C., & Cesbron-Delauw, M.-F. (2015). Toxoplasma secretory granules: One population or more? *Trends in Parasitology*, *31*(2), 60–71. https://doi.org/10.1016/j.pt.2014.12.002

Mercier, C., Dubremetz, J.-F., Rauscher, B., Lecordier, L., Sibley, L. D., & Cesbron-Delauw, M.-F. (2002). Biogenesis of Nanotubular Network in *Toxoplasma* Parasitophorous Vacuole Induced by Parasite Proteins. *Molecular Biology of the Cell*, *13*(7), 2397–2409. https://doi.org/10.1091/mbc.e02-01-0021

Mercier, C., Lefebvre-Van Hende, S., Garber, G. E., Lecordier, L., Capron, A., & Cesbron-Delauw, M. (1996). Common *cis* -acting elements critical for the expression of several genes of *Toxoplasma gondii* . *Molecular Microbiology*, *21*(2), 421–428. https://doi.org/10.1046/j.1365-2958.1996.6501361.x

Michel, V., Yuan, Z., Ramsubir, S., & Bakovic, M. (2016). Choline Transport for Phospholipid Synthesis: *Experimental Biology and Medicine*. https://doi.org/10.1177/153537020623100503

Michelin, A., Bittame, A., Bordat, Y., Travier, L., Mercier, C., Dubremetz, J.-F., & Lebrun, M. (2009). GRA12, a Toxoplasma dense granule protein associated with the intravacuolar membranous nanotubular network. *International Journal for Parasitology*, *39*(3), 299–306. https://doi.org/10.1016/j.ijpara.2008.07.011

Miller, M. (2009). The Importance of Being Flexible: The Case of Basic Region Leucine Zipper Transcriptional Regulators. *Current Protein & Peptide Science*, *10*(3), 244.

Mineo, J. R., & Kasper, L. H. (1994). Attachment of Toxoplasma gondii to Host Cells Involves Major Surface Protein, SAG-1 (P-30). *Experimental Parasitology*, *79*(1), 11–20. https://doi.org/10.1006/expr.1994.1054

Mistry, J., Chuguransky, S., Williams, L., Qureshi, M., Salazar, G. A., Sonnhammer, E. L. L., Tosatto, S. C. E., Paladin, L., Raj, S., Richardson, L. J., Finn, R. D., & Bateman, A. (2021). Pfam: The protein families database in 2021. *Nucleic Acids Research*, *49*(D1), D412–D419. https://doi.org/10.1093/nar/gkaa913

Mital, J., Meissner, M., Soldati, D., & Ward, G. E. (2005). Conditional Expression of *Toxoplasma gondii* Apical Membrane Antigen-1 (TgAMA1) Demonstrates That TgAMA1 Plays a Critical Role in Host Cell Invasion. *Molecular Biology of the Cell*, *16*(9), 4341–4349. https://doi.org/10.1091/mbc.e05-04-0281

Modrzynska, K., Pfander, C., Chappell, L., Yu, L., Suarez, C., Dundas, K., Gomes, A. R., Goulding, D., Rayner, J. C., Choudhary, J., & Billker, O. (2017). A Knockout Screen of ApiAP2 Genes Reveals Networks of Interacting Transcriptional Regulators Controlling the Plasmodium Life Cycle. *Cell Host & Microbe*, *21*(1), 11–22. https://doi.org/10.1016/j.chom.2016.12.003

Mohrmann, L., & Verrijzer, C. P. (2005). Composition and functional specificity of SWI2/SNF2 class chromatin remodeling complexes. *Biochimica et Biophysica Acta (BBA) - Gene Structure and Expression*, *1681*(2–3), 59–73. https://doi.org/10.1016/j.bbaexp.2004.10.005

Montoya, J. G., & Liesenfeld, O. (2004). Toxoplasmosis. *Lancet (London, England)*, *363*(9425), 1965–1976. https://doi.org/10.1016/S0140-6736(04)16412-X

Moore, R. B., Oborník, M., Janouškovec, J., Chrudimský, T., Vancová, M., Green, D. H., Wright, S. W., Davies, N. W., Bolch, C. J. S., Heimann, K., Šlapeta, J., Hoegh-Guldberg, O., Logsdon, J. M., & Carter, D. A. (2008). A photosynthetic alveolate closely related to apicomplexan parasites. *Nature*, *451*(7181), 959–963. https://doi.org/10.1038/nature06635

Mordue, D. G., Desai, N., Dustin, M., & Sibley, L. D. (1999). Invasion by Toxoplasma gondii Establishes a Moving Junction That Selectively Excludes Host Cell Plasma Membrane Proteins on the Basis of Their Membrane Anchoring. *Journal of Experimental Medicine*, *190*(12), 1783–1792. https://doi.org/10.1084/jem.190.12.1783

Morlon-Guyot, J., Berry, L., Chen, C.-T., Gubbels, M.-J., Lebrun, M., & Daher, W. (2014). The *Toxoplasma gondii* calcium-dependent protein kinase 7 is involved in early steps of parasite division and is crucial for parasite survival: Functional dissection of *T. gondii* CDPK7 protein. *Cellular Microbiology*, *16*(1), 95–114. https://doi.org/10.1111/cmi.12186

Morlon-Guyot, J., El Hajj, H., Martin, K., Fois, A., Carrillo, A., Berry, L., Burchmore, R., Meissner, M., Lebrun, M., & Daher, W. (2018). A proteomic analysis unravels novel CORVET and HOPS proteins involved in *Toxoplasma gondii* secretory organelles biogenesis. *Cellular Microbiology*, *20*(11), e12870. https://doi.org/10.1111/cmi.12870

Morrissette, N.S., Murray J.M., Roos D.S. (1997). Subpellicular microtubules associate with an intramembranous particle lattice in the protozoan parasite Toxoplasma gondii. *J Cell Sci*, 110(Pt1), 35-42.

Morrissette, N. (2015). Targeting Toxoplasma Tubules: Tubulin, Microtubules, and Associated Proteins in a Human Pathogen. *Eukaryotic Cell*, *14*(1), 2–12. https://doi.org/10.1128/EC.00225-14

Morrissette, N., & Gubbels, M.-J. (2020). The Toxoplasma cytoskeleton: Structures, proteins, and processes. In *Toxoplasma gondii* (pp. 743–788). Elsevier. https://doi.org/10.1016/B978-0-12-815041-2.00016-5

Morrissette, N. S., & Sibley, L. D. (2002). Cytoskeleton of Apicomplexan Parasites. *Microbiology and Molecular Biology Reviews*, *66*(1), 21–38. https://doi.org/10.1128/MMBR.66.1.21-38.2002

Moudy, R., Manning, T. J., & Beckers, C. J. (2001). The Loss of Cytoplasmic Potassium upon Host Cell Breakdown Triggers Egress of Toxoplasma gondii. *Journal of Biological Chemistry*, *276*(44), 41492–41501. https://doi.org/10.1074/jbc.M106154200

Mouveaux, T., Oria, G., Werkmeister, E., Slomianny, C., Fox, B. A., Bzik, D. J., & Tomavo, S. (2014). Nuclear Glycolytic Enzyme Enolase of Toxoplasma gondii Functions as a Transcriptional Regulator. *PLoS ONE*, *9*(8), e105820. https://doi.org/10.1371/journal.pone.0105820

Mouveaux, T., Roger, E., Gueye, A., Eysert, F., Huot, L., Grenier-Boley, B., Lambert, J.-C., & Gissot, M. (2021). Primary brain cell infection by Toxoplasma gondii reveals the extent and dynamics of parasite differentiation and impact on neuron biology. *BioRxiv*, 2021.03.15.435467. https://doi.org/10.1101/2021.03.15.435467

Mueller, C., Klages, N., Jacot, D., Santos, J. M., Cabrera, A., Gilberger, T. W., Dubremetz, J.-F., & Soldati-Favre, D. (2013). The Toxoplasma Protein ARO Mediates the Apical Positioning of Rhoptry Organelles, a Prerequisite for Host Cell Invasion. *Cell Host & Microbe*, *13*(3), 289–301. https://doi.org/10.1016/j.chom.2013.02.001

Mueller, C., Samoo, A., Hammoudi, P.-M., Klages, N., Kallio, J. P., Kursula, I., & Soldati-Favre, D. (2016). Structural and functional dissection of *Toxoplasma gondii* armadillo repeats only protein (TgARO). *Journal of Cell Science*, jcs.177386. https://doi.org/10.1242/jcs.177386

Mullapudi, N., Joseph, S. J., & Kissinger, J. C. (2009). Identification and functional characterization of cis-regulatory elements in the apicomplexan parasite Toxoplasma gondii. *Genome Biology*, *10*(4), R34. https://doi.org/10.1186/gb-2009-10-4-r34

Muñiz-Hernández, S., González del Carmen, M., Mondragón, M., Mercier, C., Cesbron, M. F., Mondragón-González, S. L., González, S., & Mondragón, R. (2011). Contribution of the Residual Body in the Spatial Organization of *Toxoplasma gondii* Tachyzoites within the Parasitophorous Vacuole. *Journal of Biomedicine and Biotechnology*, *2011*, 1–11. https://doi.org/10.1155/2011/473983

Nagamune, K., Hicks, L. M., Fux, B., Brossier, F., Chini, E. N., & Sibley, L. D. (2008). Abscisic acid controls calcium-dependent egress and development in Toxoplasma gondii. *Nature*, *451*(7175), 207–210. https://doi.org/10.1038/nature06478

Nagayasu, E., Hwang, Y.-C., Liu, J., Murray, J. M., & Hu, K. (2017). Loss of a doublecortin (DCX)-domain protein causes structural defects in a tubulin-based organelle of Toxoplasma gondii and impairs host-cell invasion. *Molecular Biology of the Cell*, *28*(3), 411. https://doi.org/10.1091/mbc.E16-08-0587

Nagel, S. D., & Boothroyd, J. C. (1989). The Major Surface Antigen, P30, of Toxoplasma gondii Is Anchored by a Glycolipid. *Journal of Biological Chemistry*, *264*(10), 5569–5574. https://doi.org/10.1016/S0021-9258(18)83584-0

Naguleswaran, A., Elias, E. V., McClintick, J., Edenberg, H. J., & Sullivan, W. J. (2010). Toxoplasma gondii Lysine Acetyltransferase GCN5-A Functions in the Cellular Response to Alkaline Stress and Expression of Cyst Genes. *PLoS Pathogens*, *6*(12), e1001232. https://doi.org/10.1371/journal.ppat.1001232

Nair, S. C., Brooks, C. F., Goodman, C. D., Strurm, A., McFadden, G. I., Sundriyal, S., Anglin, J. L., Song, Y., Moreno, S. N. J., & Striepen, B. (2011). Apicoplast isoprenoid precursor synthesis and the molecular basis of fosmidomycin resistance in Toxoplasma gondii. *Journal of Experimental Medicine*, *208*(7), 1547–1559. https://doi.org/10.1084/jem.20110039

Nakaar, V., Bermudes, D., Peck, K. R., & Joiner, K. A. (1998). Upstream elements required for expression of nucleoside triphosphate hydrolase genes of Toxoplasma gondii. *Molecular and Biochemical Parasitology*, 11.

Nakagawa, T., Yoneda, M., Higashi, M., Ohkuma, Y., & Ito, T. (2018). Enhancer function regulated by combinations of transcription factors and cofactors. *Genes to Cells*, *23*(10), 808–821. https://doi.org/10.1111/gtc.12634

Nallani, K. C., & Sullivan, W. J. (2005). Identification of proteins interacting with Toxoplasma SRCAP by yeast two-hybrid screening. *Parasitology Research*, *95*(4), 236–242. https://doi.org/10.1007/s00436-004-1291-5

Nardelli, S. C., Che, F.-Y., Silmon de Monerri, N. C., Xiao, H., Nieves, E., Madrid-Aliste, C., Angel, S. O., Sullivan, W. J., Angeletti, R. H., Kim, K., & Weiss, L. M. (2013). The Histone Code of Toxoplasma gondii Comprises Conserved and Unique Posttranslational Modifications. *MBio*, *4*(6), e00922-13. https://doi.org/10.1128/mBio.00922-13

Naumov, A., Kratzer, S., Ting, L.-M., Kim, K., Suvorova, E. S., & White, M. W. (2017). *The Toxoplasma Centrocone Houses Cell Cycle Regulatory Factors*. 8(4), 17.

Nichols, B.A., Chiappino, M.L., Pavesio C.E. (1994). Endocytosis at the micropore of *Toxoplasma gondii*. *Parasitol Res.* 80(2), 91-98. https://doi.org/10.1007/BF00933773

Nichols, B. A., & Chiappino, M. L. (1987). Cytoskeleton of Toxoplasma gondii1. *The Journal of Protozoology*, *34*(2), 217–226. https://doi.org/10.1111/j.1550-7408.1987.tb03162.x

Nicolle, C., Manceaux, L., (1908). Sur une infection a corps de Leishman (ou organismes voisins) du gondi. *C.R. Seances Acad. Sci.* 147, 763-766.

Nishi, M., Hu, K., Murray, J. M., & Roos, D. S. (2008). Organellar dynamics during the cell cycle of Toxoplasma gondii. *Journal of Cell Science*, *121*(9), 1559–1568. https://doi.org/10.1242/jcs.021089

Nolan, S. J., Romano, J. D., & Coppens, I. (2017). Host lipid droplets: An important source of lipids salvaged by the intracellular parasite Toxoplasma gondii. *PLOS Pathogens*, *13*(6), e1006362. https://doi.org/10.1371/journal.ppat.1006362

Nole-Wilson, S., & Krizek, B. A. (2000). DNA binding properties of the Arabidopsis floral development protein AINTEGUMENTA. *Nucleic Acids Research*, *28*(21), 4076–4082. https://doi.org/10.1093/nar/28.21.4076

Nyonda, M. A., Hammoudi, P., Ye, S., Maire, J., Marq, J., Yamamoto, M., & Soldati-Favre, D. (2021). *Toxoplasma gondii* GRA60 is an effector protein that modulates host cell autonomous immunity and contributes to virulence. *Cellular Microbiology*, *23*(2). https://doi.org/10.1111/cmi.13278

Olguin-Lamas, A., Madec, E., Hovasse, A., Werkmeister, E., Callebaut, I., Slomianny, C., Delhaye, S., Mouveaux, T., Schaeffer-Reiss, C., Van Dorsselaer, A., & Tomavo, S. (2011). A Novel Toxoplasma gondii Nuclear Factor TgNF3 Is a Dynamic Chromatin-Associated Component, Modulator of Nucleolar Architecture and Parasite Virulence. *PLoS Pathogens*, *7*(3), e1001328. https://doi.org/10.1371/journal.ppat.1001328

Olias, P., Etheridge, R. D., Zhang, Y., Holtzman, M. J., & Sibley, L. D. (2016). Toxoplasma Effector Recruits the Mi-2/NuRD Complex to Repress STAT1 Transcription and Block IFN-γ-Dependent Gene Expression. *Cell Host & Microbe*, *20*(1), 72–82. https://doi.org/10.1016/j.chom.2016.06.006

Opitz, C., & Soldati, D. (2002). 'The glideosome': A dynamic complex powering gliding motion and host cell invasion by Toxoplasma gondii: Mechanism of host cell invasion by the Apicomplexa. *Molecular Microbiology*, *45*(3), 597–604. https://doi.org/10.1046/j.1365-2958.2002.03056.x

Orosz, F. (2009). Apicortin, a unique protein, with a putative cytoskeletal role, shared only by apicomplexan parasites and the placozoan Trichoplax adhaerens. *Infection, Genetics and Evolution*, *9*(6), 1275–1286. https://doi.org/10.1016/j.meegid.2009.09.001

O'Shaughnessy, W. J., Hu, X., Beraki, T., McDougal, M., & Reese, M. L. (2020). Loss of a conserved MAPK causes catastrophic failure in assembly of a specialized cilium-like structure in Toxoplasma gondii. *Molecular Biology of the Cell*, *31*(9), 881. https://doi.org/10.1091/mbc.E19-11-0607

Ouologuem, D. T., & Roos, D. S. (2014). Dynamics of the *Toxoplasma gondii* inner membrane complex. *Journal of Cell Science*, jcs.147736. https://doi.org/10.1242/jcs.147736

Paing, M. M., & Tolia, N. H. (2014). Multimeric Assembly of Host-Pathogen Adhesion Complexes Involved in Apicomplexan Invasion. *PLoS Pathogens*, *10*(6), e1004120. https://doi.org/10.1371/journal.ppat.1004120

Panas, M. W., & Boothroyd, J. C. (2021). Seizing control: How dense granule effector proteins enable *Toxoplasma* to take charge. *Molecular Microbiology*, *115*(3), 466–477. https://doi.org/10.1111/mmi.14679

Panas, M. W., Ferrel, A., Naor, A., Tenborg, E., Lorenzi, H. A., & Boothroyd, J. C. (2019). Translocation of Dense Granule Effectors across the Parasitophorous Vacuole Membrane in *Toxoplasma*- Infected Cells Requires the Activity of ROP17, a Rhoptry Protein Kinase. *MSphere*, *4*(4), e00276-19, /msphere/4/4/mSphere276-19.atom. https://doi.org/10.1128/mSphere.00276-19

Panas, M. W., Naor, A., Cygan, A. M., & Boothroyd, J. C. (2019). *Toxoplasma* Controls Host Cyclin E Expression through the Use of a Novel MYR1-Dependent Effector Protein, HCE1. *MBio*, *10*(2). https://doi.org/10.1128/mBio.00674-19

Parmley, S. F., Yang, S., Harth, G., David Sibley, L., Sucharczuk, A., & Remington, J. S. (1994). Molecular characterization of a 65-kilodalton Toxoplasma gondii antigen expressed abundantly in the matrix of tissue cysts. *Molecular and Biochemical Parasitology*, *66*(2), 283–296. https://doi.org/10.1016/0166-6851(94)90155-4

Paul, A. S., Miliu, A., Paulo, J. A., Goldberg, J. M., Bonilla, A. M., Berry, L., Seveno, M., Braun-Breton, C., Kosber, A. L., Elsworth, B., Arriola, J. S. N., Lebrun, M., Gygi, S. P., Lamarque, M. H., & Duraisingh, M. T. (2020). Co-option of Plasmodium falciparum PP1 for egress from host erythrocytes. *Nature Communications*, *11*. https://doi.org/10.1038/s41467-020-17306-1

Peixoto, L., Chen, F., Harb, O. S., Davis, P. H., Beiting, D. P., Brownback, C. S., Ouologuem, D., & Roos, D. S. (2010). Integrative Genomic Approaches Highlight a Family of Parasite-Specific Kinases that Regulate Host Responses. *Cell Host & Microbe*, *8*(2), 208. https://doi.org/10.1016/j.chom.2010.07.004

Pelletier, L., Stern, C. A., Pypaert, M., Sheff, D., Ngô, H. M., Roper, N., He, C. Y., Hu, K., Toomre, D., Coppens, I., Roos, D. S., Joiner, K. A., & Warren, G. (2002). Golgi biogenesis in Toxoplasma gondii. *Nature*, *418*(6897), 548–552. https://doi.org/10.1038/nature00946

Periz, J., Whitelaw, J., Harding, C., Gras, S., Del Rosario Minina, M. I., Latorre-Barragan, F., Lemgruber, L., Reimer, M. A., Insall, R., Heaslip, A., & Meissner, M. (2017). Toxoplasma gondii F-actin forms an extensive filamentous network required for material exchange and parasite maturation. *ELife*, *6*, e24119. https://doi.org/10.7554/eLife.24119

Pernas, L., Adomako-Ankomah, Y., Shastri, A. J., Ewald, S. E., Treeck, M., Boyle, J. P., & Boothroyd, J. C. (2014). Toxoplasma Effector MAF1 Mediates Recruitment of Host Mitochondria and Impacts the Host Response. *PLoS Biology*, *12*(4), e1001845. https://doi.org/10.1371/journal.pbio.1001845

Pernas, L., Bean, C., Boothroyd, J. C., & Scorrano, L. (2018). Mitochondria Restrict Growth of the Intracellular Parasite Toxoplasma gondii by Limiting Its Uptake of Fatty Acids. *Cell Metabolism*, *27*(4), 886-897.e4. https://doi.org/10.1016/j.cmet.2018.02.018

Persson, E. K., Agnarson, A. M., Lambert, H., Hitziger, N., Yagita, H., Chambers, B. J., Barragan, A., & Grandien, A. (2007). Death Receptor Ligation or Exposure to Perforin Trigger Rapid Egress of the Intracellular Parasite *Toxoplasma gondii*. *The Journal of Immunology*, *179*(12), 8357–8365. https://doi.org/10.4049/jimmunol.179.12.8357

Peterson, C. L., & Laniel, M.-A. (2004). Histones and histone modifications. *Current Biology*, *14*(14), R546–R551. https://doi.org/10.1016/j.cub.2004.07.007

Pittman, K. J., Aliota, M. T., & Knoll, L. J. (2014). Dual transcriptional profiling of mice and Toxoplasma gondii during acute and chronic infection. *BMC Genomics*, *15*(1), 806. https://doi.org/10.1186/1471-2164-15-806

Pollack, Y., Katzen, A. L., Spira, D. T., & Golenser, J. (1982). The genome of Plasmodium falciparum. I: DNA base composition. *Nucleic Acids Research*, *10*(2), 539–546.

Ponts, N., Fu, L., Harris, E. Y., Zhang, J., Chung, D.-W. D., Cervantes, M. C., Prudhomme, J., Atanasova-Penichon, V., Zehraoui, E., Bunnik, E. M., Rodrigues, E. M., Lonardi, S., Hicks, G. R., Wang, Y., & Le Roch, K. G. (2013). Genome-wide Mapping of DNA Methylation in the Human Malaria Parasite Plasmodium falciparum. *Cell Host & Microbe*, *14*(6), 696–706. https://doi.org/10.1016/j.chom.2013.11.007

Porchet, E., & Torpier, G. (1977). Etude du germe infectieux de Sarcocystis tenella et Toxoplasma gondii par la technique du cryodécapage. *Zeitschrift für Parasitenkunde*, *54*(2), 101–124. https://doi.org/10.1007/BF00380795

Portman, N., & Šlapeta, J. (2014). The flagellar contribution to the apical complex: A new tool for the eukaryotic Swiss Army knife? *Trends in Parasitology*, *30*(2), 58–64. https://doi.org/10.1016/j.pt.2013.12.006

Qiu, W., Wernimont, A., Tang, K., Taylor, S., Lunin, V., Schapira, M., Fentress, S., Hui, R., & Sibley, L. D. (2009). Novel structural and regulatory features of rhoptry secretory

kinases in Toxoplasma gondii. *The EMBO Journal*, *28*(7), 969. https://doi.org/10.1038/emboj.2009.24

Qureshi, B. M., Hofmann, N. E., Arroyo-Olarte, R. D., Nickl, B., Hoehne, W., Jungblut, P. R., Lucius, R., Scheerer, P., & Gupta, N. (2013). Dynein light chain 8a of Toxoplasma gondii, a unique conoid-localized β-strand-swapped homodimer, is required for an efficient parasite growth. *The FASEB Journal*, *27*(3), 1034–1047. https://doi.org/10.1096/fj.11-180992

Rabaud, C., May, T., Lucet, J. C., Leport, C., Ambroise-Thomas, P., & Canton, P. (1996). Pulmonary Toxoplasmosis in Patients Infected with Human Immunodeficiency Virus: A French National Survey. *Clinical Infectious Diseases*, *23*(6), 1249–1254. https://doi.org/10.1093/clinids/23.6.1249

Rabenau, K. E., Sohrabi, A., Tripathy, A., Reitter, C., Ajioka, J. W., Tomley, F. M., & Carruthers, V. B. (2001). TgM2AP participates in Toxoplasma gondii invasion of host cells and is tightly associated with the adhesive protein TgMIC2. *Molecular Microbiology*, *41*(3), 537–547. https://doi.org/10.1046/j.1365-2958.2001.02513.x

Radke, J. (2001). Defining the cell cycle for the tachyzoite stage of Toxoplasma gondii. *Molecular and Biochemical Parasitology*, *115*(2), 165–175. https://doi.org/10.1016/S0166-6851(01)00284-5

Radke, J. B., Lucas, O., De Silva, E. K., Ma, Y., Sullivan, W. J., Weiss, L. M., Llinas, M., & White, M. W. (2013). ApiAP2 transcription factor restricts development of the Toxoplasma tissue cyst. *Proceedings of the National Academy of Sciences*, *110*(17), 6871–6876. https://doi.org/10.1073/pnas.1300059110

Radke, J. B., Worth, D., Hong, D., Huang, S., Sullivan, W. J., Wilson, E. H., & White, M. W. (2018). Transcriptional repression by ApiAP2 factors is central to chronic toxoplasmosis. *PLOS Pathogens*, *14*(5), e1007035. https://doi.org/10.1371/journal.ppat.1007035

Radke, J., Behnke, M., Mackey, A., Radke, J., Roos, D., & White, M. (2005).The transcriptome of Toxoplasma gondii. *BMC Biology*, *3*(1), 26. https://doi.org/10.1186/1741-7007-3-26

Radke, J. R., Guerini, M. N., Jerome, M., & White, M. W. (2003). A change in the premitotic period of the cell cycle is associated with bradyzoite differentiation in Toxoplasma gondii. *Molecular and Biochemical Parasitology*, *131*(2), 119–127. https://doi.org/10.1016/S0166-6851(03)00198-1

Ramakrishnan, C., Maier, S., Walker, R. A., Rehrauer, H., Joekel, D. E., Winiger, R. R., Basso, W. U., Grigg, M. E., Hehl, A. B., Deplazes, P., & Smith, N. C. (2019). An experimental genetically attenuated live vaccine to prevent transmission of Toxoplasma gondii by cats. *Scientific Reports*, *9*(1), 1474. https://doi.org/10.1038/s41598-018-37671-8

Ranish, J. A., & Hahn, S. (1996). Transcription: Basal factors and activation. *Current Opinion in Genetics & Development*, *6*(2), 151–158. https://doi.org/10.1016/S0959-437X(96)80044-X

Kingston R.E., & Narlikar G.J. (1999). ATP-dependent remodeling and acetylation as regulators of chromatin fluidity. *Genes & Development*, *13*(18). https://doi.org/10.1101/gad.13.18.2339

Rebelo, S., Santos, M., Martins, F., da Cruz e Silva, E. F., & da Cruz e Silva, O. A. B. (2015). Protein phosphatase 1 is a key player in nuclear events. *Cellular Signalling*, *27*(12), 2589–2598. https://doi.org/10.1016/j.cellsig.2015.08.007

Reese, M. L., & Boothroyd, J. C. (2011). A Conserved Non-canonical Motif in the Pseudoactive Site of the ROP5 Pseudokinase Domain Mediates Its Effect on

Toxoplasma Virulence. *Journal of Biological Chemistry*, *286*(33), 29366–29375. https://doi.org/10.1074/jbc.M111.253435

Reiss, M., Viebig, N., Brecht, S., Fourmaux, M.-N., Soete, M., Di Cristina, M., Dubremetz, J. F., & Soldati, D. (2001). Identification and Characterization of an Escorter for Two Secretory Adhesins in Toxoplasma gondii. *Journal of Cell Biology*, *152*(3), 563–578. https://doi.org/10.1083/jcb.152.3.563

Rezaei, F., Sarvi, S., Sharif, M., Hejazi, S. H., Pagheh, A. sattar, Aghayan, S. A., & Daryani, A. (2019). A systematic review of Toxoplasma gondii antigens to find the best vaccine candidates for immunization. *Microbial Pathogenesis*, *126*, 172–184. https://doi.org/10.1016/j.micpath.2018.11.003

Riechmann, J. L., & Meyerowitz, E. (1998). *The AP2/EREBP Family of Plant Transcription Factors*. 22.

Robert-Gangneux, F., & Darde, M.-L. (2012). Epidemiology of and Diagnostic Strategies for Toxoplasmosis. *Clinical Microbiology Reviews*, *25*(2), 264–296. https://doi.org/10.1128/CMR.05013-11

Roger, N., Dubremetz, J.-F., Delplace, P., Fortier, B., Tronchin, G., & Vernes, A. (1988). Characterization of a 225 kilodalton rhoptry protein of Plasmodium falciparum. *Molecular and Biochemical Parasitology*, *27*(2–3), 135–141. https://doi.org/10.1016/0166-6851(88)90033-3

Roiko, M. S., Svezhova, N., & Carruthers, V. B. (2014). Acidification Activates Toxoplasma gondii Motility and Egress by Enhancing Protein Secretion and Cytolytic Activity. *PLoS Pathogens*, *10*(11), e1004488. https://doi.org/10.1371/journal.ppat.1004488

Rosowski, E. E., Lu, D., Julien, L., Rodda, L., Gaiser, R. A., Jensen, K. D. C., & Saeij, J. P. J. (2011). Strain-specific activation of the NF-κB pathway by GRA15, a novel Toxoplasma gondii dense granule protein. *Journal of Experimental Medicine*, *208*(1), 195–212. https://doi.org/10.1084/jem.20100717

Rudlaff, R. M., Kraemer, S., Streva, V. A., & Dvorin, J. D. (2019). An essential contractile ring protein controls cell division in Plasmodium falciparum. *Nature Communications*, *10*(1), 2181. https://doi.org/10.1038/s41467-019-10214-z

Rudzki, E. N., Ander, S. E., Coombs, R. S., Alrubaye, H. I., Cabo, L. F., Blank, M. L., Gutierrez-Melo, N., Dubey, J., Coyne, C. B., & Boyle, J. P. (2020). Toxoplasma gondii GRA28 *is required for specific induction of the regulatory chemokine CCL22 in human and mouse cells* [Preprint]. Microbiology. https://doi.org/10.1101/2020.10.14.335802

Rugarabamu, G., Marq, J.-B., Guérin, A., Lebrun, M., & Soldati-Favre, D. (2015). Distinct contribution of *T oxoplasma gondii* rhomboid proteases 4 and 5 to micronemal protein protease 1 activity during invasion: ROM4 and ROM5 contribute to MPP1 activity. *Molecular Microbiology*, *97*(2), 244–262. https://doi.org/10.1111/mmi.13021

Sabin, A.B. &Olitsky, P.K. (1937). *Toxoplasma* and obligate intracellular parasitism. *Science*, 85, 336-338.

Sadak, A., Taghy, Z., Fortier, B., & Dubremetz, J. (1988). Characterization of a family of rhoptry proteins ofToxoplasma gondii. *Molecular and Biochemical Parasitology*, *29*(2–3), 203–211. https://doi.org/10.1016/0166-6851(88)90075-8

Saeij, J. P. J., Boyle, J. P., Grigg, M. E., Arrizabalaga, G., & Boothroyd, J. C. (2005). Bioluminescence Imaging of Toxoplasma gondii Infection in Living Mice Reveals Dramatic Differences between Strains. *Infection and Immunity*, *73*(2), 695–702. https://doi.org/10.1128/IAI.73.2.695-702.2005

Saksouk, N., Bhatti, M. M., Kieffer, S., Smith, A. T., Musset, K., Garin, J., Sullivan, W. J., Jr, Cesbron-Delauw, M.-F., & Hakimi, M.-A. (2005). Histone-Modifying Complexes Regulate Gene Expression Pertinent to the Differentiation of the Protozoan Parasite

Toxoplasma gondii. *Molecular and Cellular Biology*, 25(23), 10301. https://doi.org/10.1128/MCB.25.23.10301-10314.2005

Sakuma, Y., Liu, Q., Dubouzet, J. G., Abe, H., Shinozaki, K., & Yamaguchi-Shinozaki, K. (2002). DNA-Binding Specificity of the ERF/AP2 Domain of Arabidopsis DREBs, Transcription Factors Involved in Dehydration- and Cold-Inducible Gene Expression. *Biochemical and Biophysical Research Communications*, 290(3), 998–1009. https://doi.org/10.1006/bbrc.2001.6299

Sardar, R., Kaushik, A., Pandey, R., Mohmmed, A., Ali, S., & Gupta, D. (2019). ApicoTFdb: The comprehensive web repository of apicomplexan transcription factors and transcription-associated co-factors. *Database*, 2019, baz094. https://doi.org/10.1093/database/baz094

Sautel, C. F., Cannella, D., Bastien, O., Kieffer, S., Aldebert, D., Garin, J., Tardieux, I., Belrhali, H., & Hakimi, M.-A. (2007). SET8-Mediated Methylations of Histone H4 Lysine 20 Mark Silent Heterochromatic Domains in Apicomplexan Genomes. *Molecular and Cellular Biology*, 27(16), 5711. https://doi.org/10.1128/MCB.00482-07

Scallan, E., Hoekstra, R. M., Angulo, F. J., Tauxe, R. V., Widdowson, M.-A., Roy, S. L., Jones, J. L., & Griffin, P. M. (2011). Foodborne Illness Acquired in the United States—Major Pathogens. *Emerging Infectious Diseases*, 17(1), 7–15. https://doi.org/10.3201/eid1701.P11101

Scholtyseck, E., Friedhoff, K., & Piekarski, G. (1970). ber mikromorphologische bereinstimmungen bei Entwicklungsstadien von Coccidien, Toxoplasmen und Piroplasmen. *Zeitschrift fr Parasitenkunde*, 35(2). https://doi.org/10.1007/BF00259989

Schwarz, J. A., Fouts, A. E., Cummings, C. A., Ferguson, D. J. P., & Boothroyd, J. C. (2005). A novel rhoptry protein in Toxoplasma gondii bradyzoites and merozoites. *Molecular and Biochemical Parasitology*, 144(2), 159–166. https://doi.org/10.1016/j.molbiopara.2005.08.011

Semenovskaya, K., Lévêque, M. F., Berry, L., Bordat, Y., Dubremetz, J., Lebrun, M., & Besteiro, S. (2020). TgZFP2 is a novel zinc finger protein involved in coordinating mitosis and budding in *Toxoplasma*. *Cellular Microbiology*, 22(1). https://doi.org/10.1111/cmi.13120

Shandilya, J., & Roberts, S. G. E. (2012). The transcription cycle in eukaryotes: From productive initiation to RNA polymerase II recycling. *Biochimica et Biophysica Acta (BBA) - Gene Regulatory Mechanisms*, 1819(5), 391–400. https://doi.org/10.1016/j.bbagrm.2012.01.010

Shaw, M. K., Roos, D. S., & Tilney, L. G. (1998). Acidic compartments and rhoptry formation in *Toxoplasma gondii*. *Parasitology*, 117(5), 435–443. https://doi.org/10.1017/S0031182098003278

Sheffield, H. G., & Melton, M. L. (1968). The fine structure and reproduction of Toxoplasma gondii. *The Journal of Parasitology*, 54(2), 209–226.

Sheiner, L., Santos, J. M., Klages, N., Parussini, F., Jemmely, N., Friedrich, N., Ward, G. E., & Soldati-Favre, D. (2010). Toxoplasma gondii transmembrane microneme proteins and their modular design. *Molecular Microbiology*, 77(4), 912–929. https://doi.org/10.1111/j.1365-2958.2010.07255.x

Shen, T., & Huang, S. (2012). The Role of Cdc25A in the Regulation of Cell Proliferation and Apoptosis. *Anti-Cancer Agents in Medicinal Chemistry*, 12(6), 631–639. https://doi.org/10.2174/187152012800617678

Shen, B., Brown, K.M., Lee, T.D., Sibley, L.D., (2014). Efficient Gene Disruption in Diverse Strains of Toxoplasma gondii using CRISPR/Cas9. mBio 5.

https://doi.org/10.1128/mBio.01114-14

Shi, Y. (2009). Serine/Threonine Phosphatases: Mechanism through Structure. *Cell*, *139*(3), 468–484. https://doi.org/10.1016/j.cell.2009.10.006

Sibley, L. D., Niesman, I. R., Parmley, S. F., & Cesbron-Delauw, M. F. (1995). Regulated secretion of multi-lamellar vesicles leads to formation of a tubulo-vesicular network in host-cell vacuoles occupied by Toxoplasma gondii. *Journal of Cell Science*, *108*(4), 1669–1677.

Sidik, S. M., Huet, D., Ganesan, S. M., Huynh, M.-H., Wang, T., Nasamu, A. S., Thiru, P., Saeij, J. P. J., Carruthers, V. B., Niles, J. C., & Lourido, S. (2016). A Genome-wide CRISPR Screen in Toxoplasma Identifies Essential Apicomplexan Genes. *Cell*, *166*(6), 1423-1435.e12. https://doi.org/10.1016/j.cell.2016.08.019

Silmon de Monerri, N. C., Yakubu, R. R., Chen, A. L., Bradley, P. J., Nieves, E., Weiss, L. M., & Kim, K. (2015). The Ubiquitin Proteome of Toxoplasma gondii Reveals Roles for Protein Ubiquitination in Cell-Cycle Transitions. *Cell Host & Microbe*, *18*(5), 621–633. https://doi.org/10.1016/j.chom.2015.10.014

Sinai, A.P., Webster, P., & Joiner, K.A. (1997). Association of host cell endoplasmic reticulum and mitochondria with the Toxoplasma gondii parasitophorous vacuole membrane: A high affinity interaction. *Journal of Cell Science*, *110 (Pt 17)*. http://pubmed.ncbi.nlm.nih.gov/9378762/

Silva, E. K. D., Gehrke, A. R., Olszewski, K., León, I., Chahal, J. S., Bulyk, M. L., & Llinás, M. (2008). Specific DNA-binding by Apicomplexan AP2 transcription factors. *Proceedings of the National Academy of Sciences*, *105*(24), 8393–8398. https://doi.org/10.1073/pnas.0801993105

Sindikubwabo, F., Ding, S., Hussain, T., Ortet, P., Barakat, M., Baumgarten, S., Cannella, D., Palencia, A., Bougdour, A., Belmudes, L., Couté, Y., Tardieux, I., Botté, C. Y., Scherf, A., & Hakimi, M. (2017). Modifications at K31 on the lateral surface of histone H4 contribute to genome structure and expression in apicomplexan parasites. *ELife*, *6*. https://doi.org/10.7554/eLife.29391

Singh, U., Brewer, J. L., & Boothroyd, J. C. (2002). Genetic analysis of tachyzoite to bradyzoite differentiation mutants in Toxoplasma gondii reveals a hierarchy of gene induction: Bradyzoite development pathways in T. gondii. *Molecular Microbiology*, *44*(3), 721–733. https://doi.org/10.1046/j.1365-2958.2002.02903.x

Sims, T.A., Hay, J., Talbot I.C., (1988). Host-parasite relationship in the brains of mice with congenital toxoplasmosis. *The Journal of Pathology*, 156, 255-261.

Skene, P. J., & Henikoff, S. (2017). An efficient targeted nuclease strategy for high-resolution mapping of DNA binding sites. *ELife*, *6*. https://doi.org/10.7554/eLife.21856

Sloves, P.-J., Delhaye, S., Mouveaux, T., Werkmeister, E., Slomianny, C., Hovasse, A., Dilezitoko Alayi, T., Callebaut, I., Gaji, R. Y., Schaeffer-Reiss, C., Van Dorsselear, A., Carruthers, V. B., & Tomavo, S. (2012). Toxoplasma Sortilin-like Receptor Regulates Protein Transport and Is Essential for Apical Secretory Organelle Biogenesis and Host Infection. *Cell Host & Microbe*, *11*(5), 515–527. https://doi.org/10.1016/j.chom.2012.03.006

Smith, A. T., Tucker-Samaras, S. D., Fairlamb, A. H., Sullivan, W. J., & Jr. (2005). MYST Family Histone Acetyltransferases in the Protozoan Parasite Toxoplasma gondii. *Eukaryotic Cell*, *4*(12), 2057. https://doi.org/10.1128/EC.4.12.2057-2065.2005

Soete, M., Camus, D., & Dubrametz, J. F. (1994). Experimental Induction of Bradyzoite-Specific Antigen Expression and Cyst Formation by the RH Strain of Toxoplasma gondii in Vitro. *Experimental Parasitology*, *78*(4), 361–370. https://doi.org/10.1006/expr.1994.1039

Soldati, D., & Boothroyd, J. C. (1995). A selector of transcription initiation in the protozoan parasite Toxoplasma gondii. *Molecular and Cellular Biology*, *15*(1), 87–93. https://doi.org/10.1128/MCB.15.1.87

Soldati, D., Dubremetz, J. F., & Lebrun, M. (2001). Microneme proteins: Structural and functional requirements to promote adhesion and invasion by the apicomplexan parasite Toxoplasma gondii. *International Journal for Parasitology*, *31*(12), 1293–1302. https://doi.org/10.1016/S0020-7519(01)00257-0

Sommer, M. S., Gould, S. B., Lehmann, P., Gruber, A., Przyborski, J. M., & Maier, U.-G. (2007). Der1-mediated Preprotein Import into the Periplastid Compartment of Chromalveolates? *Molecular Biology and Evolution*, *24*(4), 918–928. https://doi.org/10.1093/molbev/msm008

Speer, C. A., & Dubey, J. P. (2005). Ultrastructural differentiation of Toxoplasma gondii schizonts (types B to E) and gamonts in the intestines of cats fed bradyzoites. *International Journal for Parasitology*, *35*(2), 193–206. https://doi.org/10.1016/j.ijpara.2004.11.005

Splendore, A., (1908). Un nuovo protozoa parassita de' conigli. incontrato nelle lesioni anatomiche d'une malattia che ricorda in molti punti il Kala-azar dell' uomo. *Nota preliminare pel. Rev. Soc. Sci*. Sao Paulo 3, 109-112.

Srivastava, S., White, M. W., & Sullivan, W. J. (2020). Toxoplasma gondii AP2XII-2 Contributes to Proper Progression through S-Phase of the Cell Cycle. *MSphere*, *5*(5). https://doi.org/10.1128/mSphere.00542-20

Stark, M.J. (1996). Yeast protein serine/threonine phosphatases: Multiple roles and diverse regulation. *Yeast (Chichester, England)*, *12*(16). https://doi.org/10.1002/(SICI)1097-0061(199612)12:16%3C1647::AID-YEA71%3E3.0.CO;2-Q

Starnes, G. L., Coincon, M., Sygusch, J., & Sibley, L. D. (2009). Aldolase Is Essential for Energy Production and Bridging Adhesin-Actin Cytoskeletal Interactions during Parasite Invasion of Host Cells. *Cell Host & Microbe*, *5*(4), 353–364. https://doi.org/10.1016/j.chom.2009.03.005

Stegmaier, P., Kel, A. E., & Wingender, E. (2004). *Systematic DNA-Binding Domain Classification of Transcription Factors*. 11.

Sterner, D. E., & Berger, S. L. (2000). Acetylation of Histones and Transcription-Related Factors. *Microbiology and Molecular Biology Reviews*, *64*(2), 435–459. https://doi.org/10.1128/MMBR.64.2.435-459.2000

Stiller, J. W., & Cook, M. S. (2004). Functional Unit of the RNA Polymerase II C-Terminal Domain Lies within Heptapeptide Pairs. *Eukaryotic Cell*, *3*(3), 735. https://doi.org/10.1128/EC.3.3.735-740.2004

Stommel, E. W., Ely, K. H., Schwartzman, J. D., & Kasper, L. H. (1997). Toxoplasma gondii:Dithiol-Induced Ca2+Flux Causes Egress of Parasites from the Parasitophorous Vacuole. *Experimental Parasitology*, *87*(2), 88–97. https://doi.org/10.1006/expr.1997.4187

Striepen, B. (2011). The apicoplast: A red alga in human parasites. *Essays in Biochemistry*, *51*, 111–125. https://doi.org/10.1042/bse0510111

Striepen, B., Crawford, M. J., Shaw, M. K., Tilney, L. G., Seeber, F., & Roos, D. S. (2000). The Plastid of Toxoplasma gondii Is Divided by Association with the Centrosomes. *Journal of Cell Biology*, *151*(7), 1423–1434. https://doi.org/10.1083/jcb.151.7.1423

Striepen, B., Jordan, C. N., Reiff, S., & van Dooren, G. G. (2007). Building the Perfect Parasite: Cell Division in Apicomplexa. *PLoS Pathogens*, *3*(6), e78. https://doi.org/10.1371/journal.ppat.0030078

Su, C., Khan, A., Zhou, P., Majumdar, D., Ajzenberg, D., Dardé, M.-L., Zhu, X.-Q., Ajioka, J. W., Rosenthal, B. M., Dubey, J. P., & Sibley, L. D. (2012). Globally diverse

Toxoplasma gondii isolates comprise six major clades originating from a small number of distinct ancestral lineages. *Proceedings of the National Academy of Sciences*, *109*(15), 5844–5849. https://doi.org/10.1073/pnas.1203190109

Sullivan, W. J. (2003). Histone H3 and H3.3 Variants in the Protozoan Pathogens *Plasmodium falciparum* and *Toxoplasma gondii*. *DNA Sequence*, *14*(3), 227–231. https://doi.org/10.1080/1042517031000089496

Sullivan, W. J., Monroy, M. A., Bohne, W., Nallani, K. C., Chrivia, J., Yaciuk, P., Smith, C. K., & Queener, S. F. (2003). Molecular cloning and characterization of an SRCAP chromatin remodeling homologue in Toxoplasma gondii. *Parasitology Research*, *90*(1), 1–8. https://doi.org/10.1007/s00436-002-0814-1

Sullivan WJ., Jr, Jeffers V., (2012). Mechanisms of Toxoplasma gondii persistence and latency. *FEMS Microbiology Reviews*, 36(3), 717-733. https://doi.org/10.1111/j.1574-6976.2011.00305.x

Suss-Toby, E., Zimmerberg, J., & Ward, G. E. (1996). Toxoplasma invasion: The parasitophorous vacuole is formed from host cell plasma membrane and pinches off via a fission pore. *Proceedings of the National Academy of Sciences*, *93*(16), 8413–8418. https://doi.org/10.1073/pnas.93.16.8413

Suvorova, E. S., Francia, M., Striepen, B., & White, M. W. (2015). A novel bipartite centrosome coordinates the apicomplexan cell cycle. *PLoS Biology*, *13*(3), e1002093. https://doi.org/10.1371/journal.pbio.1002093

Suzuki, Y, Joh, K., Orellana M.A., Conley, F.K. & Remington, J.S. (1991). *A gene(s) within the H-2D region determines the development of toxoplasmic encephalitis in mice*. 8.

Swain, J. E., Wang, X., Saunders, T. L., Dunn, R., & Smith, G. D. (2003). Specific inhibition of mouse oocyte nuclear protein phosphatase-1 stimulates germinal vesicle breakdown. *Molecular Reproduction and Development*, *65*(1), 96–103. https://doi.org/10.1002/mrd.10258

Swedlow, J. R., Hu, K., Andrews, P. D., Roos, D. S., & Murray, J. M. (2002). Measuring tubulin content in Toxoplasma gondii: A comparison of laser-scanning confocal and wide-field fluorescence microscopy. *Proceedings of the National Academy of Sciences*, *99*(4), 2014–2019. https://doi.org/10.1073/pnas.022554999

Swierzy, I. J., Muhammad, M., Kroll, J., Abelmann, A., Tenter, A. M., & Lüder, C. G. K. (2014). Toxoplasma gondii within skeletal muscle cells: A critical interplay for food-borne parasite transmission. *International Journal for Parasitology*, *44*(2), 91–98. https://doi.org/10.1016/j.ijpara.2013.10.001

Swiezewska, E., & Danikiewicz, W. (2005). Polyisoprenoids: Structure, biosynthesis and function. *Progress in Lipid Research*, *44*(4), 235–258. https://doi.org/10.1016/j.plipres.2005.05.002

Takatsuji, H. (1999). Zinc-finger proteins: The classical zinc finger emerges in contemporary plant science. *Plant Molecular Biology*, *39*(6). https://doi.org/10.1023/a:1006184519697

Talevich, E., & Kannan, N. (2013). Structural and evolutionary adaptation of rhoptry kinases and pseudokinases, a family of coccidian virulence factors. *BMC Evolutionary Biology*, *13*, 117. https://doi.org/10.1186/1471-2148-13-117

Templeton, T. J. (2004). Comparative Analysis of Apicomplexa and Genomic Diversity in Eukaryotes. *Genome Research*, *14*(9), 1686–1695. https://doi.org/10.1101/gr.2615304

Tenter, A. M., Heckeroth, A. R., & Weiss, L. M. (2000). Toxoplasma gondii: From animals to humans. *International Journal for Parasitology*, *30*(12–13), 1217.

Thiagalingam, S., Cheng, K.-H., Lee, H. J., Mineva, N., Thiagalingam, A., & Ponte, J. F. (2003). Histone Deacetylases: Unique Players in Shaping the Epigenetic Histone

Code. *Annals of the New York Academy of Sciences*, *983*(1), 84–100. https://doi.org/10.1111/j.1749-6632.2003.tb05964.x

Tilley, L. D., Krishnamurthy, S., Westwood, N. J., & Ward, G. E. (2014). Identification of TgCBAP, a Novel Cytoskeletal Protein that Localizes to Three Distinct Subcompartments of the Toxoplasma gondii Pellicle. *PLoS ONE*, *9*(6). https://doi.org/10.1371/journal.pone.0098492

Tomavo, S., Schwarz, R. T., & Dubremetz, J. F. (1989). Evidence for glycosyl-phosphatidylinositol anchoring of Toxoplasma gondii major surface antigens. *Molecular and Cellular Biology*, *9*(10), 4576–4580. https://doi.org/10.1128/MCB.9.10.4576

Tomita, T., Bzik, D. J., Ma, Y. F., Fox, B. A., Markillie, L. M., Taylor, R. C., Kim, K., & Weiss, L. M. (2013). The Toxoplasma gondii Cyst Wall Protein CST1 Is Critical for Cyst Wall Integrity and Promotes Bradyzoite Persistence. *PLoS Pathogens*, *9*(12). https://doi.org/10.1371/journal.ppat.1003823

Tomley, F. M., & Soldati, D. S. (2001). Mix and match modules: Structure and function of microneme proteins in apicomplexan parasites. *Trends in Parasitology*, *17*(2), 81–88. https://doi.org/10.1016/S1471-4922(00)01761-X

Tonkin, M. L., Beck, J. R., Bradley, P. J., & Boulanger, M. J. (2014). The Inner Membrane Complex Sub-compartment Proteins Critical for Replication of the Apicomplexan Parasite Toxoplasma gondii Adopt a Pleckstrin Homology Fold. *Journal of Biological Chemistry*, *289*(20), 13962–13973. https://doi.org/10.1074/jbc.M114.548891

Tonkin, M. L., Roques, M., Lamarque, M. H., Pugniere, M., Douguet, D., Crawford, J., Lebrun, M., & Boulanger, M. J. (2011). Host Cell Invasion by Apicomplexan Parasites: Insights from the Co-Structure of AMA1 with a RON2 Peptide. *Science*, *333*(6041), 463–467. https://doi.org/10.1126/science.1204988

Torgerson, P. R., & Mastroiacovo, P. (2013). The global burden of congenital toxoplasmosis: A systematic review. *Bulletin of the World Health Organization*, *91*(7), 501–508. https://doi.org/10.2471/BLT.12.111732

Torres, J. A., Pasquarelli, R. R., Back, P. S., Moon, A. S., & Bradley, P. J. (2021). Identification and Molecular Dissection of IMC32, a Conserved Toxoplasma Inner Membrane Complex Protein That Is Essential for Parasite Replication. *MBio*, *12*(1). https://doi.org/10.1128/mBio.03622-20

Tosetti, N., Pacheco, N. D. S., Bertiaux, E., Maco, B., Bournonville, L., Hamel, V., Guichard, P., & Soldati-Favre, D. (2020). Essential function of the alveolin network in the subpellicular microtubules and conoid assembly in Toxoplasma gondii. *ELife*, *9*. https://doi.org/10.7554/eLife.56635

Tran, J. Q., Leon, J. C. de, Li, C., Huynh, M.-H., Beatty, W., & Morrissette, N. S. (2010). RNG1 is a Late Marker of the Apical Polar Ring in Toxoplasma gondii. *Cytoskeleton (Hoboken, N.J.)*, *67*(9), 586. https://doi.org/10.1002/cm.20469

Tran, J. Q., Li, C., Chyan, A., Chung, L., & Morrissette, N. S. (2012). SPM1 Stabilizes Subpellicular Microtubules in Toxoplasma gondii. *Eukaryotic Cell*, *11*(2), 206–216. https://doi.org/10.1128/EC.05161-11

Treeck, M., Sanders, J. L., Elias, J. E., & Boothroyd, J. C. (2011). The Phosphoproteomes of Plasmodium falciparum and Toxoplasma gondii Reveal Unusual Adaptations Within and Beyond the Parasites' Boundaries. *Cell Host & Microbe*, *10*(4), 410–419. https://doi.org/10.1016/j.chom.2011.09.004

Tu, V., Mayoral, J., Sugi, T., Tomita, T., Han, B., Ma, Y. F., & Weiss, L. M. (2019). Enrichment and Proteomic Characterization of the Cyst Wall from *In Vitro* Toxoplasma gondii Cysts. *MBio*, *10*(2). https://doi.org/10.1128/mBio.00469-19

Tyler, J. S., & Boothroyd, J. C. (2011). The C-Terminus of Toxoplasma RON2 Provides the Crucial Link between AMA1 and the Host-Associated Invasion Complex. *PLoS Pathogens*, *7*(2), e1001282. https://doi.org/10.1371/journal.ppat.1001282

Tyler, J. S., Treeck, M., & Boothroyd, J. C. (2011). Focus on the ringleader: The role of AMA1 in apicomplexan invasion and replication. *Trends in Parasitology*, *27*(9), 410–420. https://doi.org/10.1016/j.pt.2011.04.002

Koufopanou, V., Goddard, M.R., & Burt, A., (2002). Adaptation for horizontal transfer in a homing endonuclease. *Molecular Biology and Evolution*, *19*(3). https://doi.org/10.1093/oxfordjournals.molbev.a004077

van Dooren, G. G., Reiff, S. B., Tomova, C., Meissner, M., Humbel, B. M., & Striepen, B. (2009). A Novel Dynamin-Related Protein Has Been Recruited for Apicoplast Fission in Toxoplasma gondii. *Current Biology*, *19*(4), 267–276. https://doi.org/10.1016/j.cub.2008.12.048

van Dooren, G. G., Yeoh, L. M., Striepen, B., & McFadden, G. I. (2016). The Import of Proteins into the Mitochondrion of Toxoplasma gondii. *Journal of Biological Chemistry*, *291*(37), 19335–19350. https://doi.org/10.1074/jbc.M116.725069

Vanchinathan, P., Brewer, J. L., Harb, O. S., Boothroyd, J. C., & Singh, U. (2005). Disruption of a Locus Encoding a Nucleolar Zinc Finger Protein Decreases Tachyzoite-to-Bradyzoite Differentiation in Toxoplasma gondii. *Infection and Immunity*, *73*(10), 6680–6688. https://doi.org/10.1128/IAI.73.10.6680-6688.2005

Vaughan, A. M., & Kappe, S. H. I. (2017). Malaria Parasite Liver Infection and Exoerythrocytic Biology. *Cold Spring Harbor Perspectives in Medicine*, *7*(6), a025486. https://doi.org/10.1101/cshperspect.a025486

Venugopal, K., Chehade, S., Werkmeister, E., Barois, N., Periz, J., Lafont, F., Tardieux, I., Khalife, J., Langsley, G., Meissner, M., & Marion, S. (2020). Rab11A regulates dense granule transport and secretion during Toxoplasma gondii invasion of host cells and parasite replication. *PLoS Pathogens*, *16*(5). https://doi.org/10.1371/journal.ppat.1008106

Venugopal, K., Werkmeister, E., Barois, N., Saliou, J.-M., Poncet, A., Huot, L., Sindikubwabo, F., Hakimi, M. A., Langsley, G., Lafont, F., & Marion, S. (2017). Dual role of the Toxoplasma gondii clathrin adaptor AP1 in the sorting of rhoptry and microneme proteins and in parasite division. *PLOS Pathogens*, *13*(4), e1006331. https://doi.org/10.1371/journal.ppat.1006331

Verhave, J. P., & Meis, J. F. G. M. (1984). The biology of tissue forms and other asexual stages in mammalian plasmodia. *Experientia*, *40*(12), 1317–1329. https://doi.org/10.1007/BF01951885

Vlastaridis, P., Kyriakidou, P., Chaliotis, A., Van de Peer, Y., Oliver, S. & Amoutzias, G. (2017). Estimating the total number of phosphoproteins and phosphorylation sites in eukaryotic proteomes. *Gigascience*, 6(2), 1-11. https://doi.org/10.1093/gigascience/giw015.

Waldman, B. S., Schwarz, D., Wadsworth, M. H., Saeij, J. P., Shalek, A. K., & Lourido, S. (2020). Identification of a Master Regulator of Differentiation in Toxoplasma. *Cell*, *180*(2), 359-372.e16. https://doi.org/10.1016/j.cell.2019.12.013

Walker, R., Gissot, M., Croken, M. M., Huot, L., Hot, D., Kim, K., & Tomavo, S. (2013a). The Toxoplasma nuclear factor TgAP2XI-4 controls bradyzoite gene expression and cyst formation. *Molecular Microbiology*, *87*(3), 641–655. https://doi.org/10.1111/mmi.12121

Walker, R., Gissot, M., Huot, L., Alayi, T. D., Hot, D., Marot, G., Schaeffer-Reiss, C., Dorsselaer, A. V., Kim, K., & Tomavo, S. (2013b). Toxoplasma Transcription Factor TgAP2XI-5 Regulates the Expression of Genes Involved in Parasite Virulence and

Host Invasion. *The Journal of Biological Chemistry*, *288*(43), 31127. https://doi.org/10.1074/jbc.M113.486589

Wan, K.-L., Carruthers, V. B., Sibley, L. D., & Ajioka, J. W. (1997). Molecular characterisation of an expressed sequence tag locus of Toxoplasma gondii encoding the micronemal protein MIC21Note: Nucleotide sequence reported in this paper have been submitted to the GenBank^TM database with the accession number U62660.1. *Molecular and Biochemical Parasitology*, *84*(2), 203–214. https://doi.org/10.1016/S0166-6851(96)02796-X

Wang, C., Hu, D., Tang, X., Song, X., Wang, S., Zhang, S., Duan, C., Sun, P., Suo, J., Ma, H., Suo, X., & Liu, X. (2021). Internal daughter formation of *Toxoplasma gondii* tachyzoites is coordinated by transcription factor TGAP2IX -5. *Cellular Microbiology*, *23*(3). https://doi.org/10.1111/cmi.13291

Wang, H., Lei, T., Liu, J., Li, M., Nan, H., & Liu, Q. (2014). A Nuclear Factor of High Mobility Group Box Protein in Toxoplasma gondii. *PLoS ONE*, *9*(11). https://doi.org/10.1371/journal.pone.0111993

Wang, J., Dixon, S. E., Ting, L.-M., Liu, T.-K., Jeffers, V., Croken, M. M., Calloway, M., Cannella, D., Ali Hakimi, M., Kim, K., & Sullivan, W. J. (2014). Lysine Acetyltransferase GCN5b Interacts with AP2 Factors and Is Required for Toxoplasma gondii Proliferation. *PLoS Pathogens*, *10*(1), e1003830. https://doi.org/10.1371/journal.ppat.1003830

Wang, J.-L., Bai, M.-J., Elsheikha, H. M., Liang, Q.-L., Li, T.-T., Cao, X.-Z., & Zhu, X.-Q. (2020). Novel roles of dense granule protein 12 (GRA12) in Toxoplasma gondii infection. *The FASEB Journal*, *34*(2), 3165–3178. https://doi.org/10.1096/fj.201901416RR

Wang, Z.-D., Wang, S.-C., Liu, H.-H., Ma, H.-Y., Li, Z.-Y., Wei, F., Zhu, X.-Q., & Liu, Q. (2017). Prevalence and burden of Toxoplasma gondii infection in HIV-infected people: A systematic review and meta-analysis. *The Lancet HIV*, *4*(4), e177–e188. https://doi.org/10.1016/S2352-3018(17)30005-X

Weiss, L. M., & Dubey, Jitender. P. (2009). Toxoplasmosis: A history of clinical observations. *International Journal for Parasitology*, *39*(8), 895–901. https://doi.org/10.1016/j.ijpara.2009.02.004

White, M. W., Jerome, M. E., Vaishnava, S., Guerini, M., Behnke, M., & Striepen, B. (2004). Genetic rescue of a Toxoplasma gondii conditional cell cycle mutant. *Molecular Microbiology*, 12.

White, M. W., Radke, J. R., & Radke, J. B. (2014). *T oxoplasma* development—Turn the switch on or off?: Tachyzoite control of development. *Cellular Microbiology*, *16*(4), 466–472. https://doi.org/10.1111/cmi.12267

White, M. W., & Suvorova, E. S. (2018). Apicomplexa Cell Cycles: Something Old, Borrowed, Lost, and New. *Trends in Parasitology*, *34*(9), 759–771. https://doi.org/10.1016/j.pt.2018.07.006

Williams, M. J., Alonso, H., Enciso, M., Egarter, S., Sheiner, L., Meissner, M., Striepen, B., Smith, B. J., & Tonkin, C. J. (2015). Two Essential Light Chains Regulate the MyoA Lever Arm To Promote Toxoplasma Gliding Motility. *MBio*, *6*(5), e00845-15. https://doi.org/10.1128/mBio.00845-15

Wilson, (Iain) R.J.M., Denny, P. W., Preiser, P. R., Rangachari, K., Roberts, K., Roy, A., Whyte, A., Strath, M., Moore, D. J., Moore, P. W., & Williamson, D. H. (1996). Complete Gene Map of the Plastid-like DNA of the Malaria ParasitePlasmodium falciparum. *Journal of Molecular Biology*, *261*(2), 155–172. https://doi.org/10.1006/jmbi.1996.0449

Wingender, E. (1993). *Gene Regulation in Eukaryotes*. 7.*VCH Weinheim*

Wingender, E. (1996). TRANSFAC: A database on transcription factors and their DNA binding sites. *Nucleic Acids Research*, *24*(1), 238–241. https://doi.org/10.1093/nar/24.1.238

Wolf, A., Cowen, D., & Paige, B. (1939). HUMAN TOXOPLASMOSIS: OCCURRENCE IN INFANTS AS AN ENCEPHALOMYELITIS VERIFICATION BY TRANSMISSION TO ANIMALS. *Science*, *89*(2306), 226–227. https://doi.org/10.1126/science.89.2306.226

Wong, Z. S., Sokol-Borrelli, S. L., Olias, P., Dubey, J. P., & Boyle, J. P. (2020). Head-to-head comparisons of Toxoplasma gondii and its near relative Hammondia hammondi reveal dramatic differences in the host response and effectors with species-specific functions. *PLOS Pathogens*, *16*(6), e1008528. https://doi.org/10.1371/journal.ppat.1008528

Wuitschick, J. D., Lindstrom, P. R., Meyer, A. E., & Karrer, K. M. (2004). Homing Endonucleases Encoded by Germ Line-Limited Genes in Tetrahymena thermophila Have APETELA2 DNA Binding Domains. *Eukaryotic Cell*, *3*(3), 685. https://doi.org/10.1128/EC.3.3.685-694.2004

Xue, Y., Theisen, T. C., Rastogi, S., Ferrel, A., Quake, S. R., & Boothroyd, J. C. (2020). A single-parasite transcriptional atlas of Toxoplasma Gondii reveals novel control of antigen expression. *ELife*, *9*, e54129. https://doi.org/10.7554/eLife.54129

Yakubu, R. R., Monerri, N. C. S. de, Nieves, E., Kim, K., & Weiss, L. M. (2017). Comparative Monomethylarginine Proteomics Suggests that Protein Arginine Methyltransferase 1 (PRMT1) is a Significant Contributor to Arginine Monomethylation in Toxoplasma gondii. *Molecular & Cellular Proteomics : MCP*, *16*(4), 567. https://doi.org/10.1074/mcp.M117.066951

Yamamoto, M., Ma, J. S., Mueller, C., Kamiyama, N., Saiga, H., Kubo, E., Kimura, T., Okamoto, T., Okuyama, M., Kayama, H., Nagamune, K., Takashima, S., Matsuura, Y., Soldati-Favre, D., & Takeda, K. (2011). ATF6β is a host cellular target of the Toxoplasma gondii virulence factor ROP18. *Journal of Experimental Medicine*, *208*(7), 1533–1546. https://doi.org/10.1084/jem.20101660

Yang, C., & Arrizabalaga, G. (2017). The serine/threonine phosphatases of apicomplexan parasites. *Molecular Microbiology*, *106*(1), 1–21. https://doi.org/10.1111/mmi.13715

Yang, C., Broncel, M., Dominicus, C., Sampson, E., Blakely, W. J., Treeck, M., & Arrizabalaga, G. (2019). A plasma membrane localized protein phosphatase in Toxoplasma gondii, PPM5C, regulates attachment to host cells. *Scientific Reports*, *9*. https://doi.org/10.1038/s41598-019-42441-1

Yang, C., & Stiller, J. W. (2014). Evolutionary diversity and taxon-specific modifications of the RNA polymerase II C-terminal domain. *Proceedings of the National Academy of Sciences of the United States of America*, *111*(16), 5920. https://doi.org/10.1073/pnas.1323616111

Yang, L., Uboldi, A. D., Seizova, S., Wilde, M.-L., Coffey, M. J., Katris, N. J., Yamaryo-Botté, Y., Kocan, M., Bathgate, R. A. D., Stewart, R. J., McConville, M. J., Thompson, P. E., Botté, C. Y., & Tonkin, C. J. (2019). An apically located hybrid guanylate cyclase–ATPase is critical for the initiation of Ca2+ signaling and motility in Toxoplasma gondii. *Journal of Biological Chemistry*, *294*(22), 8959–8972. https://doi.org/10.1074/jbc.RA118.005491

Yates, B., Braschi, B., Gray, K. A., Seal, R. L., Tweedie, S., & Bruford, E. A. (2017). Genenames.org: The HGNC and VGNC resources in 2017. *Nucleic Acids Research*, *45*(Database issue), D619. https://doi.org/10.1093/nar/gkw1033

Yoon, H. S., Grant, J., Tekle, Y. I., Wu, M., Chaon, B. C., Cole, J. C., Logsdon, J. M., Patterson, D. J., Bhattacharya, D., & Katz, L. A. (2008). Broadly sampled multigene trees of eukaryotes. *BMC Evolutionary Biology*, *8*(1), 14. https://doi.org/10.1186/1471-2148-8-14

Zeeshan, M., Pandey, R., Subudhi, A. K., Ferguson, D., Kaur, G., Rashpa, R., Nugmanova, R., Brady, D., Bottrill, A. R., Vaughan, S., Brochet, M., Bollen, M., Pain, A., Holder, A. A., Guttery, D. S., & Tewari, R. (2021). Protein phosphatase 1 regulates atypical mitotic and meiotic division in Plasmodium sexual stages. Communications biology, 4(1), 760. https://doi.org/10.1038/s42003-021-02273-

Zhang, M., Mishra, S., Sakthivel, R., Fontoura, B. M. A., & Nussenzweig, V. (2016). UIS2: A Unique Phosphatase Required for the Development of Plasmodium Liver Stages. *PLOS Pathogens*, *12*(1), e1005370. https://doi.org/10.1371/journal.ppat.1005370

Zhang, Y. (2001). Transcription regulation by histone methylation: Interplay between different covalent modifications of the core histone tails. *Genes & Development*, *15*(18), 2343–2360. https://doi.org/10.1101/gad.927301

Zheng, L., Roeder, R. G., & Luo, Y. (2003). S Phase Activation of the Histone H2B Promoter by OCA-S, a Coactivator Complex that Contains GAPDH as a Key Component. *Cell*, *114*(2), 255–266. https://doi.org/10.1016/S0092-8674(03)00552-X